

THE UNIVERSITY OF ALBERTA

Design of Shallow Tunnels in Soft Ground

by

Arsenio Negro Jr.

VOLUME I

A THESIS

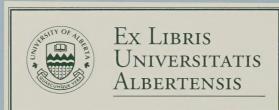
SUBMITTED TO THE FACULTY OF GRADUATE STUDIES AND RESEARCH .

IN PARTIAL FULFILMENT OF THE REQUIREMENTS FOR THE DEGREE

OF Doctor of Philosophy

Department of Civil Engineering

EDMONTON, ALBERTA
SPRING 1988



THE UNIVERSITY OF ALBERTA

Design of Shallow Tunnels in Soft Ground

by

Arsenio Negro Jr.

VOLUME I

A THESIS

SUBMITTED TO THE FACULTY OF GRADUATE STUDIES AND RESEARCH
IN PARTIAL FULFILMENT OF THE REQUIREMENTS FOR THE DEGREE

OF Doctor of Philosophy

Department of Civil Engineering

EDMONTON, ALBERTA
SPRING 1988

THE UNIVERSITY OF ALBERTA

RELEASE FORM

NAME OF AUTHOR Arsenio Negro Jr.

TITLE OF THESIS Design of Shallow Tunnels in Soft

Ground

DEGREE FOR WHICH THESIS WAS PRESENTED Doctor of Philosophy
YEAR THIS DEGREE GRANTED SPRING 1988

Permission is hereby granted to THE UNIVERSITY OF ALBERTA LIBRARY to reproduce single copies of this thesis and to lend or sell such copies for private, scholarly or scientific research purposes only.

The author reserves other publication rights, and neither the thesis nor extensive extracts from it may be printed or otherwise reproduced without the author's written permission.

Digitized by the Internet Archive in 2021 with funding from University of Alberta Libraries

THE UNIVERSITY OF ALBERTA FACULTY OF GRADUATE STUDIES AND RESEARCH

The undersigned certify that they have read, and recommend to the Faculty of Graduate Studies and Research, for acceptance, a thesis entitled *Design of Shallow Tunnels in Soft Ground* submitted by Arsenio Negro Jr. in partial fulfilment of the requirements for the degree of Doctor of Philosophy.

CALCAN TO ALL SULVION DAG

The Coft Crount s best teams are the medical and the control of the requirements of the requirements.

DEDICATION

To Dona Nair, Sr. Nene and Te.

You deserve more than just this.

To Bone Mais, Ms. Mens and To

elds such neds essa five ebla.

ABSTRACT

This work reviews and discusses the behaviour of shallow tunnels in soil. The most relevant factors controlling the ground behaviour are identified.

A comprehensive review of available design methods is presented. Existing procedures and current design practice are assessed and the deficiences of current approaches to shallow tunnel design are recognized. It is demonstrated that there is a need to improve these routines by coupling ground settlement prediction with lining load estimates. While this can be done using numerical techniques, the practice asks for simpler yet reliable procedures, presently unavailable.

Accordingly, a new design method is developed. It assumed the ground behaviour to be non-linear and time independent, and the tunnel to be shallow, single and circular. The method was developed through generalization of results obtained by two and three-dimensional finite element modelling, after assessing the ability of these techniques to portray tunnelling behaviour.

The two dimensional modelling allows relationships to be established between tunnel closure, ground mass displacements, the amount of ground stress release and the resulting ground stiffness changes. The results of the generalization process are presented in dimensionless form, through equations and charts, which allow the above relationships to be defined for distinct soil strengths,

ground stiffnesses, in situ stress conditions and for different tunnel sizes and depths.

The effects of the delayed installation of the lining are accounted for by combining the above results with an estimate for tunnel closure, developed from three-dimensional finite element parametric analyses. The lining-ground interaction is taken into consideration through an analytical closed form solution which includes the effects of the gravitational stress field.

A step by step sequence for the application of the method is presented. The method is validated by applying it to results of three-dimensional finite element analyses, model tests and to a large number of case histories. It is shown that the proposed procedure yields very sensible estimates of the tunnel performance whenever good ground control conditions exist.

ACKNOWLEDGEMENTS

Dr. Z. Eisenstein made this thesis possible and I am grateful for his support.

Financial assistance came from a variety of sources including the Natural Science and Engineering Research Council, the Fundacao de Amparo a Pesquisa do Estado de Sao Paulo (Brazil), the University of Alberta Dissertation Fellowship, the Department of Civil Engineering of the University of Alberta and also from the Fundacao Armando Alvares Penteado (Sao Paulo, Brazil).

During implementation of the 2D Finite Element program I was helped by Dr. L.V. Medeiros, Dr. D.W. Murray and Dr. D. Chan. Part of this work was done at the Pontificia Universidade Catolica do Rio de Janeiro where I was assisted by Jose Napoleao and Celso Romanel. Dr. Jose Brandt contributed tremendously in this phase, but certainly not only here!

The 'soft till' issue involved support from Drs. S.

Thomson, F. El-Nahhas and D.C.C. Sego. Gerry Cyre was
instrumental in the field and in the laboratory. But without
Ralph Wittebolle's cooperation, I wouldn't have achieved
anything.

Also, I would have been in trouble with the german literature and with the 3D analyses had Heinrich Heinz been elsewhere!

Dr. N.R. Morgenstern is to be credited for his suggestions and for having raised my interest on the drained

versus undrained issue in soft ground tunnels. I am thankful to Dr. B. Ladanyi for a discussion we had in Winnipeg from which emerged our interest on the 3D ground-lining response to tunnelling and to Dr. J.G. MacGregor for his comments on lining-ground interaction.

Paulo Branco is to be awarded for reading and commenting on the entire handwritten version of this work. Susan Evison bravely edited this tome of a thesis. By enduring my english she learned lots of portuguese!

After typing it Tanya Schulz promised she would never type another thesis in her life. No wonder! Thanks to Donna Salvian for the tables and to Denise Nickels for most of the figures.

Flavio M. Kuwajima cooperated in different ways which included loosing a squash game to me from time to time...

Many people contributed to this work and a complete list may ask for an additional volume. Some of them are those who replied to our questionnaire and are listed in Appendix B.

Once I was told by the late Arthur Casagrande that to do useful and serious research work, firstly, one would have to be sure what one is talking about. Secondly, one would have to conduct the work with integrity and ingenuity (he loved this word!). Thirdly, one would have to present it in its full transparency so it can be assessed and, more importantly, reproduced. I am grateful for his advice.

Table of Contents

Chapt	er			Page	
1.	INTE	RODUCTI	ON		
	1.1	Preamb	ole	1	
	1.2	Aims .			,
	1.3	Scope	and Thesi	is Organization10)
2.		ALIZED AIN CHA	BEHAVIOUF	R OF SHALLOW TUNNELS: STRESS AND	;
	2.1	Introd	duction		ì
	2.2	Shallo	w and Dee	ep Tunnels15	ì
	2.3	Soil F	Response t	to Tunnelling26	,
		2.3.1	Foreword	26	,
		2.3.2	Idealized	d Stress Changes27	,
		2.3.3	Idealized	d Strain Changes34	
		2.3.4	Stress and Idealized	nd Strain Changes Under Less d Conditions45	j
			2.3.4.1	Stress Paths45	i
			2.3.4.2	Ground Reaction Curves53	
			2.3.4.3	Shear Strain Development56	i
			2.3.4.4	Volume Changes	i
		2.3.5	Idealized	d Lining Action86	,
			2.3.5.1	Preamble86	,
			2.3.5.2	Good Lining Contact in an Ideally Deep Tunnel89	1
			2.3.5.3	Good Lining Contact in a Shallow Tunnel97	
			2.3.5.4	Poor Lining Contact106	
		2.3.6	Three Din	mensional Response122	
			2.3.6.1	Plane Strain Representation and Three Dimensional Response122	

			2.3.6.2	Three Dimensional Arching and Ground-Lining Response127
			2.3.6.3	Evidence of Three-dimensional Ground-Lining Response135
			2.3.6.4	Three-dimensional Ground-Lining Responses from Numerical Analyses148
	2.4	Summa	ry and Cor	nclusions163
3.	I DE AND	ALI ZED GROUNI	BEHAVIOUR	R OF SHALLOW TUNNELS: STABILITY
	3.1	Introd	duction	
	3.2	Tunnel	l Stabilit	ty
		3.2.1	Foreword	178
		3.2.2	Three-Dir	mensional Stability
		3.2.3	Two-Dimer	nsional Stability194
	3.3	The Ro	ole of Gro	oundwater210
		3.3.1	Foreword	210
		3.3.2	Generation	on of Porewater Pressure Changes .210
			3.3.2.1	Idealized Porewater Pressure Changes210
			3.3.2.2	The Effect of Gravity213
			3.3.2.3	Porewater Pressure Changes in Less Idealized Conditions214
		3.3.3		ion of Excess Pore Water s229
			3.3.3.1	Linear Elastic Consolidation229
			3.3.3.2	Non-Linear Consolidation234
			3.3.3.3	Additional Consequences of the Consolidation Process238
		3.3.4	Drained a	and Undrained Behaviour246
			3.3.4.1	Foreword246
			3.3.4.2	Steady State Seepage 247

			3.3.4.3	Total	and Ef	fective	e Stress	Paths	255
			3.3.4.4	Change	s in S	tabilit	y with	Time .	.258
			3.3.4.5	Draine Bounda	d and	Undrain	ned Resp	onse	.264
	3.4	Summar	y and Cor	nclusio	ns	• • • • • •			.275
4.	PRES	ENT ST	TATE OF TH	HE DESI	GN OF	SHALLOV	V TUNNEI	s	.285
	4.1	Introd	duction						.285
	4.2	Design	Require	ments .					.288
		4.2.1	Basic Red	quireme	nts fo	r Linir	ng Desig	jn	.289
		4.2.2	Basic Red Prediction	quireme on and	nts fo	r Displ	lacement		.301
		4.2.3	Basic Red Excavation	quireme on Stab	nts fo	r Veri	ication	of	.321
	4.3	Availa	ble Desig	gn Meth	ods				.329
		4.3.1	Foreword		• • • • •	• • • • • •	• • • • • •		.329
		4.3.2	Prediction	on of L	ining	Loads			.331
			4.3.2.1	Classi	ficati	on of N	Methods	• • • • •	.331
			4.3.2.2	Empiri Method	cal ar	nd Semi-	-Empirio	al	.333
			4.3.2.3	Ring a	nd Pla	te Mode	els		.344
			4.3.2.4	Ring a	nd Spr	ing Mod	dels		.361
			4.3.2.5	Numeri	cal Me	thods			.378
			4.3.2.6	Numeri	cally	Derived	Method	is	.379
			4.3.2.7	Effect	s in 7	wo-Dime	Dimensio ensional		.389
		4.3.3	Prediction	on of G	round	Displac	ements		.402
		4.3.4	Ground St	abilit	y Veri	fication	on		.416
	4.4	Survey	of the	Current	Desig	n Pract	cice		.426
	•	4 4 1	Foreword						426

		4.4.2	Predictio	on of	Lini	ng Loa	ads	• • • •	• • • •	• • • •		427
			4.4.2.1	Surve	ey of	Pract	tice		• • • •			427
			4.4.2.2	Resu.	lts o	f the	Sur	vey		• • •		434
			4.4.2.3	Fina	l Com	nents		• • • •				454
		4.4.3	Prediction	n of	Grou	nd Set	ttle	nent:	5			460
			4.4.3.1	Surve	ey of	Pract	tice					461
			4.4.3.2	Resu	lts o	f the	Sur	vey				466
			4.4.3.3	Final	l Com	ments		• • • •			• • •	480
	4.5	Summa	y and Cor	clus	ions	• • • • •	• • • •	• • • •	• • • •		• • •	483
5.	SHAI	LLOW TO	JNNEL MODE	ELLIN	G	• • • • •	• • • •	• • • •				508
	5.1	Intro	duction			• • • • •	• • • •	• • • •	• • • •			508
	5.2	Two-Di	imensional	Mode	ellin	g	• • • •	• • • •	• • • •		• • •	513
		5.2.1	Review of	Pre	vious	Stud	ies .	• • • •	• • • •		• • •	513
			5.2.1.1	Mode:	lling	Asped	cts	• • • •	• • • •		• • •	514
			5.2.1.2	Pred: Fini	iction	n of I	Perf	orman	nce h	эy	• • •	534
		5.2.2	Numerical	Sim	ulati	on App	plied	a	• • • •		• • •	552
			5.2.2.1	Gene: Solu	ral De	escri	otion	n of	the	• • •	• • •	552
			5.2.2.2	Disc	ussion	n on t	the S	Solut	ion	• • •	• • •	564
		5.2.3	Parametri	c St	udies		• • • •	• • • •	• • • •		• • •	576
		5.2.4	Analyses	of S	ome Ca	ase H	isto	ries	• • • •	• • •	• • •	577
			5.2.4.1	Open	ing R	emarks	5	• • • •	• • • •		• • •	577
			5.2.4.2	Alto	da B	oa Vis	sta :	Funne	el		• • •	581
			5.2.4.3	Edmon	nton :	Light nel .	Rail	l Tra	ansit	:	• • •	613
			5.2.4.4	Edmo	nton 1	Experi	iment	tal ?	Tunne	1.	• • •	653
,		5.2.5	Summary a	and Co	onclu	sions	• • • •	• • • •				717

	5.3	Three	-Dimension	al Mo	delli	ng .	• • • • •		• • • •	• • • •		725
		5.3.1	Introduct	ion .	• • • • •	• • • •				• • • •		725
		5.3.2	Available Tunnel Co	Solu nverg	tions ence	for	Esti	.mate	s of			730
		5.3.3	Review of the Finit	Thre e Ele	e-Dim ment	ensi Meth	onal	Mode	lling	by	7	737
		5.3.4	Numerical	. Solu	tion	Adop	ted .		• • • •			747
		5.3.5	Parametri	c Ana	lyses							753
			5.3.5.1	Analy	ses a	nd R	Result	s	• • • •		• •	753
			5.3.5.2	Inter	preta	tion	of t	he R	esult	s.	• • •	774
		5.3.6	Applicati	on of	the	Resu	ilts .		• • • •		8	304
			5.3.6.1	Tunne	l Clo	sure			• • • •		8	304
			5.3.6.2	Groun Tunne	d Mov 1 Fac	emen	ts Ah	ead	of th	ne	8	342
		5.3.7	Summary a	ind Co	nclus	ions					8	347
	5.4	Conclu	usion		• • • • •	• • • •			• • • •		8	350
6.	TWO	DIMENS	SIONAL MOD	ELLIN	G FOR	GEN	ERALI	ZATI	ис	• • •	8	360
	6.1	Introd	duction	• • • • •	• • • • •	• • • •	• • • • •		• • • •		8	360
	6.2	Modell Variab	ling Simploles	ifica	tions	and	Rang	jes o	f • • • • •		8	364
		6.2.1	Foreword			• • • •			• • • • •		8	364
		6.2.2	Cohesionl	.ess S	oil M	odel			• • • •		8	364
		6.2.3	Frictionl	.ess S	oil M	odel		• • • •	• • • • •	• • •	8	380
		6.2.4	Comments	on So	me Si	mpli	fying	Ass	umpti	ons	8	394
			6.2.4.1	The E	ffect	of	Janbu	ı's M	odulı	ıs K		394
			6.2.4.2	The E	ffect	of	Janbu	ı's E	xpone	ent	n 8	395
			6.2.4.3	The E Stren	ffect gth C	of ompo	the C	ohes	ive			911
			6.2.4.4	The E	ffect	of	Poiss	on's	Rati	. 0 .		323

		6.2.5	Analyses	931
	6.3	Parame	etric Analyses	939
		6.3.1	Details of the Analyses	939
			6.3.1.1 Number of Unloading Increments	s939
			6.3.1.2 Mesh Design and Influence of Lower Boundary	the 946
		6.3.2	Results of the Analyses	960
			6.3.2.1 Frictionless Soil Model Result	ts .962
			6.3.2.2 Cohesionless Soil Model Result	ts .975
			6.3.2.3 Relationships Between Surface and Crown Settlements	993
	6.4	Genera	alization of the Results	1013
		6.4.1	Opening Remarks	1013
		6.4.2	Frictionless Soil Model	1014
		6.4.3	Cohesionless Soil Model	1035
	6.5	Limits	s of the Generalized Solution	1078
		6.5.1	Extrapolation of the Numerical Results	1078
		6.5.2	Assessment of the Two-Dimensional Stability	1085
	6.6	Summa	ry and Conclusions	1102
7.	DEVE	ELOPME	NT AND VALIDATION OF A DESIGN PROCEDURE	1115
	7.1	Intro	duction	1115
	7.2	Soil-I	Lining Interaction	1117
		7.2.1	Choice of the Model: Hartmann Solution	1117
		7.2.2	Soil-Lining Interaction Analysis for Delayed Lining Installation in a Non-Linear Ground Mass	1131
		7.2.3	Influence of the Lining Presence on the Ground Settlements	1153

7.3	Guidel Proced	lines for dure	Using the Proposed Design
7.4	An Exa	ample of t	the Use of the Proposed Design
7.5	Valida	ation of t	the Proposed Method1196
	7.5.1	Verificat	ion Against a Tunnel Model Test 1196
		7.5.1.1	Model Test Procedures1196
		7.5.1.2	Soil Conditions in the Test1198
		7.5.1.3	Predicted and Measured Ground Responses1201
	7.5.2	Finite El	cion Against a Three-Dimensional ement Analysis of a Shallow
	7.5.3	Verificat Histories	ion Against Actual Case
		7.5.3.1	Foreword1212
		7.5.3.2	A Large Shielded Tunnel in Marl: The Frankfurt Baulos 23, Domplatz Tunnel1214
		7.5.3.3	Twin NATM Tunnels in Marl: The Frankfurt Baulos 25, Romerberg Tunnel
		7.5.3.4	A Small Shielded Tunnel in Till: The Mississauga (Ontario) Tunnel
		7.5.3.5	A Large NATM Tunnel in Granular Soil: The Butterberg Tunnel, in Osterode, near Hannover1246
		7.5.3.6	A Large Shield in Till: The Edmonton LRT Tunnel1257
		7.5.3.7	An NATM Tunnel in Marl: The Munich U - Bahn - Line 8/1, Baulos 18.21263
		7.5.3.8	An NATM Tunnel Built under Compressed Air: The Munich

	7.5.3.9 An NATM Tunnel Driven Through Heterogeneous Ground: The Bochum Baulos A2 Double Track Subway Tunnel1279
	7.5.3.10 An NATM Tunnel with Staged Installation of the Lining: The Sao Paulo North Extension Double Track Tunnel
	7.5.4 Analysis and Interpretation of the Results Obtained
7.6	6 Summary and Conclusions1310
8. CO	NCLUSIONS1324
REFERENC	CES1341
APPENDI	X A - RESULTS OF 3-D FINITE ELEMENT ANALYSES1406
APPENDIX	X B - LIST OF RESPONDENTS TO THE QUESTIONNAIRE1410
APPENDI	X C - NORMALIZED GROUND SETTLEMENTS
APPENDIX	X D - TWICE NORMALIZED GROUND REACTION CURVES1453

List of Tables

Table		Page
2.1	Assessments of the Effects of the Presence of the Ground Surface and of the Gravitational Stress Gradient in Shallow Tunnels	18
2.2	Shear Strain Distributions Observed in Model Tests and in Actual Tunnels in Drained Conditions	57
2.3	Plane Section Model Tests in Clay and Sand Under Drained Conditions	63
2.4	Plane Section Model Tests in Clay Under Undrained Conditions	68
3.1	Soil Properties in Johnston and Clough (1983) Analyses	219
4.1	Existing Criteria for Damage Assessment of Structures Subjected to Ground Movements	310
4.2	Damage Related to Building Distortion for Brick-Bearing Wall Structures Adjacent to Excavations (modified after Cording et.al., 1976:535)	315
4.3	Reported Ground Control Procedures in Soil Tunnelling	330
4.4	Ground Pressure Theories: A Partial Survey	338
4.5	Recommended Lining Distortion Ratios for Design Verification (after Schmidt, 1984: modified)	341
4.6	Some Review Works on Ring and Plate or Ring and Spring Models for Design of Linings Under Non-Uniform Stress Fields	350
4.7	Assumptions and Features of some Ring and Plate Solutions for Non-Uniform Stress Field	353
4.8	Assumptions and Features of some Ring and Spring Models	364
4.9	Details of Some Numerically Derived Methods for Lining Loads Prediction	382

Table		Page
4.10	Account for Three-Dimensional Effects in Two Dimensional Models	394
4.11	Features of some Methods for Ground Displacement Prediction for Shallow Tunnel Design	404
4.12	Features of some Methods for Ground Stability Verification	420
4.13	Envisaged Ground Conditions for Response of Questionnaire on Lining Design (modified after Duddeck, 1982:173)	430
4.14	ITA Questionnaire Response on Lining Design	433
4.15	Questionnaire on Ground Movements Caused by Shallow Tunnels	464
4.16	Questionnaire Response on Ground Movements	465
4.17	Type of Practice of Respondents	467
4.18	Preferred Approaches Indicated by Respondents for Ground Settlement Prediction	471
4.19	Noted Qualities for Different Settlement Prediction Procedures	476
5.1	Some Guidelines for Two-Dimensional Finite Element Mesh Design, Derived from Sensitivity Studies	516
5.2	Excavation Simulation Procedures for Tunnel Modelling with Finite Element Techniques	520
5.3	Numerical Procedures to Account Approximately for Three-Dimensional Effects of a Tunnel Advance in Two-Dimensional Finite Element Analyses	521
5.4	Classification of Prediction According to Lambe (1973)	.536
5.5	Review of Some Numerical Predictions of Shallow Tunnel Behaviour Using Two-Dimensional Finite Element Analyses	537

Table		Page
5.6	Overall Aspects of Reviewed Numerical Predictions of Shallow Tunnel Performance	543
5.7	Case Histories Selected for Analyses with the Adopted Numerical Solution	579
5.8	Typical Ranges of Properties of ABV Soils	585
5.9	Range of Geotechnical Parameters for the Variegated Soil at the ABV Site	586
5.10	Range of Geotechnical Parameters for the Red Porous Clay at the ABV Site	587
5.11	Parameters Varied in ABV Tunnel Back Analyses	596
5.12	Measured and Calculated Performance of ABV Tunnel	601
5.13	Range of Basic Soil Properties Found Along LRT Tunnel Alignment at Jasper Avenue	618
5.14	Range of Geotechnical Parameters for Edmonton Till at the South LRT Tunnel Line	619
5.15	Range of Geotechnical Parameters for Lake Edmonton Clay at the South LRT Tunnel Line	622
5.16	Range of Geotechnical Parameters for Saskatchewan Sands and Gravels at the South LRT Tunnel Line	623
5.17	Parameters Varied in the LRT Tunnel Back Analysis	635
5.18	Measured and Calculated Average Thrust Forces at Rib Joints in the LRT Tunnel	647
5.19	Measured and Calculated Performance of the LRT Tunnel	648
5.20	Results of Oedometer Consolidation Tests on Till for Edmonton Experimental Tunnel	661
5.21	Parameters of Fitted Hyperbolae for Softer Till	668

Table		Page
5.22	Parameters of Hyperbolae Fitted to Stress-Strain Curves of Till, Tested under Distinct Total Stress Paths and Drainage Conditions	681
5.23	Parameters Varied in the Edmonton Experimental Tunnel Back-Analyses	696
5.24	Measured and Calculated Average Thrust Forces at the Lower Lining Joint in the Edmonton Experimental Tunnel	709
5.25	Measured and Calculated Performance of Edmonton Experimental Tunnel	712
5.26	Results of the Numerical Simulations of the Final Tunnel Performance in Three Case Histories	722
5.27	Some Solutions for Tunnel Convergence Estimates under Time-Independent Conditions	732
5.28	Review of Some Three-Dimensional Finite Element Simulations of Tunnel Construction	740
5.29	Cases of Three-Dimensional Analyses	755
5.30	Coefficients of the Adopted U and K Relations for Sections at Different Distances Behind the Face	787
5.31	Predicted and Measured Displacements at the Face and at the Point of Support Activation in Shallow Tunnels for the Crown	809
5.32	Predicted and Measured Displacements at the Face and at the Point of Support Activation in Shallow Tunnels for the Springline	813
5.33	Predicted and Measured Displacements at the Face and at the Point of Support Activation in Shallow Tunnels for the Floor	815
5.34	Calculated and Observed Maximum Horizontal Movements of the Tunnel Face	845

Table		Page
5.35	Calculated and Observed Maximum Longitudinal Distortions at the Ground Surface, Ahead of the Tunnel Face	846
6.1	Input Parameters for Finite Element Analyses of Tunnels with the Same H/D and with a Homothetic Hyperbolic Stress-Strain Soil Model with c=0	870
6.2	Invariance of NGRC and Normalized Displacements to Changes in the Unit Weight of the Soil	879
6.3	Input Parameters for Finite Element Analyses of Tunnels with the Same H/D and with Homothetic Hyperbolic Stress-Strain Soil Model with $\phi=0$	882
6.4	Variation of the Maximum Normalized Surface Settlement with the Exponent n and with the Amount of Stress Release Allowed in the Opening	909
6.5	Ratio of Normalized Crown Displacements for n=0 to n>0, for Different Exponents n and Different Amount of Stress Release at the Opening	910
6.6	Variation of the Maximum Normalized Surface Settlement with the Cohesive Strength of the Soil and with the Amount of Stress Release Allowed	916
6.7	Variation of the Dimensionless Crown Displacement for the Different Strength Assumptions made and for the Different Amounts of Stress Release	924
6.8	Selected Variables for the Parametric Finite Element Analyses	940
6.9	Recorded Final Movements below Actual Tunnels and Tunnel Model Tests	957
6.10	Parameters used and Obtained in the Reduction of the Twice Normalized Ground Reaction Curves for the Frictionless Soil Model, for H/D=3	1016
6.11	Parameters used and Obtained in the Reduction of the Twice Normalized Ground Reaction Curves for the Frictionless Soil Model for H/D=1.5	1022

Table		Page
6.12	Parameters Used and Obtained in the Reduction of the Twice Normalized Ground Reaction Curves for the Frictionless Soil Model for H/D=6	1023
6.13	Parameters Obtained in the Reduction of the Twice Normalized Ground Reaction Curves for the Frictionless Soil Model	1024
6.14	Parameters Used and Obtained in the Reduction of the Twice Normalized Ground Reaction Curves of a Tunnel with $H/D=3$, for the Cohesionless Soil Model with $K_o=0.8$	1037
6.15	Parameters Used and Obtained in the Reduction of the Twice Normalized Ground Reaction Curves for the Frictionless Soil Model and for K _o =0.6	1045
6.16	Parameters Used and Obtained in the Reduction of the Twice Normalized Ground Reaction Curves for the Frictionless Soil Model and for K _o =0.8	1046
6.17	Parameters Used and Obtained in the Reduction of the Twice Normalized Ground Reaction Curves for the Frictionless Soil Model and for K _o =1.0	1047
7.1	Typical Relative Stiffness Ratios for Common Linings and Soils	1122
7.2	Calculation of the Reduced Unit Weight of the Soil for the Lining-Ground Interaction Analyses	1142
7.3	Calculation of the Reduced Average Ground Stiffness at Lining Installation	1146
7.4	Performance at the ABV Tunnel as Measured and as Calculated by the Proposed Procedure	1191
7.5	Measured and Calculated Ground Response in the Centrifuge Model Test 2DP by Mair (1979)	1204
7.6	Typical Properties of Frankfurt Clay used in the Analysis	1216

Table		Page
7.7	Selected Ground Parameters for Drained Analysis of Tunnel in Dense Sand-Clay Till	.1237
7.8	Selected Ground Parameters for Analysis of Tunnel in Well-Graded Sandy-Silty Gravel	.1249
7.9	Selected Parameters for Munich Marl	.1265
7.10	Measured and Calculated Performances at the Munich Line 5/9 Tunnel	.1278
7.11	Results of the Application of the Proposed Calculation Procedure to some Case Histories of Shallow Tunnels	.1297
7.12	Calculated and Measured Widths of the Final Surface Settlement Profiles in Some Case Histories	.1306

List of Figures

Figure		Page
2.1	Effect of Gravity on the Elastic Stress Paths in a Deep Tunnel	30
2.2	Stress Changes due to the Reduction of the In Situ Stress in a Deep Tunnel	33
2.3	Stress and Strain Changes Around a Tunnel	35
2.4	Stress Paths Around a Shallow Tunnel,	48
2.5	Ground Reaction Curves for a Shallow Tunnel	54
2.6	Relationship Between Crown Displacement and Factor of Safety in Drained Model Tests	64
2.7	Relationship Between Crown Displacement and Factor of Safety in Undrained Model Tests	69
2.8	Relationship Between Dimensionless Displacement of the Crown and Factor of Safety Observed in Drained and Undrained Model Tests	74
2.9	Distribution of Volumetric Strains around Shallow Tunnels	77
2.10	Schematic Representation of Specific Volume Changes with Varying Tunnel Depth	84
2.11	In Situ Stresses and Lining Loads on a Rigid Lining for Non-Slip Condition	91
2.12	Normal Stress on a Rigid Lining for Full Slip Condition	91
2.13	Equilibrium Points for Crown and Springline of a Deep Tunnel with Full Slip Interface Between Soil and Lining	96
2.14	In Situ Stresses Around a Shallow Circular Tunnel Profile Prior to Excavation	98
2.15	Stress Distributions Around a Rigid Lining in a "Shallow" Tunnel	100

Figure		Page
2.16	Points of Equilibrium of a Ground-Lining Interaction Analyses Using Finite Element Method	104
2.17	Reaction of the Support to External Gravity Loads	119
2.18	Incremental Displacement Field in the Longitudinal Vertical Plane, caused by an Incremental Advance of the Tunnel Face by Heading and Bench Excavation (after Heinz, 1984; modified)	125
2.19	Three-Dimensional Arching near the Face of an Advancing Tunnel (after Eisenstein et.al. 1984: modified)	129
2.20	Ground-Lining Response Concept for the Tunnel Crown (after Eisenstein et.al., 1984: modified)	133
2.21	Vertical Stress and Displacement Measurements at Crown Elevation for Tunnels in Frankfurt (modified after Sauer and Jonuscheit, 1976 and Stroh and Chambosse, 1973)	137
2.22	Radial Stress and Displacement at Springline Elevation for Tunnels in Frankfurt (Modified after Sauer and Jonuscheit, 1976 and Chambosse, 1972)	139
2.23	Measured Footing Pressures in the Upper Shotcrete Arch at the Munich Subway (Baulos 18.2)	143
2.24	Longitudinal Distribution of Thrust Forces at the Tunnel Crown (after Schikora, 1984: modified)	149
2.25	Radial Stresses and Displacements at the Crown Elevation (L/D=2/3)	152
2.26	Radial Stresses and Displacements at the Springline Elevation (L/D=2/3)	153
2.27	Radial Stresses and Displacements at the Floor Elevation (L/D=2/3)	154
2.28	Ground-Lining Response Curves at the Crown	159

Figure	Page
2.29	Ground-Lining Response Curves at the Springline
2.30	Ground-Lining Response Curves at the Floor
3.1	Three-Dimensional Collapse Mechanisms in Shallow Tunnels
3.2	Influence of Geometric Conditions on the Undrained Stability of Tunnel Headings in Overconsolidated Kaolin183
3.3	Undrained Stability of Fully Lined and Fully Unlined Model Test Tunnels in Overconsolidated Kaolin
3.4	Distributions of the Longitudinal Distortion Index Along A Stable and an Unstable Tunnel
3.5	Longitudinal Distortions above the Crown of a Model Tunnel Test (based on Casarin, 1977)
3.6	Stress Paths and Stress Ratio of a Soil Element at the Tunnel Crown
3.7	Local Collapse at the Roof of a Deep Tunnel in Dense Sand
3.8	Ground Reaction Curve and Stress Ratio Changes in an Element of Soil at the Crown of a Tunnel Approaching Collapse208
3.9	Short Term Pore Pressure Changes and Total Stress Distributions
3.10	Pore Water Pressure Changes in a Soil Element Adjacent to the Opening upon Decrease of Internal Tunnel Pressure220
3.11	Calculated Contours of Undrained Porewater Pressure Changes Around a Tunnel in Boston Blue Clay for two Overconsolidation Ratios (after Johnston, 1981:133,140 - modified)
3.12	Pore Pressure Coefficients for Elastic Consolidation of a Deep Circular Tunnel (modified from Carter and Booker, 1982)231

Figure		Page
3.13	Changes in Lining Bending Moments with Time during Elastic Consolidation (modified from Carter and Booker, 1984:603)	.233
3.14	Non-Linear Consolidation of a Thick Cylinder: Evolution of Radial Stress and Pore Pressures at the Rigid Lining-Soil Interface with Time (modified from Gunn and Taylor, 1985)	.236
3.15	Distributions of Surface and Subsurface Settlements before and after Consolidation (modified from Johnston, 1981:104)	.239
3.16	Schematic Flow Net in the Longitudinal Plane for a Partially Lined Shallow Tunnel during Construction	.249
3.17	Steady State Flow Nets Around Shallow Tunnels with Different Lining Permeabilities (from Fitzpatrick et.al., 1981:99 - modified)	.252
3.18	Schematic Distribution of Settlements in the Cover of a Shallow Tunnel due to Groundwater Drainage	.254
3.19	Idealized Total and Effective Stress Paths Around a Tunnel	.257
3.20	Idealized Changes in Shear Stress, Pore Pressure and Factor of Safety during and after Construction of a Plane Strain Shallow Tunnel in Saturated Clay	.261
3.21	Degree of Consolidation and Maximum Surface Settlement Evolution in a Shallow Tunnel (modified after Johnston, 1981:106)	.266
3.22	Tentative Boundaries for Undrained and Drained Responses Around a Deep, Impermeable Unlined Tunnel in an Elastic Soil	.270
3.23	Tentative Boundaries for Undrained and Drained Responses along line AB of the Cover of a Shallow and Permeable Tunnel, resulting solely from Ground Drainage	.273

Figure		Page
4.1	Displacements and Strains from Finite Element Simulation of a Shallow Tunnel	306
4.2	Classification of Some Typical Examples of Methods for Lining Load Prediction	332
4.3	Maximum Bending Moment Variation with Flexibility Ratio for a Deep Tunnel Liner from Different Ring and Plate Closed Form Solutions	359
4.4	Equivalence between Continuum and Spring Models for an Unlined Circular Opening under a Gravitational Stress Field	375
4.5	Maximum Bending Moment Variation with Flexibility Ratio for a Deep Tunnel Liner from Ring and Spring and Ring and Plate Solutions	377
4.6	Classification of Methods for Ground Settlement Prediction for Shallow Tunnels	407
4.7	Assumed Ratio Horizontal to Vertical In Situ Stresses used for Design of Shielded or Mined Tunnels in Soil	435
4.8	Ground Load Assumption Considered in the Responses for the Design of Shielded and Mined Tunnels	436
4.9	Criteria Indicated in the Responses for Ground Load Reduction both in Shielded and Mined Tunnels	440
4.10	Types of Statical Systems used for Assessment of Lining Loads in Shallow Tunnels	442
4.11	Statical Systems Applied in Shielded and Mined (NATM) Tunnels	443
4.12	Procedures for Evaluation of the Spring Constant to be used in Ring and Spring Models for Lining Design of Shielded or Mined Tunnels	445
4.13	Distribution of Respondents on the Statical System used for the Design of the Primary and Secondary Linings in Mined Tunnels	447

Figure		Page
4.14	Obligation to Account for the Non-Linear Behaviour of the Soil or the Support, in the Design of a Shallow Tunnel in Soil	449
4.15	Obligation to Account for Non-Linear Behaviour of the Soil or the Support in Shielded and Mined Tunnels	450
4.16	Consideration of Three-Dimensional Effects in the Lining Design of Shielded and Mined Tunnels	451
4.17	Factors of Safety used in the Design of Shallow Tunnels in Soil	453
4.18	Type of Practice of Respondents	468
4.19	Distribution of Respondents that Normally Perform Quantitative Prediction of Settlements Caused by Shallow Tunnelling	469
4.20	Distribution of most often used Methods for Settlement Prediction among Respondents	472
4.21	Basic Qualities of any Settlement Prediction	474
4.22	Noted Qualities of the "Empirical" and "Numerical" Approaches for Settlement Predictions Routinely Performed by Practitioners	477
4.23	Distribution of Respondents Affirming they Couple Settlement and Lining Load Prediction in their normal Design Practice	479
4.24	Distribution of Approaches Used for Coupling Ground Settlements and Lining Load Predictions	481
5.1	Examples of Stress-Strain Relations for Soil used in Shallow Tunnel Modelling	527
5.2	Triaxial Test Results on a Lightly OC Clay and Predictionsby the Hyperbolic and Jardine et.al. (1986) Models	533

Figure	Page
5.3	Stress-Strain Relations for OC London Clay under Unconsolidated Undrained Triaxial Test (after Jardine et.al., 1985:512, modified)
5.4	Types of Numerical Prediction of Shallow Tunnel Behaviour made by Two-Dimensional Finite Element Analysis545
5.5	Performance Aspects Compared in Numerical Predictions of Shallow Tunnel Behaviour by Two-Dimensional Finite Element Analyses
5.6	Comparison of Surface Settlements Calculated by Two-Dimensional Finite Element Analyses and Measured Values546
5.7	Comparison of Subsurface Settlements Calculated by Two-Dimensional Finite Element Analyses and Measured Values546
5.8	Comparison of Horizontal Displacements Calculated by Two-Dimensional Finite Element Analyses and Measured Values550
5.9	Comparison of Lining Loads Calculated by Two-Dimensional Finite Element Analyses and Measured Values550
5.10	Hyperbolic Model Representation558
5.11	Derivation of the Current Tangent Modulus
5.12	Details of the Finite Element Mesh562
5.13	Longitudinal Profile Along ABV Tunnel582
5.14	Profile of the In Situ Deformation Modulus at the ABV Site
5.15	Construction Details at the ABV Tunnel590
5.16	Assumptions and Fixed Parameters for ABV Tunnel Back Analyses
5.17	Measured and Calculated Surface Settlements at the Face of the ABV Tunnel

Figure		Page
5.18	Measured and Calculated Subsurface Vertical Displacements at the Face of the ABV Tunnel	599
5.19	Measured and Calculated Final Surface Settlements at the ABV Tunnel	602
5.20	Measured and Calculated Final Subsurface Vertical Displacements at the ABV Tunnel	603
5.21	Measured and Calculated Final Radial Stresses on ABV Tunnel Lining	604
5.22	Calculated Contours of Major and Minor Principal Strains Around the ABV Tunnel	609
5.23	Calculated Principal Strain Differences and Changes in Tangent Modulus Around the ABV Tunnel	610
5.24	Subsurface Profile of Southbound LRT Tunnel along Jasper Avenue (after Branco, 1981:modified)	615
5.25	Profile of In Situ Deformation Modulus at the LRT site	625
5.26	TBM and Lining System used at the Edmonton LRT Tunnel (after Branco, 1981:modified)	627
5.27	Assumptions and Fixed Parameters for the LRT Tunnel Back Analyses	630
5.28	Measured and Calculated Surface Settlements before Lining Activation at the LRT Tunnel	637
5.29	Measured and Calculated Final Surface Settlements at the LRT Tunnel	637
5.30	Measured and Calculated Vertical Displacements Along a Vertical Line 10 m off the Centreline of the LRT Tunnel	638
5.31	Measured and Calculated Vertical Displacements Along a Vertical Line 4 m off the Centreline of the LRT Tunnel	639
5.32	Measured and Calculated Lateral Movements in the Ground beside the LRT Tunnel before Lining Activation	642

Figure		Page
5.33	Measured and Calculated Final Lateral Movements in the Ground beside the LRT Tunnel	643
5.34	Measured and Calculated Thrust Forces at Rib Joints in the LRT Tunnel	645
5.35	Calculated Changes in Tangent Modulus around LRT Tunnel	652
5.36	Subsurface Profile of Edmonton Experimental Tunnel along 125 Avenue (Yellowhead Trail) (after El-Nahhas, 1980:modified)	654
5.37	Geotechnical Profile at the Instrumented Section 3 of Edmonton Experimental Tunnel	658
5.38	Grain Size Distributions	659
5.39	Location of Shelby Sampling and Types of Test in Edmonton Experimental Tunnel	662
5.40	Void Ratio - Effective Stress Curves from Oedometer Tests for Edmonton Experimental Tunnel Through Till	663
5.41	Drained Passive Compression Tests in Softer Till (24 - 25 m depth)	669
5.42	Consolidated Undrained Passive Compression Tests in Softer Till (11.5 m depth)	670
5.43	Consolidated Undrained Passive Compression Tests in Softer Till (21.0 m depth)	671
5.44	Consolidated Undrained Passive Compression Tests in Softer Till (28.5 m depth)	672
5.45	Variation of Initial Tangent Modulus with Confining Pressure for Till in Edmonton Experimental Tunnel	674
5.46	Effective Stress Strength Parameters for Till in Edmonton Experimental Tunnel	677
5.47	Total Stress Strength Parameters for Till in Edmonton Experimental Tunnel	677

Figure		Page
5.48	Profile of In Situ Deformation Modulus at the Edmonton Experimental Tunnel	678
5.49	Consolidated Undrained Compression Test in Softer Till with Constant Average Stress	682
5.50	Consolidated Undrained Active Compression Test in Softer Till	683
5.51	Stress-Strain Curves of Softer Till Tested under Distinct Total Stress Paths and Distinct Drainage Conditions	684
5.52	Tangent Moduli of Deformation of Till in Edmonton Experimental Tunnel for Distinct Total Stress Paths and Drainage Conditions	685
5.53	Stress Paths of Triaxial Tests on Till in Edmonton Experimental Tunnel	687
5.54	TBM and Lining System used at the Edmonton Experimental Tunnel (after El-Nahhas:1980:modified)	688
5.55	Assumptions and Fixed Parameters for the Edmonton Experimental Tunnel Back Analyses	691
5.56	Measured and Calculated Settlements after Complete Passage of the TBM at the Edmonton Experimental Tunnel	699
5.57	Measured and Calculated Subsurface Vertical Displacements along the Tunnel Centreline, after Complete Passage of the TBM at the Edmonton Experimental Tunnel	.702
5.58	Measured and Calculated Subsurface Vertical Displacements along a Vertical Line 2.5 m off the Centreline, after Complete Passage of the TBM at the Edmonton Experimental Tunnel	.703
5.59	Measured and Calculated Subsurface Settlements after Complete Passage of the TBM, at the Edmonton Experimental Tunnel	.704

Figure		Page
5.60	Measured and Calculated Lateral Movements in the Ground beside the Edmonton Experimental Tunnel before Lining Activation	706
5.61	Measured and Calculated Lateral Movements in the Ground beside the Edmonton Experimental Tunnel after Complete Passage of the TBM	707
5.62	Measured and Calculated Thrust Forces at Segment Joints in the Edmonton Experimental Tunnel	710
5.63	Calculated and Measured Zones with Maximum Shear Strain Greater than 1% in the Edmonton Experimental Tunnel	714
5.64	Calculated and Measured Zones with Maximum Shear Strain Greater than 2% in the Edmonton Experimental Tunnel	716
5.65	Conceptual Relations Between the Amount of Stress Release and Loss of Ground in a Two-Dimensional Representation	728
5.66	Radial Displacements of an Unlined Deep Tunnel in Elastic Ground (after Niwa et.al., 1979)	734
5.67	Three-Dimensional Finite Element Mesh and Input Parameters	749
5.68	Dimensionless Radial Displacements at the Crown of a Lined and Unlined Shallow Tunnel (H/D=1.6 and K=0.75)	756
5.69	Dimensionless Radial Displacements at the Springline of a Lined and Unlined Shallow Tunnel (H/D=1.6 and K=0.75)	757
5.70	Dimensionless Radial Displacements at the Floor of a Lined and Unlined Shallow Tunnel (H/D=1.6 and K=0.75)	758
5.71	Dimensionless Radial Displacements at the Crown of a Lined and Unlined Deeper Tunnel (H/D=2.8 and K=0.75)	760
5.72	Dimensionless Radial Displacements at the Springline of a Lined and Unlined Deeper Tunnel (H/D=2.8 and K=0.75)	761

Figure		Page
5.73	Dimensionless Radial Displacements at the Floor of a Lined and Unlined Deeper Tunnel (H/D=2.8 and K=0.75)	.762
5.74	Closure of an Unlined Tunnel in Elastic Ground Compared to that of Lined Tunnels in Elasto-Plastic Material	.765
5.75	Dimensionless Crown Displacements of the Shallower (H/D=1.6) Unlined Tunnel for Different In Situ Stress Ratios K	.767
5.76	Dimensionless Crown Displacements of the Deeper (H/D=2.8) Unlined Tunnel for Different Stress Ratios K	.768
5.77	Dimensionless Springline Displacements of the Shallower (H/D=1.6) Unlined Tunnel for Different Stress Ratios K	.770
5.78	Dimensionless Springline Displacements of the Deeper (H/D=2.8) Unlined Tunnel for Different Stress Ratios K	.771
5.79	Dimensionless Floor Displacements of the Shallower (H/D=1.6) Unlined Tunnel for Different Stress Ratios K	.772
5.80	Dimensionless Floor Displacements of the Deeper (H/D=2.8) Unlined Tunnel, for Different Stress Ratios K	.773
5.81	Comparison of Dimensionless Crown Displacements of the Shallower and Deeper Unlined Tunnels	.775
5.82	Comparison of Dimensionless Springline Displacements of the Shallower and Deeper Unlined Tunnels	.776
5.83	Comparison of Dimensionless Floor Displacements of the Shallower and Deeper Unlined Tunnels	.777
5.84	Ground Movements in the Vertical Longitudinal Plane of the Shallower (H/D=1.6) Unlined Tunnel	.778
5.85	Ground Movements in the Vertical Longitudinal Plane of the Deeper (H/D=2.8) Unlined Tunnel	.779

Figure		Page
5.86	U and K Relationships for the Section at the Face	.781
5.87	U and K Relationship for a Section D/4 Behind the Face	.782
5.88	U and K Relationship for a Section D/2 Behind the Face	.783
5.89	U and K Relationship for a Section 1.D Behind the Face	.784
5.90	U and K Relationship for a Section 2.D Behind the Face	.785
5.91	U and K Relationships for the Tunnel Crown	.789
5.92	U and K Relationships for the Tunnel Springline	.790
5.93	U and K Relationships for the Tunnel Floor	.791
5.94	Coefficients of the U and K Relationship for the Crown of an Unlined Shallow Tunnel (1.5 <h a="" as="" d<3.0)="" distance="" face<="" function="" of="" td="" the="" to=""><td>.792</td></h>	.792
5.95	Coefficients of the U and K Relationship for the Springline of an Unlined Shallow Tunnel (1.5 <h a="" as="" d<3.0)="" distance="" face<="" function="" of="" td="" the="" to=""><td>.793</td></h>	.793
5.96	Coefficients of the U and K Relationship for the Floor of an Unlined Shallow Tunnel (1.5 <h a="" as="" d<3.0)="" distance="" face<="" function="" of="" td="" the="" to=""><td>.794</td></h>	.794
5.97	Maximum Horizontal Displacement of the Tunnel Face Expressed in Dimensionless Form, as a Function of the Stress Ratio K	.795
5.98	Maximum Angular Distortion Along the Tunnel, at Crown Elevation	.799
5.99	Maximum Angular Distortion Along the Tunnel, at an Axis 0.3D Above Crown Elevation, as a Function of the Maximum Crown Distortion	.801

Figure	P	age
5.100	Maximum Angular Distortion of the Ground Surface Along the Tunnel Alignment as a Function of the Maximum Crown Distortion	803
5.101	Comparison Between Niwa et.al. (1979) and the Present (Averaged) Tunnel Closure Solution	807
5.102	Predicted and Measured Crown Displacements at the Face for Different Ground Types	823
5.103	Predicted and Measured Springline Displacements at the Face, for Different Ground Types	826
5.104	Predicted and Measured Crown Displacements at the Face for Different Tunnel Construction Methods	827
5.105	Predicted and Measured Springlne Displacements at the Face, for Different Tunnel Construction Methods	829
5.106	Predicted and Measured Crown Displacements at the Section the Support was Installed for Different Ground Types	831
5.107	Predicted and Measured Crown Displacements at the Section the Support was Installed for Different Tunnel Construction Methods	832
5.108	Dimensionless Crown Displacements Observed when the Support was Installed at Different Distances Behind the Tunnel Face	834
5.109	Predicted and Measured Springline Displacements at the Section the Support was Installed, for Different Ground Types	
5.110	Predicted and Measured Springline Displacements at the Section the Support was Installed for Different Tunnel Construction Methods	839
5.111	Distributions of Measured Crown Displacements after Support Installation	840

Figure	P	age
5.112	Distributions of Measured Crown Displacements at the Tunnel Face	843
5.113	Evaluation of the Ground Stress Release at the ABV Tunnel for a Two-Dimensional Numerical Simulation	853
5.114	Evaluation of the Ground Stress Release at the LRT Tunnel for a Two-Dimensional Numerical Simulation	856
5.115	Evaluation of the Ground Stress Release of the Edmonton Experimental Tunnel for a Two-Dimensional Simulation	858
6.1	Example of Homothetic Hyperbolae	866
6.2	Uniqueness of the Normalized Homothetic Hyperbolae for c=n=0	867
6.3	Ground Reaction Curves for the Crown of Geometrically Homothetic Tunnels in a Soil with a Homothetic Hyperbolic Stress-Strain Relationship (cohesionless model)	871
6.4	Ground Reaction Curves for the Springline of Geometrically Homothetic Tunnels in a Soil with a Homothetic Hyperbolic Stress-Strain Relationship (cohesionless model)	872
6.5	Ground Reaction Curves for the Floor of Geometrically Homothetic Tunnels in a Scil with a Homothetic Hyperbolic Stress-Strain Relationship (cohesionless model)	873
6.6	Normalized Ground Reaction Curves of Geometrically Homothetic Tunnels in a Soil with a Homothetic Hyperbolic Stress-Strain Relationship (cohesionless model)	874
6.7	Subsurface Settlements along the Cover of Geometrically Homothetic Tunnels in a Soil with a Homothetic Hyperbolic Stress-Strain Relationship (c=0), for Stress Release of 50%	875

Figure		Page
6.8	Surface Settlements over Geometrically Homothetic Tunnels in a Soil with a Homothetic Hyperbolic Stress-Strain Relationship (c=0), for Stress Release of 50%	.876
6.9	Ground Reaction Curve for the Crown of Geometric Homothetic Tunnels in a Soil with a Homothetic Hyperbolic Stress-Strain Relationship (frictionless model)	.884
6.10	Ground Reaction Curve for the Springline of Geometric Homothetic Tunnels in a Soil with a Homothetic Hyperbolic Stress-Strain Relationship (frictionless model)	.885
6.11	Ground Reaction Curve for the Floor of Geometric Homothetic Tunnels in a Soil with a Homothetic Hyperbolic Stress-Strain Relationship (frictionless model)	.886
6.12	Normalized Ground Reaction Curves of Geometrically Homothetic Tunnels in a Soil with a Homothetic Hyperbolic Stress-Strain Relationship (frictionless model)	.887
6.13	Subsurface Settlements along the Cover of Geometrically Homothetic Tunnels in a Soil with a Homothetic Hyperbolic Stress-Strain Relationship $(\phi=0)$, for a Stress Release of 50%	.888
6.14	Surface Settlements over Geometrically Homothetic Tunnels in a Soil with a Homothetic Hyperbolic Stress-Strain Relationship $(\phi=0)$, for a Stress Release of 50%	.890
6.15	Influence of Janbu's Modulus K on the Ground Reaction Curve of the Tunnel Crown	.896
6.16	Influence of Janbu's Modulus K on the Ground Reaction Curve of the Tunnel Springline	.897
6.17	Influence of Janbu's Modulus K on the Ground Reaction Curve of the Tunnel Floor	.898

Figure	Page
6.18	Variations with Depth of the In Situ Tangent Modulus for Three Values of Janbu's Exponent, n900
6.19	Normalized Ground Reaction Curves for the Tunnel Crown, Calculated for Different In Situ Tangent Modulus Profiles901
6.20	Normalized Ground Reaction Curves for the Tunnel Floor, Calculated for Different In Situ Tangent Modulus Profiles
6.21	Normalized Ground Reaction Curves for the Tunnel Springline, Calculated for Different In Situ Tangent Modulus Profiles
6.22	Ground Reaction Curves for the Crown and Floor, with the Displacements Normalized to the Soil In Situ Stiffnesses at Points Half a Diameter Above and Below the Tunnel Respectively905
6.23	Normalized Subsurface and Surface Settlements for 50% Ground Stress Release at the Opening, for Different Exponent n Values
6.24	Normalized Ground Reaction Curves for the Crown, Calculated for Different Cohesive Strengths of the Soil913
6.25	Normalized Ground Reaction Curves for the Springline, Calculated for Different Cohesive Strengths of the Soil
6.26	Normalized Ground Reaction Curves for the Floor, Calculated for Different Cohesive Strengths of the Soil917
6.27	Normalized Subsurface and Surface Settlements for 50% Ground Stress Release, Calculated for Different Cohesive Strengths of the Soil918
6.28	Normalized Ground Reaction Curves for the Crown, Calculated for Different Soil Strengths921

Figure		Page
6.29	Normalized Ground Reaction Curves for the Springline, Calculated for Different Soil Strengths	922
6.30	Normalized Ground Reaction Curves for the Crown, Calculated for Different Poisson's Ratios	926
6.31	Normalized Ground Reaction Curves for the Springline, Calculated for Different Poisson's Ratios	928
6.32	Normalized Ground Reaction Curves for the Floor, Calculated for Different Poisson's Ratios	929
6.33	Normalized Subsurface and Surface Settlements for 50% Ground Stress Release, Calculated for Different Poisson's Ratios	930
6.34	Distributions of Sizes and Depths of Tunnels Reviewed	
6.35	Distributions of Geotechnical Properties of the Grounds Through Which the Tunnels Reviewed were Driven	935
6.36	Distribution of the In Situ Stress Ratios in the Case Histories Reviewed	937
6.37	Distribution of Construction Methods and Distance of Support Activation in the Tunnels Surveyed	938
6.38	Normalized Ground Reaction Curve for the Springline Calculated for Different Numbers of Unloading Increments	942
6.39	Difference in the Calculated Dimensionless Displacement U for Ten and Twenty Unloading Increments	943
6.40	Differences in the Normalized Ground Settlements for Stress Release of 50%, Calculated for Ten and Twenty Unloading Increments	944
6.41	Normalized Ground Reaction Curves for the Crown, Calculated for Different Positions of the Lower Rigid Boundary	948

Figure		Page
6.42	Normalized Ground Reaction Curves for Springline, Calculated for Different Positions of the Lower Rigid Boundary	.950
6.43	Normalized Ground Reaction Curves for Floor, Calculated for Different Positions of the Lower Rigid Boundary	.951
6.44	Distribution of Subsurface Normalized Settlements for 50% Ground Stress Release, Calculated for Different Positions of the Lower Rigid Boundary	.952
6.45	Subsurface Settlement Distribution for 50% Ground Stress Release, Calculated for Different Positions of the Lower Rigid Boundary	.954
6.46	Transverse Profiles of Normalized Ground Surface Settlements for 50% Stress Release, Calculated for Different Positions of the Lower Rigid Boundary	.955
6.47	Normalized Ground Reaction Curves for H/D=3 and an Undrained Strength Ratio of 1.25	.964
6.48	Normalized Subsurface Settlements along Tunnel Axis for H/D=3 and an Undrained Strength Ratio of 1.25, Calculated for Increasing Amount of Stress Release	.965
6.49	Normalized Surface Settlements for H/D=3 and Undrained Strength Ratio of 1.25, Calculated for Increasing Amount of Stress Release	.966
6.50	Normalized Ground Reaction Curves at the Crown for an Undrained Strength Ratio of 1.25 and Different Tunnel Depths	.967
6.51	Normalized Ground Reaction Curves at the Springline for and Undrained Strength Ratio of 1.25 and Different Tunnel Depths	.968
6.52	Normalized Ground Reaction Curves at the Floor for an Undrained Strength Ratio of 1.25 and Different Tunnel Depths	.969

Figure		Page
6.53	Normalized Subsurface and Surface Settlement for an Undrained Strength Ratio of 1.25 and 50% Ground Stress Release, Calculated for Different Tunnel Depths	.971
6.54	Normalized Ground Reaction Curves of the Crown for H/D=3 and Different Undrained Strength Ratios	.972
6.55	Normalized Ground Reaction Curves of the Springline for H/D=3 and Different Undrained Strength Ratios	.973
6.56	Normalized Ground Reaction Curves of the Floor for H/D=3 and Different Undrained Strength Ratios	.974
6.57	Normalized Subsurface and Surface Settlements for H/D=3 and 50% Ground Stress Release, Calculated for Different Undrained Strength Ratios	.976
6.58	Normalized Ground Reaction Curves for $H/D=3$, $K_o=0.8$ and $\phi=30^{\circ}$.978
6.59	Normalized Subsurface Settlements for $H/D=3$, $K_o=0.8$ and $\phi=30^\circ$, Calculated for Increasing Amount of Stress Release	.979
6.60	Normalized Surface Settlements for $H/D=3$, $K_o=0.8$ and $\phi=30^\circ$, Calculated for Increasing Amount of Stress Release	.980
6.61	Normalized Ground Reaction Curves for Different Tunnel Depths, Calculated for $\phi=30^\circ$ and $K_o=0.8$.982
6.62	Normalized Subsurface and Surface Settlements for Different Tunnel Depths, Calculated for $\phi=30^\circ$, $K_o=0.8$ and 50% Stress Release	.983
6.63	Normalized Ground Reaction Curves of the Crown for H/D=3 and K _o =0.8, Calculated for Different Friction Angles	.985
6.64	Normalized Ground Reaction Curves of the Springline for H/D=3 and K _Q =0.8, Calculated for Different Friction Angles	.986

Figure		Page
6.65	Normalized Ground Reaction Curves of the Floor for H/D=3 and K _o =0.8, Calculated for Different Friction Angles	987
6.66	Normalized Subsurface and Surface Settlements for H/D=3, K _o =0.8 and 40% Ground Stress Release, Calculated for Different Friction Angles	988
6.67	Normalized Ground Reaction Curves of the Crown, for $H/D=3$ and $\phi=30^{\circ}$, Calculated for Different In Situ Stress Ratios	990
6.68	Normalized Ground Reaction Curves of the Springline, for $H/D=3$ and $\phi=30^{\circ}$, Calculated for Different In Situ Stress Ratios	991
6.69	Normalized Ground Reaction Curves of the Floor, for H/D=3 and ϕ =30°, Calculated for Different In Situ Stress Ratios	992
6.70	Normalized Subsurface and Surface Settlements for $H/D=3$, $\phi=30^{\circ}$ and 50% Ground Stress Release, Calculated for Different In Situ Stress Ratios	994
6.71	Variation of the Maximum Normalized Surface Settlement with the Amount of Stress Release and other Variables, for the Frictionless Soil Model	997
6.72	Variation of the Maximum Normalized Surface Settlement with the Amount of Stress Release and other Variables, for the Cohesionless Soil Model	999
6.73	Relationships between Normalized Maximum Surface Settlement and Relative Depth of Tunnel, Calculated for the Frictionless Soil Model, for 30% Stress Release	1002
6.74	Relationships between Normalized Maximum Surface Settlement and Relative Tunnel Depth, Calculated for the Frictionless Soil Model, for 50% Stress Release	1003

Figure		Page
6.75	Normalized Settlement Ratios for ϕ =40° and 30% Stress Release	.1004
6.76	Normalized Settlement Ratios for ϕ =40° and 50% Stress Release	.1005
6.77	Normalized Settlement Ratios for ϕ =30° and 30% Stress Release	.1006
6.78	Normalized Settlement Ratios for ϕ =30° and 50% Stress Release	.1007
6.79	Normalized Settlement Ratios for ϕ =20° and 30% Stress Release	. 1008
6.80	Normalized Settlement Ratios for ϕ =20° and 50% Stress Release	.1009
6.81	Normalized Settlement Ratios Observed in some Case Histories	. 1011
6.82	Twice Normalized Ground Reaction Curve (NNGRC) for the Crown of a Tunnel with H/D=3, for the Frictionless Soil Model	.1017
6.83	Twice Normalized Ground Reaction Curves (NNGRC) for the Springline of a Tunnel with H/D=3, for the Frictionless Soil Model	.1019
6.84	Twice Normalized Ground Reaction Curves (NNGRC) for the Floor of a Tunnel with H/D=3, for the Frictionless Soil Model	.1020
6.85	Variation of the Coefficient A with Relative Tunnel Depth, for the Frictionless Soil Model	.1025
6.86	Variation of the Coefficient B, for the Tunnel Crown, with Strength and Depth Ratios, Calculated for the Frictionless Soil Model	.1026
6.87	Variation of the Coefficient B for the Tunnel Springline, with Strength and Depth Ratios, Calculated for the Frictionless Soil Model	.1027
6.88	Variation of the Coefficient B for the Tunnel Floor, with Strength and Depth Ratios, Calculated for the Frictionless Soil Model	. 1028

Figure		Page
6.89	Twice Normalized Ground Reaction Curve (NNGRC) for the Crown of a Tunnel with $H/D=3$, for the Cohesionless Soil Model with $K_o=0.8$	1038
6.90	Twice Normalized Ground Reaction Curves (NNGRC) for the Springline of a Tunnel with $H/D=3$, for the Cohesionless Soil Model with $K_o=0.8$	1040
6.91	Twice Normalized Ground Reaction Curves (NNGRC) for the Floor of a Tunnel with $H/D=3$, for the Cohesionless Soil Model with $K_o=0.8$	1041
6.92	Slope of the Arbitrary Axes used to Obtain the NNGRC, Represented as a Function of H/D, for K _o =0.6	1051
6.93	Relationships between a_{ref} and the Friction Angle for $K_0 = 0.6$	1052
6.94	Twice Normalized Ground Reaction Curves for Tunnel Crown Calculated for $K_o=0.6$	1053
6.95	Twice Normalized Ground Reaction Curves for the Tunnel Springline, Calculated for $K_o = 0.6$	1054
6.96	Twice Normalized Ground Reaction Curves for the Tunnel Floor, Calculated for $K_o = 0.6$	1055
6.97	Variations of λ' for the Tunnel Crown, Calculated for $K_o \! = \! 0.6$	
6.98	Variations of λ' for the Tunnel Springline, Calculated for $K_o = 0.6$	1057
6.99	Variations of λ' for the Tunnel Floor, Calculated for $K_o = 0.6$	1058
6.100	Slopes of the Arbitrary Axes used to Obtain the NNGRC Represented as a Function of H/D, for K _o =0.8	1061
6.101	Relationships between a_{ref} and the Friction Angle of $K_o=0.8$	1062
6.102	NNGRCs for Tunnel Crown, Calculated for $K_o=0.8$	1063

Figure	Pa	ge
6.103	NNGRCs for Tunnel Springline, Calculated for $K_0 = 0.8$	64
6.104	NNGRCs for Tunnel Floor, Calculated for $K_o=0.8$	65
6.105	Variations of λ' for the Tunnel Crown, Calculated for $K_o=0.8$	66
6.106	Variations of λ' for the Tunnel Springline, Calculated for $K_o = 0.8$	67
6.107	Variations of λ' for the Tunnel Floor, Calculated for $K_o = 0.8$	68
6.108	Slopes of the Arbitrary Axes used to Obtain the NNGRC Presented as a Function of H/D, for K _o =1.010	69
6.109	Relationships between a_{ref} and the Friction Angle for $K_o=1.0$	70
6.110	NNGRCs for Tunnel Crown, Calculated for $K_o = 1.0$	71
6.111	NNGRCs for Tunnel Springline, Calculated for $K_0=1.0$	72
6.112	NNGRCs for Tunnel Floor, Calculated for $K_o=1.0$	73
6.113	Variations of λ' for the Tunnel Crown, Calculated for $K_o = 1.0$	74
6.114	Variations of λ' for the Tunnel Springline, Calculated for $K_o = 1.0$	75
6.115	Variations of λ' for the Tunnel Floor, Calculated for $K_o=1.0$	76
6.116	Variations of the Initial Slope of the Twice Normalized Ground Reaction Curves with K _o and H/D10	77
6.117	Extension of the NGRCs for H/D=3, $K_0=0.8$ and $\phi=30^{\circ}$	
6.118	Extension of the NGRCs for H/D=3 and $c_{\rm u}/\gamma$ D=1.25	84

Figure		Page
6.119	Reference Values used for Normalizing the NGRC of the Tunnel Crown for the Frictionless Soil Model and Components to Define the Limiting U of the Fitted Function	1086
6.120	Reference Values used for Normalizing the NGRC of the Tunnel Springline for the Frictionless Soil Model and Components to Define the Limiting U of the Fitted Function	1087
6.121	Reference Values used for Normalizing the NGRC of the Tunnel Floor for the Frictionless Soil Model and Components to Define the Limiting U of the Fitted Function	1088
6.122	Lower Bound Solution for Tunnel Collapse Pressure in a Frictionless Soil	1095
6.123	Lower and Upper Bound Solutions for Tunnel Collapse Pressure in a Frictional and Cohesive Soil $(\phi=10^\circ)$	1097
6.124	Lower and Upper Bound Solutions for Tunnel Collapse Pressure in a Frictional and Cohesive Soil $(\phi=20^{\circ})$	1098
6.125	Lower and Upper Bound Solutions for Tunnel Collapse Pressure in a Frictional and Cohesive Soil $(\phi=30^\circ)$	1099
6.126	Lower and Upper Bound Solutions for Tunnel Collapse Pressure in a Frictional and Cohesive Soil $(\phi=40^\circ)$	1100
7.1	Notations and Conventions used in Hartmann's Solution	1124
7.2	Lining Stresses, Displacements and Internal Forces Given by Hartmann's Solution	1125
7.3	Comparison of Lining Responses Calculated for Different Tunnel Depths, with and without Account of the Influence of the Ground Surface	1129
7.4	Equilibrium Points of the Soil-Lining Interaction at Tunnel Crown	1137

Figure		Page
7.5	Equilibrium Points of the Soil-Lining Interaction at Tunnel Springline	1138
7.6	Equilibrium Points of the Soil-Lining Interaction at Tunnel Floor	1139
7.7	Distribution of Final Settlements Calculated for a Tunnel Lined after 40% Stress Release, Compared to the Distributions for an Unlined Tunnel Equal Crown Displacement	1155
7.8	Distribution of Final Settlements Calculated for a Tunnel Lined after 80% Stress Release, Compared to the Distributions for an Unlined Tunnel with Equal Crown Displacements	1156
7.9	Suggested Sequence of Steps for Application of the Proposed Procedure for Shallow Tunnel Design	1161
7.10	Calculation Sheet with Geometric Ground Properties Data and Tunnel Closure at Lining Activation	1169
7.11	Calculation Sheet for Estimates of the Stress Release and Ground Stiffness at the Section the Lining is Activated	1170
7.12	Calculation Sheet for 2D Stability Verification and Lining-Ground Interaction Analysis	1171
7.13	Calculation Sheet for Iterative Analysis of the Lining-Ground Interaction	1172
7.14	Calculation Sheet for Subsurface and Surface Settlements	1173
7.15	ABV Tunnel - Input Data and Tunnel Closure at Lining Activation	1176
7.16	ABV Tunnel - Stress Release and Ground Stiffness at Lining Activation	1179
7.17	ABV Tunnel - Two Dimensional Stability Calculation and Lining-Ground Interaction	1182
7.18	ABV Tunnel - Iterative Calculation for the Lining-Ground Interaction	1185

Figure	Pa	ge
7.19	ABV Tunnel: Subsurface and Surface Settlement Calculations	87
7.20	Calculated and Measured Final Subsurface Settlements at the ABV Tunnel	92
7.21	Calculated and Measured Final Surface Settlements at the ABV Tunnel11	93
7.22	Calculated and Measured Radial Stresses on the ABV Tunnel Lining11	94
7.23	Measured and Calculated Ground Response at Tunnel Crown for the Centrifuge Model Test	05
7.24	Measured and Calculated Surface Settlement Profiles for the Centrifuge Model Test at Two Internal Pressures	08
7.25	Subsurface Settlement Distributions Calculated in a Three-Dimensional Analysis and by the Proposed Method12	11
7.26	Profile of Surface Settlements Calculated in a Three-Dimensional Analysis and by the Proposed Method12	13
7.27	Measured and Calculated Final Subsurface Settlements over the South Tunnel in the Frankfurt Baulos 23 (Domplatz) Subway	20
7.28	Measured and Calculated Final Surface Settlements over the South Tunnel in the Frankfurt Baulos 23 (Domplatz) Subway	21
7.29	Predicted Lining Loads in the South Tunnel (1st driven) Compared to Measurements in the North Tunnel (2nd driven): Frankfurt Baulos 23 (Domplatz) Subway Tunnels	22
7.30	Measured and Calculated Subsurface Settlements over the Frankfurt Baulos 25 (Romerberg) Subway12	28
7.31	Measured and Calculated Final Surface Settlements at the Frankfurt Baulos 25 (Romerberg) Subway Tunnel12	29

Figure		Page
7.32	Measured and Calculated Final Surface Settlements over Twin Tunnels at the Frankfurt Baulos 25 (Romerberg) Subway	1231
7.33	Predicted Lining Radial Stresses for Single Tunnel and Measured Stresses in Twin Tunnels at the Frankfurt Baulos 25 (Romerberg) Subway	1232
7.34	Measured and Calculated Final Subsurface Settlements over the Mississauga Sewer Tunnel	1242
7.35	Measured and Calculated Final Surface Settlements over the Mississauga Sewer Tunnel	1243
7.36	Measured and Predicted Radial Stress Distributions on the Lining of the Mississauga Sewer Tunnel	1245
7.37	Measured and Calculated Final Subsurface Settlements over the Butterberg Tunnel	1253
7.38	Measured and Calculated Final Surface Settlements over the Butterberg Tunnel	1254
7.39	Measured and Predicted Radial Stress Distributions on the Shotcrete Lining of the Butterberg Tunnel	1256
7.40	Measured and Calculated Final Surface Settlements over the Edmonton LRT Tunnel	1261
7.41	Measured and Calculated Thrust Forces on the Edmonton LRT Primary Lining	1262
7.42	Measured and Calculated Final Subsurface Settlements over the Munich Line 8/1 Tunnel	1268
7.43	Calculated and Measured Radial Stress Distributions on the Shotcrete Lining of the Munich Line 8/1 Tunnel	1270
7.44	Measured and Calculated Surface Settlements over the Munich Line 5/9 Tunnel	1275

Figure		Page
7.45	Measured and Calculated Final Subsurface Settlements over the Bochum Baulos A2 Tunnel	. 1283
7.46	Measured and Calculated Final Surface Settlement Profiles over the Bochum Baulos A2 Tunnel	. 1284
7.47	Calculated and Measured Radial Stress Distributions on the Shotcrete Lining of the Bochum Baulos A2 Tunnel	1285
7.48	Measured and Calculated Final Subsurface Settlements over the Sao Paulo North Extension Tunnel	1290
7.49	Measured and Calculated Final Surface Settlement Profiles over the Sao Paulo North Extension Tunnel	1291
7.50	Calculated Maximum Surface Distortions Compared to the Observed Maxima	1301
7.51	Calculated Tunnelling Performance Compared to Field Observations	1304
A.1	Radial Stresses and Displacements at the Crown Elevation (L/D=1/2)	1407
A.2	Radial Stresses and Displacements at the Springline Elevation (L/D=1/2)	1408
A.3	Radial Stresses and Displacements at the Floor Elevation $(L/D=1/2)$	1409
C.1	Normalized Settlements: $K_o=1$, $c_u/\gamma D=2.5$, $H/D=1.5$	1416
C.2	Normalized Settlements: $K_o=1$, $c_u/\gamma D=1.25$, $H/D=1.5$	1417
C.3	Normalized Settlements: $K_o=1$, $c_u/\gamma D=0.625$, $H/D=1.5$	1418
C.4	Normalized Settlements: $K_o=1$, $c_u/\gamma D=0.3125$, $H/D=1.5$	1419
C.5	Normalized Settlements: $K_o=1$, $\phi=20^{\circ}$, $H/D=1.5$	1420
C.6	Normalized Settlements: $K_o=1$, $\phi=30^{\circ}$, $H/D=1.5$	1421

Figure		Page
C.7	Normalized Settlements: $K_o=1$, $\phi=40^{\circ}$, $H/D=1.5$	1422
C.8	Normalized Settlements: $K_o=0.8$, $\phi=20^{\circ}$, $H/D=1.5$	1423
C.9	Normalized Settlements: $K_o=0.8$, $\phi=30^{\circ}$, $H/D=1.5$	1424
C.10	Normalized Settlements: $K_o=0.8$, $\phi=40^{\circ}$, $H/D=1.5$	1425
C.11	Normalized Settlements: $K_o=0.6$, $\phi=20^{\circ}$, $H/D=1.5$	1426
C.12	Normalized Settlements: $K_0=0.6$, $\phi=30^{\circ}$, $H/D=1.5$	1427
C.13	Normalized Settlements: $K_0=0.6$, $\phi=40^{\circ}$, $H/D=1.5$	1428
C.14	Normalized Settlements: $K_o=1$, $c_u/\gamma D=2.5$, $H/D=3$	1429
C.15	Normalized Settlements: $K_o=1$, $c_u/\gamma D=1.25$, $H/D=3$	1430
C.16	Normalized Settlements: $K_o=1$, $c_u/\gamma D=0.625$, $H/D=3$	1431
C.17	Normalized Settlements: $K_o=1$, $\phi=20^{\circ}$, $H/D=3$	1432
C.18	Normalized Settlements: $K_o=1$, $\phi=30^{\circ}$, $H/D=3$	1433
C.19	Normalized Settlements: $K_o=1$, $\phi=40^{\circ}$, $H/D=3$	1434
C.20	Normalized Settlements: $K_0=0.8$, $\phi=20^{\circ}$, $H/D=3$	1435
C.21	Normalized Settlements: $K_0=0.8$, $\phi=30^{\circ}$, $H/D=3$	1436
C.22	Normalized Settlements: $K_o=0.8$, $\phi=40^{\circ}$, $H/D=3$	1437
C.23	Normalized Settlements: $K_o=0.6$, $\phi=20^{\circ}$, $H/D=3$	1438
C.24	Normalized Settlements: $K_0=0.6$, $\phi=30^{\circ}$, $H/D=3$	1439

Figure		Page
C.25	Normalized Settlements: $K_o=0.6$, $\phi=40^{\circ}$, $H/D=3$	
C.26	Normalized Settlements: $K_o=1$, $c_u/\gamma D=2.5$, $H/D=6$. 1441
C.27	Normalized Settlements: $K_o=1$, $c_u/\gamma D=1.25$, $H/D=6$	
C.28	Normalized Settlements: $K_o=1$, $c_u/\gamma D=0.625$, $H/D=6$. 1443
C.29	Normalized Settlements: $K_o=1$, $\phi=20^{\circ}$, $H/D=6$. 1444
C.30	Normalized Settlements: $K_o=1$, $\phi=30^{\circ}$, $H/D=6$.1445
C.31	Normalized Settlements: $K_o=1$, $\phi=40^{\circ}$, $H/D=6$.1446
C.32	Normalized Settlements: $K_o=0.8$, $\phi=20^{\circ}$, $H/D=6$.1447
C.33	Normalized Settlements: $K_o=0.8$, $\phi=30^\circ$, $H/D=6$.1448
C.34	Normalized Settlements: $K_o=0.8$, $\phi=40^{\circ}$, $H/D=6$. 1449
C.35	Normalized Settlements: $K_o=0.6$, $\phi=20^{\circ}$, $H/D=6$	
C.36	Normalized Settlements: $K_o=0.6$, $\phi=30^{\circ}$, $H/D=6$	
C.37	Normalized Settlements: $K_o=0.6$, $\phi=40^{\circ}$, $H/D=6$.1452
D:1	NNGRC for Crown, $K_o = 0.6$, $H/D = 6$. 1454
D.2	NNGRC for Crown, $K_o = 0.6$, $H/D=3$. 1455
D.3	NNGRC for Crown, $K_o = 0.6$, $H/D = 1.5$. 1456
D.4 ^	NNGRC for Springline, $K_o = 0.6$, $H/D = 6$. 1457
D.5	NNGRC for Springline, $K_o = 0.6$, $H/D=3$. 1458
D.6	NNGRC for Springline, $K_0 = 0.6$, $H/D=1.5$. 1459
D.7	NNGRC for Floor, K _o = 0.6, H/D=6	. 1460

Figure						Page
D.8	NNGRC	for	Floor, K	(_o =	0.6,	H/D=31461
D.9	NNGRC	for	Floor, K	°=	0.6,	H/D=1.51462
D.10	NNGRC	for	Crown, K	(_o =	0.8,	H/D=61463
D.11	NNGRC	for	Crown, K	(_o =	0.8,	H/D=31464
D.12	NNGRC	for	Crown, K	(_o =	0.8,	H/D=1.51465
D.13	NNGRC	for	Springli	ne,	, K _o =	0.8, H/D=61466
D.14	NNGRC	for	Springli	ne,	, K _o =	0.8, H/D=31467
D.15	NNGRC	for	Springli	ne,	, K _o =	0.8, H/D=1.51468
D.16	NNGRC	for	Floor, K	(_o =	0.8,	H/D=61469
D.17	NNGRC	for	Floor, K	°=	0.8,	H/D=31470
D.18	NNGRC	for	Floor, K	·=	0.8,	H/D=1.51471
D.19	NNGRC	for	Crown, K	·=	1.0,	H/D=61472
D.20	NNGRC	for	Crown, K	(_o =	1.0,	H/D=31473
D.21	NNGRC	for	Crown, K	°=	1.0,	H/D=1.51474
D.22	NNGRC	for	Springli	ne,	, K _o =	1.0, H/D=61475
D.23	NNGRC	for	Springli	ne,	, K _o =	1.0, H/D=31476
D.24	NNGRC	for	Springli	ne,	, K _o =	1.0, H/D=1.51477
D.25	NNGRC	for	Floor, K	(_o =	1.0,	H/D=61478
D.26	NNGRC	for	Floor, K	(_o =	1.0,	H/D=31479
D.27	NNGRC	for	Floor, K	(=	1.0,	H/D=1.51480

least on a section.	DEBMN .	
tog Plogif R + 0.6.		. 5:630
tor Crown, R C TN B		
for Growin' Mis 3.8 m.		
er Apringline, K. '8, L. cm		
for Springline, 7 -		
for Floor, K. e 3.3.		
101 Fig. 1.83.73°C23		
for crown, N O Bross		
ten "1 ukc13 101		
20 (Speing: 10, 12, 1		
tor gaptarling, a s.v.		
(01 විද්යිලව, විය 1.3, සි.ක		
conserve to take the total good too		
Control of the transfer of the		
where in and the second		

1. INTRODUCTION

1.1 Preamble

The intense urban development observed worldwide in this century has enhanced the requirements for land use and has increased the general concern regarding its impact on the environment. Such factors as increased land costs and community opposition to disruption caused by new public works have forced underground alternative schemes to be contemplated and implemented. Tunnelling schemes, otherwise not considered for economic or purely technical reasons, are being increasingly favoured as solutions to a variety of urban problems. These encompass mass transport, sewerage, drainage, water and energy supply, etc. Also, recent developments in construction technology yield reductions in the costs of tunnelling operations hence construction in difficult ground conditions has become a viable proposition.

Public utilities are usually installed underground at relatively shallow depths, where, more frequently than not, "soft" ground is found. "Soft" ground is defined in this thesis to be: any incompetent, soil-like material, where a tunnelling excavation driven through it, will require some form of virtually continuous support to maintain the stability of the excavation. The underground excavation alternative minimizes social, environmental and economical impacts by reducing disturbances caused by a cut-and-cover operation. However, it can still cause appreciable

disruption. This may result from ground deformation induced by tunnelling operations, with potential environmental effects on neighbouring constructions and utilities.

The shallow ground tunnel cover may not be sufficient to attenuate the deformations induced by the underground excavation. This is the case of the system of transit tunnels built in central Germany in the last decade, for instance, the Bochum system in some locations has barely 2 m cover of post war rubble fill. In contrast to this, some tunnels of the London Underground system built late last century have up to 70 m of soil cover, for instance, at Parliament Hill on the Northern Line "tube".

Some points emerge from the preceding discussion. If anyone is aiming to plan, design or build such a structure, he has to answer a few questions beforehand. Will the cavity be stable during construction? What support or lining system should be installed and what loads will it endure during its service lifetime, with what margin of safety? What are the magnitude and distribution of the displacements induced by the tunnelling operation? What is the damage potential of these displacements on existing structures in the vicinity? These questions, although not exhaustive, must have played on the minds of the pioneering tunnel engineers, when faced with the demand of constructing an urban tunnel. As in many occasions in the history of technology, the pressing need of the structure was greater than the intellectual or scientific interest to answer the questions. As a

consequence, those questions remained unanswered or poorly answered. But the structure was built, possibly imperfectly in technical terms. Such imperfection may have resulted from the tunnel construction emboding excessive safety and cost or insufficienct safety.

When practical problems are not promptly solved by available theories or when these are not known to the practitioner, solutions are often empirically developed. By observing successful and unsuccessful past experiences, for instance (in mechanical terms, stable or unstable performance) in tunnel construction, it has been possible to develop some observational design rules. These, however, do not generate information about the margin of safety of the structure. Since these rules embody only successful experience, it is recognized that the structure built according to them will have a factor of safety greater than unity. How much greater is not easily to established. Unlike theoretical solutions that can furnish safe or unsafe design, depending on the validity of the assumptions made, empirical solutions generally provide a conservative design. The above discussion is applicable not only to soil tunnelling but to any other field of geotechnical engineering and it may be considered as a truism. However, a review of the state-of-the-art reports prepared on the subject over the last two decades (Peck, 1969, Attewell, 1977, Clough and Schmidt, 1981, Ward and Pender, 1981, to quote few) reveals that an appreciable amount of empiricism

still exists as a design basis for soft ground tunnelling. This may be surprising in view of the significant developments in soil mechanics within the same time span, with the introduction of a variety of new modelling techniques for solving increasingly difficult geotechnical problems. Persistence in using empirical or semi-empirical approaches in the practice of urban tunnel design, can be attributed to a number of different causes. One may be that some theories which have been transferred from other engineering fields are unable to fully or properly solve all aspects of shallow tunnelling. The risks in transferring behavioural or conceptual models from one scientific or technical field to a completely different field was addressed by Ladanyi, (1982). During the transfer process, the underlying assumptions of the theory being transferred are not always clearly stated and the validity of the theory may be questionable for a particular practical application. Another reason might be that the theory is too complex for routine use by non-specialized engineers in design practice.

As will be seen in the next two chapters, shallow tunnelling in soft ground involves a number of behavioural features that preclude the use of any simple theoretical model. This and the current impracticality of using more sophisticated modelling tools in routine practice, may explain to some degree, the continued use of empirical approaches. Moreover, the attraction that empiricism holds should not be disregarded, as it enables one to ensure the

ultimate performance of the structure. Tunnels being designed using fairly elaborate numerical techniques, frequently have the final design decisions made only after checking the results against known empirical rules. The opposite is also true. Tunnels being designed entirely on the basis of previous experience may only have some numerical modelling conducted, possibly just to satisfy some contractual requirement or to comply with the client's request. It is common then to find the more involved and possibly more adequate design procedures have little or no impact on the major design decisions.

The capability of numerical modelling, frequently treating the problem as two dimensional, is becoming increasingly known within the community of practioners. Their current limitations are being recognized and clients are becoming gradually concerned when their use is not treated with healthy skepticism. "The enormous developments in measurements and computing capabilities over the last two decades have drawn many researchers" — and numerically or computer oriented practitioners — "into a vortex of ever—increasing sophistication and complexity. They have become so intrigued by their ability to solve previously intractable problems that the primary objectives of research" and practice — "have been obscured" (Poulos, 1982).

As will be seen in following chapters, it has been fully recognized by tunnellers that a fairly clear

relationship exists between the magnitude of the displacements in the ground mass around the tunnel opening and the magnitude of stress eventually carried by the support system. This dependence between stress and displacements was expressed using ground-support interaction diagrams. Fenner (1938) was the first to define and obtain these diagrams analytically, using an elastic-plastic model. Obviously, the magnitude of the displacement occurring at the tunnel opening dominates the magnitude of settlement at the ground surface. Therefore, the settlement should be related to the magnitude of the stress supported by the lining. Despite this obvious connection between the two quantities, whose assessment represents the key issues of design, it is suprising to find that in practice one tends to ignore the connection (see Chapter 4). It will be noted that lining design is frequently conducted independently of settlement predictions and, in many instances, using conflicting design assumptions that finally lead to overconservative solutions for both the support system and ground control measures. A possible reason for this state of affairs is the persistent empirical approach which treats the two problems separately. Also the behavioural and conceptual models used to treat these problems were transferred from entirely different fields and in some instances, are based on conflicting hypotheses. As an example, lining design evolved predominantly from a continuum mechanics approach, whereas many prevailing

methods for settlement estimates were developed from stochastic theories. In contrast with the theories of elasticity or plasticity, the stochastic medium is typically a discontinuous particulate mass, subjected to gravitational body forces, with their movements controlled by probabilistic laws. Putting aside for a moment the discussion of the validity of using either approach (as addressed by de Mello and Sozio, 1983), it should be recognized (Eisenstein, 1982 and Eisenstein and Negro, 1985) that although convenient numerically, the separation of the problem of displacement and the issue of lining pressure predictions is entirely artificial.

It would appear that research directed towards the development of a practical procedure coupling displacement prediction with lining design is needed. It would preclude the dichotomy of surface settlement and lining load treatment. Also, enough room exists to develop a procedure that would lie somewhere between the more elaborate design approach that makes use of numerical techniques and the prevailing empirical approach for the design of shallow tunnels. This is the subject of the next item.

1.2 Aims

In broad terms, and following the reasoning of Poulos (1982), it could be suggested that any applied research to shallow tunnelling in soil, should include attempts to:

a) identify unsolved or partly solved problems that

affect existing practices;

- b) more adequately appreciate the mechanisms involved in the soil and in the behaviour of the supporting structures, whenever possible identifying the controlling parameters;
- c) develop procedures or approaches to solve the above mentioned problems;
- d) summarize the results of the research work in a comprehensive manner and in such a way that it may be used by the practitioner;
- e) validate the results of the research by applying them to practical problems and to define ranges of validity.

Sometimes, time or resource constraints or even personal preferences may channel the applied research into one or two of the summarized general points. In the present study, an effort is made to balance the importance of each of the above items.

This work attempts to develop a design procedure that simultaneously treats the problems of estimating lining loads and of predicting the ground settlements in shallow tunnels driven in soil. These activities are part of the overall design considerations of a shallow tunnel and will be discussed in Chapter 4.

To achieve this aim, a basic premise was established at the onset of the work: reasonable simplicity. The demand for simple design oriented procedures is evident from a survey carried out and discussed in Chapter 4 of this thesis. This general demand may reflect the known fact that despite how elaborate an analysis might be, "there will always be practical limitations on its ability to model real geotechnical problems" (Poulos, 1982). Such limitations are well known: uncertainties in modelling the geological profile in detail, in assessing the soil parameters, in recognizing the dominant factors that govern the behaviour, etc. These uncertainties result from a variety of reasons, ranging from economic considerations, time availability and also the present difficulties of properly simulating more complex behaviour (eg. instability after excessive straining of a structure).

Although it should be simple, the needed design procedure would have to be based on a consistent theoretical background to avoid the shortcomings of the existing empirical methods. Hence, it would have to encompass a fairly large number of variables or factors known to affect tunnel behaviour. This required that, in its development, use had to be made of fairly involved modelling techniques, (numerical and analytical), and these were selected on the basis of their recognized simplicity and reliability in solving the posed problem. However, to render the problem tractable, a considerable number of simplifying assumptions had to be made and limitations were imposed as will be seen in the following chapters. This was done, however, knowing that the predictive exercises performed to date in geotechnical engineering show differences in results that

are more related to differences in judgement between different predictors, than to differences in the methods of analysis used. One may conclude that the success in applying a method to solve a practical problem, depends as much on the qualities of the designer as on the method itself. In other words, experience in using a method is of paramount importance and in this regard it is probably easier to gather experience with a simple procedure than with a complex one (Poulos, Op.cit).

If it were possible to develop such a design oriented method, it would lie between the simpler empirical methods and the more complex numerical solutions. Ideally it would allow the practitioner to evaluate possible ranges of behaviour or responses to tunnelling, to predesign or design the support and to evaluate field data from instrumentation monitoring, as part of an observational approach to tunnel construction which enables feedback for the final design solution.

1.3 Scope and Thesis Organization

To achieve the objectives as previously described, a number of major factors will be explicitly considered in the development of the proposed design procedure. These are to account for the effects of the following:

- a) the delayed installation of the lining;
- b) the non-uniform state of stress in the soil in situ, represented by the stress gradient generated by

gravitational body forces and by a horizontal to vertical stress ratio different from unity;

- c) the non-linear response exhibited by most soils in terms of their stress-strain relationships, including dependence on stress level and strength;
- d) the stress free boundary represented by the ground surface;
- e) the interactive nature of the load transfer process developed between the soil and its support system; and

The reasons for selecting these factors as those to be appraised in the development of the method will emerge from the discussions in the next two chapters and throughout this thesis. To a large extent, the selection criteria relied initially on observations of real tunnels and on conceptual models, which have been confirmed through more elaborate models. No attempt has been made to develop a new numerical technique for the purpose of this study. Existing methods were simply adapted, to develop the proposed design procedure. This and the need to keep the method as simple as possible meant that despite the already appreciable number of variables taken into consideration, a significant number of factors had to be excluded. Hence it was decided to limit the study to single tunnels with a circular profile, driven through isotropic, time-independent continuous media, excavated full-face under free air, and without water seepage effects. Non geostatic loadings produced by a non-uniform surface or subsurface foundation loads were also

not considered. No treatment is given to special classes of soils such as those exhibiting strong post peak softening, e.g., sensitive clays.

It will be shown that the proposed procedures will furnish reasonable results whenever, "good ground control" conditions are attained. These can result from favourable ground (firm) conditions or from the use of appropriate construction techniques applied to poorer ground, where otherwise "ravelling" or "running" of the ground would occur '. Attempts will be made in this thesis to better define "good ground control conditions" and to quantify the expected behaviour.

The exclusion of some factors from this study should not lead one to surmise that they play a minor role in the behaviour of a tunnel in soft ground. For the sake of completeness, their role is briefly discussed in the following two chapters.

In Chapters 2 and 3 the idealized behaviour of shallow tunnels is presented. The influence of a number of factors affecting the behaviour is briefly discussed, using simple conceptual models whenever possible.

Chapter 4 summarizes the present state of the design of shallow tunnels with the more important available design

^{&#}x27;The Wilson tunnel, partly driven though residual soils in the Koolau Range northeast of Honolulu, is an interesting example of the varying response of the same ground to different construction technologies (see Peck, 1981). The ravelling ground response to full face excavation was changed to very favourable and stable conditions, when the tunnel was advanced in small drifts and in short longitudinal sections.

methods being reviewed. The merits of the more frequently used methods for lining design and settlement prediction are identified and critically assessed. Finally, an evaluation of the present needs and a definition of potential improvements for current practice are attempted.

Chapter 5 reviews shallow tunnel modelling using two and three dimensional finite numerical techniques. The capability of two dimensional finite element analyses to portray the behaviour of selected case histories is assessed. The need to estimate the magnitude of tunnel opening displacements prior to lining installation is justified in order to identify the amount of stress release allowed before the support is installed in the two dimensional representation. For this purpose, parametric three dimensional simulations are carried out and an approximate procedure is established to simulate displacement prior to support activation.

Chapter 6 presents numerical modelling and generalizations to be used for the development of the design model. Reduction of parameters and model simplifications are introduced. The two dimensional finite element parametric analyses are carried out from which generalized relations between stress, ground deformation profile and displacements around the opening are obtained for both frictionless and cohesionless soils.

In Chapter 7 a design procedure is developed based on results obtained in Chapters 5 and 6. Assessments of the

effect of delayed lining installation and the soil-lining interaction are made. How to obtain the surface and subsurface settlements is explained. Finally a guideline for using the design procedure in practice is established with the underlying assumptions re-stated to define the range of validity for the proposed method.

Also in Chapter 7, the proposed design procedure is compared with a number of well documented case histories and laboratory model tests. Limitations of the method and the approximations introduced for practical use are discussed.

Finally in Chapter 8 a brief summary of the research work and the main conclusions are presented. Also included are suggestions regarding future applied research on the subject.

2. IDEALIZED BEHAVIOUR OF SHALLOW TUNNELS: STRESS AND STRAIN CHANGES

2.1 Introduction

The purpose of this Chapter is to briefly review some of the more important factors affecting shallow tunnel behaviour, integrating the soil and its support system. As much as possible, the discussion will be framed within a soil mechanics background. In contrast to other geotechnical fields, such as the design of slopes, embankments and foundations, the understanding of soil tunnelling is founded predominantly on tradition and empiricism, where the soil mechanics perspective in not always clear. To put the subject in a basic form, use will be made of simple conceptual models, complemented by results from field observations, model tests and numerical analyses. Some factors will be studied separately, although it is recognized that substantial interaction exists between them. Such an approach is artificial but can be justified for a broad overview.

2.2 Shallow and Deep Tunnels

Despite the fact that a really deep tunnel does not exist, the concept of a "deep" tunnel arose for reasons of theoretical convenience. This enables two effects to be neglected in assessing the behaviour of an opening in the ground (at depth): (a) the stress field gradient across the

opening becomes negligible; (b) the influence of the stress free boundary surface is minimized.

Under conditions of plane strain and material homogeneity, the symmetry of a deep circular opening enables the pattern to be typified by the study of one quadrant. However, if effects (a) and (b) above were to be included in the analysis, then the cross section is symmetrical about the vertical axis only. Moreover, unsymmetrical patterns develop about the horizontal axis, in terms of (a) stress distributions; (b) displacement distributions; (c) possible modes of failure.

Almost all of the analytical closed form solutions available for the analysis of ground-liner interaction were developed assuming ideally deep tunnels (see Chapter 4). Then, it would be of some use to be able to identify when a tunnel could be considered "deep", but a closer look into this apparently simple question reveals no simple answer. Depending on the parameter being investigated (stress or displacement at a certain location), on the criteria to define whether a tunnel is "deep" or not, and, possibly, on the type of analysis being conducted, the answer may vary considerably. In terms of the judging criteria, two possibilities could be considered: a) negligible effect of the free surface and b) negligible effect of the stress field gradient across the opening.

A number of investigators studied the problem and the result of a brief survey into the subject is summarized in

Table 2.1. The common assumptions used in these studies are indicated in the table. Among others, all analyses considered a linear elastic ground. Mindlin (1938, 1939) was one of the first to address the subject, studying the case of an unlined tunnel. Unlike previous investigators (Schmid, 1926, Yamaguti, 1929), who studied the problem of a mass of indefinite extent, subjected to gravity, Mindlin considered a half space limited by a horizontal stress free surface. Mindlin followed and corrected the approach given by Jeffrey (1920), who studied a similar problem for the case of zero body forces, with a plate subjected to uniform tension, parallel to its straight edge. By describing the system in bipolar co-ordinates Mindlin was able to calculate the stress around the opening, but made no attempt to calculate the corresponding strains. His solution was obtained by making use of an infinite series expansion. By comparing the tangential stress at the tunnel crown for the half space condition with that for the infinite plate under gravity action, Mindlin identified that for cover to diameter (H/D) ratios greater than 0.25, the effect of the free surface becomes negligible, provided the stress field ratio K is equal to unity (K is the ratio of lateral to vertical field stresses).

For a non hydrostatic stress field defined by $K=\nu/(1-\nu)$, Mindlin found that the threshold ratio H/D depends on the Poisson's ratio (ν). For ν of 0.5, the associated threshold is again equal to 0.25, as found in his

				Crit	Criteria
Authors	Analyses	Investigated	Source	Negligible effect of the free surface at	Negligible effect of of the gravitational stress gradient at
Mindlin (1939)	Closed form solution of unlined tunnel	θ_{θ} at crown and $K = 1$	Author's equations 45 and 47 in limit (Fig. 5) compared	H/D > 0.25	Not assessed
		θ_0 at crown and $K = v/(1-v)$ with $v = 0.25$	Author's equations 57 and 58 (fig. 6) compared	H/D > 1.5	Not assessed
Evoldsen (1968)	Mindlin's solution for unlined tunnel	σ _θ above crown (interior points)	Pigures 5 and 6 of author's paper	H/D > 4	н/Б > 50
Peck et.al. (1972)	Finite element, lined tunnel, non slip, K_0 = 0.5 and 2	Max. thrust, bending moments and diameter changes	Figures 10 and 11 of author's paper	H/D > 1	Not assessed
Ranken (1978)	Finite element, lined tunnel, full and non slip, K ₀ = 0.5, fixed lin. stiff.	Thrusts, moments, diameter changes, radial displac. at crown, spring. and floor	Figures 4.2, 4.3, 4.5 and 4.6 of author's thesis	H/D > 1.5	H/D >> 5

Note: In all analyses, linear elastic, homogeneous, isotropic domain subject to gravity, circular opening, horizontal ground surface, plane strain condition and constant in situ K ratio (H = tunnel cover; D = tunnel diameter).

Table 2.1 Assessments of the Effects of the Presence of the Ground Surface and of the Gravitational Stress Gradient in Shallow Tunnels

first analysis. For ν of 0.25 (K=1/3), the analysis indicated that the effect of the free surface becomes imperceptible at H/D slightly greater than 1.5.

In both analyses, Mindlin was solely concerned with the effect of the proximity of the stress free boundary and made no attempt to assess the effect of the gravitational stress gradient.

Table 2.1 shows also the findings of Ewoldsen (1968), who carried out a parametric study by computer, using Mindlin's basic solution. Instead of inspecting only the tangential stress at the crown, as Mindlin did, Ewoldsen examined the stress at interior points within the ground mass above the crown. By removing, in an approximate way, the stress gradient effect from the solution, he showed that the presence of the free boundary surface is still discernible for values of H/D in excess of four. He also showed that the gravitational stress gradient is felt for cover to diameter ratios in the order of 50.

The inclusion of a lining in the opening highlights a special feature of shallow tunnel analysis. This refers to an overall uplift of the opening which is more pronounced when the lining is stiff. This trend to "float" is due to the fact that the resultant force generated by the excavation of the opening in a gravitational medium is vertical and upwards, being equal to $\pi\gamma D^2/4$ per unit length of tunnel. The corresponding upward movement is a consequence of the gravitational stress gradient. However,

it depends also on the deformation properties of the ground and lining and it is affected by the presence of the stress free boundary. This feature is evident when performing elastic analyses where the creation of the opening and lining installation occur simultaneously. In real tunnels, this effect is partly or completely suppressed since the liner installation is delayed. The introduction of the lining gives rise to other parameters that can be used in judging criteria for defining shallow and ideally deep tunnels. These are the thrusts and bending moments developed within the liner.

Peck et.al., (1972) reported results of finite element analyses of lined tunnels, for initial stress ratios, K, of 0.5 and 2.0, and for variable H/D ratios. Examining the magnitudes of the maximum thrust in the lining, the bending moments at the springline and the invert, as well as the changes of the horizontal and vertical diameters of the lined opening, these authors suggested that, regardless of the stiffness of the lining with respect to that of the soil, the effect of the free boundary surface becomes negligible for H/D greater than 1.0.

A more detailed study was performed by Ranken (1978), using a similar approach. For a certain relative stiffness, for a lining installed at the moment of creation of the opening, and for K=0.5, Ranken concluded that the effect of the free surface on thrusts, bending moments, diameter changes and radial displacements in the lining, is neglible

for all H/D ratios greater than 1.5. He also detected that the influence of the gravitational stress gradient across the opening, is greater than the influence of the ground surface boundary and remains at a significant level to a much greater depth (H/D>>5). Like Ewoldsen (1968), Ranken used an approximate scheme to assess the two effects separately. This was possible after realizing that the liner response at the springlines is less affected by the influence of the stress gradient across the opening (Ranken, 1978:108). Ranken also noticed that the threshold value of H/D depends slightly on the condition of the ground-lining interface, which he represented in his analysis by either full or non-slip.

The results presented so far permit one to conclude that the influence of gravity is not to be disregarded even for tunnels of appreciable depth (H/D>50). However, the effect of the free ground surface on stress, displacements, thrust and bending moments in the liner, can be considered negligible in a linear elastic analysis, for cover to diameter ratios greater than about 1.5. Although this is true when the pertinent parameters are taken at or near the opening perimeter, this conclusion may not be valid in terms of induced displacements away from the opening. Barrat and Tyler (1976) and Eisenstein et.al. (1981) presented case histories of tunnels driven in soil, with cover to diameter ratios of about 8 and 10, respectively. In both cases, appreciable displacements were recorded at the ground

surface upon tunnelling, whereas beyond small distances (about 1D) below the invert elevation, no displacements were detected. Hence, even for fairly deep tunnels, the presence of the ground surface and the action of gravity make the displacement distributions above and below the tunnel highly non-symmetrical. Eisenstein et.al., (Op.cit) also showed that an asymmetric development of plastic zones around the opening was inferred from field observations of vertical and horizontal displacements. This again reflects both the influence of the ground surface and the action of gravity. It was not possible to single out the dominant factor that caused these asymmetric responses, but, as far as the displacements are concerned, one is tempted to believe that the proximity of the ground surface may have had a preponderant role.

A deep tunnel is occasionally defined as one in which the cover to the crown is sufficiently thick so that the effect of the displacements occurring at the opening are able to attenuate, making the surface settlements negligible. Although this definition may be correct for a tunnel in a linear elastic ground, it is misleading for real ground conditions, where non-elastic and time-dependent responses may develop. Imperceptible surface settlements could hypothetically be possible in a tunnel of small cover, if the excavation is through a soil with a highly dilatant response which may compensate the inward displacements of the opening. Conversely, it is possible to conceive a tunnel

with a fairly thick cover of compressible soil, which is driven in such a way that the short term displacements are insignificant, but where time dependent effects (e.g. consolidation due to drainage towards the permeable opening) may finally induce significant surface settlements.

German authors frequently refer to "shallow" and "deep" tunnels. Possibly reflecting current practice in Germany, a design quideline for tunnels was prepared by a working group and was published by Duddeck (1980). A summary of these recommendations is presented by Heinz (1984). The distinction between shallow (H/D smaller than 2) and deep (greater than 3), according to Duddeck (Op.cit), reflects a concern with respect to the effect of the proximity of the ground surface. More than that, it expresses the need to identify the condition where the so called "partial embedding" assumption should be applied. According to this, the interaction between lining and soil in the upper 90° arch of the crown should be disregarded. In other words, the ground above tunnel crown should be taken as a "heavy fluid", able to transmit loads to the support, but unable to withstand any additional shear. As maintained by Duddeck (1980), this assumption would be applicable to shallow tunnels with limited overburden (cover to diameter ratio smaller than 2, according to Duddeck, Op.cit, or smaller than 2.5 according to Duddeck and Erdmann, 1982 and Erdmann and Duddeck, 1984). The German recommendations propose that, for H/D greater than 3 (or 2.5 according to Duddeck and

Erdmann, Op.cit and Erdmann and Duddeck, Op.cit), a complete embedding of the lining by the ground can be assumed, and a continuum model for interaction can be used. Moreover, Duddeck and Erdmann (1982) suggest that, in deeper tunnels, allowance could be make for some reduction of the primary in situ stress, as opposed to in shallow tunnels, where a full overburden condition should be assummed. A discussion of the merits and validity of these assumptions is given in other sections of this thesis. However, it should be anticipated that no field evidence has been found so far, supporting these highly consequential assumptions. The hypothesis of full overburden has the premise of a ground with no shearing resistance, which is clearly highly debatable. The assumption of no embedding in the crown region is also open to discussion. Wong (1986:34) defended it, by accepting the full development of two failure zones running upward from the tunnel, intercepting the ground surface, thus bounding a soil block free to move down, towards the opening. In other words, one would have to admit a complete collapse mechanism of the soil above the tunnel crown, in order to justify the German assumption of no embedding in that region. Although this is a possibility, it normally cannot be accepted in an urban tunnel, and therefore it has to be inspected in the design stage as an extreme condition and its risk of occurrence either minimized or eliminated. Moreover, it should not be taken as a routine hypothesis for engineering design. An involved

discussion on the consideration of extreme conditions in geotechnical design is given by de Mello (1977), who also addresses the problem with respect to soil tunnelling practice (de Mello, 1981:212). Moreover, if it is the collapse mechanisms that justify the partial embedding assumption for a shallow tunnel, there is no justification to support the selection of the region where this condition prevails (crown). In fact, the observation of collapse mechanisms for plane-section tunnels in centrifuge tests carried out in Cambridge, U.K. (e.g. Mair, 1979) and plasticity solutions of this very problem (Davis et.al., 1980), demonstrate that depending on the geometry (H/D) and on the relative strength of the material, the critical failure mechanism varies. Accordingly, the partial embedding assumption would have to be extended not only to the crown 90° arch, but also to the springline.

Since a condition of total collapse is difficult to justify as a normal or "average" (de Mello and Sozio, 1983) design hypothesis, the assumption of "embedding absence" should more feasibly be replaced by that of a "weakened" or "softened embedding". Partial or localized failure could then be accounted for, assuming a proportionally reduced deformation modulus for the soil around the tunnel, as a function of the degree of shear strength mobilization.

Additional comments on the above subject will be presented later in this Chapter and in Chapter 4.

In summing up, two conclusions emerge from the above discussion, bearing in mind that the underlying assumptions are highly idealized:

a. When studying the behaviour of the ground or lining responses strictly around the opening, the presence of the stress free boundary at the ground surface can be neglected for H/D greater than 1.5, but the influence of the gravitational stress gradient should always be taken into consideration in the design of urban tunnels.

b. When studying the displacement field around an urban tunnel or possible modes of collapse of the ground, the effect of the ground surface as well as the action of gravity should always be considered.

2.3 Soil Response to Tunnelling

2.3.1 Foreword

The following is a qualitative description of the expected response of the soil subjected to the effects of a tunnelling operation. Generally, in simple physical terms, this operation involves a) the removal of the soil within the cut profile, which produces an overall reduction in the stiffness of the ground mass; b) the reduction of the in situ stress around the opening (normal and shear stresses), causing stress changes throughout the ground mass which generate volumetric and shear strains and also pore water pressure changes; c) the change in the hydraulic

boundary conditions which affects the dissipation of the excess pore water pressures, and the ground water seepage pattern.

The tunnelling operation also involves the inclusion of a support system, which interacts with the soil, further changing the ground stress and its stiffness. Attention here will be mainly given to the ground response, as the "design of a tunnel lining is not a structural problem but ground/structural problem, with the emphasis on 'ground'" (Kuesel, 1986). It will be assumed in this section that the tunnel is driven above the water table, with fully drained conditions. Later on, in Chapter 3, the role of the water table within the system will be discussed.

The ground reaction to the advance of the tunnel excavation involves stress transfer mechanisms, which are clearly three-dimensional. A two-dimensional representation may be a reasonable approximation at a sufficient distance from the advancing face. To simplify the analysis, a two-dimensional plane strain condition will be adopted initially. The implications associated with relaxing this assumption are discussed later.

2.3.2 Idealized Stress Changes

The stress changes induced by a stress free circular opening, in an infinite plane strain, homogeneous, isotropic elastic plate, subjected to uniform vertical (σ) and horizontal $(K\sigma)$ normal external stresses, can be determined

through Kirsch's (1898) solution. This is a zero body force solution that corresponds to an ideally deep tunnel. Let us assume that the radial $(\sigma_{\rm r})$ and shear stress $(\tau_{\rm r\theta})$ at all points around the perimeter of the opening, are proportionally reduced to a fixed fraction, Σ , of the original in situ stress $(\sigma_{\rm ro}, \ \tau_{\rm r\thetao})$. Hence, at the perimeter:

$$\sigma_{\rm r}(\theta) = \Sigma \sigma_{\rm ro}(\theta)$$

$$\tau_{r\theta}(\theta) = \Sigma \tau_{r\theta0}(\theta)$$

At the crown (or floor) and springline, the shear stresses are zero, and, therefore, the radial and tangential stresses are principal stresses. For these points, it is possible to show that, after reducing the in situ stresses around the perimeter by a uniform fraction $(1-\Sigma)$, the principal stresses will be:

$$\sigma_{\rm rc} = \Sigma . \sigma$$
 [2.1]

$$\sigma_{\theta c} = K\sigma + (1-\Sigma)(2K-1)\sigma$$
 [2.2]

for the crown, and:

$$\sigma_{rs} = \Sigma . K \sigma$$
 [2.3]

$$\sigma_{\theta s} = \sigma + (1-\Sigma)(2-K)\sigma$$
 [2.4]

for the springline.

If K=1, then:

$$\sigma_{\rm rc} = \sigma_{\rm rs} = \sigma_{\rm r} = \Sigma \sigma$$

$$\sigma_{\theta c} = \sigma_{\theta s} = \sigma_{\theta} = 2\sigma - \Sigma \sigma$$

The mean normal stress and the maximum shear stress at the crown and springline are:

$$\sigma_{m} = \sigma$$

$$\tau_{\text{max}} = (1 - \Sigma) \sigma$$

The stress path corresponding to the reduction of the in situ stress is shown in Figure 2.1 as line 1-1. In this case, the stress changes of any point on the perimeter are described by a unique stress path.

If body forces due to gravity are now included, but still neglecting the effect of the stress free ground surface, the in situ principal stress at crown, springline and floor are:

$$\sigma_{\text{rco}} = \sigma_{\theta \text{co}} = \sigma - \gamma \frac{D}{2}$$

$$\sigma_{\text{rco}} = \sigma_{\theta \text{so}} = \sigma$$

$$\sigma_{\text{rFo}} = \sigma_{\theta \text{Fo}} = \sigma + \gamma \frac{D}{2}$$

respectively, where γ is the specific weight of the elastic material and D is the diameter of the opening. Mindlin's solution for a deep tunnel with gravity can furnish the magnitudes of the tangential stress at those points, for a hydrostatic state of in situ stress, after a complete release of these stresses at the opening (Mindlin, 1939:1132). For a Poisson's ratio of 0.5, the final tangential stresses at the crown, springline and floor, are:

$$\sigma_{\theta c} = 2\sigma - \gamma \frac{D}{2}$$
 [2.5]

$$\sigma_{\theta s} = 2\sigma$$
 [2.6]

$$\sigma_{\theta F} = 2\sigma + \gamma \frac{D}{2}$$
 [2.7]

The final mean normal stresses and maximum shear stresses are:

$$\sigma_{\rm mc} = \tau_{\rm maxc} = \sigma - \gamma \frac{D}{4}$$
 [2.8]

$$\sigma_{\mathsf{ms}} = \tau_{\mathsf{maxs}} = \sigma \tag{2.9}$$

$$\sigma_{\text{mF}} = \tau_{\text{maxF}} = \sigma + \gamma \frac{D}{4}$$
 [2.10]

Without gravity: crown, springline and floor stress paths: (1) - (1) (unique)

With gravity: springline (1) - (1) crown (2) - (2) floor (3) - (3)

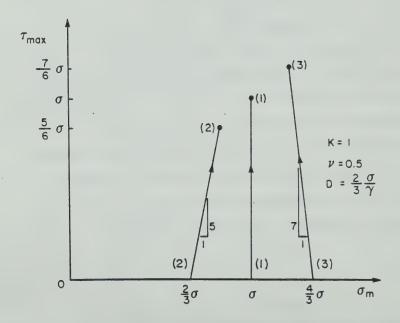


Figure 2.1 Effect of Gravity on the Elastic Stress Paths in a Deep Tunnel

Due to gravity, different elastic stress paths are identified for the crown, springline and floor (Figure 2.1). Gravity does not affect the stress path followed by the springline which exhibits a state of pure shear (no change in mean normal stress). Gravity causes a decrease in the maximum shear stress in the crown and an increase in the floor. With respect to the mean normal stress, an increase is observed in the crown and a decrease in the floor. Elastic volume changes are therefore expected to occur at the crown and floor.

The inclusion of the effect of the ground surface will further alter these stress paths. For K different from unity, some points at the opening will experience rotation of the principal stresses. The increase of shear stress in response to the stress release at the opening may cause yielding of the ground, making the stress path distort towards failure. Local failure of a soil element may eventually occur and, if further reduction of the stress at the opening is imposed, the stress path will travel down the failure line. Figure 2.2(a) illustrates this stress path for an element of soil at the opening springline, while figure 2.2(b) shows schematically the changes in stresses at interior points in the ground. This progressive stress transfer process, where the shear strength of the ground is increasingly mobilized upon the continuous reduction of the internal stresses at the opening, is the "arching" mechanism. Clearly, this mechanism is not confined to a

two-dimensional stress redistribution. Upon advance of the tunnel face, a three-dimensional arching process develops, as will be seen later. Tunnelling operations which make use of "good ground control", tend to inhibit soil failure. It will be seen that the portion CD or CE of the stress path shown in Figure 2.2(a) may involve highly detrimental consequences, which are normally not acceptable when tunnelling in urban areas. In such areas, good quality construction will tend to confine the stress path to the portion AC. In practice, the means to ensure this include, for example, the following: (a) the use of "earth pressure balance" techniques, where compressed air or bentonite slurry minimizes the stress release at the opening; (b) the use of favourable sequences of excavation and of support installation (which also controls the amount of stress release at the opening); (c) the use of continuous or discontinuous fore-polings and long spiles (which, again, attempt to reduce the stress release); (d) the practice of promptly filling or grouting the void behind the lining, or of expanding the latter against the excavated profile (to avoid full stress release at the opening or even to increase the stress at the perimeter); (e) the use of ground treatment prior to the excavation (which does not control the stress changes, but favourably changes the failure envelope of the soil).

For conditions different than those which have been asssumed, different stress path responses will be found for

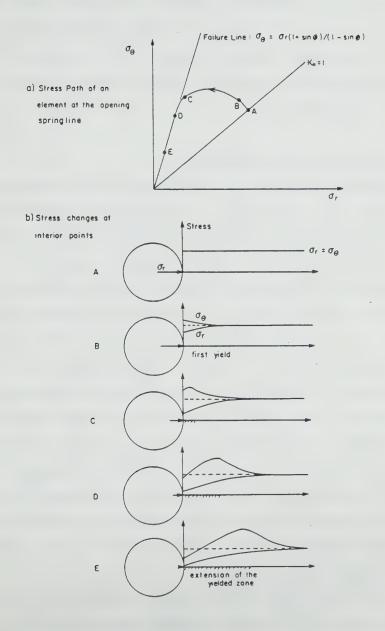


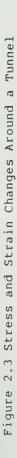
Figure 2.2 Stress Changes due to the Reduction of the In Situ Stress in a Deep Tunnel

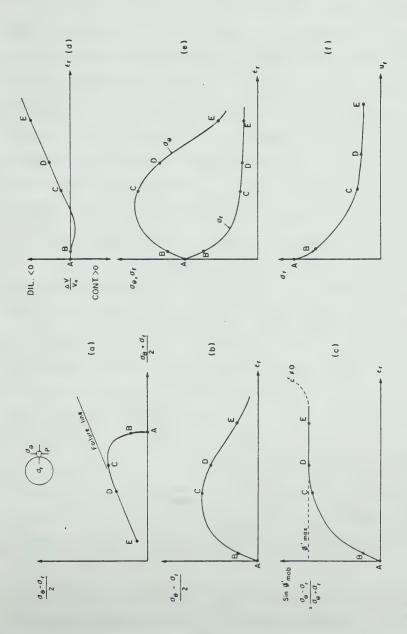
different points around the opening. It has been shown that gravity as well as the existence of the ground surface affects the stress changes. Moreover, if K is different from unity, some points around the tunnel may reach failure sooner than others.

2.3.3 Idealized Strain Changes

The stress path shown in Figure 2.2 has been replotted in Figure 2.3a. Assume that it represents the response of an ideally deep tunnel operation in a lightly overconsolidated soil, showing negligible cohesive strength under a hydrostatic in situ stress condition. We shall retain the assumption of full drainage occurring as the stresses at the opening are reduced. We shall also admit that this soil, has its "stiffness" (be it a "current" Young's modulus or a shear modulus) dependent on the mean normal stress and on the degree of shear mobilization. Also, we shall admit that upon failure, no appreciable reduction in friction angle is observed. These assumptions were already underlaid but not explicitly formulated, when the changes in stress shown in Figure 2.2 were discussed. The following is a discussion of the strain changes that will likely occur in a soil element P, adjacent to the opening.

As the idealized gradual excavation takes place, the radial stress $\sigma_{\rm r}$ is steadily reduced. From A to B, (Figure 2.3a) the ground response is nearly linear elastic and the tangential stress, $\sigma_{\rm g}$, increases proportionally to





the decrease in σ_r . The radial strain, ϵ_r , increases almost linearly (Figure 2.3b). At B some yield develops and σ_a ceases to increase at the same rate as σ , decreases. The stress path shows a more pronounced non-linear shape as does the stress-strain response (Figure 2.3b). Around point C, the maximum shear stress peaks and failure is attained soon after2. Failure is achieved with the mean normal stress reducing faster than the increase in shear. As a result, the maximum shear stress after point C starts to drop. Thereafter, the shear stress-radial strain curve (Figure 2.3b) starts showing a conspicuous downwards trend resembling a "strain-softening" response. A closer inspection, of course, reveals no "actual" strain softening since it is assumed that no reduction in friction angle occurs after failure. In fact, if the stress obliquity (the ratio of maximum shear stress to mean normal stress) is plotted against radial strain (Figure 2.3c), no actual "strain-softening" is revealed as expected. As the stress path travels down along the failure line (portion CDE in Figure 2.3a), the friction angle is fully mobilized and the stress obliquity (Figure 2.3c) remains fairly constant, provided the cohesive component of strength (c') is very small or zero. If this is not the case, the stress obliquity

² Clearly, this is a local failure condition of the soil element adjacent to the opening and it does not necessarily mean that the whole structure is at a collapse state. If this element at failure, is part of an overall stable system, then, additional unloading may alter the state of stress in the element and so cause finite increments of strains (Atkinson, 1981:59-61)

increases rapidly as the radial stress is reduced to zero, with the soil then experiencing a tensile type of failure (dotted line in Figure 2.3c).

The associated specific volume changes experienced by the soil element are shown in Figure 2.3d. Typically, in the nearly elastic portion AB of the loading process, near zero volume changes occur, as pure shear develops. Depending on the type of response of a particular soil upon yielding (stress level and history), it may show a small decrease in volume, which is soon compensated by a more pronounced trend of the soil to swell, associated with the faster reduction in mean normal stress (portion BC in Figure 2.3d). From C to E both shear strains and dilatancy will develop, their magnitudes dependent on a number of factors.

Figure 2.3e gives the relationships between tangential and radial stresses and radial strain in the soil element. While the changes in radial stress and strain display a continuous and monotonic evolution, the tangential stress presents a reverse trend after peaking around point C. In order to comply with the failure criteria, the tangential stress has to be reduced. This stress reduction results in an overall stress redistribution in the soil mass that causes stresses to be transferred to neighbouring soil elements, that may also be brought to failure.

At this point it is worth mentioning the differences between <u>localized failure</u> and <u>tunnel collapse</u>. As already pointed out, around point C in Figure 2.3, the maximum shear

stress is peaked and failure is achieved in the soil element under consideration. Provided no mechanism is created, the failed soil element will remain in place. Also by virtue of the previously mentioned stress transfer process, adjoining soil elements will be further sheared and the failure zone will propagate into the ground. Gravity will control this propagation, and it will also be affected by the presence of the ground surface. Eventually, the zones of high shear strain will create a mechanism, and the complete collapse of the ground into the opening will become possible. Tunnels in cohesionless soils such as that depicted in Figure 2.3 would reach a collapse state at points D or E with a non-zero compressive radial stress. For a given soil, the ratio H/D will regulate the distance between local failure and collapse stress states. Shallower tunnels would reach collapse at point D, closer to C and deeper tunnels at E. It is worth stressing that for a number of soils, first yield will occur at B, well before local failure is achieved. It is also important to mention that as the local failure condition is attained, both the local straining and associated displacements of the ground go uncontrolled. The risk of experiencing large settlement at the surface increases. This is why good tunnelling practice should lead to stress changes confined to within zone AC, recognizing, however, that some limited amount of yield will develop.

The radial displacement at a point in the opening, is the result of summing the radial strains from that point to

the limits of the ground mass. The displacement then reflects the combined response of points close to the tunnel and away from it. One would end up with a curve like the one shown in Figure 2.3f, that relates the reduction in the radial stress with the development of radial displacement at a particular point of the tunnel wall. In a more general case, shear stresses will also be present at the tunnel wall and the idealized tunnelling operation causes a reduction in these as well. As already assumed earlier in this section, the rate of stress decrease at the tunnel wall, is the same for both radial (or normal) stress and shear stress. The ratio between shear and normal stresses acting on the wall of the plane strain opening will be constant. The magnitude of the ratio will vary from point to point depending on the in situ Ko value. Therefore, the curve shown in Figure 2.3f will also reflect the shear stress removal upon tunnelling. It should be recalled that this curve has been obtained on the assumption that each point of the opening wall has its in situ stress reduced in decrements to a constant fraction $(1-\Sigma)$ of its original value. This curve has been referred to as a "Ground Reaction Curve", as "Convergence Curve" or a "Characteristic Line". It reveals a fact that has been long recognized: the existence of the interconnection between the magnitude of the convergence of the tunnel walls and the magnitude of the loads ultimately carried by the support system.

So far the action of the support has been intentionally put aside, since it is the topic of discussion later in this chapter. However, its role and effect on the ground response should not be forgotten. Besides restraining the amount of stress release at the opening, it may alter the stress and strain patterns shown in Figure 2.3. In general, the inclusion of an element of a different stiffness will alter the load transfer mechanisms, the development of volumetric and shear strains, as well as the so called ground reaction curve.

The soil behaviour depicted in Figure 2.3 includes a number of features that resemble those of a real soil even though a number of simplifying assumptions had to be made. But even with these simplifications, not much data is available on the behaviour of fully drained soils loaded along the stress path given in Figure 2.3a. Some preliminary test results, using the Bishop and Wesley (1975) stress path apparatus and following a loading sequence similar to that discussed, have been presented by Burland and Fourie (1985). Material tested included undisturbed and reconstituted overconsolidated London Clay, and clay samples from the Claygate Beds in Bell Common, Essex, U.K. (Hubbard et.al., 1984). Their investigation referred to the behaviour of elements of soil located underneath the bottom of an open cut retained excavation, entailing stress release under conditions of limiting passive equilibrium. This stress path - termed "passive stress relief" by the authors - has

similarities to that experienced around a tunnel. The results they have obtained confirm to some extent, the overall response that has been speculated here. The special feature presented in Figures 2.3b and c regarding the "softening" behaviour associated with the "unloading" boundary condition, has been recognized by Potts and Burland (1983) while performing a type "A" prediction (Lambe, 1973) of the retained excavation mentioned above. The addition of factors, such as the non-hydrostatic state of in situ stress, the action of gravity and of the free ground surface, the influence of support installation, the nature (and stress history) of the soil, etc. to the conceptual analysis just presented, may make the analysis even more intricate. Evidently, the detailed soil response will differ from what has been shown, but broad behaviour trends can be drawn, adopting the same type of reasoning. When all factors pertaining to a shallow tunnel are at play, two simple facts emerge. Firstly, the ground response will be clearly dissimilar for different points around the opening perimeter. No unique response will be observed at soil elements around the perimeter of a given shallow tunnel. Secondly, an obvious non-linear response will be experienced in terms of the stress-strain behaviour.

Normally consolidated and even lightly overconsolidated soils, as well as most granular non-cohesive soils undergo yielding after relatively small stress changes and their response is typically non-linear. Seneviratne (1979) carried

out some plane strain drained model tests of shallow circular tunnels (H/D between 0.5 and 0.95), in normally consolidated spetstone Kaolin. By reducing the internal tunnel pressure and monitoring the ground mass displacements through radiographic techniques, Seneviratne was able to obtain ground reaction curves such as that shown in Figure 2.3f. His results suggest that these curves ceased to show a linear pattern after less than a 10% reduction of the initial tunnel pressure (Seneviratne, Op.cit., Figure 4.10.b). For these tests, it is customary to define a "load factor" (see Atkinson and Potts, 1977). as:

 $LF = \frac{\sigma_o - \sigma_i}{\sigma_o - \sigma_c}$ [2.11]

where $\sigma_{\rm o}$ is the initial vertical stress at the tunnel axis, $\sigma_{\rm i}$ is the current tunnel pressure (uniform in a model test), and $\sigma_{\rm c}$ is the tunnel pressure at collapse. This factor, as defined, may be understood as the reciprocal of a factor of safety (FS) against global collapse of the structure. Seneviratne's results show departure from a linear response at load factors between 0.4 and 0.5 (i.e. factors of safety between 2 and 2.5). Results from similar tests in overconsolidated kaolin (Cairncross, 1973 and Orr, 1976), as well as in loose and dense sand (Potts, 1976), were conducted in Cambridge and were presented by Atkinson and Potts (1976), Atkinson et.al., (1975) and Orr et.al., (1978). Again, it is revealed that, in terms of the ground reaction curves for the tunnel crown, non-linearity is observed at load factors higher than 0.33 to 0.5 (or factors

of safety smaller than 2 to 3).

It is also customary to express a ratio called "overload factor" as:

$$OF = \frac{\sigma_{o} - \sigma_{i}}{\sigma_{o}}$$
 [2.12]

where $\sigma_{\rm o}$ and $\sigma_{\rm i}$ have the same meaning as before and $c_{\rm u}$ is the undrained shear strength of the soil.

For purely cohesive soils, Davis et.al. (1980), were able to bound fairly closely the exact tunnel collapse pressure (σ_c). This pressure is given by:

$$\sigma_{\rm o} - \sigma_{\rm c} = Nc_{\rm u}$$
 [2.13]

where N is the overload factor at collapse (also called the stability ratio). N is a function of the relative tunnel cover (H/D) and of the ratio $\gamma D/c_u$, where γ is the specific weight of the soil and D is the tunnel diameter. For a 4m diameter tunnel, driven 20 m below the surface in a stiff overconsolidated soil (for example, London Clay) with an undrained strength of 200 kPa, the ratio $\gamma D/c_u$ is smaller than 0.4. For all practical purposes, this ratio may be taken as zero. For this condition, Davis et.al., (Op.cit., Figure 13), furnish values for N ranging from 5 to 6 (lower and upper bound), for H/D of 5. Therefore, under these circumstances, the tunnel collapse pressure would be given by:

$$\sigma_{\rm o}$$
- $\sigma_{\rm c}$ =(5 to 6). $c_{\rm u}$

Judging from field observations of tunnels built in London Clay, (approximately 4 m diameter and H approximately 20 m), Ward (1969) noted that, if the overload factor, OF, is less

than 2, then the short term ground response is elastic (Ward, Op.cit.:321). This was confirmed by Attewell and Farmer's (1974:391) observations regarding the Green Park tunnel in London Clay. Combining equations 2.11 and 2.13, one finds:

$$FS = \frac{1}{LF} = \frac{N}{OF}$$
 [2.14]

For N = 5 to 6 and OF = 2, the ratio N/OF can be understood as a minimum factor of safety (FS) below which a non linear ground response would predominate. Thus, for London Clay, the factor of safety would range between 2.5 and 3.0. Similar reasoning was used by Morgenstern and Eisenstein (1970) to investigate the limits of applicability of linear elastic theories to open cut excavations. They found a limiting factor of safety against undrained base failure of 1.5 to 2.0, above which a linear response would be expected.

Hence, from model test results and from field observations of shallow tunnels, it could be said that non-linear ground response is to be expected whenever the factor of safety against collapse is less than 2 to 3.

Unlike foundations, which are designed with factors of safety sometimes in excess of 3, shallow tunnels are built with factors of safety much lower than this. It will be seen later in this thesis, that tunnels are built frequently with factors of safety of around 1.5 or less, after equilibrium with the support is achieved. Current construction techniques allow releases exceeding 20 to 30% of the

original in situ stress. Tunnelling operations tend to bring about collapse of the ground much sooner than other geotechnical constructions. This is partly due to the stress changes the soil is forced to withstand upon tunnelling. As it was shown, a typical stress path for soil elements around a tunnel combines stress changes of a conventional laboratory extension test (in the radial direction of the opening) with those of a traditional compression test (in the tangential direction). This leads to a shorter path to soil failure. For non-hydrostatic in situ stress conditions, those points around the plane strain tunnel, which do not undergo rotation of principal stresses, exhibit an even faster path to failure (e.g., points located at the springline, for Ko smaller than unity). Soil structures undergoing appreciable yielding or exhibiting low factors of safety show non-linear responses (Morgenstern, 1975). The unavoidable stress release associated with tunnelling operations and the lower factors of safety found for this type of geotechnical structure, lead to conditions where the soil response will be predominantly non-linear.

2.3.4 Stress and Strain Changes Under Less Idealized Conditions

2.3.4.1 Stress Paths

The assumptions of plane strain and fully drained conditions are maintained, but now the effects of gravity, the free ground surface and a non-hydrostatic in situ stress

condition are considered. It will be seen that tunnelling operations entailing a proportional and gradual reduction of the in situ stresses at the opening will cause a more complex ground response.

For these conditions and also to account for the non-linear stress-strain behaviour of the soil, one needs a numerical procedure, such as the finite element method, in order to obtain the stress paths of points around the opening. Using the non-linear hyperbolic elastic model described by Eisenstein and Negro (1985), (further discussed in Chapter 5), it was possible to obtain the paths shown in Figure 2.4. Clearly, other constitutive models would provide slightly different pictures but the overall response would be fairly close to that which is shown in the figure. Details of the finite element code employed (using constant strain triangles), as well as the tunnelling simulation procedure will be given elsewhere in this thesis. The plane strain circular opening was subjected to a gradual reduction of the orginal in situ stress, with no support being installed. This was done incrementally, each stress (normal and shear) decrement amounting to 10% of the initial stress magnitude at each point of the tunnel perimeter, through an "incremental stress reversal boundary condition." The tunnel had a diameter of 4 m and a cover to diameter ratio of 1.5. The soil layer was assumed to be isotropic and homogeneous. In situ stresses were calculated for Ko equal to 0.8. The selected soil properties would be typical of a lightly

overconsolidated deposit, with zero cohesive strength and a friction angle of 30°. The groundwater level was assumed to lie far below the tunnel floor, so that fully drained conditions prevailed. A constant Poisson's ratio was assigned to the soil and a pair of Janbu's (1963) coefficients, K and n, were selected in such a way that a constant tangent modulus of deformation of about 31 MPa. before tunnel excavation, was obtained. Upon each applied stress decrement, this modulus was updated as a function of the normal stress level (defined in terms of the minimum principal stress in the plane) and of the shear stress level (defined in terms of the maximum principal stress difference in the plane) relative to the shear stress at failure. Certainly, this representation is a rough approximation of the actual soil behaviour, since no account is taken of the real plastic phenomenon associated with yielding (Morgenstern, 1975). The latter is represented here in so far as the non-linear elastic modulus of the soil changes as a function of the normal and shear stress levels. The simplicity of such a numerical model and the fact that it is reported to be used fairly successfully in practice (Christian, 1980), make it attractive for the present purpose. This is so, despite the fact that in its standard formulation the input parameters are obtained from laboratory tests following stress paths that are not related to those actually observed in the soil mass surrounding the opening.

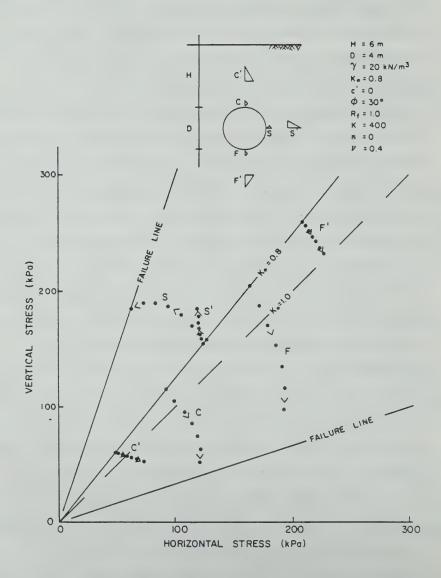


Figure 2.4 Stress Paths Around a Shallow Tunnel

Figure 2.4 shows the stress paths obtained for points C, S and F, at the crown, springline and floor, respectively, (elements located 0.25 m away from the cut profile) and for points C', S' and F', (elements at 3.0 m from tunnel wall at C' and F', and 2.5 m at S'). Although they are not principal stresses (except initially), the vertical and horizontal stresses were plotted in order to make the evaluation easier. Since the selected points are close to either the vertical or horizontal axis through the tunnel centre, both vertical and horizontal stresses have magnitudes very close to maximum and minimum stresses within the plane (less than 5% difference).

Each point of the stress paths represents the state of stress after each decrement of the in situ stress. Point "0" corresponds to the in situ condition and "6" to the final condition, at which a certain element of the finite element mesh reaches local failure. As the numerical model used has not been designed for simulation of failure control conditions, the stress paths shown represent stress changes before failure.

The paths followed at S, C and F are not dissimilar to those depicted in Figures 2.2 and 2.3. It is observed, however, that because K_{\circ} is different from unity, the principal stresses rotate at C and F between the first and second stress decrement, with no rotation observed at S. As a result, S goes faster towards failure, and this is attained after decrement number 6, before any other point

fails. Different behaviours would be noted depending on the in situ stress, geometry and ground properties, and different points may reach failure singly or simultaneously. If the soil strength was high and had a large cohesion intercept, the stress paths at C, S and F would end at the zero radial stress level with no failure being observed.

Although the magnitudes of the stress changes for points at farther locations from the opening are much smaller than at points closer to the tunnel, they will experience quite distinctive stress paths. At C', the changes in the vertical stress are smaller than in the horizontal stress. The stress path resembles that of a vertical extension laboratory test, under horizontal passive loading (passive extension test). At S', the stress path is similar to that of a conventional passive compression test, whereas at F', the path is close to that of constant mean normal stress with almost pure shear loading. Certainly, as the tunnel undergoes further unloading, these stress paths may also distort towards failure, in a similar way to C, S and F. However, they may be affected by the development of highly sheared zones or discontinuties in anticipation of the tunnel collapse.

Seneviratne (1979) and Karshenas (1979) carried out similar analyses, in an attempt to identify the drained stress paths at points around plane strain model tests.

These were conducted in normally consolidated kaolin and in dense sand. In both cases, modified versions of the Cam-clay

model were used. Test simulation included the effects of sample preparation and tunnel cutting. Examining the portions of the stress paths that correspond solely to the tunnel unloading (Seneviratne, Op.cit:Figure 6.12a, Karshenas, Op.cit:Figure 6.19 to 6.21), very similar pictures emerge. Despite the use of different constitutive models, their results agree quite well to what has been described herein. Seneviratne also performed undrained finite element analysis and noted that the total undrained stress paths are similar to the total drained stress paths, even though they pass through different points in the stress space (Seneviratne, Op.cit. Figure 6.12b).

Ng and Lo (1985) were also able to draw effective stress paths from an elastoplastic undrained finite element analysis of a shallow tunnel under plane strain conditions. Details of the finite element formulation, which takes into account an anisotropic elastic behaviour and a non-associated flow rule for plastic response and assumes a Mohr-Coulomb failure criterion, are given by Rowe et.al., (1983) and Ng (1984). Once more the stress paths are found to be very similar to those presented here. Ng and Lo go further in an attempt to identify which standard laboratory tests would better represent the stress paths they obtained numerically. They suggest that for a soil element at the crown, the effective stress path of an undrained or drained anisotropically consolidated extension test with axial stress decreasing would be similar to that obtained in the

numerical analysis. This is clearly a simplification and moreover, for other soil elements, no conventional triaxial stress paths are representative of the numerically obtained stress paths. These authors then suggest that "extreme" stress path tests bounding the "real" stress paths, should be conducted to evaluate stress path dependency of the ground.

Capellari and Ottaviani (1982) also used a non-linear elastic hyperbolic formulation to obtain representative plane strain stress paths around a shallow tunnel. They attempted to map the predominant stress paths around the opening. Their results are consistent with what has been shown here, although the division of the surrounding soil into just three stress path areas could be considered as an oversimplification. An accurate mapping would reveal a larger number of typical stress path areas.

Although the development of controlled stress path triaxial testing (Bishop and Wesley, 1975), using only servo mechanisms to ensure the follow up of a predefined stress path (Menzies et.al., 1977), enlarged testing capabilities, it seems to be quite an unlikely venture to actually follow all stress path possibilities around a shallow tunnel. Furthermore, the three-dimensional stress changes occurring in the soil, the unavoidable disturbances associated with sampling, the behaviour of soils under small strains, etc, pose additional difficulties which are possibly as relevant as the stress path dependency. So, except in very special

cases, a large degree of simplification will have to be taken in approaching a practical tunnelling problem. These factors and points will be further discussed in this thesis.

2.3.4.2 Ground Reaction Curves

The finite element analysis performed to obtain the stress paths depicted in Figure 2.4 can also furnish relationships between the radial stress and displacements, for different points around the tunnel perimeter. Figure 2.5 presents ground reaction curves thus obtained for points at tunnel crown (C), springline (S) and floor (F), which are typical for a shallow tunnel. As noted before, no unique response is observed around the perimeter, even for the case of a hydrostatic in situ stress state (see also Eisenstein, 1982 and Eisenstein and Negro, 1985). This clearly precludes any attempt to use the so called "Convergence Confinement" Method (Gesta et.al., 1980), that in its original formulation is strictly valid for ideally deep tunnels under $K_0=1$ conditions. The original concept of the ground reaction curve has been extended to account for a non-hydrostatic initial stress field for elastoplastic materials with a Mohr-Coulomb yield criteria (Detournay and Fairhurst, 1982), but the account of gravity and of the free ground surface effects have only been incorporated in an approximate form (for example; Daemen, 1975, Hoek and Brown, 1980:252). For a hydrostatic in situ stress condition, Wong (1986) used Daemen's simplified approach to include the gravity within the plastic zone only. He relaxed Daemen's original

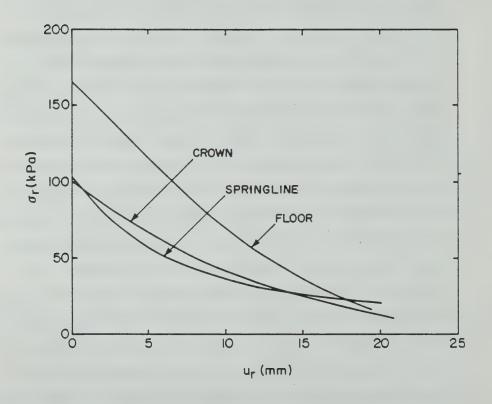


Figure 2.5 Ground Reaction Curves for a Shallow Tunnel

assumption of zero plastic volumetric strain by indroducing Ladanyi's (1974) average plastic volume strain and thereafter followed the approach of the latter author. He claimed (Wong, Op.cit, p.38) to have also included the effect of the free surface, but his derivation shows otherwise since he assumed a plastic zone of constant radius around the circular tunnel (Op.cit, p.39 and 41). This is in conflict with the development of a non-uniform plastic zone which occurs when the effects of gravity and of the free ground surface are correctly taken into consideration. In brief, Wong's formulation for ground reaction curves is another approximate solution, furnishing good results for an ideally deep tunnel, but with limited practical interest for a shallow tunnel, in view of its inherent limitations (Wong, Op.cit, p.41,42).

Numerical techniques seem to be the only effective means currently available to allow representation of stress-displacement relationships for points around shallow tunnels. It seems unlikely that any closed form solution will ever account for the stress and strain changes illustrated in Figure 2.3, and also include other relevant features of a shallow tunnel in soil. Even finite element codes are not always able to treat in a satisfying way, the boundary value problem involving the pseudo strain softening behaviour at decreasing stress levels, as is the case shown in Figure 2.3b. But if interest is limited to pre-failure conditions, the finite element method can be used to extend

the original concept of ground reaction curves, as suggested by Lombardi (1980:254), Duddeck (1980:247), Eisenstein (1982) and Eisenstein et.al.,(1984). The stress-displacement curves thus obtained would then be an end result of some fairly realistic stress-strain changes developing in the ground, and would reflect the influence of dominant features controlling the shallow tunnel response under less idealized boundary conditions.

2.3.4.3 Shear Strain Development

The development of shear strains around a plane strain shallow tunnel upon gradual unloading can be examined by numerical techniques, model testing and field observations. Preceding tunnel collapse, the growth of high shear strain zones are frequently observed. The difficulties associated with the numerical simulation of localized deformations are recognized and these are being the subject of ongoing studies. If the evolution of these strains up to tunnel collapse is a matter of interest, then it seems more instructive to examine observations made on models or prototypes.

Table 2.2 summarizes some observations made in plane strain model tests in Cambridge (UK) with soil displacements monitored by means of radiographic or photographic imagery. It also includes data derived from field instrumentation of two tunnels. Despite the fact that shear strain distributions for undrained conditions are very similar to those under drained conditions (Seneviratne, 1979:63), the

: 53:	2	1	1 -	3:5
Sheer Strain Contours (N)	7	2		, v , v , v , v , v , v , v , v , v , v
Max. Shear Strain (%)	Œ	26	•	90
n(5)	1.36	3.99	3.10	3.30
u (4)	∞ ≠	85 55	2.0	(10)
LF (3) and (FS)	(1.49)	0.96	0.81	0.95
0 (2) (KPa.)	76.1	51.7	•	
H/D d ₀ (1)	926	138	9	
#/D	0.67	0.95 138	1.20	
D (mm)	09	09	09	
× 0	9.64	9.0	~ 10	
E ₀ (HPa)	٠	٠	£ (6)	
.+ 5	50	20	15.4	
C (KPa)	%	56	9 (2)	
6011	n.c. kaolin	n.c. kaolin	o.c. kaolin (OCR = 3.5)	
Data Frim	mtatic model	etatic model	static model	
Author	(1979)	Seneviratne (1979)	Cairncross (1973) (quoted by Akkinson, et al. 1975)	
Саме	1 (02)	2 (03)	3 (D4)	

Table 2.2 Shear Strain Distributions Observed in Model Tests and in Actual Tunnels in Drained Conditions

1 5 3 1	1	la,			
Shear Strain Contours (%)		12.00	2	3,52	22 3 3 3
Max. Shear Strain (%)	~	₹	m	O	50
u(5)	0.53	2. 24	7.33	0 0	~
1	(10)	1.45 2.24	0.84 7.33	1.71 14.88	3.0
(kPa) and (FS) (mm)	0.60	0.90	~10 (1.0)	0.1.0	0.96
0 (2) (KPA)	63		ø	•	0.007
H/D 00 (1) (KPa)	140		0 2 0 0	2 10	~
II/D	0.35		1.0 210	0.5	1.48
D (mm)	09		9	09	09
K ₀	~1.0		o .	0.	0.2(7) 60
E ₀ (MPa)	(6)		110	011	1
·+ 3	15.4		ž,	~20 ~	~\$0 ***
Cu (kPa)	\$ E		1		1
Sol 1	0.c. kaolin (OCR = 3.9)		dense mand (e ₀ = 0.52)	dense sand (e ₀ = 0.52)	dense sand (e ₀ = 0.52)
Data From	static model		static model	stellc model	static model (self weight)
Author	Orr (1976) (quoted by Orr et al 1978)		Pocts (1976) (quoted by Karshenas, 1979)	Potta (1976) (quoted by Karahenaa, 1979)	Atkinson and Potts (1977)
Cane	-		\$ (05)	(90)	(70) 7

Table 2.2 Continued

53		"		1 -	
Shear Strain Contours (*)	100 P	11 1 1 1 1 1 1 1 1 1 1 1 1 1 1 1 1 1 1	2 2 2	430	3
Max. Shear Strain (V)	2	0	5	ž	
η ₍₅₎	1	1	9.	~0.6	ent
u (4) (mm)	1	3.3	~330 ~7.8	~ 50	sp lacem
LF (3) and (FS)	1.0)	(1.10)		,	e this dir
(kPa)	1	0.010	•	t	Uniform tunnel pressure at collapse "Cron" settlement at a given LF or FS; in model tests this displacement is taken at a point D/10 above tunnel crown Maximum Observed Acc. to Sketchley (1971) data Assuming zero displacement at the floor
00 (1) (KP4)	. 180 ∞	6	-300	480	FS ₂ in
D H/D 0 ₀ (1) (mm) (KP4)	1.48 ~ 180	. 48 1.8		9.3	LF or nel cro
D (mm)	09		6, 450	2,560	given lye tung ve tung lata
, M	0.2(7)	0.3(7)	35*(7) 35(7) 0.5(7) 6,450 1.81 ~300	0.8 2,560 9.3 ~480	Uniform tunnel pressure at collapse "Cron" settlement at a given LF or FS; takes at a point D/10 above tunnel crown Acc. to Sketchley (1973) data Assuming zero displacement at the floor
F ₀	1		35(2) 0	51	el pres lement oint D, rved chley (
·• £	~ \$0 *	4 5*	35*(7)	16•	Uniform tunnel pr "Crown" settlemer taken et a point Maximum Observed Acc. to Sketchley Assuming zero dis
(kPa)	- (ı		0,0	Unifo "Crow taken Maxim Acc.
Sot1	(e ₀ = 0.52)	loose sand (e ₀ = 0.69)	tunnel mainly in dense sand, cover of stiff to medium clay	"soft" till	afety (4) sent (6) 136 (10) 1-9
Data From	model model	static model (self weight)	Washington Metro (C-Line)	Edmonton sever "soft" till	Initial vertical across at tunnel Load factor and factor of safety Dissensionless crown displacement Acc. to Asárajah (1973) data Acc to Orr et al (1978), p. 168-9 From Karahenas (1979), p. 168-9
Author	Atkinson and Potts (1977) Atkinson, Potts and Schoffeld (1977)	Atkinson, Brown and Potts (1977)	Hangmire (1975)	El-Mahham (1980)	(1) Initial vertical across at tunnel axis (2) Uniform tunnel pressure at collapse (3) Load factor and factor of safety (4) "Cron" settlement at a given LF or the safe and spoint D/10 above tunnel of (3) bimenatonless crown displacement (6) Maximum Observed (1) Acc. to Nadarajah (1973) data (9) Acc. to Corte tal (1978), page 136 (10) Assuming sero displacement at the fill from Karaheraa (1979), p. 166-9
Case	Œ	o	9	=	Notes:

Table 2.2 Continued

table includes only data believed to represent predominantly drained behaviour.

Except for case 8 the tests were performed under static conditions, with the models subjected to uniform vertical surface loads, as well as uniform lateral loads. Shear strain distributions at low load factors (LF smaller than 0.5) or high factors of safety, are difficult to obtain as the observed displacements (from which strains are derived, using approximate techniques) are small. Therefore, the recorded distributions represent mainly pre-collapse conditions (LF greater than 0.6 to 0.7). It is seen that the shear strain distribution under these conditions is mainly controlled by the presence of the free boundary surface. Indeed, in cases 1 to 7, the gravitational stress gradient can be neglected, as the self-weight stress in the model material is negligible in comparison to the imposed stress field.

The shear strain distributions (for lower load factors) are controlled by the initial yielding processes and its propagation. As such, it is mainly determined by the original in situ stress (K_o value), the geometry (H/D), the strength of the ground mass and the amount of stress release allowed. Wong (1986) proposed a method to assess behavioural modes of yield propagation mainly for cohesionless soils. However, the final shear strain distributions at or around collapse, as shown in Table 2.2 are all very similar, always showing highly strained narrow zones travelling up from the

tunnel sides towards the surface. Complete tunnel collapse will occur if these zones reach the ground surface but the actual collapse mechanism will differ for distinct geometric and soil types as will be seen later. However, they encompass an overall similarity. The inclusion of gravity (case 8) through centrifuge testing does affect the shear strain pattern and its magnitude, possibly not as much as by itself but by the larger stress induced. But again, the overall picture is not much changed. In other words, shear strain propagation and collapse mechanism development is mainly controlled by the presence of the free ground surface and by the relative position of the opening.

Most of the tests represent very shallow tunnels (H/D smaller than 1.5). Undrained centrifuge tests with larger covers (H/D equal to 3.1) carried out by Mair (1979), show once more comparable response. Clearly, the high strain zones may not reach the ground surface for stronger soils or deeper tunnels. But even for the latter, the strain pattern is again similar (case 11).

The zones of high shear strain concentration tend to develop and propagate very rapidly upon tunnel unloading. This occurs for factors of safety lower than 1.4 in normally consolidated soft clay and less than 1.05 in dense sands. At this point, however, it seems worth examining the amount of displacements associated with these high strain situations. It is likely that they also will be very high.

Table 2.3 provides details of some plane strain static model tests carried out at Cambridge under drained conditions. In all cases, the field stress was simulated by the application of external loading on to the model. A flexible rubber bag installed in the circular opening allowed a uniform fluid pressure to be applied against the tunnel perimeter. This pressure was gradually reduced and the displacement field around the opening up to tunnel collapse was observed by means of radiography techniques. As the tunnel collapse pressure is known for each test, it is possible to identify the factor of safety (FS) at each stage of the internal pressure release. This factor can be related to the radial displacement (u) of the nearest point to the opening crown (on average, at 0.1 D above crown point, along the vertical axis). Figure 2.6 shows observations between crown displacements (normalized to tunnel diameter) and corresponding factors of safety for different soils and H/D ratios. In all cases, a very pronounced drop in safety is observed in the early stages of testing, which is associated with limited displacements.

The so called "loss of ground", defined as the volume of soil crossing the ideal cutting profile of the tunnel, is sometimes estimated by means of Cording and Hansmire's (1975:575 and 580) approximate rule. This volume is expressed as a percentage of the tunnel volume. If the displacement is measured at a point situated at a distance y=0.1D above the crown, the loss of ground is given by:

Test	Author	Soil ⁽¹⁾	(2) (KPa)	σ _C (2) (KPa)	H/D
D1	Seneviratne (1976)	n.c. kaolin	138	82.1	0.50
D2	Seneviratne (1976)	n.c. kaolin	138	76.1	0.67
D3	Seneviratne (1976)	n.c. kaolin	138	51.7	0.95
D4	Cairncross (1973)	o.c. kaolin	140	0	1.20
D5	Potts (1976)	dense sand	210	6	1.48
D6	Potts (1976)	dense sand	210	7	1.48

Notes: (1) All static model tests; fully drained condition; tunnel diameter D = 60 mm

- (2) For soil properties see Table 2.2
- (3) See notes (1) and (2), Table 2.2

Table 2.3 Plane Section Model Tests in Clay and Sand Under Drained Conditions

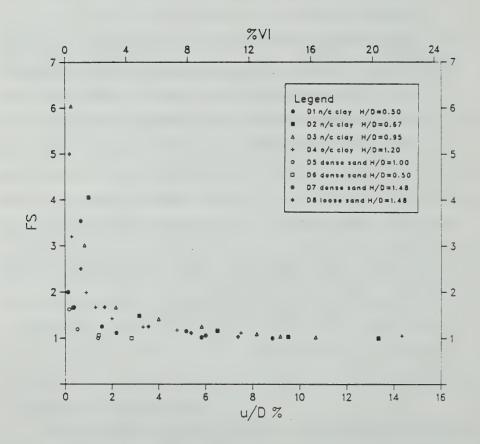


Figure 2.6 Relationship Between Crown Displacement and Factor of Safety in Drained Model Tests

$$%V_1 = \left[2 \left(\frac{D}{2} + y\right) \right] u / \pi \left[\frac{D^2}{4}\right] 100$$
= 152.8 u/D (%)

Figure 2.6 also indicates estimated ground losses for a given FS, calculated at a given stage of tunnel pressure reduction. Experience shows that despite the fact that the ground also undergoes considerable volume changes, which might be either predominantly expansive or contractive, the volume of the settlement trough at the surface is directly proportional to the volume of ground lost into the tunnel. Accordingly, as the tunnel seviceability is related to an acceptable ratio u/D, the damage potential and the degree of disruption at the surface is connected to the maximum loss of ground (%V,) that can be accepted. For most tunnels, seviceability is jeopardized if u/D exceeds 3 to 4%. Before these values are realized, however, the surface settlements are likely to be excessive in an urban environment in most instances. The corresponding limits of loss of ground are 5 to 6%. For an idealized condition of no volume change in the ground, the volume of settlement at the surface would be equal to these values of losses of ground. A "poor construction quality" as defined by Negro (1979), who extended Peck's et.al., (1972) definition of quality of construction as applied to tunnelling, corresponds to settlement volumes greater than 3%. Hence, the 5 to 6% losses of ground would likely be far too excessive. For the normally consolidated and overconsolidated clay samples tested, a factor of safety greater than 1.4 to 1.7 would

probably be sufficient to ensure tunnel serviceability by keeping the ground losses and surface settlements within acceptable limits. A lower limiting factor of safety could be postulated for dense sand, but since this type of material collapse is attained in an appreciably abrupt fashion, a limiting factor of safety for this soil could be taken as 1.2 to 1.3, for most practical purposes.

The concept of a limiting factor of safety based on acceptable deformations in a geotechnical structure is not new. It has long been used in foundation engineering. In embankment dams, it is nowadays customary to refer to a limiting rate of horizontal movements per metre rise of fill, as a controlling parameter, rather than the more traditional factor of safety for collapse (Penman and Charles, 1974 and Penman, 1986). Resendiz and Romo (1972) proposed a theoretical relationship between factors of safety from limit equilibrium analyses and the maximum horizontal displacement at the slope of an embankment, calculated by the finite element method. In tunnels through soil, this concept has not been introduced so far, possibly because it is not as evident as in other types of structures. Clearly, the factor of safety is very much dependent on the stress-strain response of the ground. Soils exhibiting pronounced post-failure stress reduction (e.g., sensitive clays), would possibly require limiting factors of safety different from the above, in order to avoid progressive failure. The soil stress-strain response is very path dependent and it was shown that no unique stress path exists around a shallow tunnel. This makes attempts to define limiting factors of safety for tunnels on the grounds of acceptable deformation, a very complex task. A way out is to rely on model testing, but even here the tunnel simulation is still highly idealized.

Comparing the suggested limiting factors of safety based on an acceptance criteria for deformation in the soil, with those previously identified for the development of high shear strain concentrations, it is seen that the former are higher than the latter. If design and construction ensure good ground control conditions (limited losses of ground and limited tunnel convergences), the development and propagation of the zones of high shear stains is unlikely or limited. Results from undrained model tests on normally and overconsolidated kaolin (Table 2.4 and Figure 2.7) also confirm these findings, suggesting that this conclusion can be fairly generalized, except possibly, for soils exhibiting strong strain softening behaviour.

Referring again to Table 2.2, it is noted that around collapse, the maximum shear strain zones progress from the opening shoulders more or less at a 45° angle between crown and springline, pointing up towards the horizontal surface. The magnitude of the maximum shear strain ranges from 3 to 24% and varies with the soil type and the geometry. Based on the available information, no shear band was identified in any of the cases reported in Table 2.2, except when a full

Test	Author	Test Type	Soil	Cu (kPa)	E ₀ (2)	$ \begin{array}{cccccccccccccccccccccccccccccccccccc$	σ ₀ (4) (kPa)	σ _C (5) (kPa)	H/D
10	Seneviratne (Seneviratne (1979) static	n.c. kaolin	26	9	0.64	138	60.4	1.00
0.2	Seneviratne (Seneviratne (1979) 🥳 static	n.c. kaolin	26	9	0.64	138	46.0	1.45
0.3	Mair (1979)	centrifuge (75 g)	0.c. kaolin (OCR = 2.8)	24	3.6	3.6 1.0	150	76.0	1.67
0.4	Mair (1979)	centrifuge (65 g)	0.c. kaolin (OCR = 1.8)	25		5.2 0.82	249	116	3.11

Notes: (1) Tunnel diameter D = 60 mm in all tests

?) Undrained "initial tangent modulus"

Ratio between effective horizontal to vertical stress (derived from measurements of negative pore water pressure, at the end of equilibrium stage in Mair's tests) (3)

(4) Total vertical stress at tunnel axis

(5) Uniform tunnel pressure at collapse

Table 2.4 Plane Section Model Tests in Clay Under Undrained

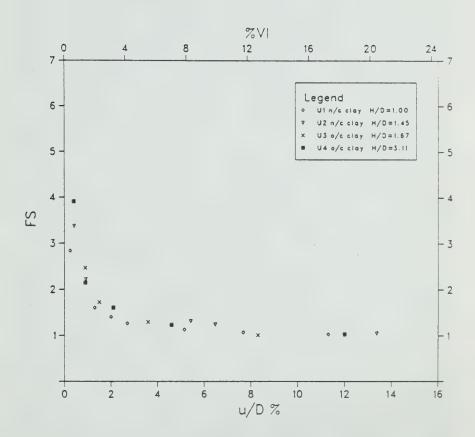


Figure 2.7 Relationship Between Crown Displacement and Factor of Safety in Undrained Model Tests

collapse condition was observed (case 8, FS=1, Atkinson and Potts, 1977:321). However, in some other model tests carried out in Cambridge, thin shear bands were detected in the soil, shortly before collapse. This was the case in some three-dimensional tunnel loading model tests performed by Casarin (1977:46). The soil was an overconsolidated kaolin (OCR=3.5), with K close to unity and an undrained cohesion of about 60 kPa. The shear bands appeared ahead of the tunnel face, dipping into it, in two undrained tests, at factors of safety lower than 1.11 (for lining placed one diameter behind the face) and 1.25 (for lining placed at the face). If these discontinuities are not clearly visible in the displacement field, they will hardly be identified through the shear strain contours. These contours are obtained on the assumption of constant (uniform) strains within each triangular element defined by three adjacent lead or silvered markers. Usually Cambridge researchers space the markers 10 mm apart. Casarin (1977) spaced them 5 mm apart, but even with this denser marker grid, his shear strain contours (Casarin, Op.cit, Figures 5.14 and 5.26) fail to identify the shear band, which was visible in his experiments. The reason for this is that the thickness of the shear band is far less than the spacing between markers. Roscoe (1970) proposed that its thickness is about 10 times the average grain size of a granular soil, while Vardoulakis (1986) suggested a factor of 16. However, observations made by Morgenstern and Tchalenko (1967) on shearbands in kaolin

samples under direct shear, indicate thicknesses of 0.1 to 0.2 mm (about 50 to 4000 times the size of a kaolin particle). The assumption of constant strain elements and the use of markers spaced at distance one or two orders of magnitude wider than the shear band thickness, allow the discontinuity to go unnoticed by backcalculated shear strain contours. The extension of Casarin's shear bands was of the order of one tunnel radius, and the maximum shear strain was calculated as 30%. Actual shear strain, within the shear band, could well have been one or two orders of magnitude higher. If formation of these thin shear zones is a matter of concern, different modelling techniques and results interpretations should be implemented. However, the subject seems to be of limited practical interest if tunnel construction is undertaken avoiding near collapse conditions. Localized shear band formation may be possibly precluded if the factor of safety against tunnel collapse is higher than about 1.5. More investigations are, however, needed to generalize this statement.

Even when this phenomenon is not present, it is a difficult task to map the shear strength mobilization around the opening, or else to define a "failure zone" from shear strain contours. Failure strains in soils are difficult to be properly assessed from laboratory testing, as they depend on the apparatus boundary conditions, type of equipment, shape and size of the testing sample, etc. Uniform straining at failure is normally not guaranteed. Moreover, the shear

strain at failure is very sensitive to the stress path experienced by the soil element before reaching failure. It was shown that the stress path around a plane strain tunnel is not unique and varies considerably from point to point. Furthermore, there is still the additional practical complication that these stress paths may differ appreciably from those normally followed in usual laboratory testing. El-Nahhas (1980) (case 11, Table 2.2) favoured a compromise, choosing a range of maximum shear strains at failure, based on tests run along selected stress paths extremes (active and passive compression tests).

The foregoing discussion showed that there is evidently a correlation between the factor of safety and ground displacements, particularly those at the tunnel crown. These displacements are affected by soil stiffness and strength, the geometry (H/D), the in situ stress condition (K_o) . Differences in these parameters may explain the scatter of data shown in Figures 2.6 and 2.7. It seems convenient to introduce a dimensionless displacement defined as:

 $U = \frac{U \cdot E_o}{D \cdot \sigma_{ro}}$ [2.16]

where, u is the radial displacement at a point of the tunnel perimeter (herein, only those at tunnel crown will be referred to), $\rm E_o$ is an initial tangent modulus of elasticity, $\sigma_{\rm ro}$ is the initial radial stress at this point (the vertical in situ stress at the crown, for instance) and D is the tunnel diameter. In a drained analysis, $\rm E_o$ is taken as a drained modulus and $\sigma_{\rm ro}$ is an effective stress. In an

undrained analysis, ${\rm E_o}$ would be an undrained modulus and $\sigma_{\rm ro}$ a total stress.

Having estimated such initial deformation moduli, on the basis of the information provided by the various authors cited in Tables 2.2 and 2.4, it is then possible to calculate the dimensionless displacement of the crown. This displacement is calculated for each decrement of tunnel pressure, for each model test, and is related to the current factor of safety. Figure 2.8 shows this relationship for all model tests discussed, including those performed under drained (series D) and undrained (series U) conditions. The introduction of a parameter related to soil stiffness reduces the test result scatter slightly, as it should. For a typical factor of safety of 1.5, the corresponding range of U would be 0.5 to 1.8, against a u/D range of 0.2 to 3.8%. Regardless of the strengths of the soils tested, U values in excess of 1.8 will generally be near the collapse condition with high shear strain concentration. The so called "good ground control conditions", would correspond to smaller U values, typically 1.0 or less. Consequently under equivalent conditions and for the same factor of safety, a softer soil may experience larger crown displacements than a stiffer soil. Indeed, the model tests show that the final collapse is attained sooner in terms of displacement for stiffer soils.

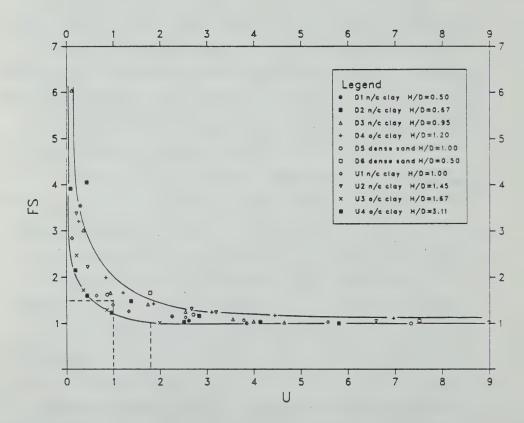


Figure 2.8 Relationship Between Dimensionless Displacement of the Crown and Factor of Safety Observed in Drained and Undrained Model Tests

2.3.4.4 Volume Changes

Unlike the development of shear strains, the time independent volume changes experienced by the soil upon tunnelling may differ from one soil type to another. The magnitudes and distribution of volumetric strains in the ground mass will depend on a number of factors. These include the mean normal stress level, the shear stress level, the stiffness of the surrounding soil (and lining if any), the stress history of the soil, the presence of the stress free ground surface, gravity and others. Volume changes due to pore water pressure changes will only be discussed briefly in this section.

An increase in shear stress may cause either compression or dilation, depending on the nature of the particular soil. A reduction in the mean normal stress will tend to cause swelling. Although the relations between volume changes and stress changes around tunnels are difficult to anticipate, it is tempting to generalize the observations made in model tests, performed under drained conditions.

Figure 2.9 shows the volumetric strains for some of the cases presented in Table 2.2. Magnitudes of strains are shown as a percentage, dilation being indicated as negative, contraction positive. Distributions (a) to (d) were obtained from static model tests, whereas (e) was obtained from centrifuge testing. Distribution (f) refers to the final volume changes derived from field observations made in the

first tunnel of Washington Metro (C-line). Most of the diagrams correspond to pre-collapse conditions, where the high degree of shearing above the tunnel may dominate and control the volume changes. Clearly, different pictures would arise for higher factors of safety (or smaller reduction of the tunnel pressure). Nevertheless some conclusions may be attempted.

Volume changes in clays depend significantly on changes of both the mean normal stress and shear stress. Soft, normally consolidated clays (Figure 2.9a and b), will frequently experience volume reduction upon tunnelling under plane strain conditions. For this type of soil, if the ground cover is small and insufficient to attenuate the straining, the tunnel collapse is reached soon after local failure is attained (somewhere around points C and D in Figure 2.3). Under these circumstances, the reduction in mean normal stress is therefore limited and the associated swelling is insufficient to balance the characteristic contraction due to the shearing and yielding observed in this type of soil. Results of tests by Seneviratne (1979), shown in Figures 2.9a and b seem to confirm this reasoning. The test with larger cover exhibits some dilation beneath the tunnel floor, which is unobserved in the shallower tunnel. In both cases, the resulting contractive volumetric strains were equal to or less than 6%, near the collapse condition.

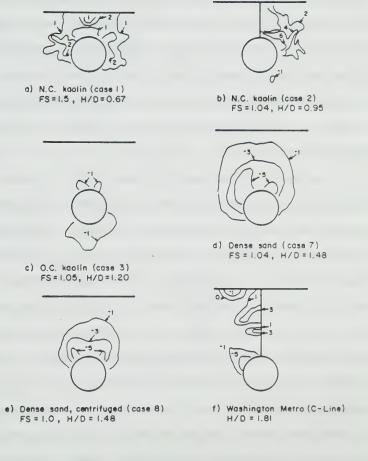


Figure 2.9 Distribution of Volumetric Strains around Shallow Tunnels

NOTE: See Table 2.2 for details. Dilation with negative sign.
Numbers refer to volumetric strain in %.

On the other hand, stiffer overconsolidated clays will generally exhibit volume expansion near tunnel collapse (Figure 2.9c). This class of soil frequently experiences dilation upon shearing, which is further enhanced by the swelling associated with a decrease in mean normal stress. The model tests conducted in Cambridge, using kaolin with an overconsolidation ratio of 3 to 4, show, however, that the magnitudes of the expansive volumetric strains were small (less than 1% as shown in Figure 2.9c, for a near collapse situation).

Volumetric strains in loose or dense sands are mainly controlled by changes in shear stress but changes in mean normal stress also have some influence. Contraction is, therefore, expected in loose deposits and dilation in dense ones. Static and centrifuge model tests carried out in dense sand (Figure 2.9d and e) confirm this. Also known is the fact that in sands, the rate of dilation increases as the magnitude of normal stress decreases. This may explain the differences observed in the distributions of volumetric strains between Figure 2.9d, where the results are from a static test with σ_{o} equal to 2 kPa and Figure 2.9e, which are from a centrifuge test with σ_o equal to 180 kPa (Atkinson and Potts, 1977:321, see Table 2.2). The proximity of the ground surface makes the shear strains concentrate above the tunnel, as shown previously. The lower normal stress level above the tunnel combined with the higher shear straining in this region, cause the higher dilation rates to

be above the tunnel, rather than anywhere else (Figures 2.9d and e). The effect of the normal stress level on the rate of dilation suggests that for two tunnels driven in dense sand, with the same ratio H/D, but at different depths, the soil around the deeper one will experience a smaller specific volume increase (total volume change divided by the tunnel volume), all other conditions being equal. Also, as it will be seen later in this chapter, the volume increase above the tunnel can be of such a magnitude that local collapse of the tunnel crown may occur, triggering a progressive mechanism that can lead to a complete collapse of the tunnel.

Figure 2.9f presents volumetric strains calculated from field measurements in the first tunnel of the Washington Metro at Lafayette Park, (Hansmire 1975:77). The tunnel was driven through dense sand and gravel in the upper half of the section and interbedded sands and clay layers in the lower half. Tunnel cover was a stiff to medium silty clay with layers of silty sands. The mixed ground condition and the presence of the lining may explain the more erratic volumetric strain distribution. However, the region above the crown seems to have experienced an overall volume increase, fairly typical for the soil types encountered there. The magnitudes of these strains (1 to 3%) compares well with those measured in model tests in dense sand and in overconsolidated clay.

Departures from the modes of behaviour just described would be expected for some special soils such as very

fissured, sensitive and collapsible clays, but no attempt will be made to address them in this general discussion.

The practical significance of the study of volumetric strains in the soil around a shallow tunnel, was briefly addressed in Section 2.2. Ideally, if the ground experiences no volume change upon tunnelling, the volume of the surface settlement troughs (V_s) would equal the volume of ground lost into the tunnel (V_1) as defined previously. Overall volume changes in the soil will make V_s greater or smaller than V_1 , according to whether the overall ground response is mainly contractant or dilatant, respectively.

Hansmire (1975:92 and 192) integrated the volumetric strains calculated in the Washington D.C. Metro tunnel through dense sands and was able to identify an overall expansion , despite some significant localized compression in lateral zones adjacent to the tunnel (Figure 2.9f). Cording and Hansmire (1975:395) extended their investigation to other single tunnels, using instead their approximate correlation to estimate the loss of ground (Equation 2.15). They noted that usually in medium to stiff clays, the volume of the settlement troughs was approximately equal to the volume lost into the tunnel. In softer saturated clays, the volumes were equivalent under undrained short term conditions, but a substantial amount of time dependent volume change may occur, leading to V greater than V,. These facts are consistent with observations made in model tests. Those authors pointed out further, that, it is mainly in granular soils that appreciable time independent volume changes may develop. Overall dilation of up to 50% of the volume of lost ground can be observed in dense sands. In loose sands, volume decrease can occur above the tunnel. Negro et.al., (1985:252) estimated a total volume decrease of almost 90% of the total volume loss (calculated as 0.42% of the tunnel volume), in an early section of a large NATM tunnel (D=10 m, H/D=0.65). This tunnel was driven for the Sao Paulo Metro, Brazil, under a loose sand cover (SPT = 1 to 6) interbedded with medium clay lenses. The large volume decrease occurred despite some cement-clay grouting above the crown, undertaken before tunnelling.

Heinz (1984:44) extended Cording and Hansmire's (Op.cit) survey on overall volume changes, by including data from a large number of NATM tunnels. He pointed out that, notwithstanding the possible inaccuracy of Cording and Hansmire's correlation for estimating V_1 (also noted by Attewell, 1977:897), the ground, in most NATM tunnels, exhibits an overall reduction in volume (around 50% of V_1). But in all fifteen NATM cases analysed, the losses of ground were smaller than 1.5% of the tunnel volume. Heinz (Op.cit:45) suggested that tunnels excavated by the NATM method may create displacement fields dissimilar to those observed in shielded tunnels and which ultimately lead to the overall ground contraction which is frequently observed. Negro et.al. (1985:58) also detected volume decreases of up to 30% of V_1 in other sections of the same NATM tunnel for

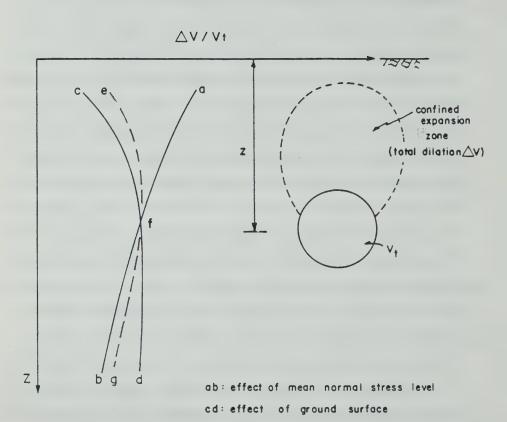
the Sao Paulo Metro, which were in a stiff fissured clay, but this behaviour was attributed to a partial drainage of the saturated clay with its associated volume changes, rather than to a time independent response. It may be argued that some of the tunnels quoted by Heinz may have also undergone a similar history, particularly in cases where dewatering well in advance of construction was not undertaken. Although an attempt is normally made to separate the time dependent from the time independent settlements in tunnels driven below the ground water level, this task is not always simple. This subject will be further addressed later on.

Eisenstein and Negro (1985), reporting three case histories of tunnels driven with different construction technologies, under a lateritic porous clay cover, mentioned the contracting nature of the overall volume change observed in the ground. This could be possibly attributed to the more or less "collapsible" structure of the surficial porous deposits frequently found in tropical environments.

Based on the effect of the mean normal stress level on the rate of dilation of sand as mentioned before, it is possible to speculate how the volume changes will develop above a given tunnel in a deposit of uniform dense sand. The study would be done with varying tunnel depths, for a fixed amount of stress release which would not cause failure. Total volume changes, ΔV , will be scaled to the volume of

the tunnel, V, to represent a specific volume change, $(\Delta V/V_{_{\! +}})$. Assume initially that the ground zone experiencing expansion above the tunnel is entirely surrounded by non expanding soil (Figure 2.10), or else, that the tunnel is sufficiently deep to have that zone not intercepting the ground surface. The specific volume change will decrease as the tunnel depth increases, as shown schematically by curve 'ab' in Figure 2.10. However, as the tunnel depth reduces, the expansion zone is intercepted by the ground surface and the integration of the volumetric strains that furnishes ΔV , is performed over an increasingly reduced area. A reduced soil cover may not be able to undergo sufficient expansion in order to compensate for the ground lost into the tunnel. Therefore, the specific volume changes should decrease as the tunnel depth decreases, possibly according to curve 'cd' in Figure 2.10. The combined effect of the mean normal stress level and of the ground surface on volume changes with tunnel depth, can possibly be described by the curve 'ef' in that figure. For a given tunnel size, the position of the inflexion point 'f' with respect to the surface, will be a function of the prescribed amount of stress release at the tunnel perimeter or, else, of the magnitude of the established factor of safety.

There is some limited evidence supporting this conceptual model. Hansmire (1975:192), from by his analyses of the behaviour of the Washington, D.C. Metro tunnels, maintains that the response depicted by the line 'cd' is



efg: both effects combined

Figure 2.10 Schematic Representation of Specific Volume Changes with Varying Tunnel Depth

correct. The maximum soil cover in this project was equal to 2.5D, and the construction technique used allowed a substantial stress release in the soil. Possibly due to these facts, Hansmire did not record that the volume expansion could not go on increasing with tunnel depth increasing. Poor ground control conditions led to crown settlements in excess of 300 mm and lining load measurements suggest that the in situ stresses were reduced by as much as 80% (Hansmire and Cording, 1985:1317). Localized collapse of the sand at the crown may have occurred and the soil zone undergoing substantial dilation reached the ground surface (Figure 2.9f).

On the other hand, model test results carried out in Cambridge and shown in Figures 2.9d and e, tend to support the behaviour represented by the curve 'ab' in Figure 2.10, or more properly by the portion 'fb', since in these cases the soil zone undergoing significant expansion seems to have been almost fully confined.

If one expects to take advantage of the ground volume expansion to account for the attenuation of ground losses and possible reduction of surface settlements, the model summarized in Figure 2.10 is of some relevance. In practice however, this is a risky venture, since proper assessment of the magnitude of ground expansion is a difficult task, where mixed soil conditions may frequently hinder expected ground dilation. Moreover, large dilations in the soil will be normally induced when substantial stress release is

permitted during tunnelling operations. This corresponds to a condition somewhere around points C or D in Figure 2.3. In other words, it is a near collapse situation, and is one that should normally be avoided in an urban tunnel. If these circumstances arise it may lead to the development of "loosening", as will be described later. The ground above the tunnel, which has already experienced considerable expansion, will undergo further volume increase, and the dense sand, in consequence, will become "looser". The term "loosening", frequently used in rock tunnelling (Szechy, 1967:136), is somewhat misleading in soils. A dense sand may remain dense even after the development of expansive volumetric strains as high as 5%. It does not become really loose, but simply less dense.

2.3.5 Idealized Lining Action

2.3.5.1 Preamble

Throughout this section a two dimensional plane strain condition will be assumed. As a rule a tunnel in soil will always require some form of support to keep the opening stable both in the short and long terms. This support is normally provided by some form of lining, which is usually continuous and for the sake of simplicity, will be assumed herein, to be a circular ring behaving as a linear elastic material.

The inclusion of a body with a stiffness different from that of the surrounding medium will change the overall

system stiffness. Some form of interaction between the soil and lining will occur, and the stress and strain change mechanisms discussed in the three previous sections, will be affected to a larger or smaller degree, depending on the relative stiffness of the soil to the lining. An early inclusion of a more rigid body within a softer medium, will cause the unbalanced loads generated by the tunnelling operation to be transferred to that body³. An equilibrium condition may eventually be reached (otherwise unattainable on the premise of an unstable ground in plane strain conditions).

Some extreme conditions are going to be briefly investigated herein. The first refers to the form of radial contact between the soil and its lining, at the instant the latter is installed. At installation, full radial contact may or may not exist. It is quite clear that a full radial contact (complete embedding by the soil) should always be preferred in practice, in order to prevent any form of load concentration (e.g., "gravity" loading) leading to unnecessary additional bending of the lining. This is more easily achieved with concrete linings cast in place against the cut ground profile (whether pumped or sprayed concrete). But for pre-cast concrete segments, steel sets and wooden lagging, steel or cast iron liner plates, some sort of lack in radial contact may frequently exist, as the cut profile

³ By "softer medium" one should understand the ground and the opening inclusive. Otherwise, the lining is normally "softer" than the ground it replaces, since some sort of deformation is always expected after its installation.

is hardly as regular as the outside profile of the liner. To minimize the voids behind it, prompt grouting or lining expansion is usually specified and undertaken. But, as a rule some space is always left behind the lining. The full radial contact condition, along all points of the soil lining interface will be referred to as "good lining contact". The condition of partial or no radial contact along the tunnel perimeter will be called "poor lining contact".

The second extreme condition refers to the form of tangential contact between the soil and lining, with the tacit assumption that a full radial contact exists. Two extreme conditions are now visualized: no slip and full slip between the soil and its support. The first corresponds to an assumption of infinite shear strength at the interface. No relative tangential displacement would then occur between the soil and the lining. This condition could be acceptable in practice, whenever the maximum mobilized shear stress does not exceed the finite shear strength of the interface. The full slip assumption considers that zero shear strength exists along the interface, allowing the soil and lining to move freely relative to each other, in the tangential direction. This condition could approximate in practice the case of a very smooth lining, placed against a very softened, or smeared ground surface. Real slip conditions may lie somewhere between these two extremes, more probably closer to the first. The outer surface of a lining is

normally fairly rough and the shear stress mobilization in the interface is likely to be small. The lining is usually installed fairly close behind the tunnel face (one to three radii behind), but still after the soil has experienced a considerable amount of displacement and stress release. As a result, the mobilized shear may be much smaller than the strength. This is further discussed in Section 2.3.5.3.

2.3.5.2 Good Lining Contact in an Ideally Deep Tunnel As with the ground reaction curve (GRC), a support reaction curve (SRC) is normally formulated. For an ideally deep tunnel under a hydrostatic in situ stress condition (K=1), a unique GRC exists and similarly, a single SRC can represent the lining action, with radial stress and displacements increasing with the load transfer onto the lining. Symmetry implies that zero bending moments exist in the lining. The condition of the tangential contact is irrelevant since the shear stresses are zero at the interface. Equilibrium is, therefore, attained at the intersection of the two reaction curves. For a linear elastic lining, the SRC is a straight line, whose slope can be predicted on the basis of the support properties and geometry (see Hoek and Brown, 1980:252, for a review on the subject). If the lining is installed before any ground displacement occurs and if it is ideally rigid and incompressible, the stress acting on the support will be equal to the field stress.

If K is different from unity, then the in situ stresses are those shown in Figure 2.11. If a rigid lining is installed without allowing any displacement and if a no slip condition is postulated, then these stresses also represent the loads the lining must withstand. If a full slip condition is admitted, with the other assumptions remaining unchanged, the stress distribution on the rigid lining will be different from the in situ stress distribution. The shear stresses at the interface are reduced to zero and, therefore, the radial normal stress will have to change in order to ensure equilibrium (see Figure 2.12). To reduce the shear stress to zero, equal and opposite shear stresses will have to be applied, forcing the soil to displace tangentially, relative to the support. If K<1, this displacement will be from the crown or the invert towards the springline. Since the lining is assumed to be rigid, no radial displacement develops at the interface and for K<1, the radial stress decreases at springline and increases at the crown (and floor), the reverse occurring for K>1. This simple fact, not always clearly understood, was correctly analyzed and interpreted by Ranken (1978:60). Ranken's (Op.cit:407,423) or Einstein and Schwartz's (1979) linear elastic analytical solutions for deep tunnels enables one to assess these effects both for a thick and a thin lining. Ranken (Op.cit:Section 3.3) presents a comprehensive discussion on the effect of the no slip and full slip assumptions on liner thrusts, bending moments and

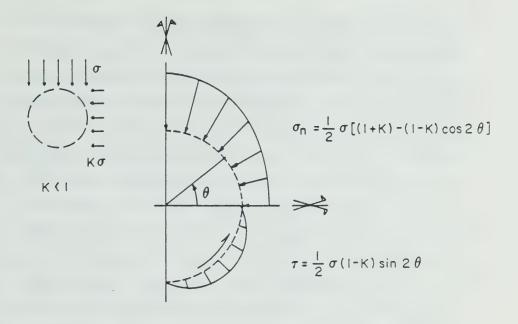


Figure 2.11 In Situ Stresses and Lining Loads on a Rigid Lining for Non-Slip Condition

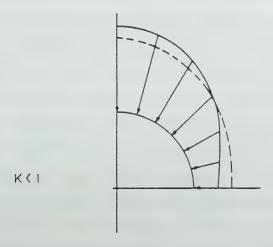


Figure 2.12 Normal Stress on a Rigid Lining for Full Slip Condition

displacements. Briefly, the slip condition does not significantly affect bending moments and lining radial displacements. The full slip assumption furnishes bending moments that are less than 10% larger than those obtained with the non-slip condition (Ranken, Op.cit:73, Einstein and Schwartz, Op.cit:513). Lining thrusts are more affected by the condition of slip. The difference between thrusts in the crown and springline are greatest for the non-slip condition, due to higher shear stresses existing at the interface. With the full slip condition, these differences are much smaller and the thrust magnitudes approach the average of the crown and springline non-slip thrust values. In other words, the greatest and lowest thrusts are always given by the non slip assumption, either at the crown or at the springline, depending on the K value (see Ranken, Op.cit:68.74).

For intermediate conditions between full and non slip, no analytical solution is available and the problem is approached by using numerical methods. This can be done using beam-spring models, with lining-soil contact represented by springs with different stiffnesses in the radial and tangential directions (for example Paul et.al., 1983:70) It can also be done using the finite element method, by including joint or interface elements (Rodriguez Roa, 1981:353, Paul et.al., Op.cit:85).

The interaction that will take place between the soil and lining when a good contact exists, takes the form of a

mutual reduction of deformations in the soil and in the lining. The insertion of a stiffer body into the opening (the lining), restrains the ground deformations. On the other hand, the complete confinement of the lining offered by the soil, restrains its deformation. The interaction becomes more complicated when it is recognized that the soil loads being transferred onto the lining depend on the magnitude of the displacements (Section 2.3.3). Additionally, loads may also be transferred from the lining into the soil, altering the so-called arching process (Section 2.3.2) associated with the reduction of the in situ stress. This may also lead to changes in stiffness of the surrounding soil, for instance, by the increase of the mean normal stress in the ground adjacent to an ovally seated lining. Both volume changes and shear strains in the ground are also inhibited by the lining. Consequently, the response of the confined and embedded support will differ from that of an isolated support subjected to external loads. Similarly, the ground response (Figure 2.5) will also be affected. Rigorously, after both elements (lining and soil) are put together, their responses are not unique but interdependent and cannot be anticipated separately, except for the case of K=1 and for an ideally deep tunnel.

Clearly, the stress and displacements found when equilibrium is achieved as a result of the soil-lining interaction process, will depend on the relative stiffnesses between both elements. These are defined in terms of

extensional and flexural stiffness ratios of the soil and the support, and are expressed in different ways. They are normally referred to as the compressibility (C) and flexibility (F) ratios. The expressions given by Einstein and Schwartz (1979:501) are preferred to those by Peck et.al. (1972:269) or Ranken (1978:339), as the first authors consider the stiffness of a perforated ground mass, which is more appropriate. They are written as:

$$C = \frac{ER (1 - \nu_s^2)}{E_s A_s (1 - \nu^2)}$$
 [2.17]

$$F = \frac{ER^{3}(1 - v_{s}^{2})}{E_{s}I_{s}(1 - v^{2})}$$
 [2.18]

in which E, ν and E_s, ν_s are elastic constants for the ground and the support, respectively, A_s and I_s are the cross sectional area and the moment of inertia of the support per unit length of tunnel, and R is the tunnel radius.

To illustrate some of the points just discussed, Figure 2.13 was prepared using Einstein and Schwartz's (1979) elastic solution for a deep tunnel under a full slip condition with K=0.5. The vertical stress field is given by $\sigma_{\rm v}$. The points for C = F = 0 correspond to a perfectly rigid support, and, as observed, despite a zero radial displacement condition, $\sigma_{\rm r}$ increases at the crown and decreases at the springline. The large difference in stress at these two points indicates that considerable bending moments exist in the lining. The points, C=F= ∞ , represent an unlined opening after full stress release. The two bold

lines correspond to the ground reaction curves for the crown and the springline, for a continuous reduction in the in situ stress at the perimeter. The points C=0 and F=∞ represent an ideally flexible tunnel, as defined by Peck (1969:245). The outward movement of the springline is equal to the inward displacement of the crown and floor, and the opening profile becomes approximately an ellipse*. The cross-sectional area of the opening does not change and, therefore, the "net" loss of ground is zero.

The radial stress becomes uniform and equal to the mean in situ stress, the bending moments are zero and lining thrusts are uniform and compressive. This is the "ideal" lining that most modern designs try to achieve. If the lining becomes compressible but remains ideally flexible (points C=1, $F=\infty$), the radial stress still remains uniform but less than the original mean in situ stress, and the crown downward displacement is larger than the springline outward movement, resulting in a "net" loss of ground. The points (F=10, C=0) and (F=10, C=1) are shown as representing intermediate behaviours. Most tunnel linings in soil have C

^{*} Peck (1969:245,246) and Muir Wood (1975:117) refer to the deformed lining profile as an ellipse. Rigorously this profile is not elliptical. If C=0, the lining circumference does not change, but just its shape. The closed form solution for C=0 and full slip interface yields crown and springline displacements of equal magnitude but with opposite sign. If the deformed profile were actually elliptical, for a given crown settlement, the outward displacement of the springline would be slightly less than the former. The difference between the two is actually less than 1% (calculations based on Selby, 1962:13). Obviously, for all practical purposes, the deformed profile can be taken as an ellipse.

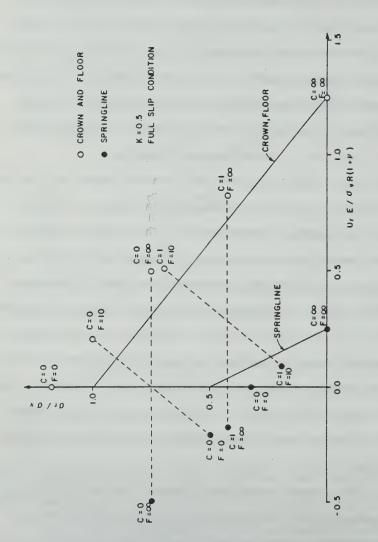


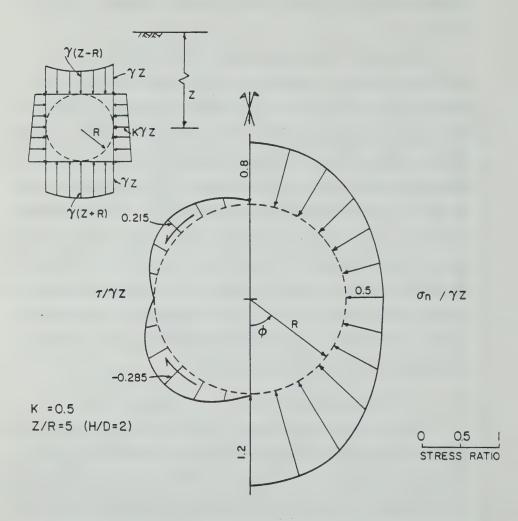
Figure 2.13 Equilibrium Points for Crown and Springline of a Deep Tunnel with Full Slip Interface Between Soil and Lining

values between zero and 2; and F values between 10 and 10,000.

Also worth mentioning is the fact that all the equilibrium points between the lining and soil shown in Figure 2.13, do not lie on the ground reaction curves for the crown or the springline. This point was raised by Pender (1979), who explained it by saying that the stiffness of the soil is not the same for the release of the asymmetric part of the in situ stress and the application of an asymmetric pressure to the tunnel perimeter by the lining. But not only this, since the equilibrium points are also affected by the stiffness of the lining. Only when this asymmetric stress is absent (deep tunnel and K=1) is it possible to review the ground and support responses independently, as is done by the convergence-confinement method.

2.3.5.3 Good Lining Contact in a Shallow Tunnel

If the tunnel is shallow, the gravity action means that symmetry of the in situ stress exists around the vertical axis only, as shown in Figure 2.14. This is given for an H/D ratio equal to 2 and K=0.5. The equation shown is derived from Hartmann (1970:215). If a rigid lining is installed without any prior displacement, and if a non-slip condition is assessed, the normal and shear stress distributions onto this lining will be different from the in situ values shown in Figure 2.14. Using Hartmann's (1972:15) elastic solution for a tunnel under a gravitational stress field, with its centre at a depth z sufficiently far from the stress free

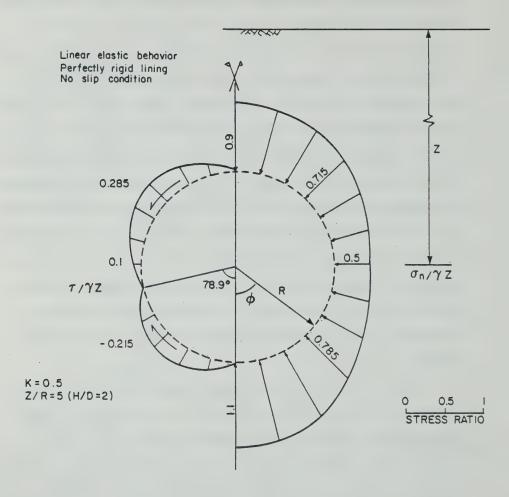


$$\begin{split} \sigma_{\mathsf{n}} &= \frac{1}{2} \gamma Z \big[(\mathsf{I} + \mathsf{K}) + (\mathsf{I} - \mathsf{K}) \cos 2\phi \big] + \frac{1}{4} \gamma \, \mathsf{R} \big[(3 + \mathsf{K}) \cos \phi + (\mathsf{I} - \mathsf{K}) \cos 3\phi \big] \\ \tau &= -\frac{1}{2} \gamma Z (\mathsf{I} - \mathsf{K}) \, \sin 2\phi - \frac{1}{4} \gamma \mathsf{R} \big(\mathsf{I} - \mathsf{K} \big) \, \left(\sin \phi + \sin 3\phi \right) \end{split}$$

Figure 2.14 In Situ Stresses Around a Shallow Circular Tunnel Profile Prior to Excavation

ground surface, one obtains the distributions of normal and shear stresses shown in Figure 2.15, where γ is the unit weight of the soil. Since the crown and floor in situ normal stresses are not equal, the rigid lining tends to "float" upon removal of the soil within the lining. The crown normal stress increases from $\gamma(z-R)$ to $\gamma(z-R/2)$, and the floor normal stress decreases from $\gamma(z+R)$ to $\gamma(z+R/2)$. The buoyant effect also causes changes in the shear stress distribution, increasing the shear in the tunnel shoulders and decreasing it in the haunches. It should be also noted that the normal stress at the springline ceases to be a principal stress as shear develops at this point. Even for K=1 there will be positive shear (from crown to floor direction) at the interface, being maximum at the springline and equal to $0.5\gamma R$.

The ratio of mobilized shear stress to acting normal stress at the soil-lining interface is a measure of shear strength mobilization. By inspecting the values shown in Figure 2.15, one notes that the risk of occurrence of a slip at the interface is highest around the tunnel shoulders. For this given geometry, in situ stress condition and support stiffness, the maximum mobilized friction angle at the interface is less than 22°. Thus, if the frictional strength of the soil-lining interface exceeds this value, or if it is smaller but has some cohesive component, appreciable tangential movement between the soil and lining may not be expected. Even if some slip does occur locally around the



$$\begin{split} \sigma_{\,\mathrm{II}} &= \frac{1}{2}\,\gamma\,\mathrm{Z}\,\left[(\mathrm{I} + \mathrm{K}) + (\mathrm{I} - \mathrm{K})\,\cos2\phi \right] + \frac{1}{4}\,\gamma\mathrm{R}\left[(\mathrm{I} + \mathrm{K})\,\cos\phi + (\mathrm{I} - \mathrm{K})\,\cos3\phi \right] \\ \tau &= -\,\frac{1}{2}\,\gamma\mathrm{Z}(\mathrm{I} - \mathrm{K})\,\sin2\phi + \frac{1}{4}\,\gamma\,\mathrm{R}\left[(\mathrm{I} + \mathrm{K})\sin\phi - (\mathrm{I} - \mathrm{K})\,\sin3\phi \right] \end{split}$$

Figure 2.15 Stress Distributions Around a Rigid Lining in a "Shallow" Tunnel

shoulders, resulting in some shear transferred to adjacent points, a full slip condition all around the tunnel profile would not exist. Shear strength mobilization decreases as the tunnel becomes deeper, as K tends towards unity and as the lining becomes more flexible.

The stress changes observed around the tunnel after installing the rigid lining, are given by the differences between the equations shown in Figure 2.14 and 2.15. Thus,

$$\Delta \sigma_{\rm p} = -1/2 \, \gamma R \, \cos \phi$$

 $\Delta \tau = 1/2 \ \gamma R \sin \phi$

By adding the integrals of these stress changes along the entire tunnel contour, a force equal to $\pi\gamma R^2$ is obtained, which is exactly the weight of the soil removed from the opening, as noted in Section 2.2.

If the circular opening is left unlined, the tangential stress at the crown, springline and floor of the "shallow" tunnel perimeter are, respectively (Hartmann, 1972:15):

$$\sigma_{\theta c} = (3K-1) \gamma (z - \frac{R}{2})$$
 [2.19]

$$\sigma_{\theta s} = (3-K) \gamma z$$
 [2.20]

$$\sigma_{\theta F} = (3K-1) \gamma (z + \frac{R}{2})$$
 [2.21]

Equations 2.5 and 2.7 derived from Mindlin's (1939:1132) solution and presented in Section 2.3.2, are particular cases of the above expressions.

Clearly, if the influence of the stress free ground surface is included, the tangential stress will differ from those given above, but the differences should be small for H/D greater than 1.5, as discussed in Section 2.2.

A more general case that includes the effect of the stress free ground surface and, perhaps, the non-linear ground response, would require numerical solution, since no analytical solution is yet available. Furthermore, in the real case, the lining is installed behind the tunnel face, after the projected tunnel profile has undergone some displacement. That could be represented in a plane strain analysis by a certain limited amount of in situ stress release at the tunnel contour.

The finite element model and simulation procedures applied for obtaining the stress paths shown in Figure 2.4 and for the ground reaction curves presented in Figure 2.5, could also be used to approach the solution of the more general case just discussed. Details of this numerical model were summarized in Section 2.3.4 and will be discussed further later in this thesis.

The construction of a tunnel of 4 m diameter with 6.2 m of ground cover was numerically simulated, assuming the following properties for the non-linear elastic hyperbolic model representing the soil:

 $\gamma = 16 \text{ KN/m}^3$

 $K_0 = 0.75$

 $\phi' = 21^{\circ}$

c' = 39 kPa

 $R_{\epsilon} = 1$

K = 330

n = 0.23

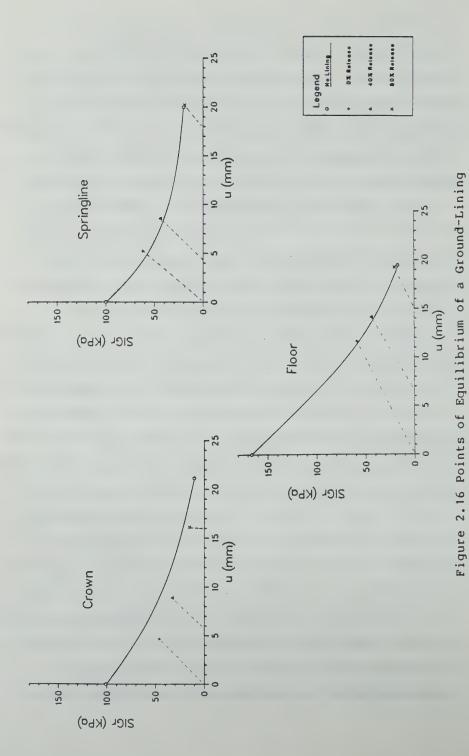
 $\nu = 0.3$

The symbols have the meanings explained in Section 2.3.4.1, and c'is the cohesion intercept of the Mohr-Coulomb envelope. A fully drained behaviour was assumed. Since Janbu's exponent, n, is non-zero, the in situ elastic modulus of soil increases with depth, being approximately equal to 24 MPa at the tunnel axis line.

The support was represented by a linear elastic material, with C = 1.8 and F = 86, with respect to the in situ elastic modulus of the soil at the tunnel axis elevation. These values could be typical for a shotcrete lining, with a reduced E value at its early age.

Four analyses were carried out, each one with different uniform amounts of in situ stress release at the opening prior to the lining installation: 0%, 40%, 80% and 100%. The full stress release corresponds to no liner installation, and enabled the construction of the ground reaction curves, in terms of radial stress and displacements, at three points of the tunnel contour: the crown, springline and floor.

These are shown in Figure 2.16. The 0% stress release analysis corresponds to the material discussed so far in this section: the lining is installed in such a way that no displacements occur before its activation. This is clearly a crude abstraction of reality, and the analyses corresponding to 40% or 80% of stress release prior to lining installation are more plausible. In these cases, the lining was introduced after the development of some displacements at



Interaction Analyses Using Finite Element Method

the opening. The equilibrium points between the lining and the soil obtained are identified in Figure 2.16. The larger stress release before support installation, obviously leads to smaller equilibrium stress and larger final displacements. The dashed lines linking the equilibrium points to the starting point of lining activation could be interpreted as support reaction curves. Unlike the radial displacements which are calculated at nodal points, it was necessary to extrapolate the calculated element stresses up to the tunnel perimeter in order to obtain the radial stresses at the soil-lining interface. This involves a certain degree of approximation.

As pointed out before, the equilibrium points do not coincide with the non-linear ground reaction curves especially at the crown. Here the ground response curve, which does not take into consideration the interaction with the lining, seems to be an upper bound for the corresponding equilibrium points. It also seems that the effect of this interaction is considerably reduced when the stress release allowed before lining installation increases.

The slopes of the dotted lines shown are measures of the stiffness of the support at each point of the tunnel contour. It is noted that for a single point, these slopes changed with variable amounts of stress release, despite the fact that the nominal values of C and F had been kept constant in all analyses. This is due to the changing value of the elastic modulus of the soil around the tunnel which

results from the unloading process. Broadly speaking, an overall reduction in this modulus would be expected and for fixed lining properties, one could envisage a stiffer support response as the amount of in situ stress release increases. This is particularly true for the crown but less evident for the other points considered. Acceptance of this arguement would lessen the impact of the relative stiffness ratios such as C and F, in a non-linear response context. It may possibly be more adequate to define these ratios in terms of a reduced average ground modulus, current with the instant of lining activation.

2.3.5.4 Poor Lining Contact

When using prefabricated lining systems, it is customary to overexcavate the tunnel profile in order to easily accommodate the support. Also, to reduce jacking forces needed to advance a tunnel boring machine, it is usual to cut a profile larger than the TBM shield. This overcut was normally done in the past by a small radial extension called a "bead", 5 to 15 mm in thickness, fixed on the leading edge of the TBM. Modern machinery design, with full face mechanical excavation, allows overcutting by means of variable length teeth, protruding radially from the face cutter. This permits a more efficient control of the excavation, allowing adjustments in the overcutting, without major disruption during tunnel advance. The voids left behind the assembled lining ring are filled with some sort of grout or the lining is expanded against the soil. Details

of construction techniques used can be found in Craig and Muir Wood (1978) and in Maidl (1984). In many cases, the voids are left unfilled for a considerable amount of time, when the grouting operation is delayed. In some other cases the grout is insufficient or inefficient (grout losses, grout settling, etc) and a void is left open in the crown region.

Depending of the size of this space behind the support, the ground response may vary. If the space is small, then with the advance of the tunnel face, a soil with sufficient stand up time will come in contact with the lining without the development of local instability or global ground collapse. If the ground has no stand up time, the void will immediately be filled with soil, but as the space size is small, then again, neither local nor global collapse will be observed. The stress changes in the soil element beside the void are clearly three dimensional, and the acting mean normal stress is possibly close to zero. In an equivalent plane strain simulation, the stress state of this element would lie between points B and D in Figure 2.3.

If the void space is sufficiently large, either local instability or global ground collapse may occur.

Distinctions will be made between these two mechanisms in following sections. In a dense sand local collapse is associated with the fall of a wedge like portion of the ground from the roof (Atkinson et.al., 1975:84). In fissured, stiff, clayey soils, local collapse may be

associated with the fall of blocks bounded by pre-existing discontinuities (Matheson, 1970). To the writer's knowledge no empirical or theoretical guidelines exist presently to limit the maximum amount of overcut space left unfilled, in order to prevent those occurrences. However, it is tempting to make use of the discussion presented on shear strain development in Section 2.3.4, based on the results of plane strain model tunnel tests. It was observed there, that a near complete collapse condition is reached in all soils tested, when the dimensionless displacement at the tunnel crown, U, given by equation 2.16, exceeded 1.8.

Out of this total figure, some displacements will occur ahead of the face and some after the soil comes in full contact with the support and loads it.

As will be seen in Chapter 5, (see also Negro et.al., 1986), the crown displacements occurring ahead of the face of shallow tunnels leads to U of not much more than 0.5, except in very soft clays. Some displacements are also likely to occur once the soil establishes a good contact with the lining. It was seen that these depend on the relative stiffness of the lining and if a very rigid support is present then the increment in U due to lining deformation is negligible. The estimate of an upper bound of the increment in U for a flexible support would preferably be made by some analyses, either as an analytical closed form solution, or numerical, such as those mentioned under the previous heading (and further discussed in following

chapters). Perhaps also, it could be bounded from available field data of real tunnel performances. Shielded tunnel cases, making use of prefabricated lining rings, offer little help in this search, as it seems practically unfeasible to identify when the soil came in full contact with the lining. Fortunately, data from NATM cases can provide some assistance, if one accepts that the shotcrete ring is likely to fulfill the requirements of good contact with the ground. In Chapter 5 of this thesis, it is shown that in all NATM cases investigated, the increment of the dimensionless crown displacement U, due to the shotcrete lining deformation after the closure of the support ring invert, is likely to be less than 0.3, with the exception of tunnels departing considerably from a circular profile (e.g., the heading of Sao Paulo Metro North extension, with a temporary heading invert, as described by Negro et.al., 1985 and Eisenstein et.al., 1986, which had a width to height ratio of about 0.5. This value may likely serve as a conservative upper bound. It is not certain how the relative stiffness of a shotcrete lining compares in reality to that of a prefabricated lining system. In both cases, there is quite a degree of uncertainty on the assessment of various parameters, for example the stiffness of segment joints, the deformation modulus of the shotcrete at its early ages, etc. However, the field data from shotcrete lined tunnels may possibly serve as a rough upper bound, since it includes the influence of a reduced deformation modulus of the hardening

concrete placed at the floor.

If the crown displacements occurring ahead of the face (corresponding to a maximum U equal to 0.5) are added to those taking place due to lining deformation (which corresponds to U between 0 and 0.3), the limiting dimensionless crown displacement increment for movement into the void space behind the lining which might produce a near collapse condition, will range from 1.0 to 1.3. If some factor of safety is included, the limiting U increment at the crown may vary from 0.5 to 0.65. From this, one could estimate a limiting crown displacement increment, and therefore, a maximum crown overbreak, which should be less than or equal to the limiting value. This approach is unquestionably very approximate and open to discussion. However, since no other guidelines are presently available, it may serve as an interim expedient to treat the problem, until a more adequate solution is formulated. Needless to say that caution should be exercised when applying the above criterion since it was developed from results of tests that made use of "well behaving" soil types under fairly idealized conditions. Minor geological details such as the presence of small sand lenses or pockets, are known to have an important role in localized collapse mechanisms (Matheson, 1970). Stiff, fissured clays, collapsible and sensitive soils may have modes of collapse which are very dissimilar to that observed in the model tests.

Unfortunately, not many documented cases in which local or global instabilities are reported in the literature can offer an opportunity to test the aforementioned criteria. Thus, verification was limited to two cases in which the writer was personally involved. One of them is the Tamanduatei Sewer Tunnel, driven in Sao Paulo, Brazil, reported by Negro (1984). The tunnel was driven with a fully mechanized TBM, with a cutting diameter of 1.79 m, a ground cover of 6.2 m and through a medium to coarse quaternary loose sand with an in situ specific weight of 17 KN/m3. An in situ elastic modulus of 4.5 MPa was estimated for this sand from static penetration cone tests carried out just above the crown elevation. The ground water level had been lowered to the tunnel haunch elevation, and some capillary rise was detected above it. Water surface tension was expected to have provided some stand up before grouting operations. Overcutting led to a void space of 5 cm behind the 10 cm thick precast segemented concrete lining. Typically, grouting was undertaken 15 hours after ring installation. Before this could take place, local collapse of the soil around the shoulders and crown was detected through six inspection holes left open in the upper segment of each lining ring under observation. Local collapse was also observed through three extensometer points installed above the tunnel crown, at 18, 34 and 48 cm above the excavation contour. The volume of material dislodged was estimated as 0.19 m³/m, or 7.5% of the tunnel volume. Using

the reasoning just presented, the limited overcutting at the crown that would bring about instability would have been 4.2 cm. Indeed, local collapse was observed with an overbreak of 5 cm. The extensometer readings indicated that it had occurred above the 5 m long body of the TBM. The length of the overcutting teeth was subsequently reduced and the overbreak was limited to about 3 cm in the crown region. No ground instability was observed thereafter in other instrumented sections.

The second case referred to is the LRT tunnel built with a TBM along Jasper Avenue in Edmonton, Alberta, reported by Branco (1981:110). Unfortunately, the geological setting of this tunnel is very particular, since the ground mass included a stiff jointed till and some dense and dry sand pockets. It is therefore a typical case where minor qeological details may have a dominant role on localized instability, and thus not ideally suited to check the aforementioned approach. A roof failure involving some 1.5 m³ (5% of the tunnel volume) of material being caved in was detected by a multipoint extensometer (ME17). Instability was limited to a fairly dry sand pocket located at and above the tunnel crown. The sand flowed into the void above the TBM leaving behind an empty cavity bounded by stiff till walls. This type of occurrance seems to have happened on other occasions along this LRT line. An in situ E value of around 50 MPa is estimated for this sand. With an excavated diameter of 6.2 m and a ground cover of 8.9 m, a

limiting overbreak of 2.2 cm at the crown would be obtained using the above criteria. The void space at the crown above the TBM body amounted to some 2 cm (Branco, Op.cit:23). Instability was observed in this section, just above the cutting head of the machine. However, no instabilities were detected when the tunnel cross section was fully embedded in till free of sand pockets.

More field evidence is needed to fully validate and perhaps extend this approach which has merit in that it relates a limiting overbreak to the amount of displacement that may trigger an instability process in the ground.

If the overbreak is left unfilled and is large enough that the ground displacements have sufficient magnitudes for instability to occur, the lining will be loaded in a very different fashion to that discussed with respect to good lining contact. While in the latter a continuum mechanics approach may be acceptable, it may not be acceptable if the contact between the lining and the soil is poor or entirely lacking. Fissures in the soil may open, soil blocks may slide or fall down and rest against the poorly confined lining ring. Running or ravelling soils, such as sands, will drop, or literally flow, from the crown and shoulders, filling the space behind the tunnel haunches, from the floor upwards. The lining will gradually be loaded by the accumulation of loosened material against it, and these loads are mainly due to the self weight of such disturbed soil. This mechanism is referred to as "loosening", and is

normally associated with large volumetric expansion above the tunnel as described previously. If the tunnel is shallow, this disturbed zone propagates upwards and may reach the ground surface, and complete tunnel collapse is achieved. If the tunnel is deep or if a stronger ground cover exists, an equilibrium situation may be encountered before this zone of disturbance reaches the surface. These ideas have been fairly well established in rock tunnelling practice for quite some time (see, for instance, Ritter, 1879, quoted by Steiner and Einstein, 1980:37). Terzaghi's (1946) rock load theory is based on them. Results of model tunnel tests in dense sands (Atkinson et.al., 1975) suggest that the loosening process is initiated by a wedge like zone experiencing large dilation above the crown. The complete collapse of the tunnel was sudden with very large movements. The ultimate failure mechanism showed two vertical slip surfaces bounding the unstable soil up to the surface, for tests with cover to diameter ratios between 1 and 4. The final loads that the lining will sustain are called "gravity loads" (Mohraz et.al., 1975; Ranken, 1978:50; Paul et.al., 1983:11). Their development will be basically controlled by the quality of the contact between the lining and surrounding soil. As pointed out by O'Rourke et.al., (1984:13), "if there is a close contact between the lining and surrounding soil, loosening may be prevented entirely or confined to a small distance above the tunnel crown".

The connection between the load development due to such a loosening condition and the amount of displacement allowed at the tunnel crown has long been recognized (for instance, Kommerell, 1940 and Terzaghi, 1946, as quoted by Steiner and Einstein, 1980:45 and 63). However, the existence of a critical crown displacement, associated with the instant the loosening processes (and the collapse mechanism) is triggered, is not as clearly recognized. Wong (1986:30 and 35) did recognize it and presented a simplified guideline to obtain the critical displacement. He proposed that at a certain point of the ground reaction curve for the crown (point b in his Figure 2.9), when the continuum mechanics approach fails to provide a solution due to numerical difficulties, a straight line tangent to this point should be used for extrapolation. The critical displacement would be obtained on this extrapolated line, assuming that the corresponding critical pressure is given by Atkinson et.al. (1975) solution for local roof collapse in sand. Wong (Op.cit:30) claims that this procedure is safe, in as far as the slope of the extrapolated line is steeper than the actual ground reaction curve, which goes undefined beyond his end point b. However, he uses a critical tunnel pressure derived from the upper bound theorem of plasticity (Wong, Op.cit:35), which is an unsafe estimate of the real critical pressure (Davis et.al., 1980:399). Since the slope of this extrapolated line can actually be very flat, despite being steeper than the actual reaction curve, the use of an upper

bound tunnel pressure may lead to quite an unsafe estimate of the critical crown displacement. Moreover, the local collapse mechanism at the roof appears to be a sole feature of tunnels in dense sands, and it has not been observed in any of the drained model tests carried out in Cambridge both in normally and overconsolidated clays with cover to diameter ratios smaller than 2. The use of a lower bound solution would have been a wiser choice. But even so, the extrapolation Wong adopted is still open to criticism, mainly because the result it leads to is highly dependent on the definition of the "end point" of the ground reaction curve, as provided by the continuum mechanics approach. Different finite element codes will provide, inevitably, different "end points" in the stress-displacement, even prior to the uncertainty associated with linear extrapolation.

Paul et.al., (1983:11) discusses critically the subject in an intuitive but sensible way, pointing out that for the development of the loosening condition, stiffer soils will require smaller deformations than softer soils. This is properly accounted for by the suggested criteria, as the dimensionless crown displacement (U) is a direct function of the in situ deformation modulus and, therefore, the limiting displacement bringing about instability is inversely related to the modulus. However, Paul et.al., (Op.cit), contemplated that in stiff soils these displacements "are so small", that even when the tunnelling operation is designed to prevent

"excessive" ground deformation, the loosening condition may possibly be achieved. If this is the case, it means that the tunnelling operation or even the tunnelling method used was inadequate for that particular situation. Indeed, the term "excessive" should be taken in relative terms. A tolerable deformation for a softer soil may well be unacceptable for a stiffer soil, as it may represent an impending collapse condition in the latter, as shown before.

The magnitude of these gravity loads are frequently related to the weight of a cerain "height" of ground above the tunnel, expressed as nD where n is a constant that is normally empirically defined (Kommerel, 1940; Terzaghi, 1943 arching theory, etc.). The value for n may be established for a particular site, on the basis of monitored performance of tunnels previously built (for instance, El-Nahhas, 1980:189; Branco, 1981:206; Corbett, 1984:185). For design purposes, these loads are supposed to act as external vertical loads (with different distributions) on the lining in the crown region, where embedding is assumed to be lacking. Some approaches assume full embedding for the remaining part of the tunnel contour (e.g., Ranken, 1978:227; Saha, 1981:32 and 34), at points where the loading system does not lead to separation of the lining from the soil (radial tension). Some other approaches also specify lateral external loads (see Szechy, 1967:267, for a review on the subject), either assuming or not assuming the embedding action of the surrounding soil (i.e. interaction

is accounted for or not).

If no embedding is assumed, then no interaction develops between the lining and the soil, and the former will be loaded only by the external gravity loads resulting from loosening and the collapse of the ground mass. Assuming that the ultimate loading system is known (magnitude and distribution), it is possible to estimate what the final lining response is likely to be. However, since the process of load build up will presumably be fairly erratic and quite unpredictable, the evolution of the lining response up to the ultimate equilibrium will also be irregular. This fact is illustrated in Figure 2.17 for a linear elastic thin circular lining, submitted to three different loading paths leading to the same final load condition. For the sake of simplicity, uniform vertical and lateral dead loads have been assumed. If the ground does not provide any embeddment, it is simple to show that the change in the vertical diameter is given by:

 $\Delta D_{v} = \sigma_{v} R^{2} \frac{1 - \nu_{s}^{2}}{E_{s}} \left[\frac{1 + K}{A_{s}} + \frac{(1 - K)R^{2}}{6 I_{s}} \right]$ [2.22]

where $\sigma_{\rm v}$ is the current vertical stress, ${\rm K}\sigma_{\rm v}$ is the current lateral stress, and the other symbols have the same meaning as before. Loading path A corresponds to a proportional increase of both the vertical and lateral stresses, similar to that experienced in an ideal excavation loading, when good lining-soil contact is ensured. Loading path B represents a case where gravity loading starts acting initially on the crown, and then lateral external loads

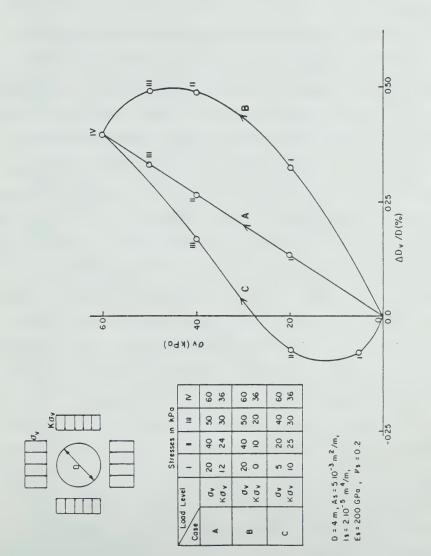


Figure 2.17 Reaction of the Support to External Gravity

Loads

build up. Finally, path C corresponds to a case of initial higher lateral loading, which reverses as the deformation increases.

The lining characteristics are given in Figure 2.17. The non-linear support reactions of an otherwise linear elastic lining, result from the non-proportional increase in external loads in cases B and C, in which the ratio K varied during the load build up. This simple analysis serves to illustrate the fact that the load transfer onto the support during an idealized uncontrolled ground loosening condition, may lead to unpredictable lining responses. This in turn may cause support distortions during load build up, which can be more critical than the final ones. The knowledge of the final gravity loads, in itself difficult to ascertain. does not ensure the prediction of lining behaviour before the equilibrium situation is achieved. Therefore, the so called loosening condition should not only be avoided in practice for its detrimental effect on the ground response (low factor of safety, large losses of ground and large ground deformation), but also for its adverse impact on the lining behaviour. Locally concentrated loads on linings have been observed in soil tunnels. Their existence has been used to contend possible misinterpretation of field measurements (Duddeck and Stading, 1985). Their occurrence in the case of good ground control and good lining contact is questionable, with the possible exception of very heterogeneous ground conditions. The accuracy and representation of the

measurements that led to the acceptance of these lining load concentrations (e.g., Kaiser and Barlow, 1986) is open to discussion (e.g. Corbett, 1984:35-198). The separation process of loads that are not related to ground pressures is always very complex, particularly when an expanded lining is used and a good contact is not assured at all points of the tunnel contour. However, from what was shown before, it is clear that higher bending moments can actually develop in linings where poor ground control conditions prevail and loosening or local collapse mechanisms develop. This was the case in the 3.2 m diameter Kenedalle Sewer tunnel in Edmonton, driven in till and sand, (Corbett, 1984), where the final dimensionless crown displacement, U, is estimated to have been greater than 1.5 in all instrumented sections. Therefore, based on the explanation in Section 2.3.4, the chances are that a collapse or near collapse condition was likely reached along this tunnel. If large amounts of overbreak or voids are left unfilled, as they were this in particular case 5, erratic lining loading is indeed to be expected, as well as higher bending moments (and, possibly, smaller thrusts) leading to a critical condition in terms of liner capacity. Unfortunately, attempts to quantify this erratic loading increase, due to poor ground control, are doomed to be sterile. Although it may sound like a truism, the unpredictable is not predictable in soil tunnelling

⁵ A construction void approximately 2 m in height and 3 m width was detected above the tunnel crown at the magnet extensometer No.3, according to Corbett, Op.cit:65)

engineering. De Mello (1981:212) poses the problem correctly:

"Surely, it is accepted that in tunnelling we automatically face a greater proportion of strictly localized conditions of heterogeneity and possible failure (...). Such conditions are those that must either be bearable and borne as unquantifiable risks, or must be resolved in design and construction by a 'change of statistical universe' (...). Our design engineering concern can only be with conditions that permit averaging and quantifications based thereon.(...)"

In this particular case, the "change of statistical universe" can include a large number of provisions, ranging from a reduction in overcutting, drainage and dewatering prior to construction, injection grouting, etc. If these measures do not ensure the aimed goals or are not feasible, one concludes that the tunnelling method in itself is not adequate for the particular site.

2.3.6 Three Dimensional Response

2.3.6.1 Plane Strain Representation and Three
Dimensional Response

So far both the ground and lining responses have been analysed in terms of a plane strain representation, which may be reasonable for a tunnel section sufficiently far from the advancing tunnel face. Ranken and Ghaboussi (1975:3-4) using an axisymmetric numerical simulation, say that this is

the case for sections at distances greater than one to two tunnel diameters from the face, if the tunnel is unlined and deep, the ground is linear elastic and the in situ stress state is hydrostatic. This suggested distance increases with increasing amount of plastic yielding in the ground. They go further by saying that if the tunnel is lined near the face (Ranken and Ghaboussi, Op.cit:5-2), and regardless of soil behaviour, the three-dimensional stress-displacement zone extends not more than one diameter behind the leading point of the tunnel liner. Field observations by El-Nahhas (1980:237,241) in the Edmonton Experimental Shielded Tunnel, indicate that the zero longitudinal strain condition is attained somewhere between one to one and a half diameters behind the point of lining activation. This is also confirmed by tunnel heading model tests conducted in Cambridge by Casarin (1977) in overconsolidated kaolin.

The ground displacement induced by a single shift of the face during tunnel advance, resembles a "flow" of soil towards the unsupported excavation (see, for example, Ranken and Ghaboussi, 1975:3-74). Figure 2.18 reproduces the results of a 3D linear elastic analysis carried out by Heinz (1984:171), in terms of incremental displacements in the vertical plane containing the tunnel axis which are caused by an incremental advance of the face. A similar picture is observed in a horizontal plane through the axis. One notes that the longitudinal component of the displacement tends to be larger than the vertical one for points ahead of the

face, with this trend being reversed as the tunnel heading region is approached. By adding the displacements of each consecutive step of face advance, it is not difficult to foresee that the total longitudinal displacements at points around and away from the tunnel perimeter, may not end up as zero, as it is normally assumed in a two dimensional representaion of a tunnel. This is confirmed by axisymmetric numerical analyses (e.g. Ranken and Ghaboussi, 1975:3-54), and by three dimensional finite element analysis (e.g. Heinz, 1984:170). As the tunnel advances, the longitudinal component of the displacements around the perimeter (against tunnel advance direction) peaks at the face, and then the soil starts moving back towards its original position. This feature was detected through slope indicator measurements by Branco (1981:112) in the Edmonton LRT tunnel. This rebound is not necessarily complete, especially in linear elastic numerical analyses (see Ranken and Ghaboussi, Op.cit:3-54 and Heinz, Op.cit:170). The practical consequences of these residual longitudinal displacements are uncertain (Heinz, Op.cit:172). If they were negligible, as suggested by the field measurements in Edmonton's LRT tunnel (Eisenstein and Branco, 1985:58), the final longitudinal strains would then be zero, as is the simplifying assumption for a 2D plane strain analyses. But during tunnel advance these strains are not zero, and therefore, the response of a strain path dependent soil would not be fully portrayed in a simplified 2D plane strain representation (Branco, 1981:112).

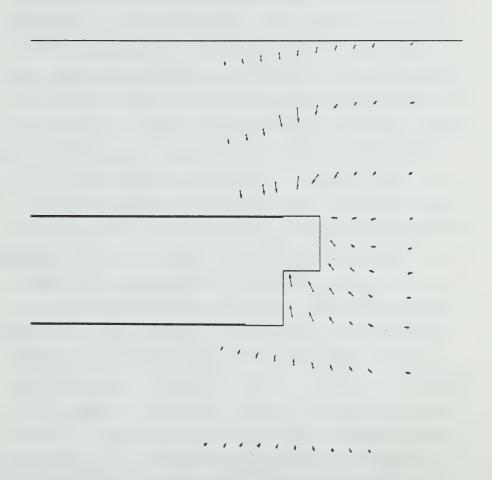


Figure 2.18 Incremental Displacement Field in the Longitudinal Vertical Plane, caused by an Incremental Advance of the Tunnel Face by Heading and Bench Excavation (after Heinz, 1984; modified)

What is important, however, is that, even if some residual longitudinal components of the displacement do remain after the tunnel face moves away, these are much smaller than the components orthogonal to the tunnel. This is particularly true if the lining is installed at a distance greater than half a diameter from the face (Ranken and Ghaboussi, Op.cit:352,354). The two dimensional transverse displacement field will predominate even more if a non-linear constitutive relationship is postulated for the soil. This is apparent from Ranken and Ghaboussi's (Op.cit:3-89, and 3-54) axisymmetric analysis using an elastoplastic cohesive and frictional model, and from a three dimensional finite element analysis using a hyperbolic non-linear elastic model for a shallow tunnel performed by Katzenbach (1981:95). Linear elastic analyses with lining installation close to the face, seem to enhance the residual longitudinal component of the displacements and also the residual longitudinal strain, and may not represent actual field conditions (e.g. Branco, 1981:112). El Nahhas (1980:236,242) derived from field displacements, longitudinal strains during tunnel advance varying from -0.4 to +0.4%, as compared with the horizontal transversel strains ranging from -3 to +3%, approximately. As mentioned before, the former decreased to zero just after the lining was expanded, while the latter remained high. Despite its narrow range of variation, the longitudinal strains may locally dominate the ground response. This is the case

around the face and heading region, when they can become the major principal strain. This is tacitly recognized in practice by the usual concern of face or face-heading stability. All these facts are fully confirmed by tunnel heading model tests (e.g., Casarin and Mair, 1981:38,39).

The three-dimensional stress-displacement zone extends also ahead of the advancing face of the tunnel. The distance of influence of this zone increases as the distance between the face and the point of lining installation decreases (Ranken and Ghaboussi, Op.cit), and also, as the soil strength decreases. Numerical analysis, field evidence and laboratory model tests, show that, typically, at distances between one to two diameters ahead of the face, the longitudinal strains are close to zero.

If one assumes that, for most tunnels, the lining is activated one diameter (D) behind the face, the region between 1 to 2D ahead and 2D behind the face is where non-plane strain conditions prevail. Within this region that fully surrounds the unsupported or partly supported excavated cavity, the stress and strain changes are dominantly three dimensional. The ground and lining responses are, therefore, affected by the longitudinal strains which had been neglected in the preceding sections.

2.3.6.2 Three Dimensional Arching and Ground-Lining
Response

In a non-pressurized tunnel, over a certain length, the in situ stresses around the contour of the expanded cavity

are fully reduced to zero. This happens even in shielded tunnels since, more frequently than not, soil overcutting is always necessary. In the idealized two dimensional plane strain ground response, the face advance was represented by a gradual and continuous reduction of the in situ stress, but they were never reduced to zero since some support was always assumed to be installed at a certain instant. Rotation (or inversion) of the principal stresses occurs not only in the transverse plane, but also in the vertical longitudinal plane through the tunnel axis, and in the horizontal longitudinal plane. Similar to that shown in the two dimensional representation (Sections 2.3.2 and 2.3.3), the shear stress increases in order to maintain equilibrium, after the total reduction of the in situ stress at the cavity wall. Therefore, the real "arching" mechanism is truly three-dimensional as illustrated in Figure 2.19 (Eisenstein et.al., 1984).

In the preceding sections, the existence of the transverse arching has been acknowledged. Terzaghi's (1943) arching theory is one of the existing approaces to study stress transfers associated with this phenomenon. A similar stress transfer mechanism develops in the longitudinal direction of the tunnel, spanning over the unsupported heading between points ahead of the tunnel face and the installed lining. This mechanism is also recognized in tunnelling practice, being referred to as the "doming" effect. Less evident but still present is the horizontal

TRANSVERSE ARCHING LONGITUDINAL ARCHING XYXYXYXYXX YYAYAYAY Section 1-1 Lining HORIZONTAL ARCHING Section 2-2 (plan view)

Figure 2.19 Three-Dimensional Arching near the Face of an Advancing Tunnel (after Eisenstein et.al. 1984: modified)

arching, again in the longitudinal direction, but with stress transfers spanning between the lining side walls and points ahead of the face. The unsupported cavity requires a three-dimensional shear stress mobilization in order to maintain equilibrium.

As the tunnel excavation and lining installation proceed, the unsupported heading moves ahead. Stress changes in the ground are caused by this advancing heading. At some section behind the face, the stress changes stabilize in equilibrium with the lining. Ground response in terms of stress changes and displacements, is therefore related to the advance of the tunnel, even in a ground with time independent behaviour as is assumed herein.

The ground response, relating radial stress and displacements as discussed in preceding sections, fully recognizes the arching occurring transversely to the tunnel, but only that. Various authors have attempted approximate approaches to account for the three dimensional effects around the unsupported heading by incorporating some additional factor into a plane strain analysis. For instance, Lombardi (1972:373, 1973:341), introduced the concept of a core disc reaction which is able to undergo progressive weakening and which generates an internal pressure that acts on the tunnel walls. Daemen and Fairhurst (1972:366), using an axisymetric finite element analysis, introduced a "proportionality factor" obtained from the radial displacement variations along the tunnel, This factor

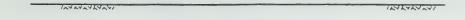
is then used to reduce the support pressure, which is assumed to have a direct relationship with the radial displacements. Amberg and Lombardi (1974:1058) introduced a ficticious body force acting outwardly into the ground. This was to account for the deviation of the longitudinal stress trajectories associated with the longitudinal arching in an axisymmetric configuration. Panet and Guellec (1974:1165) also introduced a fictitious internal pressure but selected it in such a way that the corresponding radial displacements are equal to those experienced at the face (or at the point of lining installation) in an axisymmetric tunnel. Egger (1974:1009, 1980:313) proposed another simplification by approximating the tunnel face by a half sphere. Closed form solutions relating stress and displacements are available for a sphere in a hydrostatic in situ stress state. Egger (Op.cit) combined the latter with that for a cylinder to represent the tunnel and thus approximately account for the face effect.

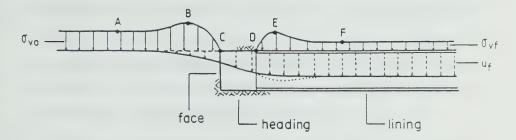
All methods aforementioned have limitations that are readily identifiable. Lombardi and Amberg's (1974:476) system of loading assumes that the maximum shear planes in the ground are orthogonal to the tunnel heading walls. The arrows shown in Figure 2.19 represent schematically the maximum principal stress trajectories. Hence the maximum shear stress is not always orthogonal to the tunnel walls (Kerisel, 1980:235). The most important limitations, common to all methods, are that they do not include gravity action,

or stress conditions whiich are not axisymmetric.

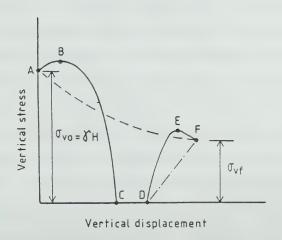
Following the Lombardi and Amberg (Op.cit) and Kerisel (1980:236) conceptual models, Eisenstein et.al. (1984:111) proposed pictorial distribution of the radial stress, $\sigma_{...}$, and radial displacements, u, along a longitudinal line at the tunnel crown elevation, which is reproduced in Figure 2.20(a). Field evidence in mining operations (for example, Wilson, 1981, quoted by Brady and Brown, 1985:376) suggest that there might be some stress concentration at point B ahead of the tunnel face (certainly not very high in shallow urban tunnels), this being followed by a rapid decrease of the vertical stress to zero at C. The radial stress should be zero along the unsupported heading (points C-D), provided that the lining is installed at a certain distance behind the face and no internal pressure is applied against the heading walls. With the lining installed, there should be an increase of vertical stress and a stable equilibrium situation is eventually attained at point F. Depending on the relative stiffness of the lining and the ground and also depending on the distance between the face and the point of lining installation, one could also expect some sort of stress concentration (point E) near the leading lining edge before final equilibrium is achieved at F.

The vertical displacement distribution is slightly more continuous, but again, some sort of concentration might be suggested, as indicated by the dotted line around point E.





a) VERTICAL STRESS AND DISPLACEMENT DISTRIBUTION ALONG THE CROWN



b) GROUND-LINING RESPONSE AT THE CROWN

Figure 2.20 Ground-Lining Response Concept for the Tunnel Crown (after Eisenstein et.al., 1984: modified)

The combination of the stress and displacement distributions shown enables one to draw a response curve of the combined soil and lining system, and this is depicted as the solid line (ABCDEF) in Figure 2.20(b). Although conceptual, this ground-lining response curve has the virtue of incorporating the main features of the actual three-dimensional stress transfer mechanisms. Similar responses would be expected at other points of the tunnel contour.

Departures from this idealized response would be expected in less ideal situations such as those respresented by unstable and sensitive soils, high horizontal in situ stresses, etc. However, in all cases, a drop in radial stress around the unsupported heading would be observed.

It should be stressed that the solid line ABCDEF in Figure 2.20(b), incorporates the response of both ground and lining, including their three-dimensional interaction. The portion ABC would represent mainly the ground response ahead of the face, but it is to some degree affected by the presence of the lining installed at D, by virtue of the longitudinal arching mechanism. Reciprocally, the portion DEF would be dominated mainly by the lining response, but again, it also expresses the interaction process between the support and the soil. The dashed curve, which is shown in the figure, would be an idealized plane strain ground reaction curve, and the chainsdotted one would represent the plane strain support reaction curve. The equilibrium point given by the intersection of these two latter curves, is

shown coinciding with the equilbrium point F, but as explained in Section 2.3.5, this should not be the case. It was also suggested in that section that the ground reaction curve can be an envelope of equilibrium points, according to variations in the liner stiffness or in the delay of liner installation.

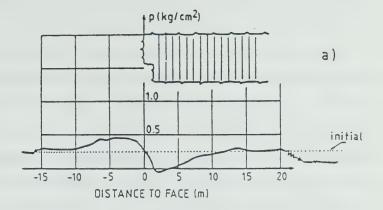
Some of a number of field observations supporting the concept of the ground-lining response just discussed are presented in the following paragraphs.

2.3.6.3 Evidence of Three-dimensional Ground-Lining Response

The assessment of the stress redistribution around the advancing face of a soft ground tunnel has not beeen fully explored in the field, mainly because stress measurements within a soil mass are difficult to obtain. The inevitable inclusion of a body of different stiffness into the ground, the stress sensor, and the installation effects frequently lead to unreliable results. Sauer and Jonuscheit (1976) reported one attempt to measure stress changes during excavation by the so called NATM. Twin tunnels were driven simultaneously in a fairly stiff tertiary clayey marl, locally known as Frankfurt clay, as part of the Frankfurt Underground Transit System (S-Bahn-Los6). Each tunnel had a circular profile with an excavated diameter of 7.7 m, running parallel at a distance apart of 4.9 m wall to wall, with a ground cover of 14.65 m. Stress measurements around the tunnels, and especially in the 4.9 m ground pillar

between the tunnels, were taken by means of several clusters of Gloetzl pressure cell. The cells were installed about three months before tunnel construction, by being carefully packed in clay filled bags which were then lowered into boreholes. The bags in place were surrounded by poured sand and the rest of the hole was filled with clay cuttings. Further details on this instrumentation can be found in Sauer and Sharma (1977). Since disturbance of the in situ stress field is unavoidable in forming the boreholes, the magnitude of the measured stress certainly does not represent their actual values (the initially recorded cell pressures, after equilibrium was attained, varied from one-fifth to one-tenth of the overburden pressure). However, the observed pressure changes are believed to provide some qualitative idea of the relative stress changes associated with the tunnel advance.

Figure 2.21(a) shows the variation of the vertical pressure readings at a point located 0.35 m above the crown of one of the tunnels. The measurements show a stress increase above the initial value as the face approaches the measuring point. A peak is reached about a half diameter ahead of the face. As the tunnel face passes below the instrument, the readings fall fairly sharply down to a minimum which is close to zero. After closure of the shotcrete ring at the invert (at about 2.4 m behind the face), the pressure readings begin to increase, up to a value which is smaller that the observed peak ahead of the



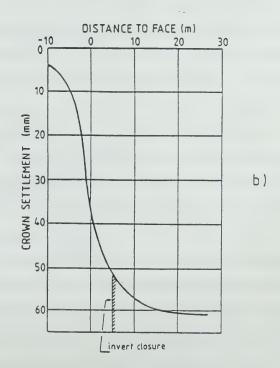


Figure 2.21 Vertical Stress and Displacement Measurements at Crown Elevation for Tunnels in Frankfurt (modified after Sauer and Jonuscheit, 1976 and Stroh and Chambosse, 1973)

face. Continued observations showed that the readings fell to a value below the initial reading after several months.

Unfortunately Sauer and Jonuscheit (1976) did not present measurements of observed ground displacements at this site. To complete the picture, data from another tunnel in Frankfurt (U-Bahnbau-Los25 Romerberg, Stroh and Chambosse, 1973) driven in the Frankfurt clay under similar conditions is presented in Figure 2.21(b). The excavated diameter and the ground cover of this tunnel were slightly less than the former (D=6.5 m and H=11.5 m). Again in this case, two tunnels were driven parallel and simultaneously at a distance of 6.2 m wall to wall. The settlements were measured at a point located 0.5 m above the crown of the north tunnel.

If the data from Figure 2.21(a) and (b) were combined, a picture similar to that shown in Figure 2.20(b) would emerge, thus confirming the three-dimensional ground-lining response concept that was postulated.

Figure 2.22(a) and (b) present similar data for the springline elevation in the ground pillar between the tunnels, as shown schematically. The Gloetzl cell was installed half a metre away from the S-Bahn tunnel wall. The horizontal displacements were observed by Chambosse (1972:Figure 75) in the U-Bahn tunnel by means of a specially designed measuring device installed from the surface, and also located 0.5 m away from the excavated tunnel wall. Unfortunately, the displacements are given as a

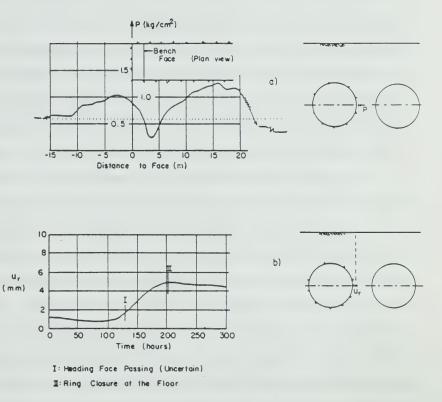


Figure 2.22 Radial Stress and Displacement at Springline
Elevation for Tunnels in Frankfurt (Modified after Sauer and
Jonuscheit, 1976 and Chambosse, 1972)

function of time, rather than of the distance to the heading face. However, some information is provided regarding the instant the face hits the instrumented section and the invert region being shotcreted, closing the lining ring (at a distance of 5 to 6 m behind the face). The same sort of response is observed at the springline as for the crown. One notes however, a minor outward radial displacement, after the support ring is closed (Figure 2.22(b)). From this data one may conclude that the concept postulated for the crown, is also valid for the springline region, thus confirming the "horizontal" side arching shown in Figure 2.19.

An outward displacement of the crown after lining installation is sometimes observed as was seen for the springline. This was noted during a careful internal levelling of the crown in a shallow tunnel built in Sao Paulo's tertiary soils. This tunnel was built by the NATM and is described in detail by Negro and Eisenstein (1981), Simondi et.al., (1982) and further summarized by Heinz (1984:273). A deep bench mark was installed in the access shaft located about 20 m behind the measuring points. The bench mark anchor was installed some 25 m below the floor elevation. A metallic invar levelling rod and a Wild N3 levelling instrument were used. The zero readings were taken soon after the first shotcrete layer was in place. The evolution of settlements was observed at two points in the lining crown. A minor but distinct crown heave was noted 1.5 to 3 diameters behind the face and it is supposed that this

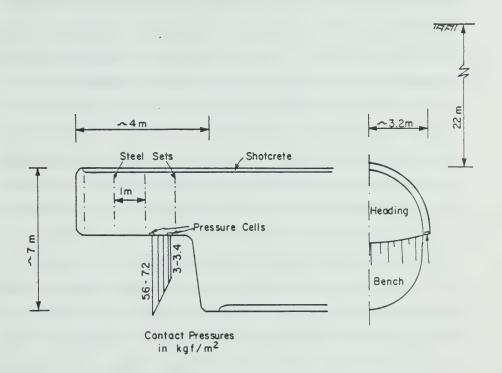
is related to the three-dimensional load transfer mechanism.

A crown heave is sometimes evident in plane strain numerical simulations of shallow tunnels with staged excavation. This was noticed by Heinz (1984:131) and Negro et.al., (1985:25), when a Lambe's (1973) Type A prediction was performed prior to the construction of a large cross section tunnel for Sao Paulo Metro, again using the NATM with shotcrete support. To some extent, a limited crown heave seems to be related to the process of numerically simulating the stages of tunnel construction in a plane strain situation. This heave may develop during invert excavation and immediate lining erection, in the two dimensional representation. In the true three-dimensional situation, the recently applied shotcrete is attached to sections already fully completed further behind, and this may generate some longitudinal bending in the upper arch shell, thus minimizing upward movement at the crown. Not to be disregarded is a possible effect of the shotcrete hardening with time, and this may also act towards reducing this trend. Despite these considerations, field monitoring of this tunnel once built, revealed some crown heave after closure of the shotcrete inverted arch (Kochen et.al., 1985: Figure 6 and Eisenstein et.al., 1986: 717). The measured heave was about half of the predicted amount.

Field evidence seems to confirm that longitudinal bending of the upper shell of the open shotcrete ring occurs upon the advance of the heading face in tunnels built by the

NATM, in a heading and bench scheme. Laabmayr and Weber (1978:88) furnish measurements of pressures in the footing of the upper shotcrete arch resting on the heading floor of a Munich Subway tunnel (Baulos, 18.2). These were measured using four contact hydraulic pressure cells installed between the shotcrete and soil. The results obtained are schematically presented in Figure 2.23. The absolute magnitude of the measured contact pressures may be debatable, considering that readings of this kind of cell are very senitive to installation procedures. However, if it is assumed that the same procedure has been used in all cells installed, the results shown can be considered in relative terms: a non-uniform contact pressure distribution prevails and it could possibly be explained by the longitudinal bending of the upper shotcrete shell supporting the heading.

One could possibly argue that the measurements could have been affected by the existence of steel ribs inserted in the shotcrete (TH channel sections were used with 89 to 108 cm height and 16 to 21 kg/m). These steel sets are said to concentrate loads and a non-uniform footing pressure would then be expected with the pressure cell reading varying according to its distance from the steel sets. However, measurements taken in more recent projects in Munich (Baumann, 1985:450), where steel ribs have been replaced by lighter lattice girders, show the same tendency. In this case, thrust forces and transverse bending moments



Note: Measurements of four cells, given by Laabmayr $\bf 8$ Weber (1978:89) for heading face at Station 85. Not to scale.

Figure 2.23 Measured Footing Pressures in the Upper Shotcrete Arch at the Munich Subway (Baulos 18.2)

were measured directly in the shotcrete lining, using a specially designed embedded gauge. Except for a broad description, no detail is given on this patented equipment. Nevertheless, the measurements indicate a non-uniform thrust force concentration in sections nearer to the advancing face (maximum thrust forces of almost 100% in excess of the average value were recorded about at one diameter behind the face). The reliability of these results have been questioned by some, on the grounds that the way the measuring equipment works was never disclosed (Gais, 1985:201). But they show, once more, that lining load concentrations may be found near the advancing heading and these could be associated with the three-dimensional loading mechanism already discussed.

Load concentrations in support sections near the tunnel face were also detected in deeper rock tunnels. This was the case in the Kielder Experimental Tunnel in mudstone, (Ward 1978:155) in which higher thrusts were measured in the steel lining ring closest to the face. This unit was installed less than 0.1D behind the front and it is suspected that a smaller load concentration would have been detected if its installation had been delayed.

Three-dimensional numerical simulations confirm some of the field evidence just discussed. The axisymmetric finite element analyses by Ranken and Ghaboussi (1975) confirm the existance of a radial stress concentration ahead of the face (Op.cit:3-5,3-69,3-85). It may exceed the in situ stress by as much as 10% depending on the conditions of the analysis.

These authors (Op.cit:3-62,3-80,3-90) also found higher thrusts in the sections of the lining closer to the face. This load concentration decreased as the distance from the face to the front of the lining installation increased. For the usual distances to the point of liner installation which is normally greater than 0.5D in soil tunnels, Schwartz and Einsteins's (1980:71,168) results indicate no load concentration occurs in closed lining rings at all. They suggest that only in cases with stiff supports and short delays of lining installation that this condition is observed. The analyses also show that the lining load concentration tends to be reduced when a non-linear constitutive relationship is postulated for the ground (Schwartz and Einstein, 1980:67,162).

Schikora (1984) presented results of three-dimensional finite element analyses for non-hydrostatic in situ stress conditions, assuming a non-linear elasto-plastic constitutive relationship for the soil and for two different schemes of face advance (full face and heading and bench). Moreover, he took into account the effect of the shotcrete hardening, by assignin increasing Young's moduli to lining rings located at increasing distances from the tunnel face. He found that while no load concentration was detected in the longitudinal distribution of the average thrust forces ther was a significant thrust variation within each lining segment regardless of whether it was a closed ring or not (see Figure 2.24). The average thrust forces steadily

increased from close to zero near the face to the final equilibrium value further behind. In each segment, the larger thrust forces occur in the leading edge, closer to the tunnel face, and smaller forces were obtained in the trailing edge. This seems to result from the non-uniform radial displacement distribution of the unsupported heading in the longitudinal direction. Upon further advance of the face, a discrete length of the stiffer support system is installed against the contour which will tend to deform more uniformly than the previously unsupported soil. This leads to higher loads in the leading edge (which potentially tend to displace more) and smaller loads in the trailing edge. The result is a 'saw-tooth' type of thrust force distribution as shown in Figure 2.24. The final thrust force distribution is obtained by superimposing the thrust increments due to a single step of face advance. This is shown as a shaded area in Figure 2.24a. Clearly, a continuous variation of thrust would be observed if both the lining and face continuously and not in finite amounts.

Hutchinson (1982:161) also found similar non-uniform thrust distributions within a liner segment, from an axisymmetric finite element elastic analyses. He pointed out further, that this longitudinal variation in liner thrust is mainly influenced by the delay in liner placement, but is also affected by the extent of the "softened" ground zone ahead and around the tunnel heading. If this type of behaviour is actually representative of that in a prototype,

then one would expect different factors of safety against liner failure at different points within the same liner segment (Hutchinson, Op.cit:167).

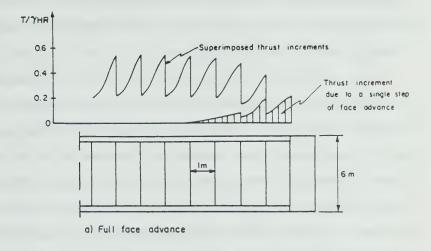
These numerical results confirm the findings by Laabmayr and Weber (1978) and Baumann (1985) which were discussed previously. The role of increasing stiffness with age of shotcrete lining in this process is not yet very clear. Also to be properly assessed are the global consequences of these findings, particularly for a heading and bench scheme, during the period that the shotcrete ring is not closed at the floor. To the writer's knowledge, just one well documented case history of a shallow tunnel failure is reported in the literature, in which the upper shotcrete shell failed under significant longitudinal bending '. The 6 m diameter tunnel, with 11 m soil cover was driven through soft and saturated organic clay (MH, with c,=20 kPa). The tunnel heading was advanced only with a fairly flat temporary invert, and closed some 3 to 4 mbehind the face (protected with a core berm). The accident was described by Cruz et.al., (1982) and was analyzed by Kochen and Negro (1985) and by Kochen et.al., (1987). Lining failure came

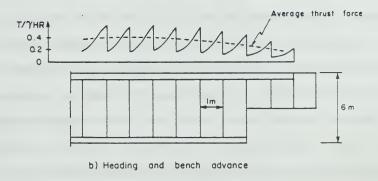
^{*} Muller (1978:31) made reference to the collapse of two tunnels in soil, apparently under similar circumstances. However, the scarcity of data available does not permit any detailed interpretation. Both tunnels were driven in marls, one for a railway scheme near Paris, in 1973 and the other for a subway scheme somewhere in Germany. Similar accidents were detected more frequently in soft rock tunnels. The failures in the Pfaffenstein tunnel in Regensburg, Germany, are an example, reported by Blindow and Wagner (1978) and by Hereth (1979). In all cases collapse seemed to have been associated with excessive drivage of the heading, without closure of the inverted arch.

after very large surface settlements (up to 300 mm) were detected in the soil, above and in front of the heading. The impending ground collapse was brought about by the failure of the lining which had not been designed to withstand large longitudinal bending stresses. Although this may be an extreme case, it seems that there is a need to investigate further the mechanisms of transient lining loading during tunnel advance, both numerically and by specific field instrumentation. The work by Pelli et.al., (1986) is an example of one such attempt, and the results they obtained confirmed to some extent the phenomenon described herein. They show further, that depending on the ground and lining properties, on the round length of the excavation, on the delay of lining installation and on the in situ stress state, tensile thrust forces may develop in the trailing edge of a liner segment. To the writer's knowledge, this has not been observed so far by field monitoring in shallow tunnels, and further investigation of the issue would be of considerable interest bearing in mind its consequential effects.

2.3.6.4 Three-dimensional Ground-Lining Responses from Numerical Analyses

In order to better assess the ground-lining response concept postulated formerly for a shallow tunnel, a three-dimensional finite element analysis was performed using the program ADINA (Bathe, 1978). Details of this study were presented by Eisenstein et.al. (1984) and Heinz





Notes: Cover H=20 m/; soil properties: γ = 21 kN/m³, K_o = 0.8, E=100 MPa, c=50 kPa, ϕ = 20°; Lining: thickness = 0.15 m, E=30 GPa. (final)

Results from 3.D FE elasto-plastic analyses.

Figure 2.24 Longitudinal Distribution of Thrust Forces at the Tunnel Crown (after Schikora, 1984: modified)

(1984:176). Complementary results will be presented herein. This type of analysis was favoured in order to identify the expected distinct response for different points of the tunnel contour, all of which in an axisymmetric analysis of a deep tunnel would be identical.

Very briefly, the analysis involved the establishment of the initial stress condition by the application of gravity loads, leading to an at-rest coefficient, Ko, equal to 0.75 expressed as a function of Poisson's ratio. Linear elastic behaviour was assumed for both the soil and lining. The former had a Young's modulus increasing with depth and was equal to 13.7 MPa around the tunnel. A Young's modulus of 5 GPa and a Poisson's ratio of 0.25 were selected to represent a shotcrete lining of 15 cm thickness. The tunnel had an excavated diameter of 3.9 m and a ground cover of 6.3 m, rendering a ratio H/D of 1.62. The relative stiffness of the support given by equations 2.17 and 2.18, were C=0.034 and F=64.2. Details of the finite element mesh design and of the boundary conditions used are given by Eisenstein et.al., (Op.cit:115) and Heinz (Op.cit:180). Full face excavation was simulated using the "birth-death" option. All the elements in the region to be excavated are initially active and at the designated step when excavation is to take place, these elements are deactivated. The lining elements, initially active as a soil material are de-activated and later re-activated as concrete. Kochen et.al., (1985) discussed in detail this feature of the ADINA code, comparing it with other numerical procedures. Tunnel advance was conducted in eight steps and two runs were performed: one with the leading lining edge located at a distance L equal to one half of the tunnel diameter behind the face and another with L equal to two-thirds of the diameter.

Figures 2.25 to 2.27 show the longitudinal distributions of the dimensionless radial displacement U, defined by equation 2.16 (normalized to the in situ radial stress), and of the radial stress ratio (current stress divided by the inital stress), for points at the crown, springline and floor for L=2D/3. Displacements were taken from points at the tunnel contour, whereas the stresses correspond to the ground stresses calculated at the Gauss points of the soil elements adjacent to the tunnel perimeter. The stresses were taken from Gauss points giving the lowest stress value and were plotted against the distance between the face and the centre of the soil element.

The mechanism that causes the longitudinal variation of thrusts in the liner, also induces variations in the ground stress and displacements that lead to "wavy" longitudinal distributions, especially behind the face, after the lining is installed (see Hutchinson, 1982:168). This effect was enhanced by the size of the elements used and by the fact that in some initial and final steps, the length of excavation round was larger than that in the central portion

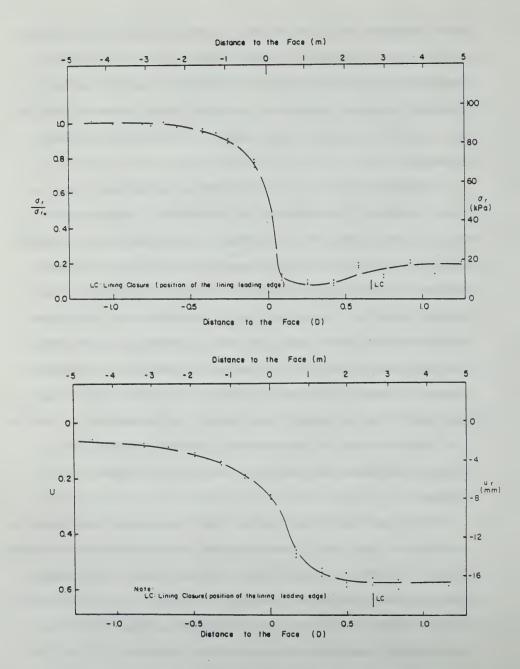


Figure 2.25 Radial Stresses and Displacements at the Crown Elevation (L/D=2/3)

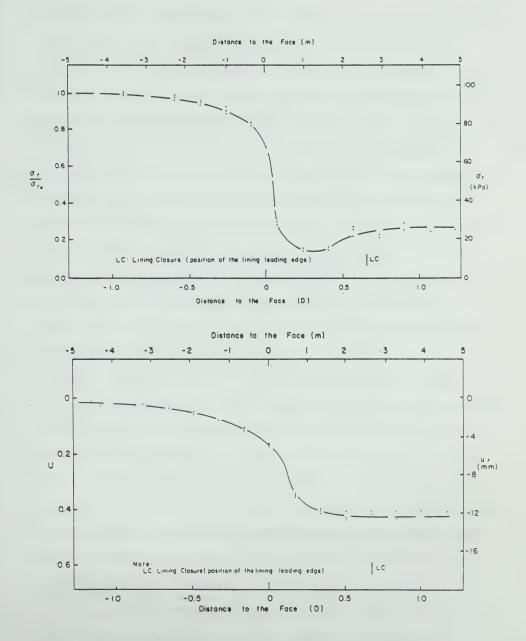


Figure 2.26 Radial Stresses and Displacements at the Springline Elevation (L/D=2/3)

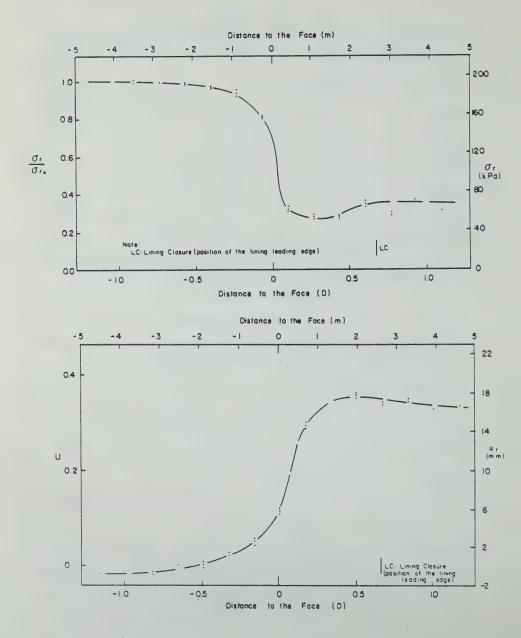


Figure 2.27 Radial Stresses and Displacements at the Floor Elevation (L/D=2/3)

of the finite element mesh. Also known to affect the results is the method used to reduce the stresses in the heading when elements are de-activated. Zones of high stress gradient, such as those found in the vicinity of the advancing heading, require small sized elements, which in turn increases the cost of the analysis considerably. To minimize these effects, only the results of the excavation of the central portion, were considered where the elements were smaller, but even so, some scatter in the stresses and displacements is present. In order to exclude this effect and therefore to obtain a response that would ideally correspond to a continuous advance of the face and a concomitan, continuous lining installation, the stress and displacement distributions were smoothed out through averaged results. This was done by superimposing output stress and displacements from three consecutive steps of the face advance, in the central portion of the mesh. and by making the face portion in these three steps coincide. The same procedure was used for points at the crown, springline and floor, for the run with L=D/2 (Appendix A). The smoothed out stress and displacement distributions found may differ slightly from that shown by Heinz (1984), a different criteria have been adopted herein.

The radial stress distributions did not show any significant concentration at any point of the tunnel contour, either ahead or behind the unsupported heading. However, it can be seen that this stress decreases sharply

from its original value for points adjacent to the unsupported heading. They do not drop to zero along the unsupported span, since they refer to points at some small distance away from the excavation contour. As a further consequence of their location, these points start to partly recover stress at some distance ahead of the leading edge of the lining. If the point were directly at the excavation line, it would experience stress increase only after the lining had been placed against it and not before.

The longitudinal gradient of the radial stress and displacement ahead of the advancing heading, show different patterns for the cases studied. The rate of change in stress is clearly greater than that for displacement.

Three-dimensional non-linear elastic finite element analysis by Katzenbach (1981:102,114,115) and Hutchinson (1982:564,568) also showed similar results, thus supporting these observations. Also the contrast seen between the measured stress and displacement rates in the Frankfurt tunnels (Figures 2.21 and 2.22) confirm this finding.

The first consequence of this fact is that the ground response, in terms of the stress-displacement relationship for points ahead of the face, is non-linear, even for a linear elastic ground. It results from the continuously changing geometry and boundary conditions of the problem, and is also affected by the presence of the lining further behind. Under these conditions, the principle of superposition is not valid and the problem requires an

incremental excavation approach, even when the ground and liner both display linear elastic behaviour. As pointed out by Ranken and Ghaboussi (1975:4-16), the sequential excavation simulation is less significant in 3D analyses of unlined tunnels in linear elastic ground. For this, the simulation of the entire tunnel excavation in just one excavation step gives results nearly identical to those obtained when the full excavation sequence is used.

Another feature observed in Figure 2.25 to 2.27 and in those in Appendix A, is that both the magnitude and distribution of the radial stresses and displacements ahead of the face are only slightly affected by the lining installation distances, for all points in the tunnel contour. This finding was confirmed also by Pelli et.al., (1986), who used a more refined three-dimensional mesh. These authors showed also that the radial displacements are not much affected by variations in the relative stiffness of the support (C from 1.4 to 14 and F from 9 x 103 to 2.4 X 105). In other words, the soil response ahead of the face is not very much influenced by the presence of the liner. Both the displacement and stress distributions behind the face are much affected by the position of the lining, and as would be expected, an increase in the unsupported heading length, ratio L/D, leads to larger radial displacements and smaller radial stresses. The same thing was noted in a plane strain simulation (Section 2.3.5), where the delay in support installation was represented by an arbitrary

reduction of the in situ stress, prior to lining activation.

The ground and lining response, in terms of the relationship between radial stress and displacement, for the three points of the tunnel contour, can be obtained from the curves shown in Figures 2.25 to 2.27 and in Appendix A. The response curves for the two distances to support installation for the crown, springline and floor are shown in Figures 2.28 to 2.30, respectively. They are presented in terms of non-dimensional stress and displacements. The dimensionless radial displacement is taken as an increment, AU, since some non-zero residual displacements were found in the boundary of the 3D mesh, ahead of the face. The curves simply confirm what has been described before. They are strongly non-linear and ahead of the face they are similar, (portions AB and AB'), although they do not coincide. The effect of the lining presence is felt slightly more at the tunnel crown, since the distances between curves AB and AB', for different L/D ratios, are larger than for the other points. For each point of the tunnel contour, the major differences in the response curves are seen for the portion BDs and B'D', which are more affected by the variations in size of the unsupported heading span and by the relative stiffness of the lining. Noteworthy, is the fact that the springline curve, for the smaller L/D value, reflects a characteristic outward movement, after the radial stress reaches a mimimum before the support is actually installed, as mentioned previously. A similar response is

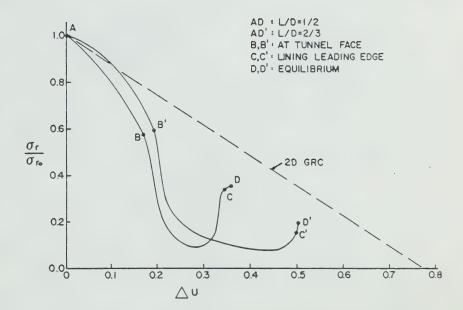


Figure 2.28 Ground-Lining Response Curves at the Crown

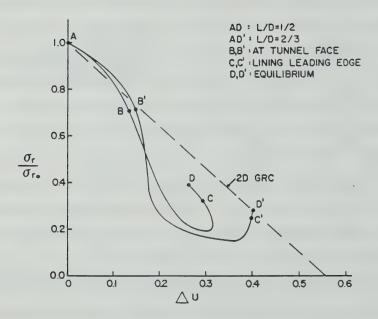


Figure 2.29 Ground-Lining Response Curves at the Springline

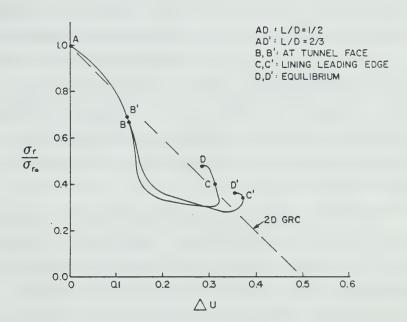


Figure 2.30 Ground-Lining Response Curves at the Floor

noted in the floor, where a small settlement is observed, after the expected heave.

For the sake of comparison, a two-dimensional finite element analysis was also performed, in order to generate the ground reaction curves for the crown, springline and floor. This is also described by Eisenstein et.al., (1984:122) and by Heinz (1984:197). Both mesh and material properties used for this analysis correspond exactly to a transverse plane section of the 3D mesh. A single step excavation was performed and no lining was installed. Stress and displacements were obtained in the same locations as in the three-dimensional analysis. The ground reaction curves thus obtained are shown as dashed lines in Figures 2.28 and 2.30.

It has been shown (Section 2.3.5) that the equilibrium points of the ground and support interaction in a plane strain simulation, do not lie on these lines. that do not account for that interaction. Therefore, it is not surprising that the equilbrium points from the 3D analyses do not coincide with these curves either. However, it seems noteworthy to point out that, with the exception of the tunnel floor point, the two dimensional ground reaction curves seem to operate as an upper bound for the equilibrium stresses and displacements of the 3D analyses. But even for the floor, the 3D equilibrium points are not too far off the 2D reaction line.

2.4 Summary and Conclusions

In this chapter the idealized behaviour of a shallow tunnel under time independent conditions was presented. An attempt was made to identify the differences between shallow and ideally deep tunnels. It was found that, depending on the criteria used, the relative tunnel depth beyond which a tunnel is said to be "deep", may vary considerably. Previous works on the subject were reviewed, and from them, two conclusions could be drawn:

- (a) When studying the tunnel lining response or the behaviour of the ground immediately around the opening, the presence of the stress free ground surface can be neglected for relative tunnel depths (H/D) greater than 1.5. However, the influence of the gravitational stress gradient should always be taken into consideration.
- (b) When studying the displacement field around a tunnel or the possible modes of collapse of the ground, the effect of the ground surface, as well as the action of gravity should always be considered.

Thus, a 'deep' tunnel, across which the stress field gradient becomes negligible and at which the influence of the stress free boundary surface is minimal, represents an idealization with limited practical value for the study of an urban tunnel.

Stress and Strain Changes in the Ground

The stress changes around an unlined opening in plane strain were investigated. The effects of gravity and of the

non-linear ground response were discussed. The associated strain changes were then studied for certain ideal conditions. Some peculiarities of the stress-strain ground response were addressed and explained in terms of the stress changes leading to soil failure around a 'deep' tunnel.

Among them are the apparent 'strain-softening' response and combined dilation ('loosening') noted after failure is reached in a frictional material. Soil failure around the tunnel may or may not lead to formation of a collapse mechanism. The results of this conceptual analysis were discussed and were extended to less idealized conditions. The consequences of the non-linear response of the ground were addressed.

Field and tunnel model test results were used to identify when the ground response to shallow tunnelling becomes definitely non-linear. It was shown that if the factor of safety against collapse is greater than 2 or 3, the ground response may be approximated by linear elasticity, but below that, a non-linear response is to be expected. Shallow tunnel construction under "good ground control conditions" involve factors of safety of about 1.5 or even less. Moreover, the path to failure in soil tunnels is short, and the degradation of safety with ground displacements is rapid. Therefore, for usual construction conditions, the soil response to tunnelling, in terms of stress and displacement relationships are typically non-linear.

The stress paths around a plane strain shallow tunnel in a non-linear ground were investigated. The prefailure stress paths were found to vary considerably from point to point around the opening, and to depend on the in situ stress state, on the relative tunnel depth and on the soil strength. If the three-dimensional stress state is taken into account, even more intricate stress paths would be observed. Evidently, it is difficult to anticipate the likely stress path. A large degree of simplification will be required in this regard when approaching a practical tunnelling problem.

The development of shear strains around shallow tunnels was examined using published results of model tests and field measurements. High shear strain concentrations were found around or at the collapse stage, their geometric pattern being mainly controlled by the presence of the ground surface and the relative tunnel depth. Despite this dependence, the shear strain patterns at collapse are all similar. Prior to collapse they are not necessarily so. These zones of high strain concentration tend to develop and propagate rapidly upon tunnel unloading. For normally consolidated soft clays, this development occurs for factors of safety less than 1.4, while for overconsolidated stiff clays and for dense sands the high shear straining becomes apparent for factors of safety less than about 1.1. The model tests indicate that there is a clear relationship between the factor of safety and the tunnel crown

displacement. Moreover, they indicate that the deterioration of safety is rapid with increasing crown displacement. To ensure serviceability, these displacements should be usually less than 4% of the tunnel diameter. For this, the model test results indicate that the factors of safety should be higher than the values given above. In other words, the requirement for tunnel serviceability or for limited ground surface settlements usually seems to imply factors of safety higher than those at which formation of high shear straining is observed.

The above analysis was repeated, reinterpreting available model test results in terms of the dimensionless crown displacement, U. This parameter seems to correlate better with the factor of safety. Regardless of the test type (drained or undrained) and the soil type, U values in excess of 1.8 will generally mean a near collapse condition, with high shear strain concentration and small factors of safety. A U value of 1 or less, corresponding to factors of safety of, typically 1.5, would represent tunnelling under 'good ground control conditions' where high ground shearing will usually not be present.

Though presented tentatively, the above criterion has the merit of recognizing the dependence between factors of safety and ground displacements. Moreover, it expresses in quantitative terms, through a limiting crown displacement, the condition at which the ground stability becomes critical. Beyond it, ground control conditions cease to be

'good', as it involves ground collapses and uncontrolled ground deformations. The criterion also indicates that, under equal conditions and for the same factor of safety, a softer soil may experience larger crown displacements than a stiffer soil. Different limiting dimensionless crown displacements may exist for different soil types. The test results available did not allow a clear definition of this aspect, though they seem to suggest a higher limiting dimensionless crown displacement for softer soils.

The proposed criterion is largely empirical. Its use for conditions different from those found in the model tests, therefore, cannot be ensured. For instance, it may not be applicable to soils showing strain softening behaviour. Before further investigations on the subject are undertaken, the criterion may be used tentatively, with due care.

The development of volume changes around shallow tunnels was also examined using published results of model tests and field instrumentation. Volumetric changes in the ground, under time-independent conditions, were found to be a function of many factors, including the mean normal stress level, the shear stress level, the relative tunnel depth, the soil type and its stress history. Typical volume strain distributions around tunnels were examined, and typical responses were identified.

A conceptual model was proposed for tunnels in sand, in which the total volume change scaled to the tunnel volume,

was related to the tunnel depth. The model assumes a fixed amount of ground stress release at the opening (a fraction of the in situ stresses) and takes into account the increase of the mean normal stress level with depth and the influence of the ground surface. As the tunnel gets deeper, the overall volume change increases up to a certain depth beyond which the volume changes becomes less affected by the ground surface and more controlled by the mean normal stress level. Thereafter, the overall volume changes decreases. This conceptual model is supported by some field and model test results.

Idealized Lining Action

In previous discussions, the action of the lining was reduced to that of some balancing stresses applied to the opening, in order to keep it stable. The actual lining action was then discussed, assuming a two-dimensional plane strain condition. Some extreme conditions were investigated, regarding the physical contact between the lining and the soil. In the tangential direction, a full and a no slip condition were assumed and the consequences of these assumptions were assessed. In the radial direction, conditions representing a full and an incomplete lining ground contact were investigated and were referred to as 'good' and 'poor' lining contact.

The support and ground responses were then analysed, assuming a good lining contact in an ideally deep tunnel. The lining-ground interaction was examined using available

linear elastic analytical solutions. The analysis was then repeated, incorporating the effect of the gravitational stress field present in a shallow tunnel case. It was noted that the shear strength mobilization at the lining-ground interface may not be very high, decreasing as the tunnel gets deeper, as the in situ stress ratio tends towards unity, and as the lining activation inside the tunnel is delayed. The actual slip conditions may lie somewhere between the full-slip and the non-slip condition, possibly closer to the second, particularly if a good lining-ground contact is ensured.

In order to include the effect of the ground surface, of the non-linear soil response and of the delayed lining installation, the results of some finite element analyses were examined. The support response was noted to vary, as the amount of ground stress release before lining activation increased. The ground stiffness reduction associated with the increasing stress release leads to different relative lining stiffnesses and different support-ground interaction, though the same lining was used in all analyses. The compressive and flexural stiffness ratios are better described, for these conditions, in terms of the current ground stiffness.

The consequences of a poor lining ground contact were then addressed. This condition is represented, for example, by a void left unfilled between the lining and soil at the crown region. If the size of this gap is small, then with

the advance of the tunnel face, the soil may come in contact with the lining without a local or global ground collapse being observed. However, if the void space is sufficiently large, either local or global instabilities may develop. In dense sands, a wedge like portion of the roof may collapse. In fissured stiff soils, blocks bounded by pre-existing discontinuities may fall and rest on the lining. Unlike the case of good lining contact, non-uniform and concentrated ground loads may develop on the lining. If the contact between the support and ground at the tunnel walls is also poor, the ground may not offer lateral confinement to the lining.

Under these conditions, the support will be loaded by the accumulation of loosened material against it, and these loads are mainly due to the self weight of the disturbed soil. This mechanism is referred to as 'loosening' and the associated loads are described as 'gravity loads'. The development of this process, which is associated with significant volume expansion above the tunnel, involves large ground movements which may not be acceptable in an urban tunnel. This loading mechanism is associated with ground conditions approaching a collapse state.

The magnitude and distribution of these gravity loads are difficult to predict, as they cannot be estimated by classical continuum mechanics approaches. Moreover, it is also difficult to predict the extent and distribution of the voids left behind the support. Hence, the definition of the

extent of the soil embedment for these conditions is uncertain.

A simple model was presented to show that even if the magnitude and distribution of the final gravity loads were known, the lining response during an uncontrolled ground loosening condition is not predictable. The support response during gravity loading depends on how these loads build up to their final values. This uncontrolled loading process can cause lining distortions which are more critical than those calculated for the final gravity loads.

The above conditions are, therefore, critical in terms of the ground response, approaching a collapse state with uncontrolled and possibly excessive movements. They are also critical regarding the lining response, which may involve large distortions or even instabilities (from lack of embedment). Consequently, they represent poor ground control conditions which are not acceptable in urban tunnelling practice. Rather than designing for them, the practitioner should identify the possibility of their development and make design provisions to eliminate them. Many ground control measures are available for that purpose. Some of them are discussed in Chapter 4.

The development of these uncontrolled tunnelling conditions depends, of course, on the soil conditions.

However, it equally depends on the size of the void space left behind the support. While the identification of the soil conditions leading to such a development are readily

made, the identification of the critical void size that may cause it is not. An approximate solution to this problem can be derived from the limiting dimensionless crown displacement, U, introduced earlier. If the uncontrolled conditions are related to a near ground collapse condition, the dimensionless displacement at the crown should be greater than 1.8. It will be shown in Chapter 5 that the maximum U developing ahead of the face of a shallow tunnel is usually smaller than 0.5 and that the increment of U due to lining deformation is generally smaller than 0.3 (for a good-lining ground contact). Therefore, the limiting dimensionless crown displacement increment for movement into the void space behind the lining, which might produce a near collapse condition, is equal to 1.0. From this, one could estimate a limiting crown displacement increment, and therefore, a maximum crown overcut, which could be less than or equal to the limiting value. Though approximate, this approach may serve as an interim expedient to treat the problem.

Needless to say that caution should be exercised when applying this criterion, which has been developed empirically and based on model test results of laboratory prepared soils. For instance, minor geological details are known to have an important role in localized collapse mechanisms. Despite this, the criterion was tested in two case histories and proved to yield sensible results. More field evidence is needed to further validate this approach,

which has merit in that it relates a limiting overbreak to the amount of displacement that may trigger an instability process in the ground.

Three-Dimensional Tunnelling Response

During tunnel advance, the longitudinal displacements in the ground are non-zero and the actual conditions are not plane strain, as assumed so far.

Numerical analyses, field evidence and results from laboratory model tests indicate that a zone in which a fully three-dimensional stress-strain state exists, extends ahead of the advancing tunnel face. The extension of this zone depends on the distance between the face and the section where the lining is installed, and on the soil strength. Typically, at distances of one to two diameters ahead of the face, the longitudinal strains are close to zero.

This three-dimensional zone also extends behind the tunnel face. As the tunnel advances, the longitudinal components of the displacements around the perimeter (opposite to the direction of tunnel advance) peak at the face, and then the soil starts moving towards its original position. This rebound may not be complete, especially in linear elastic numerical simulations. The longitudinal ground displacements may not end up as zero, as is normally assumed in a two-dimensional representation of a tunnel.

Non-linear numerical analyses, model test results and field instrumentations indicate, however, that the final longitudinal strains usually result in being very close to

zero, as assumed in plane strain analyses. Despite this, during tunnel advance these strains are not zero and consequently, the response of a stress path dependent soil would not be fully portrayed in a simplified two-dimensional plane strain representation.

What is important, however, is that even if some residual longitudinal components of the displacement do remain after the tunnel face moves away, these are much smaller than the displacement components orthogonal to the tunnel. This is particularly true if the lining is installed at a distance greater than half a diameter from the face and if a non-linear constitutive relationship is postulated for the soil. Field and laboratory observations seem to confirm this. In this regard, the two-dimensional plane strain representation of a tunnel section well behind the tunnel face can be said to be valid. However, the longitudinal strains may locally dominate the ground response at sections close to the tunnel face, when they can become major principal strains. This is tacitly recognized in practice by the usual concern with face or face and heading stability.

Based on available evidence, if one assumes that for most tunnels, the lining is activated one diameter (D) behind the face, the region between 1 to 2D ahead and 2D behind the face is where non-plane strain conditions prevail. Within this region, the stress and strain changes are dominantly three dimensional. The ground and lining responses are, therefore, affected by the longitudinal

strains which had been neglected in the preceding discussions.

A conceptual model for three-dimensional arching and ground-lining responses around an advancing unsupported tunnel heading was proposed by Eisenstein et.al. (1984). This model was reviewed and revised. Also reviewed were some approximations which were proposed by different authors, to account for the three-dimensional effects in plane strain analyses.

Field evidence supporting the conceptual model of three-dimensional ground response was reported, both for the tunnel crown and springline.

Other field evidence suggested the presence of the three-dimensional stress transfer effects. They refer to lining crown heave after invert closure, to some load concentrations in shotcrete supports near the tunnel face, and to longitudinal bending of the shotcrete shell at the crown before ring closure at the floor. Similar results were also obtained in some three-dimensional numerical simulations reviewed. The role of these effects in controlling the tunnel lining design has not been clearly established. Further investigation of this issue would be of considerable interest, bearing in mind its potential consequences.

The results of the three-dimensional linear elastic finite element analyses presented by Eisenstein et.al.

(1984) and Heinz (1984:176) were reviewed and supplemented.

A shallow tunnel construction was simulated with two different distances, L, between the tunnel face and the leading lining edge (L=D/2 and L=2D/3). The radial stress distributions in the longitudinal direction did not show any significant concentration at any point of the tunnel contour, either ahead or behind the unsupported heading. The rate of change in stress was found to be greater than that for the displacement. These results are similar to those obtained in other finite element analyses and to field measurements in some case histories.

Since radial stress and displacement gradients in the longitudinal direction are dissimilar, the ground response in terms of the stress-displacement relationship is non-linear, although linear elastic material properties have been assumed.

Also noted is the fact that both the magnitude and distribution of the radial stresses and displacements ahead of the face are generally unaffected by the lining installation distances, for all points of the tunnel contour. Similar results were reported by Pelli et.al. (1986), who showed also that the radial displacements ahead of the face are not much affected by the relative stiffness of the support. In other words, the soil response ahead of the face is not influenced very much by the presence of the liner.

Ground-support response curves were thus obtained for points at the tunnel crown, springline and floor, in terms

of normalized radial stresses and displacements. As noted earlier, the portions of these curves representing the response ahead of the face are not affected much by the lining placement position. However, behind the face, the lining placement position strongly affects the response.

Two-dimensional ground reaction curves were also obtained through a plane strain finite element analysis of the unlined tunnel, using the same material properties and a mesh corresponding exactly to a tranverse plane section of the three-dimensional mesh. It was noted that the equilibrium points obtained in the three-dimensional analysis lay close to the two-dimensional ground reaction curves, which except for the floor, seem to operate as an upper bound for the equilibrium stress and displacements of the three-dimensional analyses.

3. IDEALIZED BEHAVIOUR OF SHALLOW TUNNELS: STABILITY AND GROUNDWATER

3.1 Introduction

The idealized behaviour of shallow tunnels is further discussed herein. Two behavioural aspects, not included or superficially discussed in the previous chapter, are treated in the following sections: the stability of a shallow tunnel in soil and the role of groundwater in the ground response to tunnelling.

The discussion follows the same lines set forth earlier, in that the behaviour is studied through simple conceptual models, supplemented by results of analytical and numerical analyses. As before, the discussions will be framed within basic soil mechanics concepts. Some discussions on certain aspects are presented as mere speculative exercises, deserving further investigations to confirm or reject present interpretations.

3.2 Tunnel Stability

3.2.1 Foreword

The major interest of this study is related to shallow urban tunnels under operational conditions, in which ground displacements are to be minimized. Although this requires collapse to be precluded, the question of stability is of clear concern. It was recognized in the previous chapter

that the factor of safety of a tunnel deteriorates very rapidly with increasing ground displacements and, that, despite the specification of good ground control conditions, operational factors of safety are normally low.

Even though relevant, the stability of the tunnel lining will not be addressed here. In many cases, the lack of lining stability has been attributed more to ground instability and construction defects, rather than to the lack of structural capacity.

It was pointed out in Section 2.3.3 that soil elements adjacent to the opening may fail once their strength is fully mobilized but that this does not necessarily mean that the whole ground structure is at a collapse state. Collapse means the creation of a mechanism through which a local or global disintegration of the ground mass is experienced.

Local collapse is observed in some types of soil. When a limited part of the ground mass becomes unstable, without the creation of mechanisms which extend up to the ground surface (Sections 2.3.3 and 2.3.4). This is the case of roof collapse in dense sands and instabilities associated with heterogeneous soils such as fissured stiff clays, residual soils, etc. Such local collapse may or may not trigger a global collapse. The latter is known to occur in incompetent grounds, as all soils are supposed to be, as defined in Section 2.3.5. Zones, or bands, of high shear strain develop up to the surface and a block of the ground cover becomes unstable and slides into the tunnel.

Since in most instances the installed lining has sufficient capacity to inhibit the development of a collapse mechanism in the supported sections of a tunnel, instabilities are mainly a concern in the region of the unsupported heading advance. Except in cases of poor lining contact, global instabilities are limited, in practice, to the tunnel face or to the unsupported or partly supported heading. As a result the mechanisms involved are entirely three-dimensional.

3.2.2 Three-Dimensional Stability

With the exception of soils where local collapse prevails ', tunnel stability is mainly governed by geometric conditions. These can be defined in terms of the cover to diameter ratio, H/D, and of the unsupported heading length to diameter ratio, L/D. Depending on these ratios, two extreme collapse modes are possible, as shown in Figure 3.1. Mechanism A, corresponding to smaller values of L/D, implicates both face and roof stability. With increasing L/D, the collapse mode gradually changes to that of mechanism B where roof stability dominates. As L/D tends towards infinity (an unsupported tunnel), mechanism B becomes a two-dimensional situation. If L/D tends towards zero (fully supported tunnel except for the face), then tunnel collapse is controlled by the face stability.

⁷ Atkinson (1976) (quoted by Mair, 1977:8), showed that the differences in behaviour at collapse of 3D tunnel headings and 2D plane section tunnels is not significant for dense sands.

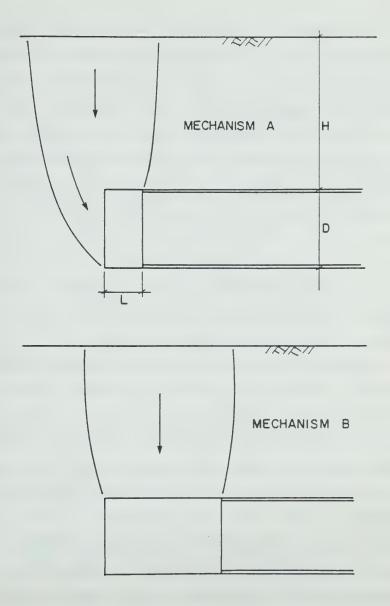


Figure 3.1 Three-Dimensional Collapse Mechanisms in Shallow Tunnels

The issue of face stability was studied by Broms and Bennermark (1967) who used the closely related solutions of both bearing capacity of piles (e.g. Skempton, 1951) and stability of deep excavations (e.g. Bjerrum and Eide, 1956) to investigate the undrained stability of tunnel faces in saturated clays. These authors used a semi-empirical approach which proposed that the stability ratio that leads to face collapse of a fully lined and deep tunnel is given by:

$$N = \frac{\sigma_{o} - \sigma_{c}}{c_{..}} = 6 \text{ to } 8$$

The symbols have the meanings given in section 2.3.3. They further suggested that the lower value should be taken as a safe reference for face stability evaluation.

Undrained static model tests of 3D tunnel headings (Casarin, 1977:51) and centrifuge experiments (Mair, 1979:116) in overconsolidated kaolin ($K_o\simeq 1$) confirmed the collapse mechanisms shown in Figure 3.1. Moreover, these tests showed that there is increasingly more displacement at the crown and less at the face as the ratio L/D increases (Casarin and Mair, 1981:36). These tests, as well as drained tests by Casarin (Op.cit:51), also demonstrated that tunnel stability decreases as the unsupported heading span increases. This is indicated by their results which are gathered together in Figure 3.2. For a given overload factor (i.e., a fixed tunnel depth, a fixed internal pressure and a fixed c_u), the factor of safety against collapse (given by equation 2.14), decreases with N increasing. As depicted in

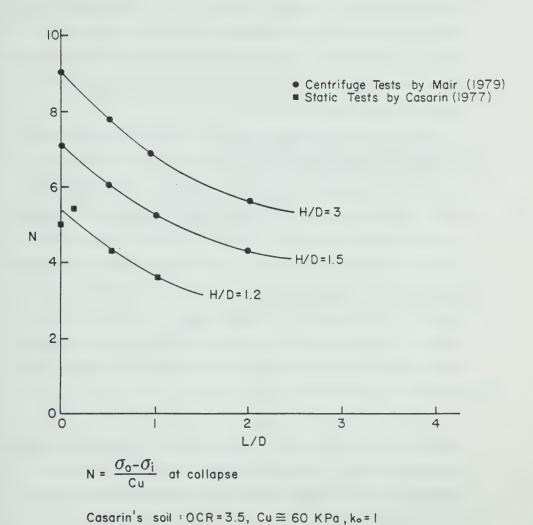


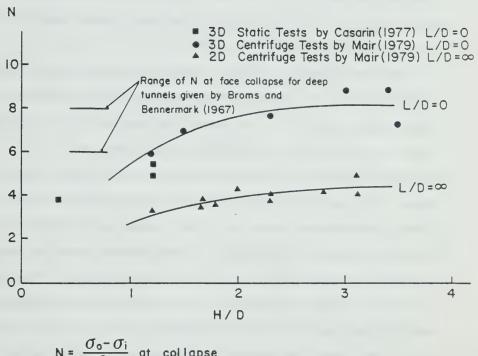
Figure 3.2 Influence of Geometric Conditions on the Undrained Stability of Tunnel Headings in Overconsolidated Kaolin

Mair's soil: OCR = 2-4, Cu = 20-25 KPa, ko = 1

Figure 3.2, N is inversely related to L/D and proportionally related to H/D. For L/D tending to infinity, N may be obtained from plane strain model representations and as L/D tends to zero, N will approach the condition analysed by Broms and Bennermark (1967).

Results of some model tests for L/D=0 situations are included in Figure 3.3. It is interesting to note that, as pointed out by Casarin and Mair (1981:40), the stability ratio N for the face of a fully lined tunnel tends towards an approximately constant value at a certain cover ratio. For H/D greater than 1.5, the stability ratio N at collapse is within the range given by the Broms and Bennermark (1967) solution, which had been formulated for an ideally deep tunnel. In other words, a tunnel with a cover to diameter ratio greater than 1.5 can be approximated by a deep tunnel solution.

The theoretical assessment of the three-dimensional stability conditions can be approached by solutions based on the Lower Bound (or Safe) and Upper Bound (or Unsafe)
Theorems of Plasticity. Examples of upper bound solutions are presented by Casarin (1975:65-69). For three kinematically admissible mechanisms in a frictionless and cohesionless soil, he produced solutions for both mechanisms A and B with varying degrees of accuracy. Davis et.al., (1980), furnished lower and upper bound 3D solutions for face stabilty (L/D=0) in frictionless soils. Muhlhaus (1985) presented a lower bound 3D solution for stability assessment



 $N = \frac{\sigma_0 - \sigma_i}{Cu}$ at collapse (See preceding figure for soil properties)

Figure 3.3 Undrained Stability of Fully Lined and Fully Unlined Model Test Tunnels in Overconsolidated Kaolin

of the unsupported heading (L/D not equal to 0) for a cohesive, frictional soil. These plasticity solutions appear to reasonably bound the actual collapse conditions seen in a number of model tests and in at least one subway tunnel (Kochen and Negro, 1985), that collapsed according to mechanism A. This case history was briefly mentioned in Section 2.3.6.3.

The assessment of actual stability conditions in the field is not always simple. The critical dimensionless crown displacement, U, of 1.8 suggested in Section 2.3.4.3, could serve as a criterion to identify impending stability problems. However, it has been derived from plane strain model tests and its use requires the knowledge of the in situ deformation modulus of the ground mass, which is not always available. Some prefer to follow the distribution of vertical displacements in the tunnel cover between the crown and the surface, especially in relatively shallow tunnels. A zero or near zero vertical straining condition within the cover depth could represent a collapse or near collapse situation, if the soil cover moves as a rigid block. However, some soils exhibit appreciable volume changes upon shearing, which may lead to misinterpretation of this model. Moreover, possible volume changes due to soil drainage and consolidation of the tunnel cover, may cause a reversal in the distribution normally expected in a homogeneous, time independent material. Resulting surface settlements may end up being larger than the crown settlements without any sign

of impending ground collapse. The situations above have been identified in a number of case histories.

Perhaps a promising practical criterion for the detection of instability problems in the field, is that proposed by Negro and Kochen (1985), and consists of inspecting the longitudinal distribution of the settlements at the crown elevation similar to the one given in Figure 2.25. If field measurements allow this curve to be obtained, then it is possible to estimate a longitudinal distortion index given by:

$$\gamma(x) = LDI(x) = \frac{\delta u(x)}{\delta x}$$

where, u(x) is the displacement at a point x. This ground distortion is a shear strain, which relates to the slope of the settlement trough, and can be interpreted as a measure of the shear strength mobilization of the soil. Therefore, it can be related to the tunnel stability condition, allowing one to identify incipient collapse mechanisms.

Figure 3.4(a) depicts the settlement and distortion distributions for a stable ground condition. The longitudinal distortion distribution resembles a Gaussian normal probability curve. If some instability process is triggered around the tunnel heading and face, a marked change in the shape of this curve is noted, even for a minor change in the shape of the settlement curve (Figure 3.4(b)). The magnitude of the maximum LDI could be taken as an index of ground control during heading advance, by referencing it to some critical shear strain. For saturated clay, the

critical shear strain would be $2c_u/E_u$ where E_u is the undrained inital tangent deformation modulus. However this criterion which is similar to that proposed by Sakurai (1981:279) says very little about the overall stability condition of the tunnel, since it may merely give an indication of some localized ground failure. This can occur without necessarily bringing the tunnel to a collapse state.

The distribution of the longitudinal distortions rather than its magnitude, furnishes a clearer indication of the overall stability of the ground cover. A minor instability trend, which otherwise goes undetected, is reflected by appreciable changes in the shape of the distribution: the LDI decreases in some regions, perhaps becoming negative at some points and increasing somewhere else. Such changes in the distribution pattern is a sign that a collapse mechanism is being formed.

The static 3D tunnel heading model tests by Casarin (1977) may be of assistance to check the proposed criterion. Figure 3.5 furnishes details of the test conditions. Variable water pressures were used to simulate a surface load that would give the field stress, $\sigma_{\rm o}$, and provide an internal pressure $\sigma_{\rm i}$, in the tunnel. An overconsolidated kaolin was tested up to undrained failure by increasing the pressure difference $(\sigma_{\rm o}-\sigma_{\rm i})$. Further details of the testing procedures can be found in Casarin (Op.cit) and Casarin and Mair (1981). The longitudinal distortions were calculated from the vertical components of the measured

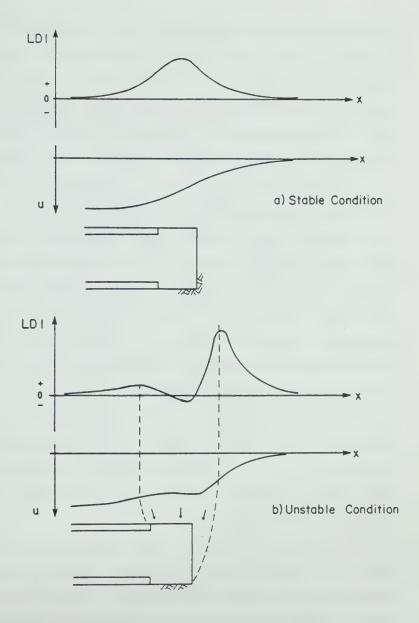
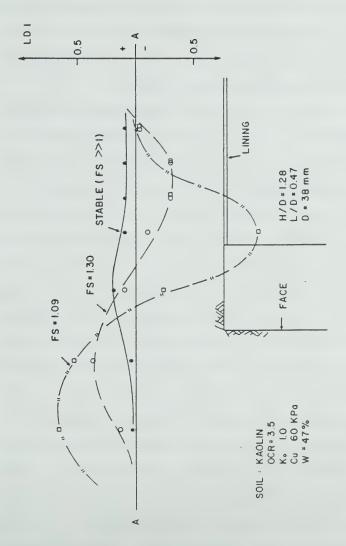


Figure 3.4 Distributions of the Longitudinal Distortion

Index Along A Stable and an Unstable Tunnel

displacements from radiographs, along a horizontal line AA situated at a distance of about a half diameter above the crown elevation. The solid line distribution was obtained from the intial displacements measured just after cutting and lining the tunnel. It represents, therefore, the ground response under stable conditions, prior to the loading which lead to failure. The broken lines correspond to the distortions calculated from the additional measured displacements, which occurred after increasing the pressure difference. These are added to the initial displacements caused by the tunnel excavation. They represent the longitudinal distortions at two loading stages, which correspond to factors of safety of 1.30 and 1.09. A very pronounced change in shape of the LDI distribution is noted with decreasing stability. Despite the fact that the model test results are directly related to the stability of a stationary tunnel heading under increasing pressure difference $(\sigma_0 - \sigma_i)$, it is believed that the overall stability of an advancing heading is fundamentally the same (Casarin and Mair, 1981:43).

The criterion above was also tested by Kocken et.al., (1987) in a subway tunnel in Sao Paulo, which collapsed according to mechanism A (see Section 2.3.6.3). By analysing, after the event, the settlements measured in six surface monuments distributed at approximately one tunnel diameter spacings along the tunnel axis , it was possible to note a change in the longitudinal distortion profile two



Ø Figure 3.5 Longitudinal Distortions above the Crown of Model Tunnel Test (based on Casarin, 1977)

days prior to the collapse, at which time the face had advanced an additional 2.4 m. Once the LDI became locally negative, a full collapse condition had already developed. A much clearer picture could have been established if the settlement points had been located closer to the tunnel crown elevation, and not at the surface.

Horiuchi et.al., (1986:756) independently developed a similar approach, using the same longitudinal distortion index. However, they preferred to relate it to some limiting index and proposed that the LDI should be calculated at a fixed point, for different positions of the tunnel face. For the reasons revealed previously this approach may not be as effective and as general as relating to the change of the LDI longitudinal distribution with tunnel advance. However, if properly calibrated for an individual site it can be proved useful as shown by Horiuchi et.al., (Op.cit). They applied their method to a large cross section tunnel built in Tokyo, through fine to medium, uniform, alluvial sand. The ground water table was at or below the springline elevation, creating flowing sand conditions which were ultimately controlled by prompt application of a sprayed chemical coating and shotcrete. The criterion was tested and calibrated against a global collapse situation of the tunnel heading, which had been experienced at the early stages of construction. At the time of collapse, the heading had been advanced with a temporary invert, some 15 m ahead of the lower bench face. The distortion index was calculated from

settlements measured through a horizontal inclinometer installed 3 m above the crown. The maximum LDI value found just before the unstable condition occurred, amounted to 1.3% (about 0.7% at ground surface). In the case of the collapsed subway tunnel in Sao Paulo, the maximum LDI found at the surface amounted to 2.5%, just prior to the failure of the organic clay cover.

Horiuchi et.al. (Op.cit:756) also proposed another monitoring index for stability of the ground. This is calculated from the third derivative of the longitudinal settlement profile. If the ground cover can be approximated by an elastic beam with a flexural rigidity, EI, and a sectional area, A, then it is possible to estimate the shear force and shear stress from its deflection curve. However, the evaluation of the third derivative requires the longitudinal deflection curve to be defined from very closely spaced settlement measurements. Also this evaluation cannot be performed if the data is too scattered. This imposes a serious restriction in using standard deep settlement point data for the evaluation of this shear index. Horiuchi et.al. (Op.cit) used data from the horizontal borehole inclinometer and calibrated this new index for the same tunnel site, finding again a good correlation with the ground stability condition. This enabled them to define a limiting shear index. The disadvantages of this approach are clear. Moreover, the need to use a continuous monitoring device for the assessment

considerably reduces the practicality of the suggested approach.

3.2.3 Two-Dimensional Stability

In spite of the fact that the actual stability condition of a tunnel exhibits a three-dimensional nature, the study of the collapse mode of a plane strain tunnel does have some practical as well as academic interest.

The theoretical assessment of the two-dimensional stability condition of the ground around a circular opening, can also be approached by plasticity solutions (upper and lower bound theorems). Lower bound solutions are sometimes formulated using the method of characteristics (Davis, 1968:354). Examples of these solutions are those presented by Davis et.al. (1980) for frictionless soils, by Atkinson and Potts (1977) for cohesionless soils, by Caquot and Kerisel (1956), D'Escatha and Mandel (1973) and Muhlhaus (1985) for cohesive and frictional soil, and others. The validity of the assumptions made and the accuracy of the solutions provided are discussed in other sections of this thesis.

The stress changes imposed on an element of soil adjacent to the plane strain circular opening have already been discussed (Sections 2.3.2 and 2.3.4). Figure 3.6(a) illustrates the stress path of a soil element 'P' at the crown of the opening, replotted from Figure 2.3(a), the same assumptions made as before. A non-hydrostatic in situ stress

condition (K_0 <1) has been assumed, and the soil was assumed to be cohesionless. As before, the initial condition is represented by point A, and local failure is approached at C. If the tunnel is shallow, a collapse mechanism may develop at D, or if the tunnel is deeper the collapse will be nearer point E. Here, the soil deformations are unrestrained and the displacements are very large. The evolution of the ratio K, horizontal to vertical stress at P, is shown in Figure 3.6(b). This ratio increases from $K_o < 1$ at A and K approaches K, at the onset of a passive type failure. If no support is provided, the stress path travels along the failure line, the ratio K remains constant and equal to Kp. If it is assumed that the tunnel is in a dense sand and is fairly deep so that it collapses at E, there is evidence showing that the collapse is initiated with the failure of a wedge shaped block of soil, sliding from the roof, as illustrated in Figure 3.7 (Atkinson et.al., 1975:84). The internal tunnel pressure at this instant could be approximated by an upper bound solution. The associated flow rule ensures that the dilation angle, ψ , is equal to the friction angle, ϕ , and this allows the wedge block to move downwards, dilating at such a rate that no separation occurs along the sliding surfaces. This is clearly an approximation of point E in Figure 3.6. Actually, the angle of dilation is smaller than the friction angle and the wedge block separates from the rest of the ground mass, and falls down. From point E onwards, the continuum mechanics approach

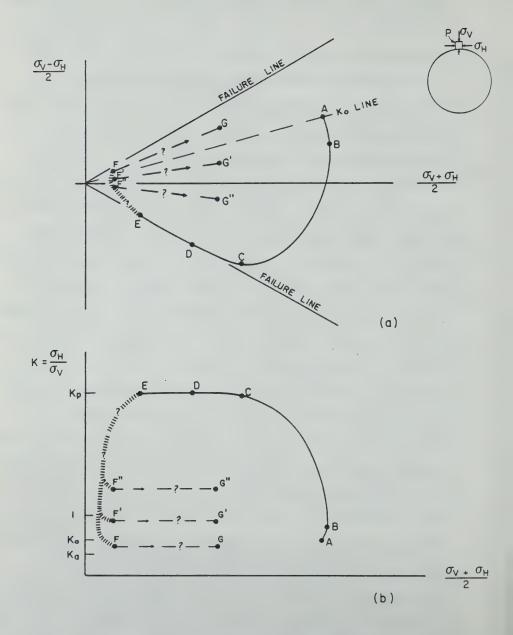


Figure 3.6 Stress Paths and Stress Ratio of a Soil Element at the Tunnel Crown

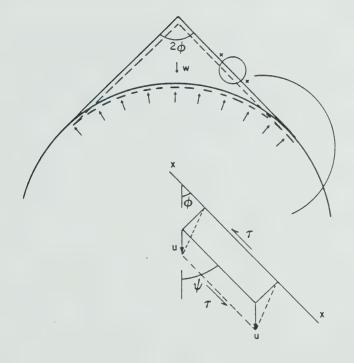


Figure 3.7 Local Collapse at the Roof of a Deep Tunnel in Dense Sand

is no longer applicable and the stress changes occurring in the soil cannot be determined. For these reasons, the following discussion should be taken as a mere speculative exercise.

Assume that after the stress release has been applied inside the opening, an ideally stiff lining had been installed. Assume also a that poor lining contact exists all around the tunnel contour, so that, up until point E the soil does not come in contact with the rigid lining anywhere. The falling block of soil at E experiences a sudden displacement, which is equal to the amount of void remaining behind the liner at the crown. The block rests against with the support and a new equilibrium situation due to this is achieved at any of the three F points shown in Figure 3.6(a). Assume now that this local ground collapse triggers a progressive failure above the tunnel crown, so that the expanded soil cover "loosens" and the failed material accumulates on the lining crown. Eventually two approximately vertical slip surfaces are formed upward from the opening, reaching the ground surface and bounding the unstable ground cover. This is observed in some model tests by Atkinson et.al. (1975). The debris accumulation process leads to an increase in the vertical stress at the failed soil element P, and any of the three G points shown in Figure 3.6(a) could represent a final equilibrium condition. The final vertical stress will not be equal to the original in situ vertical stress, as some residual shear stress is

likely to be mobilized along the vertical slip surfaces. therefore some stress will be transferred from the unstable ground As a result some stress within the unstable ground mass is transferred to the adjacent more stable ground, by some type of "arching" process.

The arching mechanism that is developed above a yielding trap door mimics the arching process above an actual tunnel in soil, but they are not rigorously alike. Terzaghi's (1936) trap door experimental results suggest that the final equilibrium point is given by G' with K>1 in Figure 3.6(a). So, this measured value of K which was greater than the in situ K_o , would be an indication that the major principal stress trajectory at points above the trap door is a concave downward arch.

Some contend, however, that there will be an inversion of the stress trajectory after roof collapse and the accumulation of loosened soil over the liner is complete. The major principal stress trajectory would again become vertical at the centreline, and the minor principal stress trajectory turns to a concave upwards arch. A marked reduction in K is would be associated with rotation of the principal stresses, from E to F in Figure 3.6(a) and (b). Final equilibrium is reached at G with a higher vertical stress existing at point P. This inverted arching configuration, resembling that taking place behind an active-state translating retaining wall or in a silo under first filling was investigated by Handy (1985) and accepted

by Wong (1986:36) for his derivation of the final vertical loading condition over a tunnel lining. Wong's proposal should also be taken as speculative, since no evidence is furnished to support it. It has, possibly the virtue of providing an upper bound value of the vertical stress, since he assumed a very conservative K ratio which was equal to the Rankine active coefficient, Ka (Wong, Op.cit.:36). Although not explicitly, Wong assumed the support to be infinitely rigid, as has been done here so far. If the lining yields under the load of "loosened" soil, the displacements at P will not only depend on the size of the void behind the lining, but also on the rigidity of the lining itself. Upon lining deformation, the vertical stress will decrease, and rotation of principal stresses may occur. The principal stress trajectory may resemble that at the start of emptying a silo filled with granular material, (Blight, 1986:36). In the upper cover portion the major principal stress is vertical and in the lower region, closer to the tunnel, it is horizontal.

It is also possible to speculate on a compromise represented by point G' in Figures 3.6(a) and (b). The fact is, however, that this alternating rotation of principal stresses or inversion of the "ground arch", has not been clearly observed, although they may explain some features detected in both the field and the laboratory. Model tests conducted in Cambridge failed to reveal this phenomenon (for example, Seneviratne, 1979:61), but this may be due to the

internal tunnel pressure being applied to the ground through a rubber bag in close contact with the soil. Under these conditions, the development of the proposed collapsed soil mechanism may be prevented. It could perhaps be better approximated by the displacement controlled model testing procedure followed by Cording et.al. (1976:15-2). These authors, however, did not furnish details of the strain or stress trajectories.

The foregoing speculative discussion is an attempt to verify the sometimes disputed assumption that the ground reaction curve of a shallow tunnel in soil, may sweep upward when a loosening state develops. This occurs after a miminum pressure is attained. It is well accepted that the stability of an underground opening is very much dependent on the post-failure behaviour of the ground. Soils exhibiting a rapid loss of strength after some peak is reached will clearly demand increased tunnel support to balance the shear strength loss. Although recent views (Read and Hegemier, 1984) question the strain softening response referred from standard laboratory testing, which is exaggerated by inhomogeneities or localization of deformations, it seems unquestionable that actual strain weakening does exist in certain classes of soils. For these, an upward ground reaction curve may result under certain circumstances. This has been proved by Nguyen Minh and Berest (1977) for a hollow sphere and by Berest and Nguyen (1979) and Nguyen and Berest (1979) for a hollow cylinder. These authors assumed

an elastoplastic material with strain softening behaviour, a Mohr-Coulomb failure criterion and a non-associated flow rule. They have shown that, unlike the classic solutions for a perfectly plastic material, this type of ground may show a point of minimum pressure in the ground reaction curve. This inversion of the curve ceases to exist, however, when the external radius of the sphere of the cylinder is large compared to the internal radius of the opening, or, in other words, when the tunnel becomes deep. Since they assumed a non-associated flow rule, their analytical closed form solutions derived for small and large strains, may not be unique (Gunn, 1984:24), as is recognized by Nguyen Minh and Berest (1979b:255). However, there is some experimental and field evidence suggesting that this may also be observed in cohesionless granular soils, which have no significant post peak strength loss.

As mentioned before, although the yielding trap door experiments do not fully correspond to a tunnel simulation because the ground displacement modes are not entirely equal, their results do show an upward trend in the stress-displacement curve after a point of minimum pressure is reached. This was observed by Terzaghi (1936:309) in displacement controlled tests he conducted in dense and loose sand, after imposing displacements of 1.4% and 2.7% of the trap door width. Ladanyi and Hoyaux (1969) also did displacement controlled trap door tests, using instead Schneebeli's (1957) rod material, for simulating a granular

ground mass in plane stress condition. Unlike Terzaghi, Ladanyi and Hoyaux performed tests with different depths of trap door burial (H/D from 2 to 5.33). In all cases, an upward trend of the pressure-yield curves was noted, with different minimum pressures for various H/D values. The tests were done for displacements of 8 to 10% of the width of the trap door. The material tested (roughened aluminum rods) had a peak friction angle of 30° and a post peak residual angle of 28°, but this difference does not explain the increase in pressure (Ladanyi and Hoyaux, Op.cit.: 12). The authors found that the pressure increase reduced as the ratio of H/D increased. The increase in pressure after a minimum was justified by Ladanyi and Hoyaux (Op.cit.:12), in terms of the enlargement of the effective width of the vertical flowing mass above the yielding door, a different mechanism to that postulated before.

From all stress controlled model tunnel tests carried out in Cambridge, just those reported by Atkinson et.al. (1975) showed an increase in internal tunnel pressure after a minimum was reached. Some eight static tests were carried out in dense sand, with cover to diameter ratio varying from 0.88 to 3.97. As described by those authors (Op.cit:84):

"... radiographs taken prior to tunnel collapse indicate that soil movements are initially restricted to a zone immediately above the crown where relatively large dilation occurs. Consequently, a collapse mechanism like that shown (...) with a wedge (...) moving downwards (...) "develops.

"Collapse of all tunnels was sudden and occurred at a well defined tunnel pressure for each test. Collapse results in sudden large movement of sand into the tunnel causing compression of the air ..." in an air-filled rubber bag simulating the tunnel pressure "... and a consequent increase in tunnel pressure to a new equilibrium value. For each test the collapse pressure and, in most cases, the final equilibrium tunnel pressure were recorded (...). Inspection of radiographs taken after tunnel collapse suggests an ultimate collapse mechanism (...) where a block of soil descends along two vertical slip surfaces ...".

It appears from this description that, had the air-filled rubber bag been absent, no increase in tunnel pressure would have been observed. This seems to support the behavioural model that had been described before, and appears to be valid only for cohesionless granular soils, as it has not been observed in tests conducted in other types of materials.

The only field evidence alluding to this type of behaviour is that noted in Washington D.C. Metro, reported by Hansmire and Cording (1985:1316). Measurements were taken in twin tunnels driven through sandy river terraces, with two different shields. Better ground control conditions were achieved in the second tunnel construction, which led to an average springline thrust in the steel ribs and wooden lagging of about 25% of the maximum thrust, given by the in situ stress ($\gamma HD/2$). The corresponding crown displacement

at equilibrium was about 1.2% of the tunnel diameter. These figures are to be compared to an average thrust of 33% and a total of 5.3% crown displacement measured in the first tunnel, where difficulties in steering the TBM, larger overcut, inadequate rib expansion, etc., were experienced. causing large ground displacements. Hansmire and Cording (op.cit:1318) stated that once sufficient ground yielding had taken place, the load in the lining increased (from 25 to 33%) with increasing ground displacement (from 1.2 to 5.3%).

If loosening is defined as an increase in the internal tunnel pressure at increasing displacement of the tunnel wall, then the preceding descriptions reveal that evidence for the mechanisms is limited. This lack of practical evidence, as opposed to the bulk of data showing otherwise, caused this concept to become a very controversial one. Researchers at MIT (Schwartz, Assouz and Einstein, 1980) contend that not only the factual evidence supporting the concept is meagre, but also that the theoretical possibility of loosening as assessed by some is questionable, even for strain softening materials. They question Daemen's (1975) approximate plane-strain analytical solution which treats loosening as a feature of a strain softening material response. Schwartz et.al., (1980:20) pointed out an inconsistency in Daemen's solution, allegedly resulting from the simplifying assumptions he made. This was that an ideally brittle material, showing the most strain-softening

response, does not exhibit any loosening at all. Schwartz et.al., (Op.cit:23) further say that the conceptual models explaining loosening by means of the arching theories are highly speculative and cannot fundamentally explain it. Results of an extensive parametric study using a plane strain analytical solution, in which the ground was represented by a piecewise linear stress-strain relationship (elastic, strain softening and perfectly plastic), are presented by these authors (Op.cit.:41). They conclude that "the often advanced opinion that strain softening ground necessarily leads to loosening is thus incorrect, nevertheless, it still cannot be concluded that strain softening never leads to loosening" (Einstein et.al., 1979:19). Recall that the analytical solutions by Berest and Nguyen (1979) and Nguyen and Berest (1979 appeared conclusive in showing that under certain circumstances loosening does occur. The analytical solution of Schwartz et.al., (1980:41) did not indicate an upward trend of the ground reaction curve simply because they assumed the medium to be infinite, whereas the solutions by the other authors assume it to be finite.

Going back to the speculative model presented before, it is possible, from the ideas presented along with Figure 3.6, to propose a stress-displacement curve as shown in Figure 3.8(a). Upon reduction of the internal stress to reach point E, local collapse develops, and the soil starts to progressively fail and accumulate over the rigid lining.

Conditions change from stress governed conditions, to a displacement controlled situation, in which the magnitude of the additional displacement, Δu , is governed by the size of the void left behind the rigid lining. The vertical stresses referred to are those acting against the lining. An increasing vertical stress is assigned to F'', F' or F, depending on the stress changes assumed at this event (Figure 3.6). As the collapsing soil accumulates over the rigid lining, the vertical stress increases according to a constant K ratio, (eq. F' to G') which is preceded by a rapid drop in K after point E is passed (Figure 3.8(b)). If this interpretive model is proven correct, the portion EFG of the stress-displacement curve would not be solely a "ground" reaction curve, since it is controlled not only by the soil properties (mainly its strength), but also by the size of the gap behind the liner, and by the liner stiffness. Indeed, if the lining were flexible, the FG portion of the curve would no longer be vertical but inclined, according to the rigidity of the support. In a stress controlled condition, not unlike that encountered in the excavation of a tunnel before the support comes in contact with the soil, the stress cannot increase, even though the ground requires it to remain stable. A stress increase will only be detected if conditions are changed to a displacement controlled situation, such as that offered by an installed support, which restrains the displacements according to its relative stiffness. If it is agreed that the final equilibrium

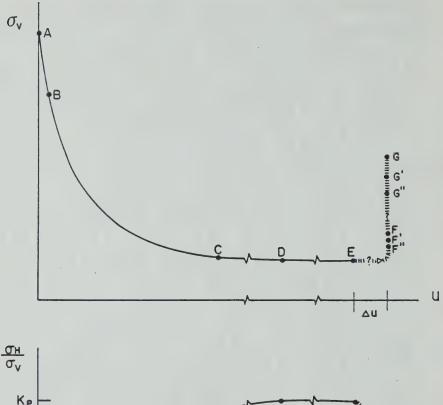


Figure 3.8 Ground Reaction Curve and Stress Ratio Changes in an Element of Soil at the Crown of a Tunnel Approaching Collapse

stress, such as that at G, can be uniquely assessed by some sort of plasticity solution, as a function of the ground properties and conditions, then the slope of the portion FG of the curve can be partly controlled by the support characteristics, being, therefore not unique.

The overall ground response resembles that of a strain softening structure loaded under displacement controlled conditions. It seems valid to relate it to the formation of inhomogeneities in the ground mass, such as the shear bands formed in trap door experiments observed some fifty years ago by Terzaghi and more recently by Vardoulakis et.al., (1981:61). If the post-failure tunnel behaviour is a matter of interest, model testing under displacement controlled conditions seems to be a promising research area. The available numerical modelling tools based on traditional elastic and plastic theoretical formulations currently seem unable to describe this mechanism.

It would be argued that loosening is likely to occur in non-cohesive granular soils at large deformations.

Typically, this might include crown displacements of greater than 1 to 2% of the tunnel diameter, and would generally be in excess of those developed in properly constructed urban tunnels. The problem was also addressed in Sections 2.3.4 and 2.3.5 of this thesis, and an expedient criterion was set up ad interim to assess the likelihood of this occurrence.

3.3 The Role of Groundwater

3.3.1 Foreword

In his 'Principles of Tunnel Lining Design', Kuesel (1986) states that if the most important part of the tunnel lining is the ground that surrounds it, the most important component of the ground is the groundwater. Groundwater plays a paramount role not only in the design of the lining but also in the overall tunnel construction and subsequent performance. The presence of water in the ground may govern tunnel heading stability, especially in cohesionless granular soil. Pore water pressure changes may control the magnitude of ground settlements, particularly those due to drainage and consolidation, and these may well exceed those developed under short term conditions. Mechanisms of soil consolidation and swelling are known to be one possible cause of time dependency of the lining loads.

A brief review of the subject is attempted in this section, with emphasis being given to the changes in porewater pressure caused by the tunnelling operation and the consequences in the overall tunnel behaviour.

3.3.2 Generation of Porewater Pressure Changes

3.3.2.1 Idealized Porewater Pressure Changes

It is recognized that even without any total stress change in the ground, the pore water pressures may be changed by a simple alteration of the hydraulic boundary

conditions. More often than not, a tunnel acts as a drain, regardless of the attempts to provide an ideal impervious lining (Ward and Pender, 1981:268). It will be assumed however that unless indicated otherwise, the tunnel contour is an impermeable boundary.

The short term, or undrained changes, in pore water pressure in a saturated soil are related to the change in volume of the soil pores. If the ground is depicted by a plane strain plate under a uniform stress field, and if the opening is circular, it can be shown that for an elastic, homogeneous and isotropic soil, the total stress path of a soil element adjacent to the tunnel is one of pure shear. No volume changes are experienced because the total mean normal stress remains constant and shear stress does not cause volumetric strains in an isotropic elastic body. If the in situ stress is non-uniform (K not equal to 1 or a gravitational stress field), then the total stress paths will generate pore pressure changes. It has been shown already that the mean total stress will vary during the reduction of the in situ total stress at the tunnel contour. Moreover, if the ground is anisotropic or inelastic, there will be generation of pore pressure changes with respect to these in situ conditions.

Short term pore pressure changes, in a saturated, homogeneous, isotropic, elastic ground, at points close to a circular opening representing a deep tunnel can be derived from elasticity without major difficulties. The in situ

total stress state in terms of polar coordinates (θ is the anticlockwise angle measured from the springline, see Figure 2.11) is;

$$\sigma_{\rm r} = \frac{1}{2}\sigma \left[(1+K) - (1-K)\cos 2\theta \right]$$
 [3.1]

$$\sigma_{\theta} = \frac{1}{2}\sigma \left[(1+K) + (1-K)\cos 2\theta \right]$$
 [3.2]

$$\tau = \frac{1}{2}\sigma \left[(1-K) \sin 2\theta \right]$$
 [3.3]

where σ is the total in situ vertical stress. If the initial ground water condition is hydrostatic and the phreatic level coincides with the ground surface, the total stress ratio, K, is given by:

$$K = K_o + (1 - K_o) \gamma_v / \gamma$$
 [3.4]

where K_{\circ} is the effective stress ratio and γ_{\circ} and γ are the unit weights of water and soil respectively.

If $\sigma_{\rm r}$ and τ at the opening are proportionally reduced to a fixed fraction Σ of their original values, only the deviatoric term $\sigma_{\rm d} = (1-{\rm K})\sigma/2$ will generate pore pressure changes. Under the assumed plane strain and fully saturated conditions, (the out of plane stress being equal to the intermediate principal stress, $\sigma_{\rm z}$), it is possible to calculate the pore pressure changes in the soil. Immediately after a partial stress release at the opening, the pore pressure, u, at points adjacent to the unlined and impervious tunnel contour will be given by:

$$u = u_o + (1-K) (1-\Sigma)\sigma \cos 2\theta$$
 [3.5]

where uo is the in situ pore pressure.

The pore pressures can be derived either using a coupled or an uncoupled approach with total stress. The

first route was followed by Carter and Booker (1982). The second approach makes use of Skempton's (1954) A and B pore pressure coefficients which are equal to 0.5 and 1.0, respectively for a saturated soil under plane strain conditions. The excess pore pressure, u-u, is non-zero if K is different from unity, it increases as the tunnel gets deeper and as the amount of allowed stress release increases. For K <1, the crown (and floor) will show a reduction in pore pressure whereas the springline will experience an increase. The transition point between the zones of potential swelling and consolidation, is at θ =45°, where the excess pore water pressure is zero. For points other than at the tunnel contour, Carter and Booker (1982) furnish initial excess pore pressure distributions, both for an impermeable and permeable opening. To simplify the solution (approached both analytically and numerically), these authors made use of the principle of superposition, by treating the individual components of the complete problem separately (reduction of mean normal stress, of the deviatoric stress, and of the pore pressure).

3.3.2.2 The Effect of Gravity

The body forces due to gravity are now included, still assuming, however, that the opening is not influenced by the stress free ground surface. For K=1, the pore pressure changes at the tunnel perimeter can be calculated from the total stress changes given by Mindlin (1939) or by Hartmann (1972), assuming a full in situ stress release is applied to

the impermeable opening (equations 2.5 to 2.7 or 2.19 and 2.21). At the crown, springline and floor, the pore pressures that will result are:

$$u_c = u_{co} + \gamma D/4$$
 [3.6]

$$u_s = u_{so}$$
 [3.7]

$$u_f = u_{FQ} - \gamma D/4$$
 [3.8]

As expected from the total stress paths shown in Figure 2.1, no pore pressure changes would be observed at the springline, since a pure shear condition prevails here. However, at the crown, there is an increase in pore pressure equal to the increase in the mean total normal stress. On the other hand, a pore pressure reduction is observed in the floor, resulting from a reduction in the mean total normal stress. Similar trends will be observed for K different from unity.

Broadly speaking, the action of gravity in a soil with K less than one, will lead to more pronounced changes in pore pressures at the tunnel floor than at the crown.

3.3.2.3 Porewater Pressure Changes in Less Idealized Conditions

Departure from linear elasticity will lead to generation of pore pressure changes, even for a deep tunnel under a uniform stress field. The likely undrained changes in pore pressure in a lightly overconsolidated soil, can be anticipated from the discussions related to Figures 2.2 and 2.3. Of particular interest are the volume changes shown in Figure 2.3(d), for an element of soil close to the tunnel

perimeter. If changes in volume are precluded upon removal of the in situ stresses, the soil will initially experience an increase in pore pressures associated with yielding which is followed by a pressure reduction as it approaches failure and beyond. The later changes are largely controlled by the decrease in the mean normal stress.

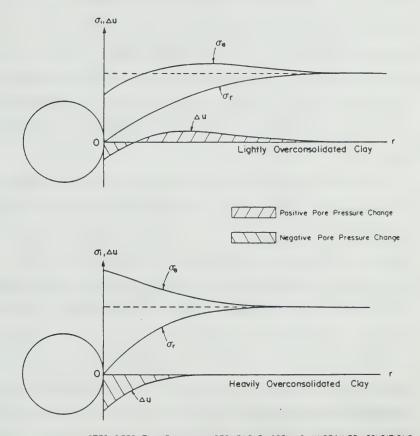
The distribution of the pore water pressure changes with distance from the opening wall, can be determined from both coupled and uncoupled approaches. The latter was favoured by Clough and Schmidt (1981:609), who combined the stress distributions furnished by an elasto-plastic closed form solution presented by Deere et.al. (1969) for a frictionless soil, with the Henkel's (1960) pore pressure coefficients. The inconvenience of this approach is that the required parameters for the solution (strength and pore pressure) must be chosen in a consistent manner, as they are not independent variables (an extensive testing program is required).

Ladanyi (1966) followed an ingenious alternative approach, adapting his former work on the expansion of a cavity in saturated clay, to the tunnel problem under a uniform stress field. This is a numerically approximate solution that takes into account the actual stress-strain curve of a soil tested in the laboratory under plane strain conditions. The piecewise integration of the stress-strain curve is done approaching it by discrete linear segments in the larger shear strain region and by fitting a curve in the

smaller shear strains region (for instance, by a hyperbola).

Ladanyi (Op.cit.) discusses the errors involved in an elastoplastic formulation in which a constant deformation modulus is assigned to the soil before plastic failure, in order to advocate the preference for the curve description model.

Figure 3.9 illustrates schematically the distributions of pore water pressure changes, (Δu), assuming a non-linear stress strain behaviour for the soil and a full stress release at the impermeable opening. They represent typical distributions for a lightly and a heavily overconsolidated soil. Plotted together are the distributions of radial and tangential total stress. As indicated, in a lightly overconsolidated soil, the pore water pressures will decrease in the region closer to the tunnel and increase further away. In a more heavily consolidated clay, the pore pressure will simply decrease. If the in situ stress is only partially released, there will be a reduction in the magnitude of the pore pressure changes, and the zones of suction may practically disappear in both cases. The magnitudes of the pressure changes also depend on the degree of overconsolidation of the clay. All these facts are supported by results of the analytical and numerical analysis presented by Clough and Schmidt (1981) and by Ladanyi (1966). Also supporting this, are the results of undrained centrifuge model tests of tunnels in saturated overconsolidated kaolin, conducted by Mair (1979:108,130).



NOTES: DEEP TUNNEL, K=1, IMPERMEABLE OPENING, UNDRAINED CONDITIONS, HOMOGENEOUS AND ISOTROPIC, NON LINEAR SOIL

Figure 3.9 Short Term Pore Pressure Changes and Total Stress
Distributions

From the plots in Figure 3.9 it is also possible to anticipate the likely changes in the effective stress. As pointed out by Ladanyi (1966), the mean effective normal stress will predominantly increase in a more overconsolidated clay and decrease in a less overconsolidated soil. In the former case, even if the opening is stable in the short term, a delayed failure process may develop if the tunnel is left unsupported as pore pressures equalize back to the initial hydrostatic condition.

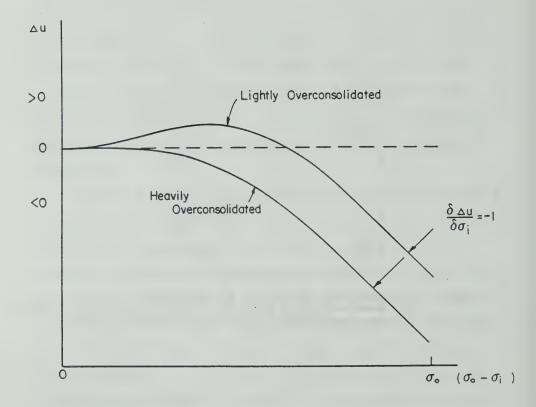
Figure 3.10 illustrates the pore pressure changes of a soil element at the tunnel contour, as the internal tunnel pressure is decreased. It was obtained using the same reasoning as before, being easily derived from Figure 2.3. The behaviour depicted is confirmed by the quoted numerical solutions and by laboratory model testing (Mair, 1979:108). As noted previously, the negative pore pressure changes can be suppressed if the in situ total stresses are not fully reduced at the opening. Moreover, if the opening contour is impermeable as supposed so far, once the critical state is attained under undrained conditions, the deviator stress, $(\sigma_{\theta} - \sigma_{r})$, remains constant. The pore pressure changes thereafter are equal to the changes in the mean normal stress. The zero volume change condition prevents the effective stress path from travelling down as in Figure 2.3. The effective stresses remain constant, and the pore pressure changes are equal to the changes in the internal

OCR	1 and 2
K _o	0.55 and 0.8
Cu/o'	0.3 and 0.45
$\gamma (kN/m^3)$	18.07
λ	0.15
κ	0.03
ecs	1.74
M	1.20 ⁽¹⁾
G/C _u	74 ⁽²⁾
k (m/s)	1.547 x 10 ⁻⁷

Notes:

- (1) Equivalent to $\phi' = 30^{\circ}$ in compression
- (2) Shear modulus to undrained strength ratio in plane strain
- (3) Cam-clay parameters taken from Carter et al (1979)

Table 3.1 Soil Properties in Johnston and Clough (1983)
Analyses



 $\sigma_{\rm o}$ = uniform in situ stress field $\sigma_{\rm i}$ = uniform tunnel internal pressure

Figure 3.10 Pore Water Pressure Changes in a Soil Element Adjacent to the Opening upon Decrease of Internal Tunnel Pressure

tunnel pressure. The curves shown in Figure 3.10 become straight lines with negative unit gradients.

A more generalized plane strain solution of the pore pressure generation problem for a shallow tunnel, including the effect of the free ground surface, a non-uniform in situ stress field, and the non-linear behaviour of the soil would require numerical techniques such as the finite element method. Examples of these are given by Branco (1987) and Samarasekera (1987). Johnston (1981), and Johnston and Clough (1983), also presented results of some finite element analyses, in which the undrained pore pressures were obtained using a coupled elasto-plastic approach assuming the Cam-clay model to represent the soil behaviour.

They simulated the construction of circular tunnels with an excavated diameter of 7.92 m and with a soil cover of 9.45 m (H/D~1.2). In their analyses, they assumed that the ground water level was at the surface, which was free draining. The rigid base of the compressible stratum located 9.45 m below the tunnel invert was also free draining. Tunnel excavation was simulated by applying the equivalent nodal loads at tunnel boundaries, in increments representing the gradual reduction of the in situ stresses. Small time increments were selected in order to ensure an undrained behaviour and the tunnel contour was assumed to be impermeable. Soil properties adopted are shown in Table 3.1, using Cambridge notation, and were said to represent those of the Boston Blue Clay. The results of two particular

analyses are shown as follows. One refers to the response of the soil in a normally consolidated condition (OCR=1 and $\rm K_o=0.55$) and the other to a lightly overconsolidated condition (OCR=2 and $\rm K_o=0.8$). The undrained strength of the clay was expected to increase with depth which led to an undrained cohesion at the tunnel axis level of about 34 kPa in the first case and 50 kPa in the second. These values are said to be typical for such soft clay content.

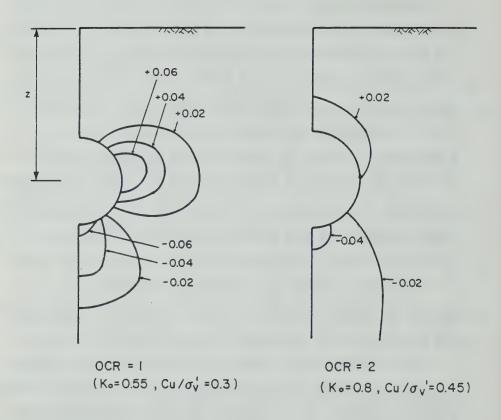
In the analyses, the tunnel perimeter was allowed to deform gradually upon the stress release, up to a pre-determined amount which corresponded to a hypothetical closure of a void left behind the lining. In both cases, this gap closure at the tunnel crown amounted to 50.8 mm and since the soil stiffnesses are not equal in the two analyses, different amounts of stress release at the opening would be expected. A larger reduction of the in situ stress should have occurred in the OCR=2 case.

Figure 3.11 presents contours of the undrained pore pressure changes, at the instant of the hypothetical gap closure. The excess pore pressures are expressed as a fraction of the in situ total vertical stress at the tunnel axis elevation. They correspond to the results shown by Johnston (1981:133,144) and reflect the effect of an increasing overconsolidation ratio for a fixed displacement boundary condition at the opening.

Despite the higher stress release necessary in the OCR=2 case to attain the same opening closure, one notes

that the magnitudes of the excess pore pressures generated in this case are much less than that calculated for the normally consolidated condition. This is partly due to the differences in strength and Ko. A maximum increase of about 11% of the hydrostatic in situ pore pressure is noted with OCR=1, against about 4% with OCR=2. Also the suction below the tunnel floor is higher for the normally consolidated case. Furthermore, the shapes of the contours are dissimilar. The zone of positive pore pressure change moved up from the springline region towards the crown as the OCR increased. The increase in the Koratio, and also the higher stress release imposed contribute to the difference. It is worth noting that the crown and floor regions tend to show pore pressure changes with opposite signs. This is attributed partly to the effect of the gravitational stress field on the ground stress paths, as explained before.

The inclusion of a support with some finite stiffness will have an effect on the generation of the undrained pore pressure changes, as it affects the stress changes in the soil. Carter and Booker (1984) studied the problem of elastic consolidation around a deep lined circular opening using numerical analyses, and assuming that the tunnel excavation is proceeding with the lining already in place. This hardly to represents reality. Johnston (1981) also included in his elasto-plastic analysis described previously, the effect of a lining installed after closure of the fictitious gap. This more closely represents the



NOTE: Values shown are ratios of pore pressure changes to the total vertical stress (γ_z) at tunnel axis.

Figure 3.11 Calculated Contours of Undrained Porewater

Pressure Changes Around a Tunnel in Boston Blue Clay for two

Overconsolidation Ratios (after Johnston, 1981:133,140
modified)

actual behaviour, in which some stress release takes place before support placement. He used the soil properties corresponding to OCR=1 (Table 3.1), but introduced a 0.508 m thick continuous, impervious concrete ring with Young's modulus varying from 0.207 to 2.07 GPa. These lower values were used to account for the presence of bolted joints of a segmented precast lining. It is interesting to compare the calculated undrained excess pore pressures developed in the soil for the two extreme lining stiffnesses (Johnston, 1981:127) with the contours obtained before lining installation (Figure 3.11). The additional deformations resulting from the lining being loaded lead to increases in the excess pore pressure profiles. The pore pressure contours are those after the soil loads are fully transferred to the support and a short term equilibrium is achieved. However, the increased suction below the tunnel is far greater than the increase of the excess pressure at the springline (about 10 times greater). The influence of the underlying rigid base restrains the soil below the tunnel from moving up, thus enhancing the negative water pressure changes (Johnston, Op.cit.: 109). So, a tendency towards an increase in suction pressures, perhaps not as much as calculated, is to be expected. It has been shown that after lining activation in a shallow tunnel the support may tend to "float" (Section 2.3.5) regardless of the position of the lower rigid base, which can partly explain the observed response in an undrained analysis.

So far it has been assumed that the tunnel contour is an impervious boundary, both prior to and after lining installation. In reality, once the tunnel heading is excavated, the soil is exposed and the radial total stress drops to zero. Also, zero pore pressures at the tunnel perimeter most likely represent the actual case, provided no supporting fluid such as compressed air, slurry, etc., is used. In any case, the tunnel contour at this instant is better depicted as a free draining hydraulic boundary. A lining with a permeability two to three orders of magnitude less than that of the soil can be assumed as impermeable for all practical purposes (Fitzpatrick et.al., 1981:99). Therefore, if such a lining is installed after the heading excavation, the tunnel contour will again become an impervious boundary. The pore pressures that underwent a substantial decrease next to the unsupported heading, may therefore, experience an increase over time as the consolidation process develops. In summing up it might be said that an undrained excavation of a tunnel in an overconsolidated clay, will induce a pore pressure response at the crown, showing a small pressure increase at points ahead of the face, followed by a pronounced decrease above the unsupported heading. Then, if an "impermeable" lining is installed and soil consolidation develops, the pore pressure will gradually rise, but normally not to its original value, as most tunnels act as drains in the long term (Ward and Pender, 1981:268).

Not much data is available on pore pressure generation in the three-dimensional stress transfer process occurring in the advancing heading of a shallow tunnel. To the writer's knowledge, no 3D results of the consolidation process around a tunnel have been made available yet. However, limited data from field measurements appears to confirm the suggested evolution of pore pressure changes at the crown. Despite the fact that in reality, an undrained response is hard to secure, the rise in water pressure ahead of the face, followed by a reduction above the heading and a partial recovery with time, has been noted near the crown of tunnels in the stiff London Clay (Barrat and Tyler, 1976:8), in a fairly sensitive and lightly overconsolidated soft qlacial lacustrine clay (Palmer and Belshaw, 1980:180), in an also sensitive, but stiffer marine clay (Ballivy et.al., 1983:349), in a stiff varved lacustrine clay (Hardy Associates, 1980:18), and in the stiff and extremely sensitive overconsolidated Leda Clay (Eden and Bozozuk, 1969:26). This overall common trend may be altered and even reversed if the heading is supported by some fluid pressure such as compressed air. This was the case in the Willington Quay Tunnel, England, driven through a soft organic alluvial silt with an air pressure of 90 kPa, which was about 40% of the overburden (Sizer, 1976:125).

As mentioned previously, the full reduction of the in situ total stress at the unsupported heading leads to a reduction in the pore pressure in the soil. They may

compensate each other, resulting in a positive mean effective stress in the soil close to the opening. This effect is more pronounced in overconsolidated soils and even if its effective cohesion intercept is negligible, the opening may remain temporarily stable despite being unsupported. This is the so called "stand up" phenomenon. With time, as the consolidation process develops, the zone of negative excess pore pressure dissipates causing the soil to swell and the effective stresses to be reduced. This may ultimately result in the initiation of a localized collapse mechanism. The span of time required to initiate the instability process is called "stand-up time", and it is a function of the magnitude and distribution of the negative excess pore pressures (hence the stress history of the soil). and of the consolidation properties of the soil. Assessment of this time is especially important when the tunnel is advanced by mining operations without a shield. The construction sequence of a staged excavation (depth of heading advance, etc.), are strongly dependent on the "stand up time" of the soil. It is therefore somewhat suprising to see this parameter being estimated in practice, on strictly empirical grounds using Terzaghi's (1946) criteria. Some limited research work has been done recently (Taylor, 1979 and Myer et.al., 1981), but the so far results obtained have not been incorporated in to routine practice.

3.3.3 Dissipation of Excess Pore Water Pressures

3.3.3.1 Linear Elastic Consolidation

The dissipation process of the excess pore pressures around a plane strain deep unlined circular tunnel in homogeneous, isotropic and elastic saturated soil, was studied by Carter and Booker (1982). As mentioned, they divided the solution of the problem into separate components which could be assembled together by superposition, to render the complete solution. They analysed the cases of a permeable and of an impermeable tunnel contour. Of relevance to the discussion are the components that lead to time dependent response. These are the removal of the deviatoric stress component, $\sigma_{\rm d}$, for the permeable and impermeable opening and of the reduction of the in situ pore pressure ($u_{\rm o}$) for the case of a permeable tunnel. The removal of the mean normal stress does not cause changes in pore pressures. Recall that the deviatoric stress component is given by:

$$\sigma_{\rm d} = 1/2 \ (1-K) \ \sigma$$
 [3.9]

The changes caused by the removal of this deviatoric component are given by:

$$\Delta u = (1-K) \sigma P \cos 2\theta$$
 [3.10]

where P is a pore pressure coefficient which is a function of the position of this point with respect to the opening (r/r_{\circ}) and of a non-dimensional time factor represented by

$$T = \frac{ct}{r^2}$$
 [3.11]

In this expression, t is the consolidation time, r_{\circ} the radius of the opening and c the coefficient of consolidation

(equal to that of swelling as linear elasticity was assumed) given by:

$$c = \frac{k}{\gamma_u m_u}$$
 [3.12]

where m_{ν} is the coefficient of volume change which is related to the constrained modulus D by:

$$D = \frac{1}{m_{ij}} = \frac{E(1-\nu)}{(1+\nu)(1-2\nu)}$$
 [3.13]

E and ν are the Young's modulus and Poissons's ratio of the soil in drained conditions.

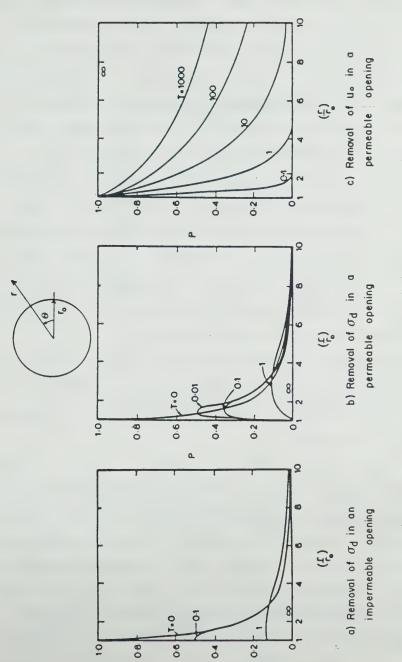
The pore pressure changes caused by the removal of the in situ pore pressure, u_{α} , is:

$$\Delta u = -P.u_{o}$$
 [3.14]

and, of course, is independent of the angle, θ .

The pore pressure coefficients, P, calculated numerically by Carter and Booker (Op.cit.) are shown in Figure 3.12. These are for a Poissons's ratio of the soil skeleton equal to zero which corresponds to the slowest rate of elastic consolidation possible (minimum c value). The pore pressure changes associated with the removal of u_o in a permeable tunnel, as given in Figure 3.12c, are independent of the Poisson's ratio (Carter and Booker, Op.cit.:1067).

If the tunnel is supported in such a way that the in situ stresses are not disturbed prior to lining installation, the changes in pore water pressures generated by the excavation will vary with time and will affect the interaction process between the soil and support. As a result, the loads onto the lining will vary with time. Provided the lining is impermeable, and despite these local



۵

Consolidation of a Deep Circular Tunnel (modified from Figure 3.12 Pore Pressure Coefficients for Elastic Carter and Booker, 1982)

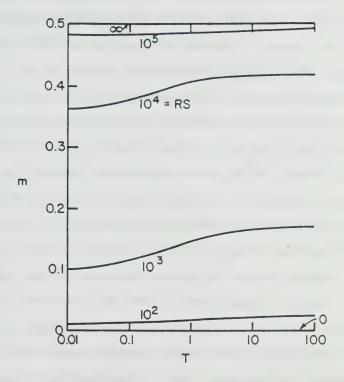
variations in load with time, it should be noted that the average radial and shear stresses at the interface will remain constant. Therefore, the average thrust force is time independent and will remain constant as it is governed by the mean normal stress removal which does not produce changes in pore water pressures. Carter and Booker (1984) studied this problem, extending their solution and by including an impervious elastic lining, and considering two types of interfaces: full and no slip. For the no slip condition, they found that the thrust force may marginally increase or decrease locally with time, (typically ±10% with respect to its short term value), as compared to the local changes in the bending moments, which may vary by as much as 100% (Carter and Booker, Op.cit.:608).

The changes in bending moments with time for the particular condition they investigated, are shown in Figure 3.13, and m is a coefficient, from which the bending moment is calculated as:

$$M = -m \frac{(1-K)}{2} \sigma r_o^2 \cos 2\theta$$
 [3.15]

The coefficients, m, shown in Figure 3.13 were calculated assuming a non-slip condition, for a lining with a constant thickness, t, equal to one-tenth of the opening radius, and for a soil with zero Poisson's ratio. Clearly, besides being a function of the time factor, m is also a function of the relative stiffness, RS, of the support to the ground, expressed as:

$$RS = \frac{2 E_s}{(1 - v_s^2) E}$$
 [3.16]



Notes: For non-slip condition, $t/r_0 = 0.1$ and $\nu = 0$ RS = $2 E_s / E(1 - \nu^2)$ relative stiffness $T = ct / r_0^2$ time factor $M = -m \cdot \frac{(1 - k)}{2} \cdot \sigma \cdot r_0^2 \cdot \cos 2\theta$ bending moment

Figure 3.13 Changes in Lining Bending Moments with Time during Elastic Consolidation (modified from Carter and Booker, 1984:603)

where E is the drained Young's modulus of the soil.

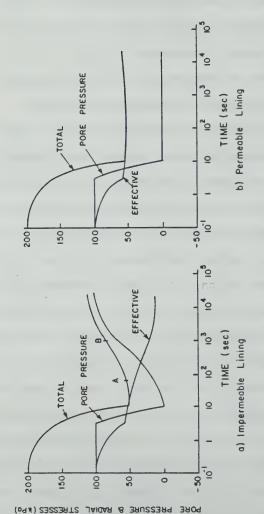
3.3.3.2 Non-Linear Consolidation

If the soil behaviour becomes non-linear, with yielding developing at some stage of tunnel unloading, pore water pressure changes will develop even for the idealized case of a deep tunnel under a hydrostatic stress field.

The dissipation of the excess pore pressures under such conditions was investigated by Gunn (1984) and Gunn and Taylor (1985), using a finite element program developed by Taylor (1984). Effective stresses were related to soil strains by means of an elasto-plastic relationship, in which the yielding condition was given by the Mohr-Coulomb failure criterion. The tunnel problem was simulated in the analysis by a thick cylinder in plane strain conditions, with an outer radius 9 times greater than the inner radius (equal to 25 mm). The initial stress state was given by a uniform total stress of 200 kPa and a pore pressure of 100 kPa throughout the cylinder. Soil properties are given in Figure 3.14. The stresses acting on the external boundary were kept constant, and tunnel excavation was simulated by a constant rate of reduction of the total stresses to a value of 50 kPa, over a time interval of 10 seconds, during which the soil response was assumed to be undrained. After this partial stress release, the nodal points at the inner boundary were fixed to represent the insertion of a rigid lining. Throughout the analysis, the outer boundary was assumed to be a permeable surface with a constant pore

pressure equal to 100 kPa. Two cases were considered with respect to the inner boundary: after "lining" installation, the inner surface was assumed to be impermeable in one case and permeable with pore pressure fixed at zero, in the other. However, before fixing the internal nodal points, the boundary was impervious in both cases.

Figure 3.14 shows the results of the finite element calculations for the two cases considered. Identical responses occurred during the undrained unloading, with the pore pressure at the opening remaining constant while the response is elastic, and decreasing with the total stress reduction after yield. In time, water migrates away from the impermeble lining and an increase in pore pressure is noted until it recovers its initial hydrostatic value of 100 kPa. Similarly, an increase in the total radial stress with time is also observed from the imposed reduced value of 50 kPa to a final lining load of about 110 kPa. The radial effective stress, however, displays a continuous reduction as the swelling process evolves. Once the consolidation process starts around the permeble lining, the pore pressure at the inner surface remains at zero, but the consolidation and drainage at points away from the contour, causes changes in the effective and total stresses. These changes are not large but an increase in both of them is evident as a steady state flow is established (water being supplied at the outer boundary), and radial seepage forces develop increasing the lining load. This increase is, however, smaller than that



E = 5 MPa, v = 0.33, Ø = 26°, C'= 0, k = 107 cm/s, angle of dilation $\psi = 0^{\circ}$, $\gamma_{\rm W} = 10$ kN $/{\rm m}^3$ 2) Up to 10s undrained unloading. Thereofter consolidation. NOTES: 1) Properties of soil skeleton

Evolution of Radial Stress and Pore Pressures at the Rigid Figure 3.14 Non-Linear Consolidation of a Thick Cylinder: Lining-Soil Interface with Time (modified from Gunn and Taylor, 1985)

observed in the impermeable case.

This expected load increase with time in an impermeable lining only occurred because the soil yielded and it would not happen for a linear elastic soil as shown before. The rate of increase in lining load should be a function of the coefficient of consolidation (or swelling), which is equal to about 10-2 cm2/s in this case. Even for a permeable lining some load increase is also expected which results mainly from seepage body forces, but the increase in this case is not very high. However, of considerable interest in both cases, is that the lining loads never recover the original 'in situ' value of 200 kPa. In the first case the final total lining load increased to 55% of the original and in the second to 31%. These increases were from the initial reduction to 25% at the end of the undrained unloading applied in both cases.

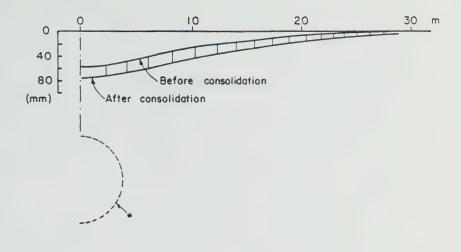
Obviously, the results just discussed cannot be fully generalized to actual tunnelling conditions, since a number of simplifications were adopted. One of them is the assumption of zero dilatancy. With respect to this, Gunn (1984) also analysed the impermeable tunnel problem assuming an associated flow rule to the Mohr-Coulomb yield-failure criteria (ψ = ϕ =26° in this case). For this case he found smaller displacements if a lining is not installed, than for the ψ =0 analysis. Also the rate at which this radial displacement takes place is higher for zero plastic volume change on yielding. Moreover, he noted also that the angle

of dilation, ψ , has minimal influence on the total stress distribution within the thick cylinder, but markedly affects the pore pressures and, consequently, the effective stresses. If a rigid and impervious lining is included, Gunn (Op.cit.) noted that the associated flow rule assumption led to an increase in the effective radial stress at the inner boundary resulting from the higher suction under the undrained loading, but a substantial drop in the effective stress occurs with time and re-establishment of the original pore pressure. The assumption of $\psi=\phi$ led to a slightly higher final total lining load of 60% of the total initial stress, compared with the 55% obtained with the $\psi=0$ assumption.

3.3.3 Additional Consequences of the Consolidation Process

Some of the consequences of the dissipation of excess pore pressures have already been pointed out in the previous paragraphs. The results of the analyses conducted by Johnston (1981) and described in Section 3.3.2.3 are useful to illustrate some points.

Figure 3.15 presents the distribution of surface and subsurface settlements before and after consolidation for OCR=1. The events occurring prior to the consolidation include undrained excavation, support of the tunnel with a 0.508 m thick impermeable lining (Young's modulus=0.5175 GPa) and closure of a void gap of 91.4 mm behind the lining at the crown. An increase in the settlement due to the



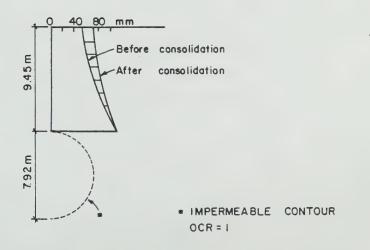


Figure 3.15 Distributions of Surface and Subsurface
Settlements before and after Consolidation (modified from Johnston, 1981:104)

consolidation is noted, but this was found to be a function of the void gap size. For an OCR=2, almost no increase in settlement was noted (Johnston, Op.cit.:136) and, actually, they even decreased locally by virtue of the swelling and associated heave developed in the high suction zones below the tunnel. Also when the gap size was reduced to 50.8 mm, for OCR=1, only a marginal increase in surface settlement was noted with time (Johnston, Op.cit.:131).

These results broadly confirm field observations in lightly to heavily overconsolidated clays showing that most of the settlement measured develops within a short term during tunnel excavation, and that those due to time dependent factors account only for a small fraction (if any) of the total displacements observed (see for instance, Barrat and Tyler, 1976:7). If the ground control is efficient (represented by a smaller void gap in the numerical analysis), then the degree of disturbance and remoulding induced in the clay is reduced and the long term fraction of settlement is considerably reduced. For instance, Palmer and Belshaw (1980:179) reported an increase of less than 15% in settlement over sections of the Thunder Bay tunnel one year after the drivage, when good ground control was exerted. This may be compared with an almost 100% increase, also after one year, in a length where poorer ground control prevailed. This occurred in a zone where a slightly more unfavourable stratigraphy existed, due to a slightly thicker clay cover (Belshaw and Palmer, 1978:578,

Palmer and Belshaw, 1979:168). Poorer ground control can be understood in terms of higher stress releases in the opening and therefore the associated increase in both shearing and pore pressure changes. Higher long term displacements are observed mainly in very soft to soft, normally to very lightly overconsolidated soils, such as the Mexico City clay (Rodriguez et.al., 1983:432, Schmitter and Moreno, 1983:406), the San Francisco's recent bay mud (Clough et.al., 1983:140), and some alluvial clayey or silty soils in Japan (Hanya, 1977:776), in Newcastle, U.K. (Sizer, 1976:34) and in Ireland (Glossop and Farmer, 1979:70). The length of time required to stablize displacements in these cases, varied from 20 to 300 days. Clearly, if the tunnel acts as a drain, the steady state flow that eventually develops will further increase these settlements.

Another important consequence of the consolidation processes around tunnels in soil, is the change in lining loads that has been referred to before. Peck (1969:250) presented results of long term observations of average all-around soil pressures on tunnel linings in different clayey soils, showing that in some cases they tend to increase at almost linearly with the logarithm of time. Peck also showed similar trends for the relative increase in the tunnel horizontal diameter. Tunnellers use different (and conflicting) jargon when alluding to this phenomenon, calling it 'squeezing' or 'swelling'. Considerable controversy has been raised on the subject. Some authors

prefer to treat the problem using the framework of 'classical' soil mechanics, attributing it simply to the 'primary' (non-linear) consolidation of the soil (Atkinson and Mair, 1981:20, Gunn, 1984:21, Gunn and Taylor, 1985:75, and others). If this is so, the rate of increase in lining loads attenuates in a log time plot, as in Figure 3.14. Some of Peck's (1969) data seems to follow this trend. Others contend that the phenomenon is solely controlled by the creep behaviour of the soil medium or to the 'secondary' consolidation of the clay, giving loads which increase at a constant rate in a log time plot. The ground response is interpreted by means of viscoelastic function, in terms of deviatoric creep (e.g. Sakurai and Yamamoto, 1976, Carter and Booker, 1982) and of volumetric creep (Carter and Booker, 1983). Others use viscoelastic - plastic models to represent the time-dependent response (e.g. Sakurai, 1970), or viscoplastic models (Nguyen Minh, 1986).

Despite the considerable computational and modelling efforts undertaken, not much has emerged from these approaches in practical terms, as far as soil tunnelling is concerned. Attempts to simulate observed field responses by the proposed numerical models has largely been avoided. A superficial overview on the subject may possibly suggest that, more often than not, the time dependent lining load response can be explained in terms of the equalization of pore pressures in a "classical" consolidation framework. For the London clay tunnels, most of them driven through the

less fissured 'blue' horizon, it is inviting to draw a parallel between observed responses and the long term behaviour of first-time slides in cuttings in London clay. The delayed failures in a number of cuttings in the more fissured upper 'brown' zone, were attributed to the very slow rate of pore pressure stabilization. This process was not very clearly understood prior to research conducted at Imperial College in the early seventies and summarized by Skempton in 1977. Time spans in excess of 40 to 50 years were recognized as being required to equalize the negative pore pressure changes and to recover an equilibrium condition. It would not be surprising to identify similar delayed responses in terms of lining load build up or of diameter change, in tunnels excavated through the less fissured soil. Vaughan and Wallbancke (1973) noted that the back estimated coefficient of swelling in a cut in the Blue London clay, from field measurements of pore pressures, was not dissimilar in magnitude from those obtained from laboratory testing of small undisturbed samples.

All London clay tunnel case histories reported by Peck (1969) involved continued monitoring up to about 10 years or less. The much longer time required to stabilize the ground response could have possibly eluded Peck's scrutiny, since in the sixties this fact was not fully appreciated. The data he reported could well have lain in the early or mid portions of the lining load-log time plot as in the segment AB in Figure 3.14(a). The linear extrapolation of the loads

in the log-time plot led him to suggest the use of a design lining load, equal to the fully recovered averaged in situ stress $(1+K)\gamma z/2$ for heavily overconsolidated swelling clays such as the London clay (Peck, Op.cit.:258). However, the rate of load increase may attenuate in the long term and the final lining loads may stabilize at a lower average stress level. If this interpretation of the time-dependent behaviour of tunnels in London clay is correct, then Peck's recommendation regarding the long term loads on a lining can only be accepted as a design hypothesis. Moreover, it is a conservative assumption, as it is equivalent to ignoring the ability of the soil to withstand shear. The long term progressive failures in slopes of cuttings in London clay, revealed that the effective strength parameters of the soil approach, 40 to 50 years after excavation, the "fully softened" or "critical state" condition. These values are lower than the peak strength but higher than its residual values (Skempton, 1977:267). This reduced strength could enable the soil to carry some load caused by the excavation unloading, and allow the lining to achieve final equilibrium under loads smaller than those in situ.

A review of the data quoted by Peck (1969:252) on tunnels in London reveals that in all cases he studied but one, the maximum long term average lining loads ranged between 44 and 83% of the in situ stress. These were calculated using a K_o profile given by the average Skempton (1961) and Bishop et.al. (1965) for London clay. One case

lies above that range, showing a local maximum around 98% of the total in situ stress. The final load measurements in this tunnel built in 1942 with a reinforced concrete lining, showed some scatter, and an "average" maximum of 90% could also be interpreted.

Although debatable, Peck's suggestion of a full overburden load for the final tunnel liner design pervaded unchallenged in practice, possibly because it is, in many instances, not a critical design loading. Modern tunnel design calls for flexible linings with low bending moments. The assumption of full overburden, therefore, tends not to aggravate the lining design, since it can be accommodated by a nominal increase in lining thickness at marginal costs. Moreover, prefabricated lining systems have their sections largely controlled by conditions other than ground loads, such as handling, assembling and shield loads.

On the other hand, one could also argue that since soil tunnels are frequently built with fairly low factors of safety, some sort of "drained" creep response under sustained shear stress could possibly be expected. Bishop (1966:124) showed that London clay samples subjected to constant shear stresses around 90% of peak strength, can be brought to failure under drained conditions. He also pointed out that the creep rate does not stay constant at any stage in his tests, which precludes the use of simpler rheological models to solve the problem. Depending on the factor of safety applied to the peak strength, Bishop detected that

the creep rate increased or decreased. Although in reality, the shear stress may not remain constant as in Bishop's tests, it is possible to accept that this creep response may not be significant whenever the factor of safety against tunnel collapse is high.

The aforementioned discussion stands on a very speculative basis. 'Primary' consolidation may account for a large portion of the observed time dependent loads but creep or 'secondary consolidation' may well have role in this load build up process. This may be the case in softer, recent organic clay deposits, subjected to a high stress release by the tunnelling operation. There is a clear need of investigations of these phenomena as related to its effect on a soil tunnel response. The comments by Ladanyi (1982:6) regarding the effect of time in rock structures, is equally valid here. Too few cases of long term observations in soil tunnels are available, or if so, the time of observation is generally too short, in order to allow a proper understanding of the effect of time on the soil response.

3.3.4 Drained and Undrained Behaviour

3.3.4.1 Foreword

As any other geotechnical structure, there is a practical need to identify the likely response of the soil around a shallow tunnel, in terms of the of generation and dissipation of excess pore pressures with time. The method of analysis used to anticipate the ground response (eq.

settlement prediction, lining loads, factors of safety, etc.), as well as the selection of the soil input parameters, normally require the identification of the problem within two extremes: a fully drained or a fully undrained condition. The distinction between these two extreme conditions lies in the rate of loading compared to the rate of pore pressure redistribution. The former is connected to the rate of tunnel advance and the latter to the rate the pore pressures equalize towards a steady state condition, which occurs as the excess pore pressures are dissipated and, possibly, as a new hydraulic boundary condition is created.

Recognizing that a tunnel frequently acts as a drain in the long term, it is appropriate to briefly explore how a steady state condition is achieved in a shallow tunnel.

3.3.4.2 Steady State Seepage

If the tunnel is being driven through an ideally incompressible and saturated granular material, and if no fluid pressure is applied to a stable heading (the opening is under atmospheric air pressure), then there will be changes in the hydraulic boundary conditions of the permeable ground domain. As a result, a flow regime will be estabilished with the tunnel heading acting as a drain. If the soil is assumed to be isotropic and homogeneous, and the lining is assumed to be impervious, a seepage flow net can be drawn, for instance for a condition of no depletion of the original groundwater level (permanent water supply to

the system). The water flow will obviously be three-dimensional, but its pattern longitudinally to the tunnel will ressemble that shown schematically in Figure 3.16. This approximate flow net has been drawn ignoring all surface tension effects, and assuming that at a distance from the opening, the water regime is hydrostatic and is not affected by the tunnel. The flow channels 1, 2 and 3, receive out of plane water flow contributions (3D flow supply from the upper and sole aguifer, around the sides of the lined impervious tunnel). This makes the flow net slightly different from that given by Glossop (1978) who assumed a plane strain situation, in which the flow at points far behind the face was fully intercepted by the impermeable lining (the water above the tunnel being unable to migrate to points below it). A point such as A (Figure 3.16) will exhibit a near hydrostatic pore pressure. At B, above the permeable heading, the pore pressure will be very small, as the vertical flow towards the crown is nearly uniform and one dimensional, and thus the total hydraulic head is close to the elevation head. At point C, the pore pressures will be higher than at B, but smaller than A. But if C was moved further to the left, its pore pressure would approach the initial hydrostatic value.

For the present conditions and assumptions, if the heading is advanced continuously, a point like A in Figure 3.16 would experience a drop in pore pressure, followed by an increase once the opening below it is lined. The recovery

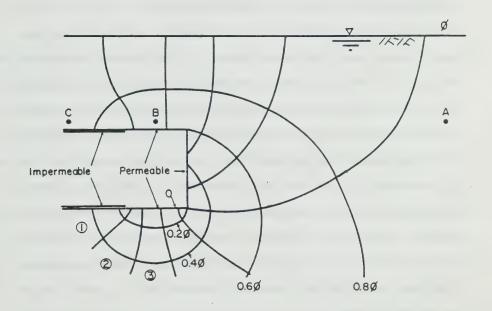


Figure 3.16 Schematic Flow Net in the Longitudinal Plane for a Partially Lined Shallow Tunnel during Construction

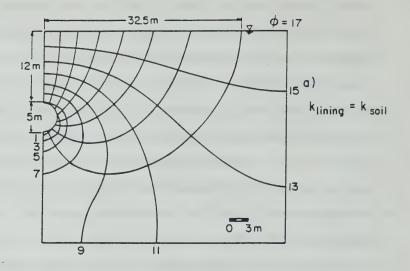
in pore pressure may be only partial if the lining has a finite permeability. The transient hydraulic boundary conditions in an advancing heading, may also explain some of the observed changes in pore pressures above tunnels mentioned in Section 3.3.2.3. However, the rate of change in this idealized case will be solely controlled by the rate of tunnel advance and so is time independent.

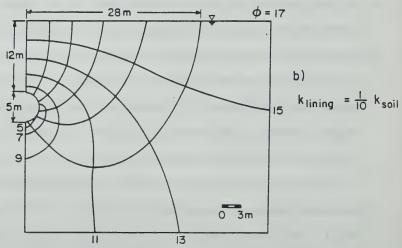
Once the heading has moved further away, a two-dimensional flow may develop if the lining is permeable. Fitzpatrick et.al. (1981) presented a number of flow nets for different conditions that included the varying geometry (ground cover, diameter and depth to impermeable bedrock), varying the lining permeabilities, non-homogeneities in the ground profile, anisotropic permeability and the effect of compressed air. In all cases, they considered that a strong aquifer recharge is present, so that the water table will not be drawn down by the tunnel drainage. They have shown that this assumption is fairly easily met in practice for relatively impervious soils (k smaller than 10-7 cm/s), since, a water recharge corresponding to 2 to 3 cm of rainfall per year will be sufficient to keep the groundwater table at a constant level.

Figure 3.17 shows two flow nets from Fitzpatrick et.al., (Op.cit:99) for a given geometry, but for two distinct ratios of soil to lining permeability (1 and 10). One notes that in the first case (which represents a fully permeable lining condition, whenever its thickness, is

small), along the vertical flow line towards the tunnel crown, the total hydraulic heads are nearly equal to the elevation heads. Therefore, the steady state pore pressures along the symmetrical axis above the tunnel are nearly zero. If the lining has a permeability smaller than the soil, the pore pressures above the tunnel are non-zero. In Figure 3.17(b), the pore pressure at the crown is equal to a head of about 4 m of water. Nevertheless, in both cases the pore pressures above the tunnel experienced a reduction with respect to the original in situ condition.

If the soil is compressible, the ground cover will consolidate upon drainage and settlement will develop. Points located below the tunnel will also experience a reduction in pore pressures and will consolidate as well. If the tunnel construction was performed in such a way that the in situ total stress was not altered, and if the lining had a non-zero permeability, then the resulting ground drainage would induce a long term settlement distribution along the cover similar to that shown by the solid line(b) in Figure 3.18(b). Note that at the crown, the settlement due to this process is non-zero as the rigid tunnel lining also settles due to the consolidation of points located below the floor. If one adds this settlement distribution to the immediate displacements induced by the unavoidable changes in the total stress caused by the tunnel construction (dashed curve (a) in Figure 3.18), the resulting settlement distribution could be that given by the dotted-dashed curve (c). This





Note: Total equipotential hydraulic head ϕ calculated for a zero elevation head at tunnel floor.

Figure 3.17 Steady State Flow Nets Around Shallow Tunnels with Different Lining Permeabilities (from Fitzpatrick et.al., 1981:99 - modified)

curve is similar to that shown for after consolidation in Figure 3.15, the difference being that the permeable tunnel condition allowed higher long term settlement to develop. A near zero vertical straining condition can therefore result without being associated with a near collapse situation, as pointed out in Section 3.2.2. This feature has been observed in a number of tunnels driven through soft, normally or lightly overconsolidated clays (for example, by Terzaghi, 1942:185 in the Chicago Subway, by Glossop and Farmer, 1979:71 in the Sewer Tunnel at Sydenham, Belfast, etc.). In this type of soil, the settlement associated with the drainage may become significant, and perhaps as large as those developed in the short term by the tunnel excavation. However, if the soil is overconsolidated or if the lining is impermeable, then the long term increase in settlement will be a small fraction of the immediate settlement. An approximate assessment of this long-term settlement was done by Howland (1981) for some of the soft clay cases just referred to. Howland simply used Terzaghi's one-dimensional consolidation theory, only taking into account the changes in pore pressure given by the steady state flow net. Despite the obvious simplification, the calculated surface settlement compared well with that measured at different times after tunnel construction.

The consequences of a steady state flow regime on the loads of a fully permeable lining have not received much attention. One reason for this could be that a lining is

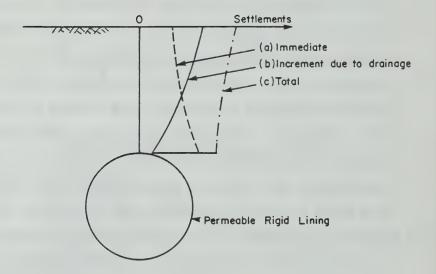


Figure 3.18 Schematic Distribution of Settlements in the Cover of a Shallow Tunnel due to Groundwater Drainage

normally designed to be impermeable and therefore the regime is not established. But if it does, one has to take into account the effect of the steady state pore pressures on the effective stresses, even for a hypothetical case of a lining installed without affecting the in situ stresses. Atkinson and Mair (1983) were one of the first authors to address this problem. They questioned the frequently made assumption, that the total load on a tunnel lining is substantially reduced if the latter is made permeable. For very idealized conditions, (they assumed a deep tunnel, no drawdown, and no soil strains after lining placement), they showed that the long term loads are the same regardless of the lining being permeable or impermeable. Their generalization seems debatable and was questioned by others (Hungr, 1985 and Gunn and Taylor, 1985). The limited numerical evidence shown in Figure 3.14 and discussed previously, does not fully support Atkinson and Mair's statement. The magnitude of the soil strains both before and after lining placement, seems to significantly affect the total lining loads. Nevertheless, their conclusion is possibly a valid one, and further research seems needed to clarify the subject.

3.3.4.3 Total and Effective Stress Paths

A proper assessment of the stress paths around a shallow tunnel is not possible without involved numerical analyses. However, to illustrate a few points, one can follow Atkinson and Mair's (1981:22) simplified reasoning.

The total and effective stress changes in an element of isotropic saturated soil near the contour of a deep tunnel will be considered under plane strain conditions. A uniform in situ stress state is assumed and two types of soil are considered: normally consolidated and overconsolidated.

Tunnel excavation and support installation is considered to be performed in an undrained condition, immediately followed by a consolidation stage. The stress changes are assumed not to cause soil failure.

Figure 3.19 shows the total stress path, ABC, this element of soil may experience (assumed to be unique for both soil types). Point A represents the in situ stress state, and u the original hydrostatic pore pressure. From A to B, the opening is unloaded and the in situ stress reduces under undrained conditions. An overconsolidated soil (oc) will react developing negative excess pore pressures and at the end of this unloading proces (point B'), the pore pressure will be u_{oc} , smaller than u_{o} . For the normally consolidated soil (nc), it will be assumed that the partial unloading is such, that a positive excess pore pressure develops, and at the end of construction (B''), the pore pressure is u_{nc} , larger than u_{o} . Following the construction period, consolidation occurs and is fully completed at the C points. If, for simplicity, the changes in total stresses during this process are ignored, as in Terzaghi's linear consolidation theory, points B and C coincide and no change in the mean total normal stress or shear stress develops. If

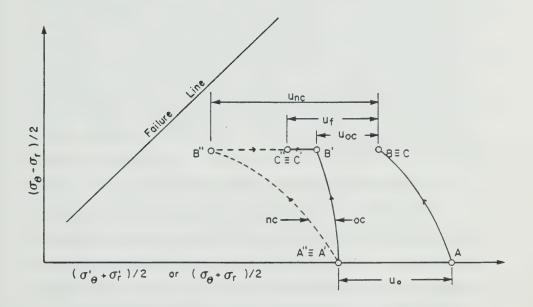


Figure 3.19 Idealized Total and Effective Stress Paths
Around a Tunnel

the lining has some finite permeability, a steady state flow towards the tunnel will finally be established in both cases and a final equilibrium pore pressure u_f, such as those given by the flow nets in Figure 3.17, is attained at C. The overconsolidated soil will swell to C', with the effective stress path moving towards failure. The normally consolidated soil will consolidate towards C'', away from failure, the factor of safety thus increasing. Under the assumed conditions, the paths B'C' or B''C'' lead to pure volumetric straining, whereas along A'B' or A''B'', only shear strains develop.

3.3.4.4 Changes in Stability with Time

One reason to identify what kind of response the soil will exhibit in terms of pore pressure changes, is the assessment of the ground stability. Strictly speaking, the stability to be investigated is that of the ground and lining combined. However, if it is assumed that after heading excavation, the support is installed with good soil contact and with sufficient structural capacity, the concerns are generally limited to the ground stability during the unsupported heading advance, (Section 3.2.1.). Therefore, it is normally assumed that the plane strain stability condition of a tunnel is not critical, if the three dimensional stability of the heading has been ensured. Despite this generally being the case, it is worthwhile to address the plane strain stability problem of a hypothetical tunnel in which the lining action is represented by an

internal tunnel pressure and the opening contour is assumed to be partly permeable.

For these idealized conditions it is tempting to draw a parallel between other geotechnical structures and the shallow tunnel problem. Bishop and Bjerrum (1960:469) investigated the changes in the stability conditions of open cuts in clay. They suggested on theoretical grounds that, due to the negative excess pore pressures that are generated in the undrained unloading of an excavation, the reduction in effective stresses with swelling and the establishment of steady seepage leads to a critical long term condition in terms of stability. In an open cut, the in situ stresses at the cutting profile are fully reduced, and therefore the reduction in the mean principal stress tends to dominate the pore pressure changes. Negative pore pressure changes are likely to occur, irrespective of the shear stress changes and possible effects of the rotation of principal stresses.

Under these simplified assumptions, the stability response of a shallow tunnel with time is likely to be distinct from that of an open cut. The reason for this is that the undrained pore pressure response in a tunnel depends on the amount of stress release allowed by the construction. Figure 3.20 depicts the possible changes in the average shear stress, pore pressure and factor of safety for a shallow tunnel in overconsolidated and normally consolidated clays. It has been assumed that tunnel construction is performed in undrained conditions, with pore

pressure redistribution occurring thereafter. Also, it has been supposed that the average shear stress along potential slip surfaces above the crown, remains constant during the consolidation process. This may not be correct if a lining is installed which restricts displacements in the opening. Even if the ground is assumed homogeneous, isotropic and elastic, it is known that the total stresses at the beginning and at the end of the consolidation process will not be the same if a displacement boundary condition is introduced (Lambe and Whitman, 1969:417,489). It was also shown (Figure 3.14), that the total stresses change in a consolidation process involving time-dependent plastic behaviour of the ground. Nevertheless, it will be assumed, for discussion purposes, that the shear stresses remain unchanged after construction.

It was shown in Section 3.3.2 (for instance, Figure 3.10), what the likely changes would be in pore pressures of a soil element close to the tunnel, upon a decrease in the tunnel internal pressure. From this, the pore pressure responses during the undrained unloading can be qualitatively estimated. Depending on the amount of in situ stress release, on the degree of overconsolidation of the soil, and on the final pore pressures developed at equilibrium, the pore pressures in an overconsolidated soil may or may not reach a minimum at the end of construction. Consequently the long term stability condition may or may not be a critical one (Figure 3.20a).

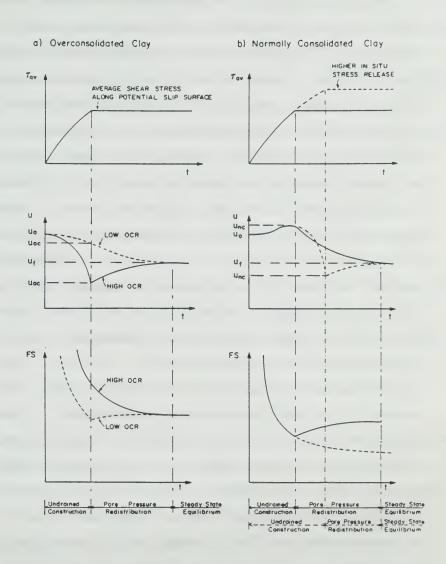


Figure 3.20 Idealized Changes in Shear Stress, Pore Pressure and Factor of Safety during and after Construction of a Plane Strain Shallow Tunnel in Saturated Clay

If the construction induces different degrees of shear stress mobilization in a normally consolidated clay (Figure 3.20b), the pore pressure response may be somewhat dissimilar. For limited in situ stress release corresponding to a good ground control condition, the pore pressures may show an increase by the end of the undrained tunnel construction, followed by a decrease with time. The associated change in the factor of safety will indicate a critical condition in the short term rather than in the long term. However, if the construction technique is poor and allows substantial plastification of the soil around the opening during the undrained unloading process, then the pore pressure changes may become negative close to the tunnel and one could speculate that a critical long term stability condition may develop.

If the tunnel contour is assumed to be fully impervious, so that a hydrostatic condition is re-established with u_f equal to u_o , and if good construction is applied with reduced amount of in situ stress release, then the most likely responses are similar to those shown by the solid lines in Figure 3.20a or b. Hence for the overconsolidated soil, the critical stability situation is in the long term and in the short term for the normally consolidated soil. The limited amount of evidence from theoretical studies, field observations and model testing discussed in Section 3.3.2.3, suggest, however, that for these described conditions (particularly if the ground

control is good), the undrained changes in pore pressures in the tunnel cover are likely to be small, compared with those found in other geotechnical structures. In contrast to an open cut excavation, the mean principal stress in the cover of a shallow tunnel does not decrease as much. Thus, the pore pressures may be controlled mainly by the shear stress changes, which are limited if the construction quality is good. Therefore, one might suggest that the changes in the factor of safety after the undrained tunnel construction could be relatively small, whenever the tunnel contour is impermeable.

Unlike Bishop and Bjerrum's (1960) suggestion for slope excavation, which has been proven correct both through numerical simulations and by interpretation of actual cases (see, for example, Kenney and Uddin, 1974 or Eigenbrod, 1975), the discussion with respect to tunnels should be taken as speculative. Finite element simulations for generation and dissipation of pore pressures seem to provide a valid approach to check this conjecture. Static model tests of tunnels in conditions resembling those established here, both for normally and overconsolidated kaolin (Seneviratne 1979:64) appear to confirm what has been suggested: that critical stability is in the short term for OCR=1 and in the long term for OCR>3.

3.3.4.5 Drained and Undrained Response Boundaries

To the writer's knowledge, no quantitative criteria have been made available so far, allowing the classification of a tunnel response as drained or undrained. Legitimate treatment of this problem would require, for instance, an approach similar to that followed by Eigenbrod (1975) for slope excavation, extended to cover an ample range of influencing parameters, and necessarily including the three dimensional nature of the tunnel heading advance.

The definition of the degree of consolidation in a plane strain tunnel problem is not as simple as in a one-dimensional situation. In a shallow tunnel, both positive and negative excess pore pressure dissipation occurs simultaneously and the usual definition of the compression at a certain time, divided by the final compression, may not be satisfactory, as the consolidation swelling process may have a balancing effect. For this reason, Johnston (1981:103) introduced an excess pore pressure constant, U., as

$$U_{e} = \int_{A} |\Delta u| dA \qquad [3.17]$$

and, defined a degree of consolidation as

$$U = 1 - \frac{U_e}{(U_e)_{max}}$$
 [3.18]

The non-dimensional time was expressed by Johnston (Op.cit.:105) as:

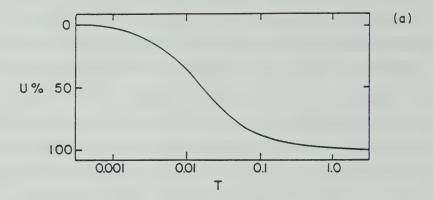
$$T = \frac{ct}{z^2} \cdot \frac{(1-2\nu)}{2(1-\nu)}$$
 [3.19]

where c is the coefficient of consolidation defined in terms of the soil elastic constants at the tunnel axis elevation,

and z is the drainage distance, taken as the depth to the tunnel axis. Both the surface and the rigid base at 2z below, were taken as free draining boundaries in his analysis. A plot of the degree of consolidation, U, against T is shown in Figure 3.21(a), using the lining and soil properties (OCR=1) given in Section 3.3.2.3, and assuming a gap closure of 91.4 mm (same conditions that led to the settlements shown in Figure 3.15). One notes that most of the consolidation process has taken place before T=0.1.

For comparison, the maximum surface settlement is shown in Figure 3.21(b). It is expressed as a percentage of the final surface settlement at the tunnel axis, plotted against the non-dimensional time factor. It is noted that most of the settlement takes place before T=1.0. The evolution of the maximum surface settlement lags behind the degree of consolidation. This is caused by the negative excess pore pressures below the tunnel floor (Figure 3.11) that dissipate more rapidly than the positive excess pressures elsewhere. The faster swelling (and heave) associated with the former, initially hinders the overall settlement trend, which is controlled by the consolidation of the positive excess pore pressure area around the springline. This process occurs at a lower rate and has a longer drainage path (Johnston, Op.cit.:105).

Also worth noting in Figure 3.21b is the fact that the time dependent settlement, in this case (normally consolidated clay, impermeable lining and a large void gap



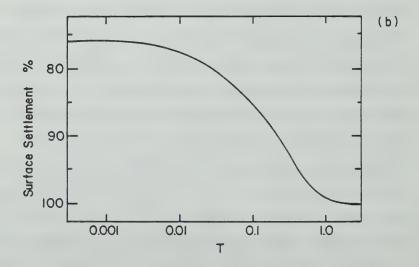


Figure 3.21 Degree of Consolidation and Maximum Surface Settlement Evolution in a Shallow Tunnel (modified after Johnston, 1981:106)

behind it) is responsible for less than a quarter of the total surface settlement. This fraction is reduced to 14% when the fictitous gap is reduced to 50.8 mm (Johnston, Op.cit.:131) and to 11% for a 50.8 mm gap when the OCR is increased to 2 (Johnston, Op.cit.:136). This confirms that, with good ground control and an impermeable lining, for both lightly and more overconsolidated soils, the time independent settlements are far greater than the time dependent ones. The latter are considered negligible for all practical purposes.

Curves as shown in Figure 3.21 are useful to evaluate the amount of time required for a fully drained response to be achieved. However, they are only applicable to the limited conditions (Johnston, 1981), and therefore it is worth investigating the influence of some extreme conditions.

For a deep unlined tunnel with an impermeable contour, the linear elatic consolidation solution provided by Carter and Booker (1982:1070) can furnish some assistance.

Equation 3.10 and Figure 3.12(a) give the pore pressure changes at any point around the tunnel, for some dimensionless time factor, T. Recall that the Poisson's ratio of the soil skeleton is equal to zero, which corresponds to the slowest rate of consolidation (Section 3.3.3.1). By using the same definition of the degree of consolidation introduced by Johnston (1981:103), in terms of the absolute modulus of excess pore pressure

[3.20]

over the total area of the soil around the circular opening, it is possible to numerically integrate the curves shown in Figure 3.12(a), for each of the time factors given. One is then able to say that, for T smaller than 0.1, the consolidation process is incomplete, with less than 10% of the consolidation having occurred. On the other hand, it is noted that for T greater than 100, the consolidation process is nearly complete, with more than 90% of the consolidation having occurred. Bearing in mind the definition of the time factor T given by the equation 3.11, one can easily establish practical boundaries for undrained and drained behaviour.

The following points are established for an elastic, isotropic and homogeneous ground. For the consolidation process of the excess pore pressures generated by the shear stress changes around an unlined and impermeable deep circular opening, one can say that:

- 1. tunnels with diameters D, such that $D>\sqrt{40ct}$
 - will exhibit negligible (U<10%) consolidation over a time interval t, after the full release of the in situ stresses under undrained conditions:
- 2. tunnels with diameters D, such that $D < 0.02 \sqrt{ct}$ [3.21] will exhibit appreciable (U>90%) consolidation over a

time interval t, after the full release of the in situ stresses under undrained conditions.

The chart shown in Figure 3.22 is readily obtained following similar reasoning used by Vaughan (1974) for the dissipation of pore pressures in embankment dams. If one takes, as an example, a deep 4 m tunnel in blue London clay, with a consolidation (or swelling) coefficient of about 10⁻⁴ cm²/s, one notes that over a time period of one year, the redistribution process of the excess pore pressure can be taken as negligible.

It is possible that the above analysis can provide some insight into a deep tunnel case, but for a shallow tunnel or in the case where the lining is permeable, it may not be adequate. Another extreme situation that could be envisaged, is that of a shallow tunnel built in such a way that the installation of a rigid lining does not disturb the in situ stress condition and in which the pore pressure changes are solely produced by a change in the hydraulic boundary condition at the tunnel contour. If it is assumed that the tunnel lining is fully permeable, a steady state seepage flow net similar to that shown in Figure 3.17 may eventually be formed. If the ratio, H/D, is small, the pore pressures along line AB (inset in Figure 3.23) in the ground cover, will end up being very close to zero. A nearly uniform gravitational flow is established along AB, with an average hydraulic gradient equal to one, since the total hydraulic head losses are approximately equal to the elevation head losses. This is so even for anisotropic flow conditions with horizontal permeability greater that the vertical (see, for

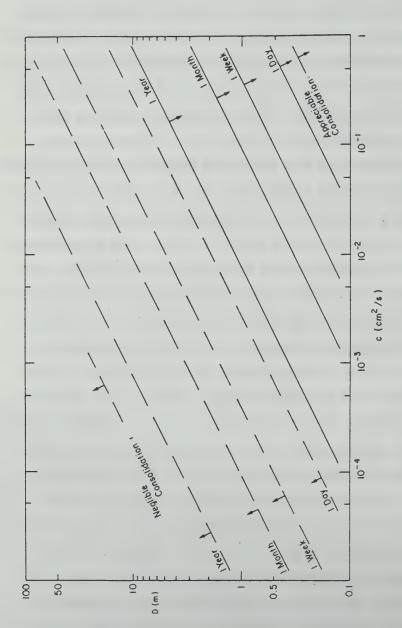


Figure 3.22 Tentative Boundaries for Undrained and Drained Responses Around a Deep, Impermeable Unlined Tunnel in an Elastic Soil

instance, Fitzpatrick et.al, 1981:102).

If one admits that the dissipation process of the nearly triangular excess pore pressure distribution along AB is a unidimensional one, and also ignores possible total stress changes with time, the consolidation of soil elements in the tunnel cover along the symmetry line can be assessed simply by Terzaghi's theory. Therefore, it can be said that for a time factor T smaller than 0.008, the consolidation along AB is incomplete * with less than 10% of the process developing. On the other hand, the consolidation along AB will be nearly completed, with more than 90% of excess pore pressures dissipated, for T greater than 0.848.

For the consolidation process along the line of symmetry, AB, of the tunnel cover due only to excess pore pressures generated by the change in the hydraulic boundary condition at the fully draining tunnel contour, one can say that:

- 1. tunnels with depth of cover H, such that $H > 22.361 \sqrt{ct} \hspace{1cm} [3.22]$ will exhibit negligible (U<10%) consolidation over a time interval t, after tunnel construction;

^{*,} For this particular case $T = 4ct/H^2$, as a double drainage condition was assumed, H being the depth of the cover.

The above boundaries are also approximately valid for tunnels which are partly draining (lining with a finite permeability), provided the initial excess pore pressure distribution along AB is close to linear.

Again, the chart shown in Figure 3.23 can be easily obtained. One may consider, as an example, the large cross section tunnel built for the Sao Paulo Subway system, described by Eisenstein et.al., (1986:713). The tunnel was driven through a stiff, silty-sandy clay layer, with a coefficient of consolidation of about 10^{-2} cm²/s. The 3 m cover of this soil, underlies a saturated sandy horizon, assumed to be fully draining. Somewhere between one to four weeks, a fully drained condition should have been established. Indeed, the field instrumentation, which included deep settlement points and some hydraulic piezometers, did indicate so (Negro et.al., 1985:58). As another example, one can take the Thunder Bay (Array 2) tunnel, driven through a silty clay-clay layer, to give a cover of 8 m. The material has a c value of about 10-3 cm2/s (Lo and Rowe, 1982:165), and neglecting any other excess pore pressures generated except those due to some drainage, one concludes that only after more than a year could almost full cover consolidation be assumed. If a fully drained condition is set at some sand layer boundary at say 2 to 3 m above the tunnel crown, then, the time required to achieve an appreciable consolidation condition would drop to somewhat less than a year. This is more consistent with the

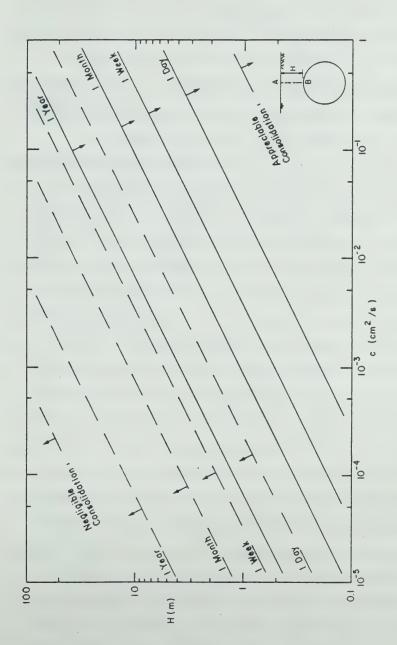


Figure 3.23 Tentative Boundaries for Undrained and Drained Permeable Tunnel, resulting solely from Ground Drainage Responses along line AB of the Cover of a Shallow and

field instrumentation observations made by Palmer and Belshaw (1980:181) who concluded that a near steady state flow condition towards the tunnel existed after a period of one year.

In practical terms, other tentative boundaries could be established to distinguish undrained from drained ground response, by possibly using other less idealized assumptions. The foregoing discussion, perhaps serves more as a simple means of approaching the problem, rather than an attempt to establish general criteria. One feature that should not be overlooked is the different rate of pore pressure equalization and displacements evolution in time, that has been illustrated by a numerical simulation, but is also known to occur in practice. It is believed that even more realistic approaches to the problem will always require some degree of simplification. This will be required on account of the three-dimensional nature of the problem, or on account of stratigraphic singularities frequently found in a site, or on minor hydrogeological details, that have major effects on the rate of pore pressure change with time. A considerable degree of judgement will always be required to accommodate any criteria, simple or otherwise when applied to real situations where such features are normally present. Nevertheless, it would be highly desireable to extend the approach just discussed to more general, but still simplified conditions, such as those that might include the action of gravity, the longitudinal plane strain heading problem, and the axisymmetric heading case. The validity of any criteria emerging from these simplified approaches should ideally be tested against some fully three-dimensional consolidation analyses of a shallow tunnel, that, to the writer's knowledge have not been made available so far.

3.4 Summary and Conclusions

The idealized behaviour of shallow tunnels was further discussed in this chapter. Two behavioural aspects not included or only superficially discussed in the previous chapters were addressed: the stability of a shallow tunnel in soil and the role of groundwater in the ground response.

Tunnel Stability

Though the lining stability can also be a matter of concern, only ground stability problems were addressed in this section. As noted in Chapter 2, even under good ground control conditions, the factors of safety involved in soil tunnelling are usually low and stability deteriorates rapidly with increasing ground displacements. Ground collapse was defined as the creation of a mechanism, through which a local or global disintegration of the ground mass is experienced.

Except for cases of poor lining contact, the ground instabilities are usually restricted to the unsupported length of the tunnel, involving collapses at the face or at the heading. The collapse mechanisms are thus usually

three-dimensional.

The groundwater conditions aside, it was shown that the 3D stability of the ground is usually controlled by geometric conditions as well as by the geotechnical parameters (soil strength). An exception to this rule is dense sand, where the stability is less affected by the geometric conditions.

Model test results indicate that the factor of safety decreases as the unsupported heading length increases and as the relative tunnel depth (H/D) decreases. For H/D greater than about 1.5, undrained model tests indicate that the stability ratio or overload factor becomes constant, and the "face only" stability approaches that for a deep tunnel.

Plasticity solutions are useful tools for anticipation of stability problems in a design stage. They may be of little help for the assessment of global stability problems during construction. Different criteria were examined for stability assessment in the field.

The limiting or critical dimensionless crown displacement, U, of 1.8 suggested in Chapter 2, though useful at a design level and of some help for interpretation of field monitoring, may be inconvenient, as it requires the knowledge of the in situ deformation modulus of the ground mass, which is not always available.

The zero vertical straining along the soil cover may not be a reliable criterion for conditions involving appreciable ground volume changes (contraction or dilation).

The use of critical shear strains as a stability index is also of little help, as it may indicate some localized ground failure, that may or may not bring the tunnel to a collapse state. In other words, it may indicate soil failure, but it may not identify the formation of a collapse mechanism.

A perhaps, more promising criterion was suggested. It consists of observing the shape (and sign) of the distribution of longitudinal distortions, calculated from the longitudinal distribution of ground settlements at a certain elevation above the tunnel crown. This criterion was tested against the results of a tunnel heading model test in saturated kaolin and furnished consistent results. Moreover, it was tested in a subway tunnel where a global collapse mechanism was observed. It was shown that the instability experienced could have been identified well before the global collapse occurred.

The idealized stress changes in the crown of a plane strain tunnel, driven through a cohesionless soil approaching collapse, were investigated. The stress changes following ground collapse cannot be determined, so a speculative discussion was undertaken. Possible interpretations were attempted and their consequences analysed.

The relevance of the above discussion is related to the shape of the ground reaction curve of the tunnel crown after collapse stage is reached. There is some evidence that at

this stage, the ground reaction curve of a shallow tunnel in soil may sweep upward, when a 'loosening' state develops after a minimum pressure is attained. The ground stress thus, would not be uniquely related to the ground displacements.

The phenomenon can be explained for soils exhibiting loss of strength after a peak strength is mobilized, provided the tunnel is not deep. For other types of soil, no definite explanation was found for the upward trend of the ground reaction curve, inferred from some limited experimental observations in sand.

A speculative model explaining this phenomenon was described. In it, the apparent ground response after collapse is not only a function of ground properties, but is also controlled by the support system. Traditional continuum mechanics approaches may not be adequate to test the validity of this interpretation. A physical or numerical verification of its validity would require simulations under displacement rather than stress controlled conditions.

The relevance of the subject seems to be confined to the post collapse response of a tunnel in non-cohesive granular soils, an area which has not been sufficiently investigated by research in soil tunnelling.

The Role of Groundwater

Though the present research does not involve the study of time dependent ground response due to consolidation, or of other effects related to the presence of water, the

subject is important and deserves some consideration.

The presence of water affects the ground stability condition, the settlement magnitude and distribution as well as the lining loads.

The generation of excess pore water pressure was studied through available plane strain analytical and numerical solutions. The development of short term excess pore pressures around an opening is controlled by a number of parameters. The influence of some of these parameters was studied under idealized conditions: the effect of the in situ stress ratio, the effect of gravity, and the effect of the amount of stress release allowed. For less idealized conditions, results of published numerical solutions were interpreted to assess the influence of other factors controlling pore water pressure generation: the influence of non-linear stress-strain properties of the soil, the effect of the overconsolidation ratio, the effect of the ground surface, and the effect of the tunnel lining. In the discussions above, the tunnel contour was assumed to be impervious, an assumption that was later relaxed to assess the likely ground responses for conditions closer to those found in real situations. Results of pore pressure generation analyses, under the three-dimensional tunnelling could not be found. A qualitative assessment of pore pressure changes for these conditions was attempted, taking into account the hydraulic boundary changes associated with the advances of the tunnel heading and lining. Results of

some field observations supporting this assessment were discussed.

A full reduction of the in situ stresses may create appreciable negative excess pore pressures around an unsupported heading. This effect is more pronounced in overconsolidated soils, and may explain the ability of some soils to stand up over a certain period of time. The subsequent swelling process will govern the pore pressure equalization and the opening stability, thus controlling what is called the 'stand-up-time'. Though the process governing the phenomenon is fairly well understood, no theoretical criterion has been advanced so far to assess the 'stand-up-time'. Despite being an important parameter which may control contruction sequences, it is presently estimated using purely empirical approaches.

The dissipation of excess pore water pressures around a plane strain tunnel was then studied by means of available analytical and numerical solutions. The linear elastic consolidation around a deep and lined impermeable tunnel, shows that the average support thrust is time-independent, although, thrust forces may vary locally (within±10%) along the tunnel contour. Local changes in bending moments are higher (up to 100% with respect to the short term value).

The above analysis cannot fully explain the increase of lining loads with time in certain tunnels. If the non-linear stress-strain behaviour of the soil is taken into consideration, the results of numerical simulations indicate

that an increase in the average thrust value can indeed occur as the pore pressures equalize. The results indicate that the lining loads increase at a non-linear rate with the logarithm of time. Moreover, they show that in the long term, the lining loads stabilize at a higher level than the short term level but lower than that given by a full overburden assumption. Evidence from cuts made in fissured overconsolidated soils such as the 'brown' London clay, suggest that the time required for pore pressure equalization may exceed 40 to 50 years. It would not be surprising to identify similar time dependent responses, in terms of lining load build up, in tunnels excavated through the less fissured 'blue' London Clay.

The above discussion was presented to suggest that the lining load increase with time, observed in some soil tunnels, can be simply explained in terms of non-linear 'primary' consolidation. The linear increase of loads with the logarithm of time suggested by Peck (1969) for tunnels in London Clay, would have resulted from observations gathered over too short a time interval (10 years or less). Had the monitoring been extended to larger time intervals, one might have observed lining load stabilization at levels lower than full overburden, contrary to Peck's interpretation. However, the possibility of 'secondary' consolidation or creep in certain conditions, should not be disregarded. Nevertheless, it can be said that the time dependent ground response will be minimized if provisions

are made to restrain the consequences of the non-linear response of the soil. In other words, if higher factors of safety are used, reflecting smaller amounts of ground stress release, prompt lining activation, etc., the time-dependent components of the ground response will be attenuated.

Similar consequences regarding ground settlement development upon pore pressure dissipation were discussed, using available numerical results of 2D non-linear consolidation around shallow tunnels. The time dependent settlements were noted to decrease, as the degree of overconsolidation of the soil increases and as the amount of ground stress release allowed decreases. For good ground control conditions, the short term movements represent the major part of the total ground displacements, unless the lining is permeable and the tunnel acts as a drain. Otherwise, the time dependent components of the movements are small.

The consequences of the development of a steady state seepage into a permeable tunnel were examined, in terms of settlement generation and lining load change. The steady state flow into an unsupported heading in a pervious and incompressible soil was studied. If the tunnel is continuously advanced under these conditions, pore pressure changes will be observed at a point above the tunnel crown. The rate of change in this idealized case will be solely controlled by the rate of tunnel advance, which controls the transient changes in the hydraulic boundary conditions. The

observed response is, in this case, totally time independent.

The assessment of the ground stability requires the identification of the ground response, in terms of the generation and dissipation of the excess pore water pressures. The two-dimensional stability of a partly permeable tunnel, supported by internal stresses, was studied in order to illustrate the problem in qualitative terms. Though some parallel could be drawn with the stability of an open cut, the ground response may be dissimilar, as it is affected by the variable amount of stress release allowed in the plane strain model. The porewater pressures may or may not reach a minimum at the end of the undrained reduction of the internal stresses. Depending on the degree of overconsolidation of the soil, on the final steady state pore pressures and on the amount of stress release, the stability of the tunnel for these idealized conditions, can be critical either in the short or the long term.

Tentative criteria were developed in order to identify the likely response of the ground around a tunnel in terms of the consolidation process for certain idealized conditions. The linear elastic consolidation solution by Carter and Booker (1982) was used to identify the amount of pore pressure equalization around a deep, impermeable and unlined tunnel for different coefficients of consolidation, different tunnel sizes, and over different time intervals. A

second criterion was developed for another extreme condition, in which the amount of consolidation in the soil cover of a shallow tunnel was investigated. In this criterion, the excess pore pressures were reduced to those resulting from a change in the hydraulic boundary conditions at the tunnel contour, which is assumed to be fully pervious. It would thus represent the equalization process resulting from the drainage of the tunnel cover.

Other similar criteria could have been developed using different approaches. For instance, the consolidation around the unsupported tunnel heading during face advance, could be studied, approximating it by available solutions for the three-dimensional consolidation around a pervious sphere. The foregoing discussions did not attempt a general solution to the problem. Rather, they served as examples of simple lines of approaching it. A more accurate solution would be more complex, and it is believed that a considerable degree of judgement would still be required when applying any criterion of this type to real situations. This judgement will always be needed once it is recognized that minor stratigraphic features or soil heterogeneities, have a major influence on the rate of pore pressures changes with time. Moreover, it was pointed out that the rate of pore pressure equalization may be different from the rate of ground displacement evolution with time.

4. PRESENT STATE OF THE DESIGN OF SHALLOW TUNNELS

4.1 Introduction

This chapter presents discussions on design requirements and on available design methods for single shallow tunnels. Its main purpose however, is to review current design practice and to attempt an identification of the present needs for design method improvements. The discussion will be limited mostly to those design aspects where the geotechnical role is more evident.

The design of soil tunnels involves a number of similarities with respect to the design of other soil structures. At the same time, there are also some peculiarities that make it distinct from the others.

As in foundation design, there is need to satisfy the stability condition of the ground and to anticipate the magnitude of displacements induced by construction. While the total loads in a foundation are more or less readily estimated, since the interaction between super-structure and the ground is routinely ignored, it is not possible in tunnels to disregard the interaction between the support and the ground. Both the magnitude and distribution of these loads are needed for the structural design, particularly for the primary lining.

Also, unlike foundation engineering where there is ample room for manipulating the working loads in the foundation elements by changing the superstructure, the

ability to "select" these loads in soil tunnels is rather limited. Lining loads depend predominantly on the soil but also on the construction technology. If the latter is defined by other imposed boundaries, very little room is left to manipulate the working loads on a primary support.

As a direct consequence, while in foundation practice ample factors of safety are normally found, in soil tunnelling, safety factors (of the ground mass) tend to be much smaller, not unlike open cut excavations in soil. Being far from collapse, foundation problems are often successfully treated using linear elasticity, whereas the latter is frequently found to render poorer results in soil tunnelling practice. Also, as pointed out by Gunn (1984:5), it should be noted that in the case of foundations, one of the primary interests is the estimation of displacements at points of the ground where the external load is applied. In contrast, in soil tunnelling one is interested in displacements not only at the tunnel contour where the loads are "applied", but also further away, at the ground surface. The "applied loads", instead of being well defined as they are in the foundation problem, are one of the unknowns. It is, therefore, much easier to find certain elastic constants that would very closely fit an observed response of a foundation, than of a tunnel response. Since it is difficult to obtain a representative Young's modulus from laboratory testing, the use of empirically adjusted elastic parameters confirmed by measured foundation performance became fairly

widespread in practice (e.g., Poulos and Davis, 1980:102). This procedure can hardly be used in soil tunnelling, except in some particular cases. The rate of time independent deformation (unrelated to consolidation or creep) of foundation or earth fill structures is generally governed by their construction rate, provided the major part of the loads are of a self-weight type. This rate is measured in the spans of weeks, months or years. By contrast, the rates of advance of a soil tunnel are measured in terms of hours or days. This has a major impact in the potential damage induced in construction adjacent to the tunnel (Cording and Hansmire, 1975:610). The rapidly changing loads and displacements induced by an advancing tunnel, create a situation which is more critical than in other geotechnical structures. Less time is available for existing neighbouring structures or utilities to interact with their foundations and to redistribute the additional loading generated. As discussed previously in this thesis, time dependent deformations normally represent a small fraction of the total deformations in the soil around the tunnel. Exceptions to these rules include the remarkable cases of subway and railway tunnels built in Oslo, Goteborg and Stockholm (Holmsen, 1953, Karlsrud and Sander, 1978, Broms, 1978). The tunnels driven through bedrock (mostly sedimentary rocks in the Oslo area, and granites in the Stockholm region) acted as drains, and caused pore pressure reductions in any deposits of marine clays which overlay the bedrock.

Resulting settlements of more than 100 to 200 mm have been recorded over periods of 3 or more years, in contrast to negligible short term displacements induced in the rock during construction.

4.2 Design Requirements

The requirements for the design of a shallow tunnel may vary according to its proposed use (highway, rail or subway, sewage, water supply with low or high pressure, etc).

Different operational criteria may be found with respect to safety, tolerances, maintenance, service life, etc. The establishment of these criteria is discussed in detail by O'Rourke et.al. (1984:4). However, there are some requirements which are common to any situation. They refer to:

- 1. The stability of the excavation;
- 2. The integrity of the support, both in the short and long terms:
- 3. The integrity of existing neighbouring structures, utilities and environment, both in the short and long terms.

There is an overall agreement that these are the basic requirements controlling the design of shallow tunnels through soil in urban areas (for instance, Peck, 1969:226, Clough and Schmidt, 1981:604, Resendiz and Romo, 1981:3, Ward and Pender, 1981:261). Also it is quite clear that these three requirements are largely interrelated. The

separation is, nonetheless, convenient for discussion purposes.

For a given site and geometry, requirement (1) is chiefly controlled by the construction technology. Condition (2) is given by the magnitude and distribution of the loads onto the support, mainly with respect to its structural capacity. Long term changes in the overall physical conditions should not be disregarded (bordering new constructions affecting the active loads or lining deterioration processes affecting the structural capacity, for example). Requirement (3) is mainly controlled by the short and long term displacements induced by the tunnel.

Clearly, another requirement which is common to the design of other geotechnical structures, is the assessment of the ground conditions and properties. The subject will not be specifically treated herein as it is beyond the scope of this work. However, a few relevant comments will be made whenever necessary.

Although arbitrary, it is thus convenient to separate the tunnel design, with respect to the geotechnical aspects, into three major activities: i) lining design, ii) prediction of displacements and iii) stability verification.

4.2.1 Basic Requirements for Lining Design

It can be said that the first requirement for lining design is the selection of the lining type. This is a rather important design decision, which is not always simple and

has far reaching consequences. The decision depends on a variety of aspects including tunnelling method, costs, schedule, supply availability, local traditions, performance requirements (water proofing, corrosion potential, etc.), maintenance requirements, etc. Despite its relevance, the subject goes beyond the scope of this study. The reader is thus referred to some review works such as those by McBean and Harries (1970) on precast concrete segmented linings; by O.M.T.C. (1976) on lining for transit systems; by Craig and Muir Wood (1978) on lining practice in the United Kingdom; by Maidl (1984) on lining practice in Germany; by Clough (1980) on lining practice in the U.S.A.

If the support construction of a single tunnel is staged, including primary ("temporary", "immediate" or "initial") and secondary ("permanent" or "final") linings, the design of the former is where the geotechnical component is normally more evident. If the assessment of the support ability to sustain loads is an exercise of confronting predicted loads against the structural capacity of the lining, again, it is in the design of the primary support that the geotechnical role is more apparent.

The operational loads of a primary lining results, among other factors, from the interaction process between the soil and lining. Within the present work, it will be assumed that these loads represent the controlling factor of the lining design. In some instances this is known to be a

gross simplification, as can be the case in precast concrete segmented linings, where either handling, transporting, stocking, erecting, shoving, expanding or grouting loads may control the design. The identification of the most critical loading configuration is not always immediate. This was the case in the 1.79 m sewer tunnel built in Sao Paulo, partly described in Section 2.3.5.4. The 100 mm thick unreinforced segmented concrete, with four pieces per ring, showed some longitudinal open cracks in certain location which did not coincide with the existing stress relievers. These were initially attributed to excessive transversel bending and to an alledged inefficiency in design of the stress raisers. It was felt possible that these did not reduce the stress in the concrete section sufficiently to ensure crack localization. After an extensive review program in which all phases of construction were monitored, it was identified that the cracking mechanism was triggered by the shoving forces that the full face TBM applied to the spigot pins, used to interlock the circumferential joints. The pins, made out of a high strength but ductile and light plastic compound, expanded against the mating holes walls, under the axial compression generated during the TBM advance. Tensile stresses, sometimes in excess of 6 MPa were estimated in the concrete due to this effect and exceeded the concrete tensile strength. A minor modification to the spigot pin and hole design eliminated the problem.

Even in the case of cast-in-place shotcrete lining, where pre-construction loads are absent, there are some concerns about transient loading conditions which may be more critical than the final, plane strain operational loading. Some of these conditions were discussed in Section 2.3.6.3, involving three-dimensional loading mechanisms, that depend on the scheme of the excavation (for instance, possible longitudinal bending of the upper shotcrete shell in the heading). The limited available field and numerical simulation results discussed in that section, indicate that such transient conditions may in fact exist. It is, however, uncertain if they are more critical than the final loading of the primary lining, or else, in what conditions they can critically prevail. An obvious and extreme case is that where the heading is advanced with the inverted floor arch lagging well behind. This construction scheme is frequently advocated by contractors for its economics and construction ease, and is appealing, particularly for large cross-section tunnels. Wittke et.al., (1986) studied this problem as applied to rock masses. There is an apparent need to investigate the subject within the soil tunnelling context, where a very limited advance of the heading without ring closure is normally practiced.

Under operational loads, structural failure of a circular tunnel lining which has good contact with the ground, can result from reaching a limiting stress, under the combined action of thrust forces and bending moments.

Shear failure or lining buckling are not normally observed in shallow tunnels of this type (Peck, 1969:255, Deere et.al., 1969:101).

For these conditions, the basic requirement for lining design involves computations of moment and thrust, and comparing these with limiting moment and thrust combinations causing failure. The moment-thrust interaction curves are helpful tools to assess lining capacity. Their generation and use are not within the scope of the present work.

Examples of applications of this approach to the tunnel support design can be found in works by Sgouros (1982), Paul et.al., (1983:70), O'Rourke et.al. (1984:65), Hansmire (1984:40), Kaiser and Barlow (1986).

For concrete linings with good contact against the soil, the assumption of linear lining response furnishes a conservative design, particularly for relatively stiff supports with larger load eccentricities. This is because if the actual non-linear response of the concrete is accounted for when cracks are developed, the eccentricity decreases, and a higher thrust value is permitted for a reduction in moment capacity. As pointed out by O'Rourke et.al. (1984:67), non-linear analysis shows that concrete linings do not fail by excessive moment, but rather by thrust which

^{&#}x27;If the ground control is good, and for a good lining contact with the soil, the lining of a circular or near-circular tunnel section is not normally provided with shear reinforcement. Rather, the lining thickness is adjusted to resist shear, if this is actually needed. Paul et.al., (1983:136) provides guidelines for shear failure verification in concrete linings.

is affected indirectly by the bending moment. Paul et.al., (1983:144) provides a simple procedure to take into account the positive action of the non-linear behaviour of concrete sections in lining design. However, as most modern lining designs aim for small eccentricities (negligible bending moments), the assumption of a linear response for the lining does not lead to excessively conservative design, and will be taken as a rule in the present work.

Factors of safety applied to the lining design result normally from the combined application of specified capacity reduction factors to the section and of load factors to the design loads. This usually provides factors of safety that are equal to or greater than two. As noted by Paul et.al. (1983:134,136), that while there appears to be little reason to use reduction factors different from that prescribed for other structures in appropriate design codes, the load factors should be distinct especially when ground loads are conservatively estimated. Additional cautions regarding the use of structural codes are discussed by O'Rourke et.al. (1984:22).

Once the lining capacity has been assessed, an additional design requirement for the primary lining is the verification of its deformations or diameter changes, which must be acceptable both terms of capacity and serviceability.

The primary lining is usually designed to withstand all transient loads developed during construction as well as the

"short-term" ground loads. The secondary lining is provided to ensure a safe support for the tunnel under possible increased "long-term" ground loads, as well as any other additional loading resulting from future changes in the overall physical conditions. For instance, if the primary lining has been installed in a dewatered ground, it is customary to design the secondary lining to withstand the loads due to water pressures that may eventually be recovered. This is an arbitrary assumption, as it is readily recognized that upon an increase in pore water pressure, the effective stresses will be changed, and possibly the total stresses. Hence, the primary lining loads are likely to be changed as well. If the secondary lining is already in place, the changes in ground stresses and pore pressures will lead to changes in the support loads, that generally will be shared by the combined primary and secondary lining system. To the writer's knowledge, no analysis has been made available so far showing how these load changes will be partitioned between the primary and secondary supports. It deserves a thorough investigation. Peck (1969:247) suggests, however, that the changes in effective stresses will lead to small alterations in the moments and the increase in water pressure will lead to a fairly uniform all-round pressure that also does not induce appreciable bending in a circular lining.

The action of capillary tensions in the water, especially in fine grained soils, should not be overlooked.

Dewatering is generally conducted in such a way that the drawdown phreatic surface is brought below the tunnel floor elevation. Inevitably, a considerable part of the soil lying above this new phreatic surface will remain either saturated or partly saturated, by virtue of surface tension. The soil zone within the capillary head will be subject to negative pore pressures. The extension of this zone and the magnitudes of these pore pressures will depend on the pore size distribution of the soil. For materials finer than a medium sand, this zone may well cover a sizeable amount of the tunnel cross-section. The negative pore pressures will increase the effective stresses which may remain non-zero, even after the tunnel is cut through. This improves tunnel stability and increases the ground stand up time. This effect has been identified in some tunnel cases, one of them being the sewer tunnel built in Sao Paulo, briefly discussed in Section 2.3.5.4. Neither the interaction between this phenomenon and heading stability, nor the mechanisms of stress changes developing upon the phreatic surface raise after the tunnel is built have been subjects of formal investigation.

While it was customary in the recent past to provide a tunnel with distinct primary and secondary support systems, there appears to be a worldwide effort to develop a single lining scheme, fulfilling both short and long term requirements. This trend is represented by precast concrete segmented linings with new waterproof sealing techniques,

developed in the U.K., Japan, U.S.A., Germany and Brazil over the last 10 years. Along the same lines, the development of the extruded liner system in the U.S.A., U.S.S.R. and Germany should be referred to, (see, for example, Babendererde 1986). Moreover, recent advances in shotcrete technology indicate that more tunnels are being built with the staged application of a shotcrete support which acts as the sole and final lining. As a result, the once common practice of leaving the primary lining design to the contractor (Peck, 1969:247) is being gradually reviewed and abandoned, notably outside the U.S.A.. The practice is being replaced by the detailed lining design being conducted by the owner or the consultant. It usally provided an opportunity for the contractor to come up with an alternative design, whenever it is felt that some benefit may be gained with this. The once somewhat neglected primary lining design is currently becoming a lively integral part of the tunnel design, notably when shotcrete is used. As a result, the present design trend is to consider the primary lining system (with some allowance for physical deterioration with time, if appropriate) as an integral part of the final support. Consequently, consideration should also be given to the long term creep characteristics of the primary shotcrete lining, which may lead to a portion of the ground loads initially sustained by it, to be shared by the combined primary and secondary lining system.

While the above discussion covers the basic requirments for lining design, it is not uncommon to have the finished tunnel later subjected to other loading conditions such as the construction of a parallel tunnel, an adjacent open cut excavation, etc. These are special problems that require individual analyses. A review on the design of two parallel tunnels was presented by Ranken (1978:161), who also presented the results of a parametric plane strain finite element analyses that can be useful for a preliminary assessment of the problem. By representing the soil behaviour through a linear elastic model (in some selected cases, an elasto-plastic model was also used), Ranken investigated the influence of the distance between the tunnels (pillar width) and the influence of the construction sequence (tunnels built simultaneously or not). His studies were not limited to the effect on lining loads, but also included the effect on ground displacements. The charts and tables presented can be used for preliminary design purposes, bearing in mind, however, the conditions modeled (linear elasticity, K equal to 0.5, plane strain representation, tunnel fully lined or unlined). The combined use of these results and of Peck's (1969:255) recommendations based on observed performance of neighbouring tunnels, may serve as an interim design approach, until a more generalized procedure is developed.

As for the effect of open excavations beside an existing tunnel, very little has been done regarding a

general design procedure for this class of problem, since Peck's (1969:257) discussion on the subject. Provided the tunnel diameter is small in comparison to the depth of the adjacent open cut (this could be the case of jacked pipe tunnels or "mini-tunnels"), the tunnel could be approximated by a small diameter pipe using some of the design methods recently developed for buried pipelines adjacent to deep trench excavations. The subject has been attracting increasing interest since the late seventies, especially in the U.K. Most of the available methods treat the pipe as an elastic beam embedded in an elastic foundation, but neglect the presence of the pipe when estimating the ground displacements induced by the adjacent excavation, which will cause the pipe to distort. The displacements are estimated on empirical or theoretical grounds. Crofts et.al., (1977) favoured the first treatment, developing an "upper bound" method, which was later criticized for offering too conservative an estimate of the additional pipe straining induced by the adjacent excavation (Symons, 1978:213, O'Rourke, 1978:215). However, Crofts et.al. (1977), possibly concerned with the large horizontal ground movements frequently observed in trench excavations in the overconsolidated London Clay, neglected the vertical component of bending in the buried pipe. The authors presented a revised form of their method (1978:217), and later included the effect of the pipe joints in their approach (Tarzi et.al., 1979). The entire method was finally

re-published in 1981 (Crofts et.al., 1981), but still, the effect of the vertical component of ground displacement was never considered. However, this can be estimated using the approach developed by Rumsey and Dorling (1985). They extended the results of parametric plane strain finite element analyses of a linear elastic soil (with constant elastic modulus or linearly increasing with depth) obtained by Kyrou (1980). Rumsey and Dorling (Op.cit.:37) developed also an alternative empirical predictive method, based on the observed performance of pipes in a large number of field experiments. This can be used in an ancillary manner with their numerical approach. They enable the net resultant maximum movement of the pipe to be assessed and, from which, the maximum pipe strain can be conservatively estimated.

Nath (1983:1410) showed that the plane strain approximation of the problem can furnish ground displacements that agree within 10% of the maximum movements calculated at the symmetry transverse plane of a three-dimensional analysis, provided the open cut has a width to depth ratio less than 1/3 and a length to depth ratio greater than 2. Results from 3D analyses (Kyrou and Kalteziotis (1985)) confirm Nath's findings, showing also that the maximum bending moments in the pipe are found near the ends of the open cuts.

While the above methods can provide some guidance to the design check of small diameter tunnels under the effect of a nearby excavation, they cannot be applied to larger tunnels which may entirely disrupt the assumed induced displacement pattern. Moreover, the tunnel approximation by a simple elastic beam may not hold any longer as the resulting transverse bending of the lining may be as large as the longitudinal bending. Presently, there is no simple solution to the problem although it is believed that there is room for its development, following approaches similar to those used for buried pipes. Inevitably, the required analyses will have to be more involved. An example of one of such analysis is given by Medeiros et.al., (1982), involving an unusual situation where a 6.2 m diameter tunnel was built through the site of an underground subway station, prior to its cut and cover excavation.

4.2.2 Basic Requirements for Displacement Prediction and Damage Estimate

Another requirement for urban tunnel design is the prediction of ground movements due to the tunnel construction and, after that, the evaluation of their effect on neighbouring structures and utilities, or, broadly speaking, on the environment. Conceptually, this requirement is similar to that for the lining design, since it involves an estimate of some quantities (displacements) and an assessment of some capacity (ability of nearby structures to withstand the anticipated movements).

However, unlike the design of the lining, in which the stress and strain interaction between the support and ground

is normally taken into account, the interaction between the ground and nearby structures is usually not accounted for. In general practice, footing loads are calculated using a frame analysis in which it is assumed that no foundation displacements occur. Then settlements are estimated as though each footing were not structurally connected to the rest of the frame. In other words, the changes in loads in the structural elements due to the induced movements, or, the change in the ground displacements due to the presence of the structure are normally ignored, or only roughly assessed (de Mello, 1969:121).

A proper analysis for the tunnel problem would demand a coupled solution, in which the nearby structure would be fully portrayed (including its foundation elements) and the tunnel construction adequately simulated. Rigorously, this analysis should be carried out including the structure construction simulation and the interaction of the foundation with the ground. An example of this, is the finite element analysis conducted by Larnack and Wood (1972), who took into consideration both immediate and long term settlements. In such a simulation, the effect of both structure and soil stiffness changes during building construction should not be disregarded (also shown by De Jong and Harris, 1971). After this, the tunnel simulation should be performed, allowing the full interaction between soil, lining and building structure. To the writer's knowledge, results of such numerical exercise have not been

made available yet and seem to be too involved for routine application. Despite this, there is a considerable academic and practical interest in conducting some limited parametric studies of this type, representing typical conditions frequently encountered in practice.

A compromise has been favoured in recent studies summarized by Attewell et.al. (1986:237). In these studies, the interaction between the ground and the existing structure at the surface is fully accounted for. The ground surface displacements induced by the tunnel are estimated, the presence of the existing structure is neglected. Equivalent loads applied to the ground surface, causing those estimated displacements, are numerically calculated. These loads are then used as implosed boundary conditions to the combined soil-structure interface . The final foundation settlements are obtained as well as the additional loads induced in the structure, as a result of the tunnel induced movements. Attewell et.al. (Op.cit.:250-277) were able to derive design charts applicable for particular conditions from which the maximum stresses in the structure are determined. These could be compared to stress-based criterion for the onset of damage.

The above method has not been sufficiently tested but it is felt that it has potential for practical use. An important limitation it presents is related to the procedure adopted to define the ground displacements induced by the tunnelling operation. This was done in a semi-emprical way,

assuming a fixed volume of settlement at the surface
(Attewell et.al., 1986:246) and a settlement distribution
profile given by a normal probability curve. The fixed
settlement volume assumption is very arbitrary and does not
take into account the basic parameters controlling the
generation of ground movement. The development of analyses
accounting for these effects is yet to be seen.

The absence of such results forced the practitioner to establish empirical rules, derived directly from observations made in prototypes. From practice it was noted that there are two main sources of damage to structures associated with nearby tunnelling activities. They are the specific differential settlements and the specific differential lateral displacements induced in the ground by the tunnel excavation. The first is the difference in settlement between two points at the ground surface, or at the foundation elevation, divided by the original distance between these two points. It is also called angular distortion, or, simply, distortion. The second is the difference in horizontal displacement of the same two points, again divided by the distance between these points. It is also called lateral strain or transverse strain.

Prediction of these displacements or strains can be performed numerically. The finite element analysis described in Section 2.3.4.1, used to obtain the stress paths shown in Figure 2.4, can also be used for this prediction. Figure 4.1 shows the settlements and lateral displacements, obtained

through this non-linear elastic analysis. They are calculated at the ground surface, for two degrees of in situ stress release: 30% and 60%. Also readily obtained are the surface distortions and the lateral strains at the surface. The inset shows the distributions of subsurface settlements and of vertical strains along the tunnel cover. Strains and displacements increase with the amount of stress release allowed. Maximum distortion is observed at the inflexion points of the settlement troughs, but the maximum lateral displacements and maximum lateral strains are noted elsewhere. Also noted are zones of lateral compression closer to the tunnel axis and of lateral extension further away, near the edge of the troughs. Both maximum ground shear distortions and maximum lateral strains at the surface have, basically, the same order of magnitude, a fact recognized by Cording et.al., (1976), through field measurements. However, these maxima develop at non-coinciding points.

In the above analysis, no support was installed in the tunnel and the existence of buildings at the surface was also ignored. If the interaction between the ground and any building had been accounted for, the displacements and strain distributions shown in Figure 4.1 would have been different. A structure at the surface normally has sufficient stiffness to flatten out the settlement trough beneath it. Field measurements confirm that this can be taken as a normal rule (see, for example, Breth and

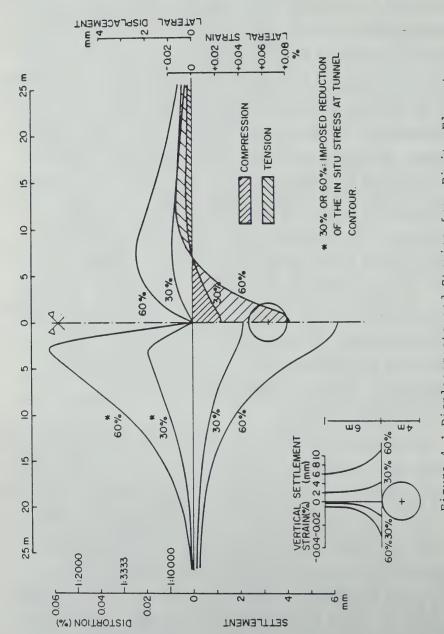


Figure 4.1 Displacements and Strains from Finite Element Simulation of a Shallow Tunnel

Chambosse, 1975:331). Hence, predictions of strains and displacements at the surface, ignoring building-ground interaction, will usually overestimate the magnitude of those variables, by some unknown amount.

Lateral strains seem to control the potential damage to structures located over underground long wall mining. The scale and extent of the induced subsidence under these circumstances are such, that the differential settlements over the limited extent of a typical surface construction are small, despite the magnitude of the settlements being one or two orders greater than that in urban tunnelling. In this latter case, the width of the structure is of the same order as the depth of the tunnel and its diameter. The structure will then be subjected to combinations of both lateral straining and differential settlements and their effects are difficult to separate (Cording et.al., 1976:519). However, from Figure 4.1, it can be anticipated that damage to a building located closer to the centre line is more likely to be associated with the shearing distortion of the ground, whereas for a building closer to the edge of the settlement trough, the damage potential is controlled by the tensile lateral strain that predominates here. Field evidence shown by O'Rourke et.al., (1976) on brick-bearing-wall structures seems to confirm this.

Two damage categories are usually identified (partly following Skempton and MacDonald, 1956:730):

a) Architectural damage: involving initially the

appearance of the structure, and is related to cracking and separations in panel walls, floors and finishes; in the extreme it may involve functional damage of building utilities, impairment of services, such as jammed doors, pipe breakage, etc.

b) Structural damage: impairing the stability of the building, which is associated with cracks and distortion of the main support elements, etc.

Experience shows that damage of the first type precedes that of the second for most building structures. Therefore, the structures will normally become unserviceable before any structural instability occurs which would endanger building occupants. This seems to facilitate the definition of a damage criterion as it will be mainly related to architectural or functional aspects. However, this may actually cause the criterion to become fairly subjective, as pointed out by Peck et.al., (1956:778). The degree of damage considered to be evident may vary from observer to observer. Moreover, the tolerance towards these damages will have different thesholds among individuals and from place to place.

It seems acceptable that most damage (prior to collapse) manifests itself as cracking, resulting from tensile strain in a structure (Burland and Wroth, 1975:616). This tensile strain results from differential settlements (inducing bending and/or shearing in the structure) and from lateral strain, caused by tunnel excavation. The tensile

strain is not readily predictable from estimated ground movements. Therefore other indices have been introduced to directly correlate damage with displacements. As noted before, since surface lateral strains are of the same order of magnitude as surface distortions, the empirical attempts to define damage criteria mainly made use of the latter. Many authors (see Table 4.1) related the occurrence of damage to the observed maximum distortion between the structure footings, after eliminating the rigid body tilt of the building. Skempton and MacDonald (1956:762) presented examples of the calculation of tilt. Although easy to calculate once the structure settlments are known, the anticipation of building tilt is very difficult as it requires full knowledge of the superstructure details and its interaction with the foundation. Thus, structure distortion is usually conservatively anticipated ignoring the tilt. Attempts to correlate the greatest distortion and the maximum settlement or the maximum differential settlement were criticized (Terzaghi, 1956:775). This type of correlation may hold for specific building types on particular and well defined soil units or for specific geological sites, but it may not be valid in a more generalized way. The relationship between these quantities is strongly dependent on the uniformity of the soil and on the distribution of loads over the structure foundation.

Ward (1956) contended that damage would be better related to the maximum curvature (second derivative) of the

Authors	Movement	Index	Availability of a limiting index criteria for damage
Skempton and MacDonald (1956:731)	4	Maximum angular distortion, with rigid body tilt discounted	.Y. 68
Meyerhof (1956:774)	«	Maximum angular distortion, with rigid body tilt discounted	Yes
Bjerrum (1963)	«	Maximum angular distortion, with rigid body tilt discounted	Yes
Ward (1956:783)	*	Maximum curvature (d ² u/dx ²)	No
Polshin and Tokar (1957:404)	*	Deflection Ratio	Yes
Burland and Wroth (1975:623)	A/B	Deflection Ratio	Yes
Kerisel (1975:463)	æ	Radius of curvature	Υ e s
Cording et al (1976:534) and O'Rourke et al (1988:656)	æ	Average angular distortion with rigid body tilt discounted	Yes
Breth and Chambosse (1975:336)	æ	Maximum angular distortion, with rigid body tilt included	√. es

Note: A = structure self weight
B = tunnelling or open cut excavation
A/B = structure is weightless

Table 4.1 Existing Criteria for Damage Assessment of Structures Subjected to Ground Movements

deformed structure foundation. Kerisel (1975) advocated in favour of the radius of curvature of the deformed ground profile, particularly in relation to the damage of old structures. In both cases, it is assumed implicitly that the tensile strains causing cracking result mainly from bending (related to the curvature). This may not be the case in some instances, as these strains may also develop diagonally, due to shear deformation of the structure (for example, see Burland and Wroth, 1975:619). In general, as pointed out by Cording et.al., (1976:529), local curvatures of the soil settlement trough induced by a tunnel are not as significant as the distortion, since the structure is able to bridge or level out small local curvatures. Moreover, curvature is difficult to measure with accuracy in practice, as it is very sensitive to data scatter and as it requires very narrow spacing of settlement points across the subsidence trough. For these reasons, Cording and Hansmire (1975:610) preferred to relate damage to the average settlement slope or average distortion.

Burland and Wroth (1975), following the work by Polshin and Tokar (1957), favoured the use of a deflection ratio to assess building damage. This ratio is defined as (Burland and Wroth, Op.cit.:616) the maximum displacement relative to the straight line connecting two reference points a distance L apart, divided by this distance. If L is taken as the transverse length of the structure, the ratio will be related to the average settlement distortion.

Table 4.1 lists some of the existing approaches to evaluate building performance upon settlements. The limiting relative displacement criteria usually distinguishes the structure type (framed, load-bearing walls, etc.), structure width to height ratio, type of damage, etc. Most of the allowable settlement criteria derived from empirical observation of building damages is related to the settlement of its foundation under its self-weight. Therefore, most criteria are not actually applicable when settlements are due to the tunnelling construction. In the latter case, the building already exists with all finishes and plaster in place, and the rate of movements are much higher than that due to the structure weight. Moreover, by the time the tunnelling settlements develop, the structure has already been subjected to movements due to its own weight, and may already sustain strains close to the critical. Minor additional straining might soon bring it to a condition of damage.

It is believed that the criteria by Burland and Wroth (1975) could be adapted for this different condition, as it is, like that by Polshin and Tokar (1957), based on the fundamental causes of building damage and makes use of a plausible behavioural model. The allowable settlements, (expressed as deflection ratios), are defined for different building structures as a function of a critical tensile strain at which cracking of cladding and finishes (and not structural elements) would become visible. According to

these authors, this strain varies from 0.03 to 0.1% (the lower portions of the range applying to reinforced concrete and the upper to brick or blockwork with cement mortar) and an average of 0.075% could be taken for most structures. Limiting deflection ratios were calculated for different buildings represented by a weightless rectangular beam of unit thickness, with different length to height ratios, under combined modes of deformation involving bending and shear. Different criteria were established for frame buildings (that tend to flex under shear), for load-bearing walls (that crack under bending) and for masonry buildings undergoing hogging (crack in the upper edge upon bending).

Out of the approaches listed in Table 4.1 only those due to Kerisel (1975:436), Breth and Chambosse (1975:336), Cording et.al., (1976:534) and O'Rourke et.al., (1978:656) are actually related to tunnelling excavation problems. The limitation of Kerisel's approach has been already discussed. The damage criterion by Cording et.al. (Op.cit.) and O'Rourke et.al., (1978) are fully empirical and are derived from field observations made in structures adjacent to tunnels and open cuts recently excavated in the U.S.A..

These authors proposed that the average angular distortion (discounting tilt) causing architectural damage in brick-bearing walls and frame structures adjacent to the excavations, are those exceeding the limits 1:1000 and 1:750 respectively. These distortions are much less than that given by the approaches related to settlement of structures

under their own weight. As explained, this is due to the higher rate of movements associated with excavations, to the presence of residual strains in the structure prior to the excavation, and also to the lateral strains that are induced in the ground. Moreover, the aging process in the structure might also have a role in producing these relatively low distortion limits.

Table 4.2 reproduces the description of damages related to the building distortions for brick-bearing wall structures summarized by Cording et.al., (1976:534), and O'Rourke et.al., (1978:656). Needless to say that the table should serve as a broad quideline, and that individual cases will normally require additional judgement. Traditional underpinning methods are known to induce appreciable distortion (values of as much as 1:400 have been reported) which may cause serious cracking in a building (Peck et.al., 1956:779). Hence, considering the low threshold distortion value for architectural damage, it seems unlikely that traditional underpinning methods can be used to prevent this type of damage. Moreover, these methods may ultimately solve problems related to differential settlement, but will hardly avoid the effects of lateral straining. Some more modern techniques, such as inclined jetted piles ("pali-raddice") or jet grouting, seem to show better potential for solving this problem. (see for instance, Guatteri et.al., 1986:190).

If the anticipated ground movements are expected to cause architectural damage, the current attitude is, to

Description of Damage	Associated average ground surface distortion with rigid body tilt discounted *
Threshold of architectural damage	1:1000
Architectural damages, including cracks and separations up to 6 mm wide, sticking doors	1:1000 to 1:300
Functional damages, such as jammed doors and windows, breakage of window panes, restrictions in building services; cracks and separations up to 25 mm wide; lintel instability	1:300 - 1:150
Spalling of stone cladding	1:150 - 1:125

Angular distortion and lateral strains assumed to be approximately equal.

Brick-Bearing Wall Structures Adjacent to Excavations Table 4.2 Damage Related to Building Distortion for (modified after Cording et.al., 1976:535) firstly balance the anticipated costs of architectural repair works in the building against the costs of protective or ground controlling procedures. In many cases, the former costs are lower than the latter. If this is not possible or acceptable, the second approach is to improve the tunnel construction quality by selecting the most efficient construction method or sequence in terms of ground control. The third alternative is to condition the soil by using techniques that may improve the ground response. The fourth and last measure (usually the most expensive) is to contemplate modern underpinning techniques that can effectively reduce the risk of damage, without creating transient conditions that might be more critical than those due to the tunnelling process.

The subject, already complex, may become even more intricate, when there is also a need to consider the longitudinal distortion of the ground ahead of the tunnel face. As noted by O'Rourke et.al., (1978:650), upon tunnel advance, a building is subjected to a settlement wave that causes a three-dimensional warping of the structure, even if its final distorted configuration can be approximated by a plane strain representation. This effect can be better understood through the plots shown in Figure 4.1, considering for instance, that the 30% curves correspond to the displacements induced at a transverse plane containing the tunnel face and the 60% curves representing the final plane strain condition. It is readily recognized that both

angular distortion and horizontal straining will develop in vertical planes parallel to the tunnel axis during tunnel excavation. This three-dimensional distortional effect in neighbouring structures has not been studied so far, and perhaps, requires further investigation. Less frequently addressed, but certainly not less important, are the concerns regarding the effects of tunnelling induced settlements in neighbouring buried utilities (mains, gas pipes, etc.). Only recently the subject started attracting increasing interest. Howe's (1982) review on damage control for distribution systems, revealed that the major cause of buried pipe fracture is movement induced by open cuts and tunnelling operations. Provided the diameter of a buried pipe is small compared to the tunnel, it is customary to ignore the interaction between the pipe and the soil, as far as ground movements caused by the tunnelling operation are concerned. In other words, the prediction of ground movements is done independently, neglecting the existence of the utility buried in the ground. However, for assessment of the additional straining resulting from tunnelling induced ground movements, the interaction between the pipe and the surrounding soil is taken into consideration in a simplified way.

The evaluation of damage risk in buried pipes can be based on either a breaking strain (or stress), or on a maximum strain (or stress) for unserviceability. Crofts et.al., (1977:174) suggested that if the factor of safety

applied to limiting strains is less than 5/3, there will be an unacceptable risk of breakage or unserviceability. For instance, according to Carder et.al., (1985:21), the maximum acceptable ultimate tensile strain for a new cast iron pipe is 0.2%. Strains due to other causes, not directly related to tunnelling induced ground movements, should be added in assessing that factor of safety. These authors further suggested that, if the factor of safety is greater than 4, breakage or damage will be unlikely.

Assessment of additional straining by tunnelling operations is frequently done by assuming the buried pipe is to be represented by an infinite elastic beam embedded in an isotropic elastic foundation, represented by a sub-grade reaction modulus. The ground movements predicted separately are used as an imposed displacement boundary condition, and bending moments, stress or strains can be calculated solving the appropriate differential equation. This approach has been followed by Takagi et.al. (1985) and by Yeates (1985), both works providing design charts resulting from parametric numerical analyses of steel pipes. The first authors study the behaviour of continuous pipes transverse to the tunnel, assuming that they deform according to the normal probability curve as suggested by Peck (1969). To corroborate their method they compared predicted and measured bending stresses in an instrumented test pipe, installed above a large shallow tunnel. The results were encouraging. Yeates (1985) used a similar approach and went

further by including the case of a continuous pipeline parallel to the tunnel axis. To do this, he used the expression for the cummulative normal probability curve suggested by Attewell and Woodman (1982) to represent the ground settlements parallel to the tunnel axis. Unlike Takagi et.al., (Op.cit.), who only considered the vertical component of the induced displacements, Yeates (Op.cit.) considered also, but separately, the effect of the horizontal movements parallel to the pipeline axis. Using the treatment by Poulos and Davis (1980:74) for axially loaded piles, Yeates provided elements to estimate the maximum tensile pipe strains at points of maximum hogging, both transversely and parallel to the tunnel. Again, the analysis requires an independent estimate of the horizontal displacement as an input. Throughout his derivation, Yeates made a number of conservative assumptions, which lead him to claim that his predictive method is safe, although comparison with field measurements has not been provided.

Takagi et.al., (1985:107) also studied the influence of mechanical joints in ductile iron pipes, and showed that they have suprisingly little effect in the numerical results obtained. This was attributed to the standard lengths of these pipes (4 to 6 m) as compared to the usually wider transverse widths of settlement troughs of shallow tunnels. Yeates (1985:137) reached a similar conclusion independently.

A comprehensive review of the available methods for assessment of the consequences of tunnelling induced ground movements on buried pipelines was recently published by Attewell et.al. (1986:122). These authors provided a number of solutions for the problem and presented examples of applications for a variety of practical conditions. In these solutions, the ground displacements induced by the tunnel construction are estimated semi-empirically by assuming that their distribution follows a normal probability curve (see Section 4.3.3), and by empirically estimating the volume of ground settlements. An improvement on this fundamental aspect of the solution would be desirable.

Although extremely useful, the above methods need to be properly correlated to actual observed performance in order to be fully validated. Not many case histories are available for this purpose, however. The use of centrifuge modelling (e.g. Kusakabe et.al., 1985) may be helpful in this assignment.

If the size of the buried utility is comparable to that of the tunnel, the simple approach just discussed may not be valid. The induced displacements may be affected by the presence of the utility (an old tunnel, for instance), and in this case, a more complicated numerical analysis will be required, allowing the complete interaction between utility, ground and tunnel to be accounted for. An example of this type of problem and analysis was shown by Hansmire et.al., (1981), and related to a sewer tunnel built with a clearance

of just 0.5 m over an old twin subway tunnel in New York City. A simplified two-dimensional plane strain finite element analysis was performed in order to assess the effect of the tunnelling including jacking forces, on the existing tunnels. Details of this study are presented by Ghaboussi et.al., (1983), who also evaluated the action of jacking the TBM in the new tunnel on the old subway lining, by means of a simplified three-dimensional finite element analysis.

As mentioned earlier, whenever it is anticipated that the induced ground displacements will likely cause damage to neighbouring structures or utilities, the tunnel design should call for ground control measures. The design of such measures are currently taken as an intergral part of tunnel design. The subject will be briefly covered in the next section, as it is also closely related to the ground stability control.

4.2.3 Basic Requirements for Verification of Excavation Stability

Lining design requires that the support capacity is sufficient to withstand soil loading conditions so that collapse of the supported opening is precluded.

This, and the assurance that good lining-soil contact exists reduces the verification of the tunnel stability to issue of the heading excavation in terms of local or global ground collapse. As noted in Section 3.2.2, the problem is fully three-dimensional and its complete solution is rather

involved. Available methods for stability assessment are applied to very idealized conditions, and the current design approach is to bound the correct solution, using fairly extreme assumptions and a large amount of judgement.

The basic requirement, as in any other stability calculation, involves the evaluation of driving forces and resisting forces, with their comparison allowing the assessment of a factor of safety. This is preferably done through the limit theorems of plasticity (upper and lower bound solutions), which enable the correct factor of safety to be bounded. Except in cases where the collapse mechanism is fairly well defined beforehand, normal design decisions are not solely based on conventional limit equilibrium calculations. These are upper bound solutions formed from the condition that the mechanism is kinematically admissible, and, therefore, they may provide unsafe estimates of the factor of safety.

Available solutions for the stability of tunnel headings are applicable to homogeneous soils, represented either by a frictionless material or by a frictional and cohesive material. The action of pore pressures are not rigorously accounted for. Solutions that assume the soil to be a purely cohesive material could represent the case of a heading excavation in saturated soil under fully undrained conditions. Therefore, at the design stage, it is necessary to identify the pore pressure responses in terms of the rate of dissipation compared to the anticipated rate of tunnel

advance. As no general solution has yet been made available for the three-dimensional consolidation process around an advancing heading, the practitioner is compelled to adopt simplified approaches to the problem, as the one presented in Section 3.3.4.5. From these approaches, the most likely response, from fully undrained to fully drained is identified, and the most adequate stability solution is selected for the case under investigation. Usually the lower bound approach of the three-dimensional stability problem of the face or heading will suffice. Being a "safe" solution, fairly low global factors of safety are generally accepted (from 1.1 to 1.3), provided the ground conditions and properties are well known.

If the likely response of a saturated ground during tunnel advance can be assumed to be fully drained, then the stability evaluation of the tunnel face or heading should ideally be performed in terms of effective stresses, with pore pressures obtained from flow nets. However, to the writer's knowledge, no solution to this fairly complex three-dimensional problem including the action of steady state pore pressures, has been developed so far. Upper bound work rate calculations seem to provide an easier path for this development, but they are not available, except for dry soils (for example, Casarin, 1977:65). De Mello and Sozio (1983), proposed a two-dimensional approximation, treating the tunnel face as a long wall mining face and using a limit equilibrium approach. This is obviously an

oversimplification that may be accepted only for comparative purposes.

Once the support is installed and an equilibrium is reached, the overall stability of the combined soil-lining system will generally increase, by virtue of the inclusion of the stiffer and stronger support element. This increase in safety is not apparent from the discussion on the idealized changes in stability with time, presented in Section 3.3.4.4 (Figure 3.20), since there, the contribution of the support in the overall safety was intentionally neglected. Actually, the assessment of safety in the combined system is usually not attempted, but rather, factors of safety are separately estimated for the ground and for the lining, in the final, long-term plane strain situation. Different factors of safety are therefore assessed, using the equilibrium loads resulting from the interaction process between the soil and the support, and the acceptance of these factors is analysed independently. There is no pre-established minimum safety factor for the soil under this condition. As noted in Section 2.3.4.3, the minimum acceptable factor is defined in terms of the maximum tolerable ground deformation. The limited amount of tunnel model test data analysed in that section, indicated that a "good ground control" condition would be achieved, whenever the dimensionless crown displacement, U, was smaller than 1, and this would correspond to factors of safety greater than typically 1.5. This value should not be taken as a rigid

reference, as different amounts of settlements or losses of ground would be expected for different soil types for the same factor of safety. Hence, values lower than 1.5 may be acceptable for stiffer or denser soils (possibly 1.3 to 1.4), and higher factors may be required for softer or looser soils (e.g., 1.6 to 1.7), for the same amount of acceptable loss of ground or tunnel closure (see Figures 2.6 and 2.7). Summing up, the assessment of the final long-term factor of safety of the ground is generallly not, in itself, a mandatory design requirement. Provided that the stability of the face and heading is fully ensured, that lining capacity is sufficient (both for short and long terms) and that the final ground displacements are acceptable, the assessment of the final factor of safety of the ground is generally an accessory design evaluation. Only in some special conditions this rule may not prevail. Exceptions to it sometimes involve cases where good lining-soil contact is not ensured. This is the case, for example, of tunnels lined with precast support elements and with a delayed application of grout to fill the voids behind them.

Another important requirement for the ground stability evaluation is the adequate assessment of soil strength. This point deserves special consideration particularly when dealing with some stiff fissured soils. The effect of soil fissures on the strength of the soil mass was analysed by Bishop (1966) and Marsland (1972), among others. The controlling role of these fissures in the short term

stability of a large cross section tunnel (10 m diameter, approximately) built in Sao Paulo, Brazil, described by Negro et.al., (1985) and Eisenstein et.al., (1986), was addressed by Negro et.al., (1985:187). The spacial distribution of fissures and other weakness facies, in this stiff sedimentary silty clay, was found to be erratic and the spacing ranging from 5 to 30 cm, or about 1/200 to 1/30 of the tunnel diameter. If the criterion by Deere et.al., (1969:1-15) for jointed rock masses was applicable to this case, it could be said that the ground mass around the tunnel would behave as a fairly homogeneous continuum (average fissure spacing less than 1/50 of the tunnel diameter). The strength of this soil was investigated by means of unconfined compression tests in a number of undisturbed cubic specimens with sides ranging from 4 to 22 cm. It varied from 0.7 MPa for the smallest specimens to 0.05 MPa for the largest. If Bishop's (1966) proposed relationship relating the strength of the intact soil to that of the fissured soil mass expressed as a function of fissure spacing, is accepted, then, the former would be found to be about 1.5 MPa and the latter 0.2 MPa, after a best fit of strength data with sample size is performed. In this particular case, tunnel stability would be better assessed using a strength compatible to the lower figure above, which better represents the strength of the ground mass.

Also not to be overlooked in the design stage is the action of possible water seepage into the heading. Steady state seepage during tunnel advance such as that discussed in Section 3.3.4.2 may generate localized piping mechanisms that may trigger an instability process, particulary in fine draining ground masses. This effect was investigated (Taylor, 1980) by modelling a plane strain tunnel failure in a homogeneous silt in a centrifuge, under the action of ground water seepage. Stratigraphic details and local hydrogeologic features have a major influence in this process and require a great deal of investigation. Proper assessment of potential problems of this nature is rather complex, as it involves three-dimensional transient flow which is highly affected by the above features. However, qualitative evaluation of difficulties can be performed under simplified two-dimensional assumptions, particularly when studying alternative means to control the groundwater flow (see, for instance, De Mello and Sozio, 1983).

Another basic requirement is the selection and design of ground control measures needed to ensure the stability of the excavation, whenever it is assessed that the tunnelling scheme does not present adequate safety. It is not unusual to find designers or owners leaving the design of ground control measures to the discretion of the contractor. This is partly due to legal and contractual dispositions found in some countries or due policies of some authorities. Modern attitudes toward risk sharing contract types are forcing

this condition to be changed. Technically speaking, it is highly advisable to include the design of ground control measures as an integral part of the tunnel design. The subject is beyond the scope of the present work, but for the sake of completeness, Table 4.3 has been prepared and summarizes the most common expedients and means to exercise ground control or ground conditioning presently used in soil tunnelling in urban areas. The primary objectives of these processes can be stability control or also reduction in ground displacements. Some processes may have broader actions and functions than indicated, but those shown seem to be sufficient for an initial assessment of their technical virtues. The list of techniques and references included do not intend to be complete, but only illustrative. Also, some processes may be classified in more than one technique group, or they may also be used in a combined way. No attempt has been made to include comments on costs since they may vary considerably, thus not allowing a general assessment to be made. Grouted soil anchors or bolts could be included in group E, combining the actions of processes E2 and E3m when suspension grout is used. Their effectiveness as a ground control technique has, however, been questioned (Laabmayr and Weber, 1978:82, Steiner et.al., 1980:321, for example), and therefore they are not included in the table. When used in stiff, residual soil masses, where the behaviour is controlled by preserved parent rock features, grout bolting can, however, be an

effective control measure.

Other techniques that could be potentially considered include electro-osmosis and lime stabilization, but their applications for ground control in soil tunnelling have not been reported to the writer's knowledge.

4.3 Available Design Methods .

4.3.1 Foreword

In this section, a survey of existing methods of shallow tunnel design is attempted with attention being paid to their features and limitations. It includes procedures that are highly dissiminated among practitioners, as well as others not so well known, despite their merits. No attempt is made to review each method in detail, as this has been done to variable extent by different authors in the recent past. These review works, however, are referred to as additional sources for reference. Although the survey was undertaken in order to be as complete as necessary, to allow a comprehensive classification of existing methods, it is far from exhaustive. This is partly due to the extremely large number of design procedures developed over the last two to three decades in different countries and published in different languages, being therefore, not always accessible. To make the survey simpler, brief and less tedious, the review covers groups of methods rather than individual methods, unless deemed necessary. Attention is given to

	Technique Group	Process	Action	Function	Comments	Recent References
4	A Staged excavation	1 Heading and bench 2 Side drift or galleries 3 Multiple drift method, etc.	Reduces unit size of face excavation, reduces influence of fasures and weakness facies in ground mass stability.	Increase stability of excavation, may reduce settlements also.	Usually not suitable for machanized excavation schemes applicable to medium or large size openings; reduction in ground displacement depends on excavation and support schemes.	All Negro and Elementein (1981); Al and All Elementein et al (1986); Al Vasiahth (1988); Parker and Robinson (1983)
øa.	Controlled stress release in ex- casation or sup- port application.	a sharty, bentonite a shield on hydroshield 2 Earth pressure bal- a noc shield. 3 High demaity shurry- shield shield 4 Extruded shield	Allows excavation or sup- port installation under adinticed in situ stress release; reduces shear in ground mass.	Reduce ground displacements and increases ground stability.	Presently used in TBM schemes only. Can induce ground heave, including B4.	Bi: Watanabe (1984); B2; Clough et al (1983); B3; Sasanabe et al (1986); Matauxaki et al (1986); B4; Novak (1984); Babendererde (1986);
U	C Presupport Techniques	Continuous steel pipe forepoling 2 De grouting forepoling 3 Prench awa 4 Blade shield 5 Marche-avant	Allows excavation under protection of pre- intealled aupport or linings may reduce in eitu extrema release if pre- support is stiff enough.	Improve local ground stability and possibly global stability, ground displacement control may be marginal.	Global stability only with long forepoling.	Cir Mihiwaki (1984); C2: Lunardi et al (1986). C4: Gruner (1918), C5: Lunardi and Louis (1984).
۵	Groundwater control techniques	1 External or internal dewatering 2 Compressed air 3 Chemical coating	Minimize or eliminate ground water flow, or its consequence, may increase soil strength.	Improve either local or global stability of the ground, reduce fish of piping or 'flowing' ground condition.	May increase ground displacements by drainage and consolidation (01 and b2) D3 currently used with shotcrete support also.	Dir Krischke and Weber (1981) D2: Strobl (1986), Yoshida et al (1986), D3: Horiuchi et al (1986)
LI .	Ground Improvement Techniques	2 Replacement grouting 2 Replacement grouting 3 Compaction grouting 4 'Claquage' grouting 5 Freezing	Increase ground mass strength, reduce its de- formability, and possibly its permeability.	Improve global and local atability. Reduce settlements. May improve groundwater control.	Hay induce ground heave, Ez refers to techniques in which soil is mixed in place by hydraulic or mechanical action with auupension groutes Settlement is balanced by heave in El, if per- formed simultaneously to tunnel advence.	And an and clough (1980), Gasters et al (1986), Highlacci et al (1986), Elleges and Baker (1984), Baker et al (1983), Ed. (1981) et al (1982), Es'recer a Garbe (1980), Hettier (1979) Schmid (1981).
6.	F Exclusion Tech- niques	1 Slurry trench walling 2 Sheet pile walling 3 Tangent pile walling	Confine unstable zone, limiting extension of subsiding ground zone; may reduce hydraulic gradients.	Protect naighbouring articutes against ex- cessive vertical move- ments.	Hovements above tunnel not prevented but increased amount of lateral ground movement will depend on flexural rigidity of walls if may not be appreciably reduced.	F1 and F2: Hanya (1981).

Table 4.3 Reported Ground Control Procedures in Soil Tunnelling

procedures developed in the recent decades as well as older methods that are often used in present days.

4.3.2 Prediction of Lining Loads

4.3.2.1 Classification of Methods

Once the lining type has been selected and its dimensions preliminarly defined'°, the internal lining forces have to be calculated, in order assess the lining capacity. These loads can be calculated using a variety of methods which can be classified in one of the five main groups shown in Figure 4.2. The terminology adopted is fairly commonly used, but for clarity some explanations will be presented in the following sections.

It is clear from the discussions presented in Chapter 2, particularly in Sections 2.3.5 and 2.3.6, that all models used for predicting lining loads are to some extent an approximation of the prototype. Maffei (1982) thoroughly discussed this aspect and classified the available methods which take into account the ground-lining interaction, into two groups: those in which the ground loads onto the lining are imposed and those in which lining loads result from the stress redistribution upon the stress release representing tunnel excavation. It is believed that this distinction may

[&]quot;" This is basically done on the basis of functional or construction impositions: minimum clearance of concrete forms for cast-in-place linings, minimum thickness of concrete segments allowing handling and complying joints, design requirements, minimum thickness imposed by standards and code provisions, etc.

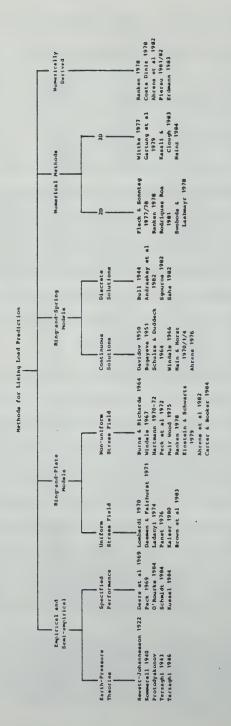


Figure 4.2 Classification of Some Typical Examples of

Methods for Lining Load Prediction

be too subtle for practical purposes, since a particular method can belong to any of the two classes, depending on the way the structural system is loaded. The purpose of the classification is, therefore, not fulfilled. Moreover, it may be argued that the stress release representing the excavation, as it is performed in a number of numerical simulations, may be understood also as an imposed loading condition. Maffei's classification identifies the types of load onto the lining-ground system (gravity load versus actual excavation loading), but does not classify the methods of calculation according to the grounds on which they are based. The latter approach was favoured by Katzenbach (1981:14) and it is followed here in a different form.

4.3.2.2 Empirical and Semi-Empirical Methods

These are methods based on observations of successfully completed tunnel supports or simply based on past experience. Some of them were developed using less simple theoretical frameworks. Nevertheless, they tend to include a considerable amount of empiricism in their assumptions. As discussed in Section 1.1, these methods include an unknown, but normally wide, margin of safety. Sometimes, if the range of cases or situations used as a basis for its development was limited, or it was developed for a particular site and construction technology, and then applied to a different scenario, it may furnish an unsafe design.

These methods can be divided into two sub-groups: the earth pressure theories and the methods in which the lining performance is determined beforehand.

Earth Pressure Theories

The earth pressure theories normally provide ground pressure envelopes (reduced overburden criteria) to be applied to the lining, from which the internal support forces can be calculated, using known solutions from structural analysis (for a monolithic ring sections, see Szechy (1967:343) for a summary of these solutions). It is a common assumption in almost all these methods that the earth pressure loads are independent of the ground displacements, and that the support is not embedded in the soil. The soil is assumed to be acting only as a source of load. By neglecting the ground-lining interaction, a conservative lining design is attained. However, the displacement independent earth pressure load assumption may or may not lead to a conservative lining design.

It seems that the above assumptions correspond to conditions of poor ground control, represented by a poor lining contact with the soil and by a large degree of "ground loosening". These features were discussed in Section 2.3.5. These conditions are hardly acceptable in normal practice nowadays, but could represent a common situation in the past, when most of these methods were developed. The Hewett-Johannesson (1922) method can be pointed out as a singular departure from this rule, as it

suggests that the horizontal earth pressures should be selected appropriately, between the active and passive extreme cases. This is an attempt to define ground loads which are compatible with the deformantion mode of the lining. However, this merit is obliberated by several weak points and inconsistencies (the assumption of a rigid lining as opposed to the acceptance of different modes of lining deformation, is one of them).

Some earth pressure methods are based on soil arching or silo theories, for example Terzaghi (1943). The assumption in shallow tunnels of vertical shear failure planes reaching the ground surface with full shear strength mobilization, reveals, once more, conditions of poor ground control, and large ground displacements.

Newmark (1964:14) studying the design of underground protective construction under the effect of a pressure pulse at surface, suggested that pressure attenuation with depth could be estimated taking into consideration the ground arching effect which may be present if the construction roof yields. He recognized, however, that the degree of arching would vary with the amount of roof deformation. Therefore, he modified Terzaghi's theory in order to include the deformation but neglected the soil self weight.

As an academic exercise, the writer followed the same reasoning for the case of a yielding roof, including the soil self weight and both the cohesive and frictional components of strength. Shear stress along the vertical

shear planes was assumed to be linearly proportional to the displacements. The distribution of the vertical displacement of the yielding soil cover was assumed to be a known exponential curve. With these assumptions, Terzaghi's arching theory was re-derived and the solution of the equilibrium differential equation furnished a relationship between the pressure over the support and the displacement profile above it. The rather lengthy expression included terms that required numerical integration. This approach could explain, at least qualitatively, ground pressure development in excess of those provided by Terzaghi's original theory, whenever soil shear strength is only partly mobilized. However, it can not fully explain the development of pressures smaller than Terzaghi's, as noted by Ladanyi and Hoyaux (1969:12) in trap-door experiments, and by Gais et.al., (1986:61) in the Munich Subway. The reason for this lies on the assumptions made. It was accepted that the shear transfer mechanism develops only along the vertical shear planes, which were assumed to be fully developed at the onset before any displacement occurs. The solutions would be correct if these failure planes existed as pre-sheared surfaces. However, this is not true, since they are progressively formed as a result of ground deformations as the soil goes towards collapse. A more likely interpretation of pressure development with soil displacement was presented in Section 3.2.3.

In its original version, Terzaghi's arching theory may be said to approximate a near collapse situation and possibly be represented by point G" in the schematic ground reaction curve shown in Figure 3.8. Therefore, for good control conditions, represented by the portion BC of that curve, (in which the failure planes are not fully developed), Terzaghi's theory would furnish ground loads either above or below the actual equilibrium load.

Therefore, it can provide either a safe or unsafe estimate of loads, depending on the magnitude of the displacements occurring in the field. This was also noted by Wong (1986:232).

Table 4.4 presents a brief summary of some earth pressure theories. Some of them were originally developed for rock masses but include soil tunnels as special cases. Other methods were included for their historical significance and some for their popularity among designers. A few illustrative comments are added as well as indications of works where some of these methods were extensively reviewed, notably Szechy (1967), Deere et.al., (1969) and Steiner and Einstein (1980). The use of these earth pressure theories seems to be diminishing in practice, in favour of methods that include the lining-ground interaction and that the acknowledgement that loads are displacement dependent. However, they can still provide useful guidance once they are calibrated with field data from a particular site and for a specific construction technique. Under these

Survey
A Partial
Theories:
Pressure
Ground
4.4
Table

Review	In (1):211 in (2):37	In (1):211	In (1):209 and In (2):45	ests In (2):75	In (1):356 and in (3):34	In (1):213	In (2):53 and In (3):44	In (2):70	roof in (1):206 and in (3): IV-17	(3) Dearm at al (1969)
Comments	Only 'gravity' loads, for deep tunnels; first method for lining load assessment	Derived from experiments in dry sand	Only 'loosening' loads, for shallow tunnels; loads directly related to the amount of crown settlement	Based on observations in timber supports and in tests on timber blocks; observational approach	Developed for shielded tunnels; first approximate attempt to account for soil-lining interaction	Parabolic shaped dead load over support; deep tunnel assumption; very used in Soviet Union	"Rock Load Theory", based on Kommerell's and Blerbaumer's data	Developed for timber supported tunnels; similar to Terzaghi (1946)	Actually a method for stability analysis; based on Kotter's differential equation; valid for flat roof	1) Chainer and Pinobelin (1980).
Author	Ritter (1879)	Forchheimer (1882)	Kommerell (1912, 1940)	Bierbaumer (1913)	Rewett-Johnannesson (1922)	Protodyakonov	Terzaghi (1943)	Stini (1950)	Balla (1963)	. (1901)

conditions, they can be used to extrapolate experience within that site and for that particular method of construction, but they may furnish incorrect load predictions if used outside the framework in which they were developed.

Methods that Specify Tunnel Performance

The second subgroup includes methods in which the lining performance is specified beforehand, and they represent an improvement over to the former methods. Here the lining flexibility is taken in consideration, as opposed to using the rigid lining concept suggested by the others. This more recent design approach is based on the concept of the "ideal lining" put forward by many modern tunnelers, notably Peck (1969). The lining is represented by a ring which is very rigid in uniform compression and very flexible upon bending. It is consistent with modern design trends that lead to negligible bending moments under limited ground losses.

Different versions of this design approach have been presented by different American designers, including Deere et.al. (1969:95), Peck (1969:257), Peck et.al. (1972:266), O'Rourke et.al. (1984), Schmidt (1984), and Kuesel (1986), among others. This approach, which in reality is a criterion that goes beyond the prediction of lining loads, can be briefly stated as: "Flexible circular tunnel linings should be designed for a uniform ring compression, corresponding to the overburden pressure at the springline, plus an arbitrary

imposed distortion measured as a percentage change in radius" (Kuesel, 1986:6). The full overburden assumption proposed by Peck (1969) resulted from his interpretation of field data and was critically reviewed in Section 3.3.3.3 as generally being a conservative design assumption. Clough and Schmidt (1981:615) contend that it is a fair assumption but they do not provide factual evidence supporting it. Schmidt (1984) extended Peck's recommendation regarding the imposed distortion for design verification, and put forward ultimate lining distortion ranges for different soil types (see Table 4.5). These recommended values were derived from field observations and are to be used for design, although higher distortion values have already been reported under extreme circumstances. For example, Schmitter and Moreno (1983:406) report total diameter changes as much as 6% in the precast segmented lining used in a Mexico City tunnel, without support collapse.

The maximum bending moments resulting from these imposed lining distortions can be calculated from elastic beam theory (Morgan, 1961:41, Deere et.al., 1969:99 or Craig and Muir Wood, 1978:190):

$$M_{\text{max}} = 3 \text{ E I } \frac{\Delta R}{R^2}$$

According to this empirical approach, the relevant point is to ensure that the anticipated distortions are acceptable in terms of the serviceability of the lining (offset and water leakage aspects, mainly). This attitude results from the fact that in most soils, if a good

Soil Type	Ultimate Range		
Stiff to hard clay (OF < 2.5 - 3)	0.15	-	0.40
Soft clays or silts (OF > 2.5 - 3)	0.25	-	0.75
Dense or cohesive sands, most residual soils	0.05	-	0.25
Loose sands	0.10	000	0.35

Notes:

- (1) Add 0.1 0.3% for tunnels in compressed air, depending on air pressure.
- (2) Add appropriate distortion for external effects such as passing neighbouring tunnels.
- (3) Values assume reasonable care in construction, and standard excavation and lining methods.

Table 4.5 Recommended Lining Distortion Ratios for Design Verification (after Schmidt, 1984: modified)

lining-ground contact is ensured, the displacements needed to mobilize appreciable passive resistance in the soil are small compared to the lining's capacity for distortions. Field data reveals that even in soft soils, diameter changes of less than 1% in a flexible lining are entirely resisted by the mobilized shear stress in the soil (O'Rourke et.al., 1984:16).

In addition to the above requirements, the approach requires adequate consideration of the possibility of buckling. Peck et.al. (1972:267) suggested that in soft clays, the overburden stress should be

$$\gamma z < \frac{3E_sI_s}{R^3}$$

for buckling to be prevented.

As noted by Craig and Muir Wood (1978:197), this criterion is more conservative than Morgan's (1961:45) lining collapse pressure, p, given by:

$$p = \frac{3E_sI_s}{R^3} + \frac{E}{1+\nu}$$

where E and ν are the elastic constants of the soil.

Deere et.al., (1969:50) present another simple and partly empirical equation for assessment of the buckling of a thin walled cylinder embedded in soil, represented by a coefficient of radial ground reaction, C. The uniform all-round pressure causing instability is given by:

$$p = 2 \sqrt{\frac{C E_s I_s}{R^3}}$$

All three equations above are conservative for a uniform lining load, but they are not strictly valid for non-uniform loading conditions. They can provide an unsafe

estimate of lining buckling if the ground-lining contact is poor (Deere et.al., Op.cit.:51), with local concentrations of ground loads. Otherwise, they show that buckling of usual lining systems due to external pressures is very unlikely for customary tunnel depths and tunnel sizes. Buckling becomes a matter of concern when the lining is very thin or when the external pressures are significant, such as in the case of high water heads in undersea tunnels.

Some weak points are apparent in this empirical approach of lining design. The assumption of uniform ring compression is not consistent with the need to account for distortional bending. Also the full overburden assumption is debatable, particularly when considering that the approach is valid for good lining contact and good ground control conditions. Nevertheless, this empirical method is very useful for a preliminary dimensioning of the lining, which requires a more detailed design analysis afterwards.

Finally, it should be noted that the above empirical methods could be used together with the observational method, as described by Peck (1969). This could form a third empirical group besides these two already described. Steiner and Einstein (1980:311-380) call this group, the "Empirical Observational Methods", and discuss their potential use in rock tunnelling. Their methodology and ideas could be extended specifically for soil tunnelling.

4.3.2.3 Ring and Plate Models

These are mainly analytical models in which the ground is represented by a plate and the support of a circular opening, corresponding to the tunnel excavation, is represented by a continuous ring. Both ring and plate are assumed to be in a state of plane strain, depicting a cross section of the tunnel far from the advancing face and unaffected by the three-dimensional stress transfer process. Solutions developed by these models are based on continuum mechanics approaches and most of them are of the closed form style, therefore very easy to handle. Without any exception, existing solutions assume the plate to be of infinite extent and therefore it is accepted that the presence of a stress free ground surface does not influence the analysis. With respect to the lining and its interaction with the ground, it was shown (Section 2.2) that the presence of the ground surface has negligible influence, if the cover to diameter ratio (H/D) is greater than 1.5. Therefore, the infinite plate is not a restrictive assumption for tunnels with ground cover of not shallower than 1.5 diameters. However, neglecting the gravitational stress gradients, as most models of this group do, is a more restrictive assumption, since most cases encountered in practice present a cover to diameter ratio for which the effect of these gradients is not small.

The ring and plate models are divided into two categories, according to whether the type of in situ

stress field which they assume is uniform or non-uniform. The former subgroup includes mostly analytical models which are axi-symmetrically solved as a result of the geometric, the stress state and the material symmetries. The latter include solutions in which the distortional component of the initial stress state is present or in which stress non-uniformity is simply caused by the action of gravity. Therefore, the solutions take advantage of, at least one plane of symmetry, and usually two.

Uniform Stress Field Solutions

These solutions are collectively included in the so called 'convergence-confinement' models. As explained in Section 2.3.5 they are only applicable to the ideal deep tunnel case with K equal to unity. By virtue of this fact, the equilibrium between the ground and the lining can be assessed by solving a set of two equations. One represents the ground reaction in terms of radial stress and displacement at the tunnel wall and the other represents the support reaction in terms of the same variables. The particular state of stress assumed and the assumption of isotropy ensures that the two functions describing the ground and support reactions can be independently assessed. The evaluation of the interaction process is greatly simplified since no distortion of the lining occurs under these conditions.

The overall simplicity of the problem allowed the introduction of relatively complex constitutive

relationships for evaluation of the ground response, including different stress-strain models, yield criteria and volume change hypotheses. An excellent review of the subject was presented by Brown et.al. (1983). As for the support response, available solutions treat it as a linear elastic material, and they are presented by Daemen (1975) and reviewed by Hoek and Brown (1980).

The capability of the available solutions to model complex ground responses, include for instance, elastic-brittle plastic behaviour, non-linearity of stress-strength criteria, accounting for short and long term strength, rate dependent strength and stiffness, and associated and non-associated flow rules for the treatment of volumetric strains. Despite this, the assumption of a uniform stress field seems to be excessively restrictive when one is dealing with shallow tunnel design. If applied to a non-uniform in situ stress condition, the convergence-confinement method will only provide the ground and support responses in terms of average stress and displacement since the distortional component of the stresses are not considered. It will furnish indications of the mean ground pressure or mean lining thrust and mean ground losses at equilibrium, which may be of some help for a qualitative design estimate. However, the impossibility of assessing the development of lining bending is a crucial limitation of this approach. Perhaps this is one of the reasons why practitioners seldom use this method for shallow tunnel design. Past and recent attempts to generalize the model to non-uniform stress field (e.g. Kastner, 1949, or Detournay and Fairhurst, 1982) were limited to the evaluation of the ground response. The interaction with the support system was still neglected.

For a proper assessment of the equilibrium between lining and soil, an independent evaluation of the ground response before lining activation is required. This class of solutions cannot provide the tools for this task.

The applicability of the convergence-confinement method to the design of shallow tunnels was objectively undertaken by Branco and Eisenstein (1985). This was done by comparing predictions by this method with field measurements from two tunnels driven through Edmonton Till, one with H/D equal to 1.4 and the other equal to about 10. In both cases, K was close to unity, and the effect of the gravitational stress gradient was present in both, obviously more so in the shallower case. These authors used Kaiser's (1980) formulation for the ground response. The results they obtained showed poor agreement for the shallower tunnel, and better but not fully satifactory agreement for the deep tunnel, even when the displacements developed before lining installation (as measured in the field) were accounted for. They attributed the discrepancies to the non-axisymmetric mode of deformation noted in both cases prior to lining activation, which was due to the presence of the free ground surface and to the effect of the gravitational stress field.

In both cases, the in situ stress field was non-uniform, despite the stress ratio being close to unity. Available solutions do not account adequately for this stress field non-uniformity and even when the stress and displacement developments prior to lining installation are properly accounted for, the method does not provide satisfactory predictions. These facts, as well as others addressed in the conference "Analysis of Tunnel Stability by

Convergence-Confinement Method" of the Association Francaise des Travaux en Souterrain (Paris, 1978) '' make this approach not fully applicable for the design of linings of shallow tunnels. Nevertheless, Figure 4.2 provides references to some representative solutions among this group.

Non-Uniform Stress Field Solutions

These are solutions in which the in situ stress non-uniformity is due to the stress ratio, K, being not equal to unity or due to gravitational stresses. Most of them were surveyed by a number of authors, to variable degrees of detail, and therefore, another review would simply be redundant. A summary of the most representative review works on the subject, presented over the last two decades, is presented in Table 4.6. As indicated, the methods reviewed include not only the ring and plate solutions but also ring and spring models, which will be discussed in the next section. Apart from the reference to

^{&#}x27;' English translation: In Underground Space, Volume. 4, No. 4, 5 and 6, Pergamon Press, 1980.

the methods reviewed by each review author, the table indicates the availability of comparisons of results provided by those methods. These are provided by some authors in terms of dimensionless moment or thrust coefficients as a function of the lining's flexibility and compressibility ratios. Finally the table has a few comments providing the main issues focussed by each review work.

Among these review works, that by Katzenbach (1981) is referred to as one of the most comprehensive register of methods available. Another notable work is that by Erdmann (1983), who provides one the best assessments of each method reviewed, including the basis of their derivation, assumptions used and furthermore, a detailed comparison of results obtainable by those methods. Part of his original work, written in German, was summarized in English by Duddeck and Erdmann (1982), Erdmann and Duddeck (1983) and Duddeck and Erdmann (1985). Also worth mentioning is the work by Ranken (1978), who provided perhaps the most detailed assessment of the assumptions used for the development of ring in a plate solutions (external and excavation loading, ground-lining interface hypothesis, thin and thick lining assumptions, effect of tunnel depth, etc.).

Despite all these review works, it was decided to prepare a summary table, in which the important assumptions of each ring and plate derivation could be easily assessed and compared. Table 4.7 includes most of the closed form analytical solutions developed over the last quarter

Review Author	Methods Reviewed Co	Comparison of Results	Comments
1. Szechy (1967)	Zuraboy and Bougayeva (1962) ² ; Bodrov-Gorelik ² , Polygona) Hethod'; Davidov (1950) ² ; Varga (1961) ² ; Meissner (1964) ² ; Orlov (1954) ² ; Rozas and Kovaca	X X	Mostly methods used in eastern countries; worked example provided. Only qualitative comparisons between methods available.
2. Duddeck (1972)	Rosza (1963) ² , Schulze and Duddęck (1964) ² ; Bougayeva (1951) ² , Voellmy (1937) _I Windels (1967) ; Morgan (1961) ² , Helsaner (1963) ; Durth (1969) ² ; Windelm (1966) ²	«	Comparison of ring-spring and ring-plate solutions, assessment of 2nd order effects. Bending moments and thrust forces compared.
3. Duddeck (1973)	Morgan (1961) 1_1 Schulze and Duddeck (1964) 2_1 Windels (1966) 2_1 Windels (1967) 1_1 Hein (1970) 1_1 Hein and Horet (1979) 2	«	Comparison of bending moments methods developed mainly by German authors.
4. Mohraz et al (1975)	Burns and Richard (1964) ¹ , Hoog (1968) ¹ , Peck et al (1972) ¹	. «	Assessment of effects of loading assumptions: external, excavation and gravity loadings. Solution for last two types SAP F.E. program. Methods developed by American authors.
5. Craig & Muir Wood (1978)	 Craig & Muir Wood (1978) Morgan (1961) 1 Muir Wood (1975) 1 Curtis (1976) 1 Schulze and Duddeck (1964) 2 Curtis (1974) 	KA A	Only qualitative comparison between methods. Emphasis on British methods compared to others.
6. Ebaid & Hammad (1978)	Davidov (1950) ² ; gngelbreth (1961) ¹ ; Zurabov & Bougayeva (1962) ² ; Peck et al (1972); Mulr Wood (1975) ¹ ; Curtle (1976)	٧ .	Quantitative comparison of bending moments provided by methods reviewed.
7. Ranken (1978)	Morgan (1961) , Mulr Wood (1975) ¹ , Curtis (1976) ¹ , Burns and Richard (1964) , Dar and Bates (1974) ¹ , Roeg (1968) ¹ Peck et al (1972) ¹ , Ranken (1978) ²	<	Quantitative assessment of effects of lining loading assumption. External and excavation loading analytical solutions compared. Comparison with FE solutions. Gravity loading case studied through numerical simulation.
8. Katzenbach (1981)	Voellmy (1937) Morgan (1961) Engelbreth (1961) Heisaner (1963) Mindela [1967] Harbaann (1970-1972) Schulze and Duddeck (1964) Mindela (1966) Hain (1968) Hain and Horst (1970, 1971, 1974)	¥ X	Mainly a comprehensive register of methods within a classification system.

Table 4.6 Some Review Works on Ring and Plate or Ring and Spring Models for Design of Linings Under Non-Uniform

Stress Fields

Review Author	10r	Metho	Methods Reviewed	Comparison of Results	Commente
9. ¹ Duddeck	9. Duddeck & Erdmann (1982)		Schmid (1926), Voellmy (1937), Engelbreth (1961), Horgan (1961), Schulze and Duddeck (1964), Windels (1966), Hujr Wood (1975), Curtin (1976), Einstein and Schwartz (1979), Ahrens et al (1982)	4	Review provides quantitative comparison of results provided by most methods reviewed, in terms of thrust forces and bending moments.
10. Erdmann	10. Erdmann & Duddeck (1981) As No. 9	3) As No. 9		«	A slightly more detailed review than the above, extending the assessment of effects of the no-slip and full-slip assumptions on lining loads.
11. Paul et al (1983)	al (1983)	Ranken et al (1978) Richarda (1964) i E Morgan (1961) i Mul	Ranken et al (1978) i Einstein et al (1980) i Burns qud Richards (1964) i Dar and Bates (1974) i Hoeg (1968) i Morgan (1961) i Mult Wood (1975) i Curtle (1976) i Peck et al (1972)	NA (1972)	A brist review of closed form solutions of 'hole-in-a-plate' type developed in english-speaking countries.
12. Erdmann (1983)	(1983)	Schmid (1926), Vos Schulze and Dyddeck Horgan (1961), Hyl Engelbreth (1961), Durth (1969), Hain	Schmid (1926)], Voellmy (1917) ¹ , Ahrena et al (1982) ¹ , Schuize and Dyddeck (1964) ² , Wingela (1966) ² , Curtis (1974) ¹ , Morgan (1961) ² , Apix Wood (1975), Wingela (1967) ² , Engelbreth (1964) ² , Peck et al (1972) ² , Binstein & Schwagtz (1979) ³ , Durth (1969) ² , Hain & Horst (1970, 1971) ² , Ahrena (1976) ²	A (979)	Most comprehensive review, including discussion on assumptions of each method, summary of equations and comparison of results given by most methods.
13. O'Rourke (1984)	e (1984)	Peck et al (1972) 's Schwartz & Eingtein Richard (1964) ', Ho	Peck et al (1972) ¹) Mult Mgod (1975) ¹ , Ranken et al (1978) ¹ ; Schwartz & Eingtein (1980) ¹ , Ourtis (1976) ¹ , Burng & Richard (1964) ¹ , Hoeg (1968) ¹ , Dar & Bates (1974)	ž	A brief historical review of some closed form solutions developed in english-speaking countries.
14. Duddeck (1985) 6. Duddeck & Erdmann	(1985) 6 6 Erdmann (19	Duddeck (1985) 6 The same methods reviewed by C Duddeck & Erdmann (1985) and Erdmann and Duddeck (1983)	The same methods reviewed by Duddeck & Erdmann (1982) and and Erdmann and Duddeck (1983)	*	Combine previous reviews by the same authors; discuss effects of non linearities, of hinges in precast linings segments, use of methods reviewed for shield tunnelling and NATM.
Notes: 1:		Ring-and-Plate solutions.			
2;		Ring-and-Spring solutions			
Α:		Available in the review			
NAN	Not availab	NA: Not available in the review			

Table 4.6 Some Review Works on Ring and Plate or Ring

and Spring Models for Design of Linings Under Non-Uniform

Stress Fields (Continued).

century. All solutions were derived assuming a plane strain condition and also that the lining is installed in close contact with the surrounding ground prior to any displacement development. Recognizing that this latter assumption can hardly be a reasonable approximation of the reality, some authors put forward approximate correction factors to account for the ground stress release caused by the delayed installation of the lining. Hartmann (1972:43) discusses stress reduction factors that would be pplied either to the specific weight of the ground or to the depth of the tunnel (the distinction between the two approaches is subtle as his solution accounts for gravity). According to this author, these factors would be empirically evaluated from field measurements. Muir Wood (1975:124) proposed an arbritary reduction of 50% of the in situ stresses on account of the delayed lining installation. Schwartz and Einstein (1980:75) suggested correction factors, derived from axisymmetric finite element analyses, to be applied to the calculated thrust or moments. Hutchinson (1982:175) questioned the criteria provided by Schwartz and Einstein, and proposed a reviewed procedure for the factor which is applied to the lining thrust.

Moreover, all solutions included in Table 4.7 assume both lining and ground to be linear elastic, homogeneous and isotropic materials. Most of them consider an "excavation loading" condition as opposed to a few that adopt an "external overpressure loading" condition. The latter

Special Features and Comments	Assume elliptical mode of deformation. Initial atress distribution incompatible with slippage condition. Only distortional component of atress is considered. Error in plane atrain assumption (corrected by M. Wood, 1975).	Developed for analysis of buried structure subjected to overpressure. Use extensional shell theory to model liner.	Include second order effects (genmet- ital non-linesity). Approximate ac- count of deviations of lining section from ideal circle during assemblage.	Full alip solution is incorrect (Ranken, 1998).20 and Echastz and Einstein, 1980:18). Solution was later corrected by Ranken, 1978.	Include second order effects (geometrical non-linearily). Uses Flugge cylindrical shell theory to model liner.	Developed from Burns and Richards (1964) solution.	Lining is represented by a thick elastic cylinder.	Elliptical mode of deformation. Include both uniform and districtional erress components but initial stress distribution not compactible with alippage condition. Approximations for partial allip, for stress release prior to liner installation and for effect of lining joints in flexibility.
Lining Lining Thickness Compressibility	Incompressible	Compressible	Incompressible	Compressible	Compressible	Compressible	Compressible	Incompressible
Lining	Thin	Thin	Thin	Thin	Thin	Thin	Thick	Thin
Lining-Ground Interface	Full alip	Both no and full slip	Both no and full slip	Both no and full slip	Both no and full slip	Full slip	No slip	Full slipp
Account For Gravity	o Z	N O	O Z	No	× 0	ON.	No	Ş
In Situ Stress Ratio (K)	Any	٧/(١-٧)	Any	Any	Any	Any	v/(1-v)	Any
Loading	Excavation	External overpressure	Excavation	External overpressure	Excavation and external overpressure	External	External overpressure	Excavat lon
Year	1961	1964	1967	1968	1970-72	1972	1974	1975
Author	Morgan	Burns & Richards	Windels	Hoeg	Hartmann	Peck, Hendron and Mohraz	Dar and Bates	Mulf Wood
	-	~	М	*	S	φ	7	0

Table 4.7 Assumptions and Features of some Ring and Plate

Solutions for Non-Uniform Stress Field

Special Peatures and Comments	Correct account of the distortional in attu stress component for full allp. His solution to be superisposed to Muir Wood's for the uniform component to get complete solution. Approximation for partial allp. Treatment of soil creep through visco-electicity.	Most complete set of solutions for 8 conditions of a deep tunnel, including second order effects.	Uses Flugge's shell theory to model liner but neglect second order effects.	Same derivation of Einstein and Schwartz, 1979. Include approximate account of delayed lining installation (corrected by Mutchinson, 1821/15) and of ground yielding.	Uses Flugge's Shell Theory to model liner. Parametric analyses presented by Erdann (1981:78). Include second order effects.	Uses cylindrical shell theory to model liner. Include coupled analysis of elastic consolidation, assuming impermeable lining. Solution obtained by nonerical integeration (not analytical). Results presented in graphs.
Lining Lining Thickness Compressibility	Incompressible	Compressible	Compressible	Compressible	Compressible	Compressible
Lining Thickness C	Thin	Thin and thick	Thin	# Pink	Thin	Thin
Lining-Ground Interface	Both no and full alip	Both no and full alip	Both no and full alip	Both no and full alip	Both no and full alip	Both no and full alip
Account For Gravity	Š	ON	8	2	Pertly	Q.
In Situ Stress Ratio (K)	Any	Any	Any	Any	Any	Any
Loading Ir	Excavation	Excavation and external over-	Excavation	Excavation	Excavation	Excavation
Year	1974-76	1978	1979	1980	1982	1984
Author	Curtie	10 Ranken	11 Einstein and Schwartz	12 Schwartz and Einstein	13 Ahrens, Lindner and Lux	14 Carter and Booker
1	oi	-	-	+	-	-

Table 4.7 Assumptions and Features of some Ring and Plate

Solutions for Non-Uniform Stress Field (Continued).

implies that the opening has been excavated and supported before the stress field is applied to the plate and could represent the case of a backfilled culvert. The lining acts as a "rigid inclusion" in the perforated plate and therefore thrusts, bending moments and lining displacements are overestimated, when compared to the "excavation loading" solutions in which the opening is excavated and supported after the stress field is applied to the plate. This latter condition more approximately represents the real tunnel situation. Differences in thrust and displacement calculated with the two loading assumptions, are more pronounced than the differences in moment or shear, but they tend to decrease as the relative stiffness of the lining to the ground decreases (Mohraz et.al., 1975:137, Einstein and Schwartz, 1979:508).

Most solutions take the field stress ratio is an independent variable but two of them, define it as a function of Poisson's ratio. All solutions, but one, do not account for the gravitational in situ stress field in the infinite plate and so treat the problem as an ideally deep tunnel. As pointed out previously, while the effect of the stress free ground surface can be accepted as negligible for H/D greater than 1.5, the influence of gravity cannot be neglected in the interaction analysis between ground and lining for most shallow tunnels.

The method by Ahrens et.al., (1982:268) is, in essence, a deep tunnel solution, since it neglects the in situ stress

gradient across the opening. However, to account partly for the effect of gravity, the uniform vertical stress field is taken as the in situ vertical stress at the crown elevation, γH , and the uniform horizontal stress field is taken as the in situ horizontal stress at the springline elevation, $K_{\rm o}\gamma (H+R)$. Consequently, the results become dependent not only on the absolute tunnel depth, H, as in other deep tunnel solutions, but also on the relative depth of the tunnel, H/D. Erdmann (1983:78) later explored this method, reducing it to an actual deep tunnel solution by making the ratio H/D equal to infinity. The only method that takes the action of gravity fully into consideration (including the heave caused by the unequal vertical stresses) is that by Hartmann (1970,1972).

The majority of the solutions consider both the case of full and no slip conditions at the ground-liner interface and assume the lining to be a thin membrane whose behaviour is approximated by thin shell theory. Only these solutions by Dar and Bates and by Ranken are entirely based on the theory of elasticity (thick lining solutions). Despite both types of solutions being applicable to linings of any thickness, rigorously only those assuming the lining to be thick, are strictly correct for all lining thicknesses. However, as noted by Ranken, (1978:312), provided the ratio of lining thickness to the mean lining radius is smaller than 0.1, the two solutions furnish essentially the same results. The preference for the thin lining appproach is due

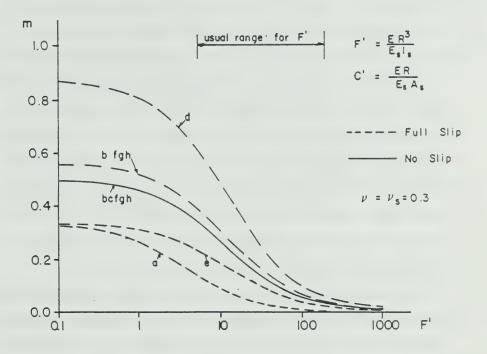
to its easier manipulation in practice as opposed to the thick liner solutions which result in cumbersome equations. Some of the solutions assume the liner to be incompressible or inextensible under thrust (compressibility ratio, C, equal to zero), despite being responsive to distortion or bending (finite flexibility ratio, F). All solutions were analytically derived, and except for one, they are presented in closed-form. The exception is the Carter and Booker (1984) method where a numerical integration is required to obtain an explicit solution which is presented in charts. All solutions neglect geometric non-linearity except for those by Windel, Hartmann, Ranken and Ahrens. These four were developed using second order theory and therefore they furnish, for instance, slightly different bending moments. The second order moments arise from differences in the internal and external liner radii, even for a uniform stress field. However, as noted by Schwartz and Einstein (1980:367), these second order terms are of small magnitude for usual lining thicknesses and therefore could be neglected for all practical purposes.

Except for solutions by Morgan (1961) and Muir Wood (1975) (which included some inaccuracies in their derivations, later amended by others, see Table 4.7), the external loading solutions for deep tunnels (solution by Peck et.al. therefore excluded), furnish almost the same values for thrust forces and bending moments. Figure 4.3, which includes part of Erdmann's (1983) data, illustrates

this point and shows that bending moments from those solutions essentially coincide within the usual range of relative stiffnesses found in practice. Similar results are found regarding thrust forces (Erdmann, Op.cit.:111,112).

The most complete set of solutions for the deep tunnel situation is that provided by Ranken (1978), who corrected and further developed previous closed form solutions. The most useful solution regarding the application to the shallow tunnel case, is that by Hartmann, as it fully accounts for the action of gravity. It is very suprising that this solution, which is older than those most frequently used (e.g., Peck et.al., Muir Wood-Curtis, Einstein and Schwartz) is rarely referenced in the literature. Even in West Germany, where his method was published, no reference was made to it except a simple mention in Katzenbach's (1981:122) survey, without any further comments (see Table 4.6). A possible explanation for this solution to have passed unnoticed and not have raised larger interest, is the fact that it has been presented in four separate and lengthy parts between 1970 and 1972, including its very long and complex derivation comprising over three hundred and forty algebraic equations. Notwithstanding this, it is the single most valuable solution of this group for the shallow tunnel problem. The complete solution by Hartmann for the excavation loading will be presented and discussed in other sections of this thesis (Chapter 7).

$$M_{\text{max}} = m \left[\frac{1-K}{2} \cdot \sigma_{\text{V}} \cdot R^2 \right]$$



- l. Legend: a. Morgan (1961), b. Windels (1967), c. Hartmann (1970,1972),
 - d. Peck et al (1972), e. Muir Wood (1975), f. Curtis Muir Wood (1976),
 - g. Einstein and Schwartz (1979), h. Ahrens, Lindner and Lux (1982)

Notes: I. Solutions a,d,e and f assume C^1 equal to zero (incompressible lining). The others (b, c, g and h) were calculated for a virtually incompressible lining with C^1/F equal to 5×10^{-4} .

- 2. Hartmann solution has been reduced here to a deep tunnel situation.
- 3. Maximum bending moment at springline or at crown/floor.

Figure 4.3 Maximum Bending Moment Variation with Flexibility
Ratio for a Deep Tunnel Liner from Different Ring and Plate
Closed Form Solutions

Broadly speaking, one of the major limitations of these solutions is the assumption of a plane strain condition and therefore the inability to account for the inevitable three-dimensional stress transfer associated with the delayed lining installation. If the lining design is understood as an exercise in behaviour prediction, to which some safety criteria is applied, the unavoidable ground stress relaxation taking place before support application cannot be neglected. Available empirical approaches to account for this effect are too arbitrary to be reliable. Some approximate numerical approaches, that will later be reviewed, are more adequate, but still have limitations, such as ideally deep tunnel assumption.

The assumptions of linear elasticity, homogeneity and isotropy are other shortcomings of these methods. One may concede that if the ground-lining contact is good, and if ground control conditions are also good once the support is fully installed, additional ground or lining deformations are likely to be small compared to the movements of the soil occurring before lining installation. Schmidt (1984) noted total lining closures of less that 0.03 to 0.3% of the tunnel diameter after the support was installed). However, the question regarding the "elastic" modulus of the groundto be used in the analysis remains unanswered. Besides the usual heterogeneities in the ground properties and their variation with depth, the stress paths at points around the opening are different (Section 2.3.4.1), and different

stress-strain responses should be anticipated. Even if an initially homogeneous ground condition exists, by the time the support is installed and the interaction with the ground is developed, a non-homogeneous ground condition would have been generated. Prior to lining activation, the soil around the opening would have undergone different degrees of straining, exhibiting stiffnesses which differ from the in situ value (Section 2.3.5.3). It will be seen later in this thesis that the potential of the ring and plate solutions could be improved if an independent procedure is developed to take these effects into consideration.

4.3.2.4 Ring and Spring Models

These are models in which the ground is represented by springs that provide reactions which are displacement dependent (Winkler type of reaction). The lining is depicted by a continuous ring when the ground-spring embedding is also continuous, or by a segmented ring formed by interconnected segments or beams, when the ground-spring embedding is of a discrete type. Accordingly, the solutions are analytically approached by treating the ring as an elastically embedded shell, or numerically approached by treating the liner as a frame which is elastically supported at its nodes. While in the first group, the final solution of the basic differential equation (usually of 4th order on radial displacements) may be obtained either analytically or numerically, the second group requires the solution to be obtained by numerical methods, like finite element analyses.

Figure 4.2 furnishes typical examples of methods of ring and spring type, according to the type of embedding or solution adopted. Like ring and plate solutions, these also assume a plane strain state, and handle non-uniform loading stress conditions.

All methods indicated in Figure 4.2 and others have been surveyed by various authors to a large extent. Therefore, a case by case review of methods will not be attempted herein, but an overall discussion on the assumptions and basic features will be presented. A summary of the most representative review works on the subject is presented in Table 4.6. The table provides an indication of the methods reviewed and the availability of comparisons of results from different approaches which assess the influences of the particular assumptions made. A noteworthy contribution is that by Duddeck and Associates who paid considerable attention to comparative studies between the ring and spring models, mostly developed in West Germany, and ring and plate models, which have been particularly favoured by English speaking authors. Perhaps the most complete review work is that by Erdmann (1983). Besides presenting the bases of the methods they reviewed, a thorough discussion is introduced on the correspondence between ring and spring and ring and plate models (Erdmann Op.cit.:25,90), largely based on the work by Ahrens et.al., $(1982)_{-}$

For the sake of completeness, Table 4.8 has been prepared, with the intent of providing brief indications of the most important assumptions and features of some ring and spring models, which are not always readily recognizable. Although most of the solutions indicated are based on the assumption of continuous subgrade ground reaction and are analytically developed, the discrete ground reaction models using numerical solutions, like the one by Andraskay et.al., (1972), seem to be more popularly used in practice. In the latter, the ground reaction is simulated by beam or spring elements positioned at the nodes of the lining frame. When this simulation is performed and the lining is loaded the liner and springs will deform and both will share parts of the imposed load, according to their relative stiffnesses. Some of the springs will compress, while others will be extended under tension, possibly in the crown region. Some reason that if the latter were to represent the soil, they should not withstand tensile stresses, and therefore they should be removed from the statical system. This arguement is problematical, particularly in the case of a uniformly loaded ring since the same reasoning asks that all springs around it to neglected as they all undergo tension. Some others contend (see Sections 2.2 and 2.3.5.4) that a fully developed failure zone will be generated above the tunnel, confined by two slip surfaces running upwards from the opening and intercepting the ground surface (e.g. Windels, 1966:265). Therefore, the soil above the tunnel crown would

1	Author	Year	Ground	Embeddment	Type of Springs	Loading	Lining Compressibility	Solution Formulation/ Presentation	Special Features and Comments
-	Bull	1944	Discrete	Partial	Radial	Localized (crown)	Compressible	Numerical (programmable)	Iterative solution; computer program developed by Mathia (1974).
2	Davidov (after Szechy, 1967)	1950	Continuous	Completa	Horizontal	Hypothetical all round distribution	Incompressible Closed form	Closed form	Deep tunnel loading. Use equivalent elastic subgrade reaction. Elastic embedding correctly fulfilled at spring-line only.
c	Bugayeva (after Szechy, 1967)		1951 Continuous	Partial (except upper 90°)	Radial	Localized (crown)	Incompressible Closed form with tabulat coefficient	Closed form with tabulated coefficient	Compatibility of displacements at springline and floor only. At other points arbitrary ground reaction.
4	Schulze and Duddeck	1964	1964 Continuous	Partial (except upper 100.)	Radial	Approx. in situ stresses (gravity partly accounted)	Incompressible	Numerical (de- aign charta)	Hay or may not include effect of inter- face shear stresses. Takes radial in situ stress at springline. Assumes equal radial stresses at crown and floor (approx. equal to overburden stress).
w	5 Windels	1966	1966 Continuous	Partial (except upper 90°)	Radial	Approx. in situ stresses (gravity partly accounted)	Incompressible Design charts (iterative procedure)	Design charts (iterative procedure)	May or may not include effect of interface shear stresses. Rad. stress at crown and floor equal to overburden. Partial acc. of geom. non linearity (linearited And order effects acc. to Erdmann, 1981:98). Approx. acc. to pre-activation lining deformations.
٠	6 Hain and Horst	1970	1970 Continuous	Partial (variable)	Radial 6 Tangential	In aitu stresses (gravity included)	Compressible	Numerical (programmable)	Tangential aprings included only in the basic theory, not in the aclution. Include linearised did order effects. Adapted for non circular profiles. Do not account for load changes due to

Table 4.8 Assumptions and Features of some Ring and Spring

Models

Author	Year	Ground	Embedding	Type of Springs	Loading	Lining Compressibility	Solution Formulation/ Presentation	Special Features and Comments
Hain and Horst	1971	1971 Continuous	Partial	Radial	In mitu stresmes (gravity included)	Compressible	Numerical (programmable)	Correct account of load changes due to linking heave. Include geometric non linearity.
Hain and Horst	1974	1974 Continuous	Complete	Radial & Tangential	In situ stresses (gravity included with K = v/(1-v)	Compressible	Numerical (programmable)	Correct account of load changes due to lining heave. Include linestized 2nd order affects and account for pre-activation lining deformations.
Ahrene (after Erdmann, 1983)	1976	1976 Continuous	Partial	Radial 6 Tangential	Radial 6 In attu atreasee Tangential (gravity included)	Compressible	Programmable (iterative procedure)	Tangential aprings included in the basic derivation. Full account of geometric non linearity. Lining with time dependent non linear (plastic) constitutive law.
10 Sgouros Saha	1982	Discrete	Partial (no tenaion radial springs)	Radial 6 Localized Tangential (crown)	Localized (crown)	Compressible	Finite Element	Finite element formulation (three nodes beam element and aprings). Lining with non linear piece wise eleatic representation
11 Andraskay, Hofmann and Jemelka	1972	Discrete	Partial (except upper 90°)	Radial	Reduced in situ atress	Compressible	Computer Program (STRESS)	Computer Program Reduced overburden stress by Voellmy (STRESS) (1933) arching theory.

Table 4.8 Assumptions and Features of some Ring and Spring

Models (Continued).

not be able to withstand any additional shear, and could not provide an embedment to the support ring in that area. Although this is an actual possibility, particularly if ground control conditions are deficient, it is hardly acceptable in a normal urban tunnelling situation since it implies the existance of an extreme collapse condition as a design hypothesis. As discussed in Chapter 2, the magnitude of ground movements are likely to be large for this condition and probably unacceptable in routine urban tunnelling. When ensuring limited and acceptable ground losses by selecting adequate ground control measures, the dimensionless crown displacement (Section 2.3.4.3) is likely to be smaller than that tentatively established for a near collapse condition. Thus, it would be reasonable that the crown embedment can be accounted for in the lining design. Normally the partial embedment assumption leads to more conservative bending moments and thrust forces in the lining.

Except for Ahrens (1976), who assumed a non-linear (plastic) behaviour for the liner, all other solutions assume linear elasticity, both for the lining and the springs. Duddeck and Erdmann (1985:257) showed results of an analysis in which the non-linear constitutive behaviour of a concrete lining was taken into account. While the thrust forces in this analysis were not much changed, the magnitude of the maximum bending moment decreased by about 33%. A safer estimate of lining loads is usually obtained from the

assumption of linear elasticity for the support and this is possibly why this assumption is normally accepted.

This agrees with findings by Paul et.al., (1983:137) who also performed analyses assuming a non-linear behaviour for the concrete lining as discussed earlier. Moreover, these authors showed that, for this sort of lining response, a partial or non-slip condition at the lining-ground interface will furnish lower ultimate (failure) thrust loads than the full slip case (Paul et.al., Op.cit.:87).

Most commonly the embedment is provided for by radial springs only, which would mimic the tangential slip case. Solutions by Schulze and Duddeck (1964) and Windels (1966) may or may not include the shear stresses at the lining-ground interface as active loads into the system. If these stresses are neglected, their solutions correspond to Muir Wood's (1975) original solution (see Table 4.7) and therefore they are formally inaccurate, as they do not take into consideration the deformation components due to the full slippage condition (see Section 2.3.5.2). For a given radial spring constant'2, if tangential springs are also considered in the analysis, a stiffer ground response can be anticipated, which in turn leads to smaller bending moments and thrust forces in the lining. In other words, the assumption of radial springs only, normally leads to a safer

^{&#}x27;2 The spring constant or spring modulus is defined as the stress-displacement ratio at a point of the lining ground interface, in terms of radial or tangential components, with units of force/length's. This terminology will be preferred to the also used terms "Winkler constant" (or modulus) and "ground-reaction constant" (modulus or coefficient).

estimate of lining loads (depending on the assumed value for the spring modulus).

Two main groups of ground load assumptions are identified in Table 4.8. The first refers to a localized gravity loading condition in the crown region only, where the lining is not embedded. This would be the case of a tunnel in a fairly self supporting ground, experiencing loosening that results in localized loads. This corresponds to what has been defined in Section 2.3.5.1 as a "poor lining-ground contact", under conditions of poor ground control. The second refers to an in situ stress load condition, assuming that the lining is installed before any ground stress redistribution occurs. In this case, the loads are not localized but distributed all around the lining perimeter. While most solutions within the second group take full account of the action of gravity (gravitational stress gradient all across the tunnel profile), the methods by Schulze and Duddeck (1964) and Windels (1966) account for the effect of gravity only partly. Similar to the ring and plate solution by Ahrens et.al., (1982), they assume equal active stresses at the crown and floor, therefore avoiding the unbalanced vertical force that would heave a shallow tunnel. The active radial stress at the springline is taken as the in situ horizontal stress at the tunnel axis elevation. However, their different assumptions of interface shear stress results in vertical and horizontal active stress distributions, which are non-uniform but are

symmetric with respect to the vertical and horizontal axes of the tunnel. The approximate account of gravity makes their solution to be dependent on the relative depth of the tunnel.

As discussed in Section 2.2, the coupled assumption of partial embedding and of in situ ground loads (full overburden) is questionable since they are incompatible. If the lack of embedding in the crown region requires the assumption of complete collapse of the tunnel cover and the development of two shear failure planes, running up to the ground surface, then the full overburden load assumption is in conflict. It implies zero shear strength along the two slip surfaces, which is not acceptable as a design assumption for most soil types. In other words, if lining embedding is taken as partial, then for consistency, the ground loads should be represented by a reduced in situ stress resulting from soil cover arching between the two slip surfaces. This is what Andraskay et.al., (1972) assumed in their solution and it is frequently adopted in practice.

Most of the solutions available are not expressed in closed form or in design charts, therefore requiring a small frame computer to be used. To make the solution simpler, the closed form approaches usually assume the lining to be imcompressible in thrust (compressibilty ratio equal to zero). Some of the existing solutions take into consideration the second order effects of the theory of elasticity. This geometric non-linearity is either accounted

for completely (e.g. Ahrens, 1976), including the lining shortening by tangential compression, or partly, when only 2nd order effects due to bending deformation are considered (e.q., Windels, 1966). Schulze and Duddeck's (1964) solution and others disregard these effects, assuming that the lining deformations are small and that equilibrium conditions can be verified in the undeformed lining geometry. However, Duddeck (1973:267) and Duddeck and Erdmann (1985:256), have shown that these assumptions may have some influence on the calculated moments, but have little influence on the thrust forces. In typical subway tunnels (6 m in diameter and steel or cast iron linings) these effects are negligible. However for larger tunnels (10 m in diameter or more), the complete account of geometric non-linearity may increase maximum. bending moments by up to 50%, or up to 20% if the lining shortening is neglected.

While most of the solutions available were developed for a circular lining profile, some of them accommodate non-circular cross sections. This is the case in the continuous solution by Hain and Horst (1970), and of the discrete solutions based on finite element formulations, such as that by Andraskay et.al., (1972) or Sgouros (1982). This is, perhaps, one of the features that make these latter solutions very attractive for practical use. This capability is not available in any of the ring and plate solutions discussed in the previous section.

A point that normally raises interest is how a ring and spring solution relates to a ring and plate one. Broadly speaking, the methods in Table 4.7 are unrelated to most methods included in Table 4.8, since they imply different representations for the ground and ground-liner interaction. For instance, the partial embedding frequently assumed in the ring and spring models has no parallel solution in the ring and plate models. Moreover, the former assumes spring constants which are usually arbitrary and non-representative of the continuum solution ground response. For instance, the radial spring constant, $K_{\rm r}$, is in many instances, related to the soil's constrained modulus (D).

$$K_r = C \frac{D}{R} = C \frac{(1-\nu)}{(1-2\nu)} \cdot \frac{1}{(1+\nu)} \frac{E}{R}$$

where R is the mean radius and C is an empirical constant. Schulze and Duddeck (1964:107) recommend that C be taken as equal to one. Windels (1966:266,273) suggests C varyies between 2/3 and 3/2.

The German recommendations for lining design (Duddeck, 1980), suggest that C be taken as equal to one. Hence for a Poisson's ratio of 0.3, $\rm K_r$ would be about 0.74E/R. Some other authors (Ebaid and Hammad, 1978:61, Sungur, 1984:21, for instance) suggest that the independent variable $\rm K_r$ be taken as

$$K_r = \frac{1}{1+\nu} \frac{E}{R}$$

This expression is obtained from the uniform convergence of a deep tunnel in elastic ground under a uniform stress field. The latter gives, for the same Poisson's ratio, K.

equal to 0.77E/R. The minor difference in $K_{\rm r}$ by both approaches did not invite much discussion, but the actual equivalence between the spring models and continuum models remained unsolved.

As noted by Sgouros (1982:32) and Paul et.al.,

(1983:21), ring and spring discrete solutions normally used
do not fully account for the interaction between the lining
and ground, which is more properly treated by the continuum

(ring and plate) models. This is due to the usual
assumptions of partial embedment of the lining, of radial
ground action only and of fairly arbitrary discrete spring
constants. Nevertheless, the works by Hain and Horst

(1974:14), Sonntag and Fleck (1976), Ahrens et.al.,

(1982:271) and the review work by Erdmann (1983:27,90), have
shown that a complete correspondence between ring and spring
continuous solutions and ring and plate continuum models is
possible. Hence, complete embedment and the introduction of
both radial and tangential springs are required for full
correspondence between the two types of elastic solutions.

Such a correspondence is fairly easily assessed for an unlined circular tunnel in a gravitational stress field.

What is required is the determination of the radial spring constant,

$$K_r = \frac{\partial \sigma_r}{\partial u_r}$$

and of the tangential spring constant

$$K_t = \frac{\partial \tau}{\partial u_t}$$

The radial and tangential stresses, $(\sigma_{\rm r}, \tau)$, and the

displacements, (u_r, u_t) , can be obtained, from Hartmann's (1970,1972) solution. By taking into account the effect of tunnel heave under the gravitational stress field, as suggested by Hain and Horst (1974:13), the spring constants can be easily determined from Hartmann's (1972) equations, 178,140 and 180,141. The resulting constants are given in Figure 4.4, which include also their value for the special case of an ideally deep tunnel.

It is worth noting that for a complete correspondence, both K_r and K_t should be expressed as a function of the position angle, ϕ , the in situ stress ratio, K, the position of the stress free boundary, n, and, of course, of the elastic constants, E and ν . If an unique average radial spring constant is to be considered (independent of ϕ), as in many ring and spring models, this value can be derived from the expression for K_r in Figure 4.4. Considering a range of in situ stress ratios between 0.6 and 1.0, of Poisson's ratio of 0.3 to 0.4, for shallow tunnels with cover to diameter ratios between 1.5 and 6 (n=2 to 11), a corresponding range of values for the mean radial spring constant is found:

$$\bar{K}_r = (1.05 \pm 0.06) K_{ro}$$

or, approximately

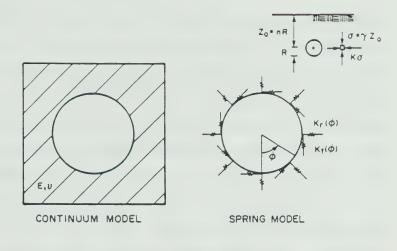
$$\bar{K}_r \simeq \frac{1}{1+\nu} \frac{E}{R} = K_{ro}$$

The latter can be taken as a reasonable approximation for equivalence between spring and continuum models of an unlined circular tunnel. The lined tunnel case could be

approached in a similar manner, again using Hartmann's closed form solution. The resulting expressions for K, and K, would, however, result in a more complex form. More importantly, the spring constants become functions of the relative stiffness of the lining (C and F), as pointed out by Hain and Horst (1974:14). For the case of a deep lined tunnel and for a non-slip condition, Erdmann (1983:90) was able to find explicit expressions for the radial and tangential spring constants (for the uniform and the non-uniform in situ stress components), derived from the ring and plate closed form solution by Ahrens et.al., (1982:269). The latter discussed in detail the correspondence between the two types of models for both full and no slip cases. Erdmann (1983:27) reviewed previous works on the subject and summarized the findings of different authors in a comparative form.

For discrete ring and spring solutions, the correspondence with continuum solutions is not as simply found. The numerical approach involves substantial approximations, one of them being the development of some tangential shear even for a uniform loading condition. This results from the usual representation of the springs by bars of finite length, in the radial and tangential directions.

Figure 4.5, that partly reproduces data from Erdmann (1983:117,118), furnishes a comparison between the maximum bending moments (at the lining crown) calculated from Schulze and Duddeck (1964) solution and from the ring and



$$\kappa_{r} = \kappa_{r0} \frac{(1+\kappa)(1+\frac{1}{2n}\cos\phi) + (1-\kappa)(\cos2\phi + \frac{1}{2n}\cos3\phi)}{(1+\kappa)(1+\frac{1}{4n}\cos\phi) + (3-4\nu)(1-\kappa)(\cos2\phi + \frac{1}{4n}\cos3\phi)}$$

$$K_{t} = K_{ro} \frac{(1+K) \frac{1}{2n} \sin \phi - (1+K) (\sin 2\phi + \frac{1}{2n} \sin 3\phi)}{\left\{-(1+K) \frac{1}{4n} \sin \phi + (1+K) \left[(3-4v)\sin 2\phi + \frac{1}{4n}\sin 3\phi\right]\right\}}$$

with

$$\kappa_{r0} = \frac{1}{1+v} \quad \frac{E}{R} \ , \qquad n = \frac{z_0}{R} \quad , \qquad \kappa = \frac{\sigma_H}{\sigma_v} \label{eq:kr0}$$

Deep tunnel: n + =

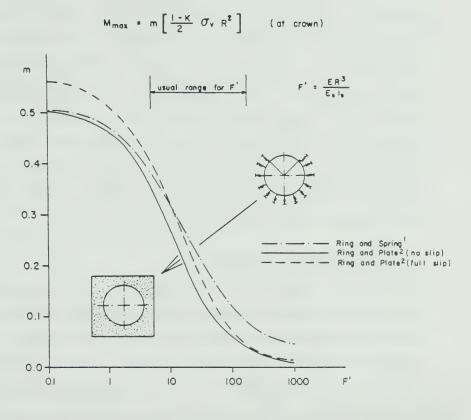
$$K_r = K_{r0} = \frac{(1+K) + (1-K) \cos 2\phi}{(1+K) + (3-4v) (1-K) \cos 2\phi}$$

$$K_{t} = \frac{-K_{r0}}{(3-4v)}$$

Figure 4.4 Equivalence between Continuum and Spring Models for an Unlined Circular Opening under a Gravitational Stress Field

plate model by Ahrens et.al., (1982), both for a deep tunnel situation and for different flexibility ratios. The former solution assumes a constant radial spring modulus equal to the constrained modulus of the soil divided by the tunnel radius. In both cases, Poisson's ratio is equal to 1/3 and the lining is virtually incompressible. Although the solutions do not precisely correspond to each other, since the ring and spring model uses a constant and arbitrary spring modulus, some conclusions can be drawn from the comparison. For a usual range of flexibility ratios, the Schulze and Duddeck solution (which includes the effect of the in situ shear stresses) tends to overpredict the bending moments. For a typical flexibility ratio, F', of 100 (this might represent a shotcrete lining of a subway tunnel in a stiff clay), the Schulze and Duddeck method gives bending moments approximately 100% higher in the no slip condition and 75% higher in the full slip situation when compared with the ring and plate solutions. The conservative estimate of moments results from the assumptions of radial springs only and from the partial embedment hypothesis. For the thrust forces, Erdmann (1983:116) shows similar trends, with the ring and spring solution giving values of 45% to 20% in excess for this typical F' figure.

The ring and spring solutions have limitation very similar to those of the ring and plate models, but have some advantages over the latter. The main limitations for both include the disregard of the ground stress relaxation due to



NOTES: I. Ring and Spring by Schulze and Duddeck (1964) including shear stress load g at interface; radial springs with $Kr = \frac{1-\nu}{1-2\nu} \cdot \frac{1}{1+\nu} \cdot \frac{E}{R}$ where $\nu = 1/3$; C' = 0 and $H/D = \infty$

2. Ring and plate solution by Ahrens et al (1982) , for H/D = ∞ , $-\nu$ = 1/3 , $\rm F^{\prime}$ / C'= 3000 .

Figure 4.5 Maximum Bending Moment Variation with Flexibility Ratio for a Deep Tunnel Liner from Ring and Spring and Ring and Plate Solutions

the three-dimensional stress transfer, and the linear elastic representation of the material properties. The discrete solution group, however, may have some advantage provided a better procedure is developed to estimate more realistic active ground loads and spring constants. These need to account for the different degree of ground straining and softening taking place before lining activation at different points of the tunnel contour. The latter was considered in an analysis performed by Costa Diniz (1978:42), who used a lower spring constant at the crown and floor regions and a higher one at the springlines.

4.3.2.5 Numerical Methods

These are the methods which make use of procedures such as the finite element analysis for prediction of lining loads. Ring-and-spring models, in which a 'discrete' approach is used (see Section 4.3.2.4), also use numerical solutions, which can even be a finite element analysis (for example, Sgouros, 1982). To distinguish from the latter model, those called 'numerical' would be the methods that treat both lining and ground as a continuum.

The present solution has been introduced here only for the sake of completeness. The use of finite element techniques in shallow tunnel design, is treated in detail in other sections of this thesis.

By treating the problem as a continuum, these methods allow lining loads and ground displacements to be obtained simultaneously. This is, perhaps, the most important feature

of this group of models.

As indicated in Figure 4.2, the numerical methods are divided into two sub-classes: two-dimensional and three-dimensional analyses. Examples of the first type are reviewed in Section 5.2.1, whereas Section 5.3.3 reviews applications of the second category.

The main difficulty involved in a two-dimensional numerical simulation of a shallow tunnel, is how to account for the actual three-dimensional effects. Since this problem is common to other 2D methods for lining load prediction (ring-and-plate and ring-and-spring models), the subject is treated separately in Section 4.3.2.7.

An assessment of the ability of 2D finite element analyses to predict lining loads in tunnels actually built is made in Section 5.2.1.2. A brief review on the lining representation and lining material modelling is included in Section 5.2.1.1. Further comments on the subject are included in Section 5.2.2.1. Different contributions on the subject are described in those sections. Noteworthy are the works by Fleck and Sonntag (1977,1978) on the influence of lining discretization and on comparisons between solutions where the ground is represented by a continuum and by discrete springs.

4.3.2.6 Numerically Derived Methods

These are methods derived from parametric numerical analyses, (numerical modelling) with results generalized for certain ranges of conditions using dimensional analysis.

Bending moments or thrust forces are thus obtained by means of dimensionless coefficients obtained from sensitivity studies that normally make use of a numerical procedure such as the finite element method.

This type of design method development has become very popular in foundation engineering over the last two decades. The work by Poulos and Davis (1980) is a noteworthy contribution towards a comprehensive treatment of pile foundation design and makes use of elastic-based theory for the analysis of complex ground-pile interaction problems. In soil tunnelling engineering, this approach has not yet become as popular, but a few contributions have been noted already over the last decade. Some of these are included in Table 4.9. All of them are derived from finite element analyses for either plane strain or three-dimensional conditions, and assuming the materials to be homogeneous and isotropic. Other authors presented notable contributions resulting from fully axisymmetric parametric finite element analyses (e.g., Ranken and Ghaboussi, 1978, Schwartz and Einstein, 1980, Hutchinson, 1982). While they are helpful in providing an insight to the behaviour of the lining-ground interaction, they are of restricted practical value whenever the distortional in situ stress component is neglected. Therefore they will be omitted in this brief review.

The solution by Ranken (1978:223) was developed for the special case of a uniform vertical localized gravity pressure load in the crown region, and therefore is only

applicable to ground control conditions or lining-ground contact in which this type of loading may develop. The effect of the stress free ground surface was intentionally neglected in his plane strain elastic analysis and the lining-ground interface was represented by a full slip condition. This was numerically simulated by means of an interface element which allowed not only the tangential slippage but also the radial separation of the liner from the ground when locally loaded. This ensured an interaction by compressive radial stresses only (no contact tension). The solution was presented in the form of dimensionless equations for moment and thrust. The coefficients are assessed from tables and diagrams as functions of the position of the localized load and of the flexibility and compressibility ratios. By superimposing the results from two or more uniform loading geometries, it is possible to estimate the lining moments and thrusts for non-uniform localized active loads. However, the superposition method can only be accepted, as an approximation, since the problem is geometrically non-linear with respect to the loading and the resulting interface separation.

Costa Diniz (1978) on the other hand developed a very useful method applicable to tunnel profiles of elliptical shape with a horizontal major axis, as used in some double track subway tunnels. In his plane strain elasto-plastic ground (with fixed strength parameters) and elastic lining representations, he assumed complete support embedment,

Author	Year	Loading	Analysis Details	Solution Formulation	Comments
7. Ranken	1978	Localized gravity (uniform and non uniform over vari- able arc length).	2D, FE plane strain; deep tunnel; full allp; interface element allowing map agration between ground and lining (partial embedding at crown); linear elestic behaviour; circular cross sections.	Momente (M) and thruste (T) from Solution for non uniform local- equations, tables and charts, for ized loads obtained by super- C between 0,01 and 3 and F from position (thus approximate). 1 to 1,000 [1].	Solution for non uniform local ized loads obtained by super- position (thus approximate).
2. Costa Diniz	1978	Excavation loading (in aitu dresses with gravity for K = V/(1-v)).	20, FE plane strain, shal- low tunnels no slips com- plate embeddennt elasto- plastic behaviour (c = 50 RPa and \$= 30°, fixed); elliptic cross sections with horizontal major axis.	M and T at crown, apringline and floor from equations and chare for Z/B between 1: and 2, B/t between 7.5 and 30, E ₂ /E from 0.33 to 0.67(2).	Approximate equations furnished for quick estante of moment and thrust at springline.
3. Ahrens et al 1982	1982	Excavation loading (approx. in aitu atreases with gravity partly accounted, for any K).	10, FE plane strain; shal- low tunnel; both no and full slip (vith a special inter- face element; partial embeddment (no cover ele- ments over the 90° arch at crown); linear elastic; circular cross section.	M. T and radial displacement at particular points, from equations and charts, for an incompregable liner with \$\text{p} from 5 to \$00^{13}\$.	Loading condition not fully compatible with shallow tunnel assumption.

Table 4.9 Details of Some Numerically Derived Methods for

Lining Loads Prediction

200	AUTHOR TEST	Loading	Analysis Details	Solution Formulation	Comments
4. Pierau	4u 1981	Stepwise excavation simulating actual 30 construction process (in situ stresses with K - v/(1-v).	10, Fr analyses of shallow tunnel; no slip; completed subseding; linear slattic behaviour; double track tunnel; non-circular cross section with 8m height and 10m width; inclined tunnel face (65*).	10, FE analyses of shal- awithous surface settlement, from completed ambaddings linear chetra, for ground covers warying elastic behaviour; double from 5 to 25m, for shotcrete thick- trons settlon with 8m height modulus from 10 to 50HPs (**0.3) and 10m width inclined tun- to 0.41; constant shotcrete modulus.	. in
5. Erdmann Erdmann Duddeck	ann 1993 ann 6 1984 eck	Stepwise excavation simu- lating actual 3D construc- tion process (deep tune) stress field with any K).	3D axisymmetric FE analyses of deep tunnel, with plane symmetric fond axisymmetric) stress flaid, no alip; complete ambeddment; linear elastic behaviour; two distances for delayed lining instillation; fixed lining thicknessed.	Reduction factors to be applied to thrust, moment and radial displacements, obtained from ring and place model. Factors given as a function of lining compressibility or flaxibility ratios and of the distance from face to lining edge.	Treatment of non symmetric in situ stress field similar to the approach by Hanafy & Emery (1980, 1982).

(2) A: half of major axis length (horizontal); B: half of minor axis length (vertical); Z: depth to tunnel axis; t: lining thickness

(3) β : flexibility ratio = ER³/E_BI_B

(1) $C = \frac{(1-\sqrt{2})}{(1+\sqrt{2})} = \frac{E}{E} = \frac{R}{A} + F = \frac{(1-\sqrt{4})}{(1+\sqrt{2})} = \frac{E}{E} = \frac{R^3}{6}$

Table 4.9 Details of Some Numerically Derived Methods for

Lining Loads Prediction (Continued).

fully accounting for the effects of the ground surface and gravity. He assumed, however, the stress ratio to be a function of the Poisson's ratio. Bending moments and thrust forces are obtained at three points of the lining contour from an equation whose coefficients are obtained from ingeniously designed diagrams. These coefficients are a function of the tunnel depth ratio, of the cross-section geometry, of the relative thickness of the lining and of the support-soil stiffness ratio. The method was elaborated for use in urban subway tunnels supported with shotcrete lining, and his analysis almost completely covered the normal range of conditions found in large cross section tunnels. No comparison of results between this method and other solutions or field measurements was made available to assess its potential.

Ahrens et.al., (1982) developed a similar method, but assumed linear elastic relationships and a circular tunnel profile. This method was reviewed and summarized by Heinz (1984:306). Furthermore, the lining was assumed to be only partially embedded, as all of the ground cover represented by the prism of elements overlying the upper 90° crown arch was not discretized in their analyses. This would thus represent the conservative assumption of complete soil cover collapse. With respect to the ground loading, Ahrens et.al., (1982) used the same assumption introduced in their analytical solution for the ring and plate model: a deep tunnel stress field, with the vertical stress equal to the

overburden stress at the crown elevation and with the horizontal stress equal to the in situ horizontal stress at the springline elevation. The solution that results is dependent on the relative depth, not only due to the loading assumption, but also because in their numerical simulation the ground domain was bounded by a stress free ground surface. Their solution furnishes moment, thrust and radial displacements at particular points of the lining contour. These are obtained from equations and design charts covering a large range of lining flexibilities, but with the conservative assumption that the support is incompressible. This method accounts also for both no and full slip at the lining-ground interface. To represent the slippage condition, Ahrens et.al. (1982:266) introduced an infinitely rigid one-dimensional bar element radially linking the soil to the lining. These elements would thus transmit the axial loads only. This approach was used earlier by Ranken (1978:96) who claimed that, in order to avoid distorting the analysis results, the same elastic properties of the ground should be assigned to the bar elements, with cross sectional areas selected to "fill" the gap behind the support. If lining properties were assigned to the bars (as Ahrens et.al. (1982) apparently did), the results obtained would be equivalent to that of a liner with its thickness increased by an amount equal to the size of the gap.

Pierau (1981,1982) carried out some three-dimensional parametric finite element analyses of a shallow tunnel, in

which the actual construction was fully represented, including the stepwise excavation and application of the support. Linear elasticity was assumed and constant elastic properties were assigned to the simulated shotcrete lining. The non-circular tunnel cross section was kept constant in all his analyses (8 m height by 10 m width). The in situ stress ratio was assumed to be a function of Poisson's ratio and a rigid boundary was placed at 0.2 m below the tunnel invert. The results of his parametric studies are presented in terms of bending moments, thrusts and displacements at particular points of the lining contour. They are expressed graphically as a function of the ground cover, lining thickness and the elastic properties of the soil. Although his results are not readily generalized as he did not reduce his data in a dimensionless form, and used some specific and fairly particular assumptions, this was the first attempt to develop a procedure that fully accounts for the three-dimensional nature of the tunnelling construction.

Erdmann (1983) and Erdmann and Duddeck (1984) presented results of a particular type of three-dimensional finite element analyses, in which the problem was represented axisymmetrically, but the stress field was assumed to be non-symmetric. Their approach was similar to that adopted by Hanafy and Emery (1980 and 1982), with, the non-symmetric stresses and displacements expanded into Fourier series (Hanafy and Emery, 1982:205). The actual sequence of construction of a deep tunnel was fully represented by

Erdmann (1983:174), including the stepwise excavation and application of the support. The latter was designed to simulate a shotcrete lining, with three assumptions regarding its stiffness: a constant modulus (of 15 GPa), and two different variable moduli assumption (from a near zero modulus at the lining edge to 15 GPa one diameter behind, in both cases). The parametric study assumed linear elasticity for the ground as well as for the support. Solutions were obtained for two distances between the tunnel vertical face and the leading edge of the liner (a quarter and a half the tunnel diameter, D). Some of their results assume that the ratio between the flexibility and the compressibility ratio is constant (in these analyses, they assumed a uniform lining thickness equal to 0.03D). Correction factors were then obtained by relating the thrusts, moments and displacements calculated in the 3D analyses, with those from the ring and plate solution by Ahrens et.al. (1982). Each of these factors were split into two components, one being applied to the zero term of the Fourier series expansion and the other to the term two. The solution is applicable to any in situ stress ratio, to any tunnel size, for appreciable ranges of soil stiffness, compression and bending stiffnesses of the lining.

From the results provided by Erdmann (1983:193-205) it can be suggested that the influence of the increasing shotcrete stiffness with time (or with distance to the face) on lining displacements, thrust or moments, is nearly

equivalent to a net increase in the delay of the application of a constant stiffness lining. Although this point requires further investigation, it is believed that for all practical purposes, this influence can be accounted for in an analysis by using an increased unsupported heading span and a constant stiffness liner. Any simple or general rule to account for the effect in this way cannot be formulated at the moment. A unique rule may not be found as it will depend on the combined rates of shotcrete hardening and lining placement. But as those rates do not vary too widely, it is believed that some criterion may emerge in the future from some combined parametric analyses.

Despite the deep tunnel assumption and other more or less restrictive assumptions, the method developed by Erdmann entails an appreciable generality as compared to Pierau's. It is believed that with a progressive reduction of computing costs and, more importantly, with the development and widespread implementation of user friendly pre and post-processing software, more comprehensive analyses of this type will become available in the future.

This group of methods for lining load estimates are particularly promising for the development of solutions for conditions not covered by the available procedures. An example of such conditions is the non-circular tunnel cross sections built by staged excavation with shotcrete support, like studies by Costa Diniz (1978) or currently by Heinz (1987).

A special procedure that intentionally has not been included in Table 4.9 is the method by Baudendistel (1973). His procedure does not allow the procurement of lining loads, but rather, it gives the minimum required thickness of an unreinforced concrete liner for a circular shallow tunnel, to avoid either compressive or tensile failure (with some safety margin). This method was developed from plane strain, finite element analyses, with the soil represented by an elasto-plastic model, with three pairs of strength and stiffness parameters. Baudendistel's design charts cover tunnels with diameters ranging from 6 to 12 m, and soil covers from 5 to 160 m. He considered also in situ stress ratios ranging from 0.2 and 1.0, and a no slip condition. Unlike other plane strain methods reviewed, Baudendistal (Op.cit.) devised an approximate procedure to account for the stress relaxation prior to lining installation. This procedure will be discussed in the next section. His design method thus defines a minimum concrete thickness for delayed lining installation (support applied at one or one quarter of a diameter behind the face).

4.3.2.7 Account for Three-Dimensional Effects in Two-Dimensional Models

With the exception of those methods for lining load prediction which were numerically derived using three-dimensional finite element analyses, such as that by Pierau (1981) or Erdmann (1983), or those that on a case by case basis, make use of a fully three-dimensional numerical

analysis (e.g. Heinz, 1984:141), none of the other methods reviewed in the previous sections, take the actual three-dimensional stress transfer process that occurs with the tunnel advance directly into account.

Most of the methods reviewed approach the tunnel problem as a plane strain situation in a transverse section normal to the tunnel axis. Therefore they are unable to take into consideration the ground displacements and the ground stress changes that take place before the support is installed and the lining-ground interaction starts. In those methods, it is usually assumed that the liner has been installed before excavation started, and consequently, they will normally provide displacements which are smaller and lining loads which are larger than those that should actually be observed.

The greater ease associated with a two-dimensional treatment, compared to the more expensive, involved and time-consuming three-dimensional approach influenced many to introduce approximate methods to account, at least partly, for the actual 3D nature of the problem. Most of these methods have in common, the assumption that the 3D situation can be approximated by a succession of 2D plane strain representations transverse to the tunnel axis. Therefore, the out of plane stresses are principal stresses and the shear stresses acting on these planes are zero. In the 3D case, non-zero shear stresses develop on these planes, as a result of the equilibrium and displacement compatibility.

The tunnel closure in the 3D unsupported heading is thus smaller than the closure in the 2D unstressed opening. In order to make the 2D representation closer to the 3D condition, the opening is never left unsupported. Otherwise, a complete unload of the final opening, in which the stresses around it are reduced to zero, followed by the installation of the lining, would inevitably lead to an unstressed support condition. No ground-lining interaction would take place in a time-independent situation. Unless time dependent responses are expected (consolidation or creep), this simulation would lead to unreliable estimates of ground movements or lining loads.

The effect of the longitudinal stress transfer or arching, is normally incorporated in the 2D representation by the introduction of some balancing internal stresses in the opening, even in sections that represent the unsupported tunnel length. This is achieved by two or three different procedures, which at the end, correspond to smoothing out the longitudinal stress distribution shown in Figure 2.20(a). The extreme stresses at B,C,D and E are not accounted for and the stress state is assumed to gradually change from A to F in a continuous way, not unlike the development of the displacements shown in the same figure. Correspondingly, the ground response result is equally gradual, as shown by the dashed curve in Figure 2.20(b). These different procedures are defined and calibrated in such a way that the final results of the 2D model in terms

of displacements or stresses, approximate as closely as possible, those observed in an actual 3D configuration. It should be pointed out that, regardless of how rigorously each of these procedures is incorporated or implemented into the two-dimensional model, they are all not more than a faint approximation of the real phenomenon. Their merit lies in the fact that they attempt to bring the 2D solutions closer to the actual conditions. However, their qualities should not be interpreted in terms of the generality of their assumptions or of the degree of rigour they exhibit. Rather, they should be evaluated in terms of their degree of simplicity for practical use and of their ability to offer results that better approximate the reality.

No attempt will be made herein to assess in depth the virtues of each available procedure to account for 3D effects in 2D models. But, they can be inferred to some extent by comparing the features of these procedures. For this purpose Table 4.10 has been prepared, gathering some representative approaches selected from many of those available.

Most of the procedures focus on estimates of lining loads, but those developed as numerical simulation techniques for two-dimensional finite element analyses, are in principle, also applicable for ground displacement predictions. Actually, some of the latter group were designed basically for the last purpose (Table 4.10, procedures, 9, 15, 16, 17 and 18).

The procedures reviewed were classified according to the models they are to be applied to: convergence-confinement (uniform stress field solutions), ring and plate models with non-uniform stress fields and numerical models (basically, the finite element method).

Table 4.10 presents also the type of approach adopted in each case to simulate the 3D effects. Some of the approaches applied to numerical models were reviewed by different authors (see, for example, Eisenstein, 1982, Katzenbach and Breth, 1983:202, Heinz, 1984:111, Kochen et.al., 1985:205 or Rowe, 1986:98). As mentioned earlier in this section, the 3D effect is usually simulated in the 2D model by introducing some internal balancing stresses to the section of the tunnel to be. This can be performed by a gradual stiffness reduction of the ground material within the tunnel profile (tunnel "core"). However, as noted by Kochen et.al., (1985:205), this may not be enough to cause movements in the soil mass, since for instance in a numerical simulation, the ground mass is in equilibrium with the stress field and the nodal forces may not be altered by a simple change in the ground stiffness. Hence the stiffness reduction is always followed by reducing the ground stress around the contour, which can be partial (as in Swoboda and Laabmayr, 1978 method) or total (as in Schikora, 1982, 1983). The partial reduction involves an additional approximation, as it requires acceptance of the principle of superposition of two different structures (Maffei,

Assumptions and Comments	Face effect represented by a core disc in plane strain or atreas, progressively weakened (yielding and reduction of darc hickness) generating internal tunnel pressure. Arbitary linear distribution of radial displacement along tunnel.	Stress field reduction linearly proportional to the radial displacement variations along unlined tunnel obtained from axiaymetric linear elastic finite element analysis. Neglects ground-liner interaction.	Stress field reduction back analysed from field instrumentation. Reduction factor to be applied either to the specific weight of soil or to the depth of the tunnel (in solutions accounting for gravity).	Progressive removal of concentric layers of elements with full stress release within the tunnel section, before lining installation. Extent of removal defined as to cause 15% or 100% of elastic convergence of tunnel contour (empirically related to the lining leading edge position at D/4 and 1D behind the face, respectively).	Tunnel face approximated by a sphere in uniform stress field. Convergence at face thus obtained for elasto-plastic ground, hence reduced tunnel pressure in the axisymmetric model.	Convergence curve at tunnel face obtained by intro- duction of fictitious body forces outwardly oriented, causing the deviation of the longitudinal stress trajectories in an axisymmetric configuration.	10 effect represented by a fictitious internal pressure selected such a way that the 2D radial displacement is equal to the 10 backsymmetric one, at the section being considered. Linear alastic and slasto plastic axisymmetric FE analyses of unlined tunnel were used to obtain pressure-distance to the face distribution. Good correspondence between perforated 2D and 1D models for distance to the face greater than D/4.
Type of Development	Analytical	Numerical	Empirical	Numerical Simulation	Analytical	Analytical	Numericel
Approach Type	Core stiffness reduction	Ground atress reduction	Ground stress reduction	Progressive core removel	Ground stress reduction	Ground stress reduction	Ground atress reduction
Where	Conver gence -Confinement	Convergence-Confinement	Ring and Plate	Finite element (non linear)	Convergence-Confinement	Convergence-Confinement	Convergence -Confinement
Year	1972,	1972	1970,	1972,	1974	1974	1974
Author	1. Lombardi	2. Daemen & Fairburst	3. Hartmann	4. Bacdendistel	5. Egger	6. Amberg & Lombardi	7. Panet & Guellec Panet & Guenot

Table 4.10 Account for Three-Dimensional Effects in Two

Dimensional Models

Assumptions and Comments	Arbitrary reduction of ground stresses by 50% of their in situ values.	Staged excevetion of the tunnel face, with progressive removal of elements and full arreas release at the zone being excavated. Concurrently, lagged application of the support. Attempt to represent sequential construction as in the NATM:	Stiffness of tunnel core reduced by 50%. Ground stress reduction estistated from the avolution of settlement of crown with face advance, as measured in the field. Staged excavation of tunnel face.	Ground etress reduction factors obtained from 3D FE linear elastic analysis of an unlined deep tunnel, for $K_0=0.5$ and for a given non circular cross acction, with three excavation sequences. Different reduction factors for crown, springline and floor, obtained by relating the longitudinal distribution of radial displacements with a linear relationship between the latter and the radial stress.	Tunnel core represented by multiple element layers each with a fraction of the ground stiffness. The sum of the stiffnesses of all layers is equal to the atiffness of the intact ground. 3D analysis of unlined tunnel provide relationship between closure and distance to the face. 2D analyses furnish relation between closure and layer stiffness fraction. Thus a rule is established between cumulative stiffness of layers and distance.	Ground-liner closed form solution with a core modulus reduction factor included. Load seduction factors defined as thrust and moment ratios with and without core stiffness reduction. Thrust load factor versus lining-face distance obtained from antaymentic FE elastic analyses of lined tunnels (relationship corrected by Mutchinson, 1982;175). Thus a relation (valid for thrust only).
Type of Development	Empirical	Numerical	Numerical empirical	Numerical	Numerical aimulation	Analytical and Numerical
Approach Type	Ground atress reduction	Progressive core removal	Stiffness and stress reductions	Ground stress reduction	Core stiffness reduction	Core stiffness reduction
Where	Ring and Plate	Finite element (incremental analysis)	Finite element (incremental analysis)	Finite element	Finite element (incremental analysis)	Ring and Plate
Year	1975	1978 1979 1984 1985	1978	1979 1984 1985	1979	1980
Author	B. Muir Wood	9. Wanniner & Breth Wanninger Negro et al Katzenbach Elsenstein et al	10. Svoboda & Laabmayr Svoboda	11. Baudendistel	12. Ven Dillen et al Obnishi et al	13. Schwartz & Einstein

Table 4.10 Account for Three-Dimensional Effects in Two

Dimensional Models (Continued).

Assumptions and Comments	After removal of moil elements within the tunnel, the in situ stresses are reduced arbitrarily, what which represents the stress transfer into the ground. Once the liner is installed, the rest of balancing stresses are released and ground-liner interaction develops.	Reduce stiffness of soil elements within the tunnel to near zero and reduce gradually the in situ stresses around tunnel contour. Monitor displacement at crown. Once a predetermined displacement at crown is reached (sps site), activate liner and continue unloading esteminated.	Approach and assumptions similar to Tan (1977) but using a stream relaxation technique. Moreover, ground-lining interaction starts when any point of excavated profile comes into contact with the lining. Hence, unlike the former, not all points will come onto the line at the same time. Also, the rate of stream relief is not constant around the contour, being intitially greater at the errorn than at the floor (Lo and Rowe, 1982:216). Requires empirical estimate of a 'gap' parameter.	Approach and assumptions similar to Svoboda and and Labhmayr (1978). Core stiffness reduction factor empirically assessed (back analyses). Full stress extaled around softened core contour. Also ataged excavation of tunnel face.	Displacement boundary condition at tunnel contour. Rate of displacement imposition given by longitudinal analyses (axisymmetric and plane strain). Hagmitude of displacements imposed apparently by trial and error. Non-uniform displacements imposed around contour (maximum at crown).
Type of Development	Numerical	Numerical aimulation	Numerical empirical	Numerical empirical	Numerical
Approach Type	Ground stress reduction	Ground stress reduction	Ground atress reduction	Stiffness and stress reductions	Imposed tunnel convergence
Mhere	Finite element	Finite element (incremental analysis)	Finite element (incremental analysis)	Finite element (incremental analysis)	Finite element (incremental analysis)
Year	1981 1975 1982 1985	1985	1981 1983 1983 1986 1986	1982 1982 1983 1985	1985
Author	14. Zagottis Rocha Schikora & Fink Baumann et al	15. Tan Clough et al	16. Rowe et al Lo and Rowe Rowe et al Bowe and Kach Rowe Ng et al	17. Schikora 6 Fink Schikora Baumann et al	18. Ohta et al

Table 4.10 Account for Three-Dimensional Effects in Two

Dimensional Models (Continued).

1982:162). By reducing the ground stresses around the contour, some ground displacements towards the softened core are induced and the core reacts against them. Thus balancing stresses are generated around the contour of the tunnel to be, which result from the interaction between the softened and the unsoftened ground areas. The analytical approach by Schwartz and Einstein (1980) differs slightly from other core stiffness reduction procedures, as they assumed a softened core inclusion before application of the stress field (subtracting the displacements induced in this phase from the final solution).

Another procedure, which is implemented numerically only, is the progressive core removal (for example, Baudendistel, 1972, Wanninger and Breth, 1978, Negro et.al., 1984). It consists of a complete piecewise removal of portions of the tunnel core, followed by the partial application of the support in these portions, as in a staged excavation of a tunnel. In essence, it also involves a reduction of the central core stiffness, as each part of the ground removed is assigned a zero stiffness (for instance, by deactivating the corresponding elements). It involves as well, an overall reduction of the in situ stress around the opening, as the ground stresses around the partial excavation profile are reduced to zero in each portion that has been removed.

As the support in this procedure is generally activated after the excavation, it is initially unstressed, and will

pick up load as the removal procedure is extended throughout the tunnel section. As a consequence, it will normally underestimate the lining loads. The results obtained for a full face one step excavation are obviously meaningless.

Another procedure is the gradual reduction of the in situ stress around the tunnel contour or gradual boundary stress reversal in a fully perforated ground mass (core stiffness previously reduced to zero). The 3D longitudinal arching effect is simply represented here by the gradual reduction of the internal stress initially set equal to the in situ values. The advantage it offers in relation to the core stiffness reduction approach is that it eliminates one fictitously created unknown, namely, the core stiffness, as well as its rate of softening. The disadvantage it contains is that the balancing internal stresses have an undefined distribution around the excavation profile. In the core stiffness reduction, this distribution results automatically from the interaction between the softened and unsoftened ground zones. Some interpretations may indicate that a non-uniform release of the in situ stresses around the tunnel occurs. Stresses at the tunnel crown (in a 2D repesentation) decrease at a faster rate than elsewhere (for K<1), and the ground stress redistribution developing towards a more uniform lining load condition than that given by the in situ stress field ratio (Branco, 1981:201, Branco and Eisenstein, 1985, Lo and Rowe, 1982:216). Most methods of this class assume a uniform rate of stress release for

all points around the opening. The latter assumption avoids the inclusion of an unknown and yet arbitrary variable (the non-uniform rate of stress release around the contour). Besides being simpler, it tends to be a safer one with respect to the development of bending moments in the lining at equilibrium.

Swoboda (1985:1653) made reference to the use of non-uniform release of in situ stresses around tunnels in two-dimensional simulations. However, to the writer's knowledge, results of such a simulation have not been made available so far.

An alternative procedure to the imposed boundary stress approach is the displacement imposed boundary condition. This was the approach favoured in some analyses by Negro and Eisenstein (1981), by Resendiz and Romo (1981) and by Ohtea et.al. (1985). This alternative may be attractive when dealing with TBM excavated tunnels, where the size of the void between the outer surface of the liner and excavation walls is relatively well defined. But for other tunnelling procedures (e.g. NATM), it may not be as clearly handled, since a physical gap behind the lining is not present. Although not exactly a displacement boundary method, the approaches by Tan (1977) and Rowe et.al. (1981) combine a ground stress reduction procedure with a following the gap closure around the opening. The lining is activated and interaction is started when the soil comes in contact with the support. Again, this procedure appears to be adequate

and relevant for TBM excavated schemes, but less applicable to NATM schemes. Moreover, to account for the displacements developing ahead of the face in the real situation, the gap behind the lining has to be increased by some amount, which can be approximated in the 2D representation by using a slightly larger excavated tunnel diameter (e.g. Rowe and Kack, 1983:300). This approximation requires an independent evaluation, either empirical (from field measurements) or numerical (necessarily three-dimensional).

As indicated in Table 4.10 some of the procedures were developed for generalization, using an analytical framework (e.g. Lombardi, 1972, 1973 and Egger, 1974). Others are based on numerical developments, for instance, Panet and Guellec (1974) using an axisymmetric solution, or Baudendistel (1979) using an actual 3D finite element analysis. The latter assumes along with Daemen and Fairhurst (1972), a linear relationship between radial displacements and stresses, to obtain ground stress reduction factors for different delayed lining distances. The discussions in Chapter 2 demonstrated that generally speaking, this is an oversimplified assumption that should not be accepted, as it tends to underestimate the loads acting on the lining installed some distance behind the tunnel face. The exception is for ground behaviour close to linear elastic, which could be acceptable in some rock tunnels, but not in soils. A more adequate development is that by Panet and Guenot (1982:199) in which the stress reduction factors were

derived from non-linear ground reaction curves which accounted for an elasto-plastic behaviour of the soil.

Some other developments are entirely empirical, (Muir Wood, 1975, or Hartmann, 1972), in which suggested reductions in ground stresses are either arbitrary or based on back analysed field performances. A large number of the methods included in Table 4.10 are not formulated in a generalized way, but represent numerical simulation procedures to be applied in finite element analyses. They are usually performed incrementally and on a case by case basis. Such is the case for all methods applicable to finite element analyses (eg. Wanninger and Breth (1978), Swoboda (1979), Van Dillen et.al. (1979) or Rowe et.al. (1983)). Their potential practical use is limited as they require a tunnel design load based on finite element solutions, which may not be available in many routine situations.

Unfortunately, most of these methods that do not require a finite element approach were developed for uniform stress field solutions, therefore being of limited practical value for shallow tunnel design. Only three are set in non-uniform stress field conditions, of which two are empirically developed. The other (Schwartz and Einstein, 1980), although originally formulated for a non-uniform stress field, fails to provide a definite criteria relating the load reduction factor applied to the non-uniform stress component (especially bending moments) to the distance of delayed lining installation. The core stiffness reduction

factor they introduced was related to that distance under uniform stress conditions (axisymmetric analyses). They assumed the same relation would be valid under a non-uniform stress state (3D analyses). Moreover, the method is valid only for deep tunnels and does not account for gravity effects. If the deep tunnel problem is of interest, then a better and more accurate approach is that by Erdmann (1983), which is directly derived from three-dimensional parametric analyses and therefore does not involve the inherent approximations of Schwartz and Einstein's (Op.cit.) method.

The present review reveals that, except for some fully empirical procedures, there is not a single solution, not even an approximate one, to account for three-dimensional effects in non-numerical two-dimensional models. applicable to shallow tunnels. Such a model would thus account for the gravitational stress field and for the presence of the stress-free ground surface.

4.3.3 Prediction of Ground Displacements

The number of methods available for the prediction of ground displacements is considerably smaller than those for lining loads. This simplified the survey on the subject, which was still quite extensive but certainly not exhaustive. The review of methods is presented in the same format used for the lining load prediction. Similarly, a classification of methods, according to the type of development on which the method is based, is presented in

Figure 4.6. In the majority of the cases, the prediction is restricted to estimates of vertical displacements in the ground, so that they will be simply referred to as methods for settlement prediction. Other reviews of ground settlement predictions were presented by Schmidt (1969), Szechy (1973;1035), da Fontoura and Barbosa (1985), for example. They included methods that are also applied to mining subsidence, but these will not be covered herein.

Four main groups of methods are identified, as indicated in Figure 4.6, and are discussed in the following. The third group shown, include those methods which are entirely based on the numerical simulation of the problem. They are performed on a case by case basis, using any type of numerical technique, for instance, the finite element method. Examples of applications of this approach to ground settlement predictions are numerous and will not be covered specifically here. References to these applications were made in Section 4.3.2 and they will be extended in Chapter 5, where the subject will be discussed in more detail.

To facilitate the review, Table 4.11 was prepared, including examples of the other three groups of calculation methods. Indications of the underlying assumptions, summaries of the developments, descriptions of the basic requirements for input and the type of output supplied by each method are given. The conditions to be fulfilled for the application of these methods in practice can be gathered from these indications on an individual basis. The

Features and Comments	Developed for shield driven subway tunnels. Valid only for Japanese conditions and construction procedures. Considers 4 ground conditions and 4 types of shield. Relates maximum surface to overburden and to overload factor.	Shielded driven tunnels. Only for Japanese soil conditions as well as construction procedures. Considers 3 types of ground conditions and 4 shield types.	Settlement calculated from linear elastic solution (approximate) of a hole in a semi-infinite plate. Assumes zero body forces and uniform interesh pressure reduction in the opening (K = 1). Developed from Jeffery (1920) solution for atresses. Suggests that transverse settlement profile at surface can be obtained assuming a normal probability curve.	Settlements due to yielding (loosening) of granular soils. Assumes full development of plastic flow. Darived from observations in trap-door experiments. Takes into account dilatancy due to shear (empirically). Requires an independent estlaste of crown settlement. Neglects ground movements prior to yielding.	Settlements due to yielding (loosening) of granular soils. Postulates plastic flow zones in the ground. Assumes no volume change. Distinguishes losses through the face and through tunnel contour. Approximates settlement trough by straight line segments. Limits of subsiding zone defined from a Rankine active state assumption. Requires independent estimate of crown settlement.	Settlements over shielded tunnels driven in saturated clays (undrained condition). Uses slastoplastic solution of hole in infite plate, developed by Ladanyi (1974), for uniform stress field (deep tunnel, R ₀ = 1). If overcutting is large (large gap), sasumes a crown settlement equal to the unrestricted radial displacement of the deep tunnel solution. If overcutting is small, assumes a crown settlement equal to the physical overcutting app. plus the radial displacement of face, plus an empirical parameter, related to the construction quality. The face displacement is taken as 1/3 of the total unrestrained plane strain displacement.	Calculates loss of ground from linear elastic solution of hole in a plate problem (deep tunne), $K_0=1$). Assumes that the volume of settlements at surface is equal to the loss of ground. The width of settlement profile derives from Rankine active state consideration.
Output of Method	Transverse settlement profile at surface	Maximum surface settlement	Maximum surface settlement	Maximum surface settlement and trough width subsurface settlements along vertical axis	Transverse settlement profile at surface	Subsurface settlement distribution along vertical axis	Maximum surface settlement and width of settlement trough
Type of Development	Empirical	Empirical	Semi-Empirical	Sent-empirical	Semi-empirical	Semi-empirical	Semi-empirical
Author/Year	1. Hanya (1977)	2. Fujita (1982)	3. Limanov (1957)	4. Murayama & Maraucka (1969) (also see Yawamoto & Okuzono, 1977)	5. Szechy (1973:1048)	6. Lo et al (1984)	7. Herzog (1985)

Table 4.11 Features of some Methods for Ground Displacement

Prediction for Shallow Tunnel Design

Features and Comments	Derived from earlier applications of stochastic theory to the solution of subsidence problem (works by Littuinssyn in the fifties and sand sixties). Assumes that the profile is given by a normal probability curve. Shape of the curve (position of infeation point) defined empirically, as a function of ground conditions and relative tunnel depth. Requires independent estimate of maximum surface extinement. For clays in undrained condition, it can be calculated by making the volume of settlement equal to the loss of ground, estimated from the elastic plastic solution of hole in infinite plate (K ₀ = 1). Else, the maximum settlement is estimated empirically from past experience.	Modified version of Peck-Schmidt method. Requires independent estimate of the surface settlement volume which is equal to the loss of ground plus the overall ground volume change. Presents procedure to estimate the broken down components of the loss of ground. Provides indication for estimating overall ground volume changes in dense sands.	Modified version of the former two methods. Provides empirical indications for estimates of the losses of ground and settlement volumes in clay and gamular soils, as a function of the overload factor and of the construction quality. The overall volume changes in the ground are also empirically estimated.	Introduces a minor modification into Peck-Schmidt method. Additionally, it proposes that the longitudinal profile of settlements can be approximated by a cumulative probability curve (error function), which is used to fit available data only.	Assumes that the transverse settlement profiles at surface and below surface are approximated by normal probability functions. Like in the previous method, assumes that the longitudinal distribution of settlements (along tunnel axis and parallel to it, both at surface as well as body it; can be proximated by a countaitive probability curve. The latter is obtained by integration of the subsidence surface generated by a spheric. Opint's source of loss. Displacements at directions other than vertical are obtained by integration of strains calculated on the assumption of erro volume changes in the ground. Requires an independent astisate of the final settlement volume, what is done expiritelly. Requires an entisate of the final settlement at the face is 1/2 of the final settlement. Design charts are provided to facilitate applications.
Output of Method	Transvarae settlement profile at surface	Transverse settlement profile at surface	Transverse settlement profile at surface	Transverse settlement profile and longitudinal profile along the exis, at surface	Complete displacement field above the tunnel
Type of Development	Semi-empirical	Seni-empirical	Semi-empirical	Semi-empirical	Semi-empiritomi
Author/Year	8. Schmidt (1969) Peck (1969)	9. Cording and Manamire (1975)	10. Attewell (1977)	11. Yoshikoshi et al (1978)	12. Attevell and Woodman (1982) Attevell et al (1984;53) Attevell et al (1984;53)

Table 4.11 Features of some Methods for Ground Displacement

Prediction for Shallow Tunnel Design (Continued).

od Features and Comments	ent profile tunnel in gravitational atrees field with $K_0^{a-\sqrt{(1-v)}}$ (v from 0.1 to vition along 0.4 thus K_0 from 0.1 to 0.67). Assumes full in situ atrees release at the opening. Settlement distributions are conveniently normalized introduces an empirical multiplying factor (4 < 1), to correct the calculated displacement on account of construction procedures, lining type and soil conditions. Pactor 4 = 0.4 to 0.5 for soil conditions and construction methods found in Madrid. Solution developed for a rigid boundary located 4D below tunnel floor.	bove tunnel actuated for shielded tunnels (with or without compressed air) in actuated clay (undrained condition). Derived from non linear hyperbolic) elastic 2D FE analyses of shallow circular tunnel. Apparently in situ ground stiffness assumed independent of Kg. Identifies losses due to (a) acreas release at the face, (b) radial closure of tunnel valla. For (a) assumed a 2D longitudinal representation (with rigid lining and face subjected to uniform internal presents. Fransverse displacement profile auto to (a) from 2D transversal representation and uniform acreas field condition (Kg and no body forces). For (b) assumed also a 2D plane strain representation and displacement boundary condition at the opening (requires independent estimate of a uniform tunnel closure). Requires CU titaxial test results: Final estiments by superposition. Final simulation of ground loss (a).	profiles shallow circular tunnel in gravitational stress field. Assumes $K_0 = v/(1+v) \text{ with } v = 0.45 (K_0 = 0.82), \text{ but assess influence of } v \text{ (and } K_0). Longitudinal and transversal settlement distributions of ground surface presented in conveniently normalized form, for H/D from 0.5 to 2.0. Includes account for ground creep and layered soil conditions.$	ttlement Derived from linear eleatic 3D FK analyses of lined shallow tunnel, with larger (non-circular) cross-sectioned area. Assumes $K_D = \nu/(1-\nu)$ and parametric results cover a limited range of application. The study aconcentrated more on lining (shotcrete) dealgn. See section 4.3.2.6 for further details.
Output of Method	Transverse settlement profile at surface and subsurface settlement distribution along along vertical axis. Lateral displacements at surface.	Transveree settlement profiles at any elevation above tunnel	Transverse and longitudinal surface settlement profiles	Maximum surface settlement
Type of Development	Numerically derived	Numerically derived	Numerically derived	Numerically derived
Author/Year	13. Sagameta and Oteo (1974) Sagameta et al (1961) Oteo and Sagameta (1982)	14. Resendiz and Resendiz (1982) Romo and Resendiz (1982)	15. Ito and Hisatake (1982)	16. Pierau (1981, 1982)

Table 4.11 Features of some Methods for Ground Displacement

Prediction for Shallow Tunnel Design (Continued).

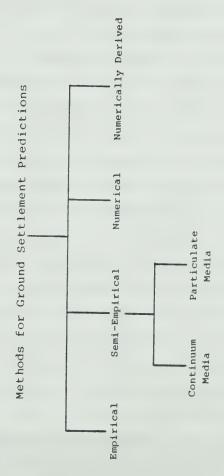


Figure 4.6 Classification of Methods for Ground Settlement Prediction for Shallow Tunnels

limitations of each method can be deduced from the information on their development and on their assumptions. A global evaluation of each group of methods is attempted in the following.

The fully empirical methods are those which were developed from the observation of the performance of tunnels previously built. As noted in Sections 1.1 and 4.3.2.2, they may include an unknown, normally wide safety margin. They are usually developed for applications in a particular site, for a specific set of ground conditions, and for certain types of construction schemes, which formed the data base from which the methods were elaborated. Applications outside these ranges of conditions may not be successful, as the extrapolation of results is not usually based on fundamental properties that control the phenomenon. This is perhaps the most serious limitation of these methods, which otherwise yield effective results when used within their specific range of validity. Only two published examples of methods belonging to this category are included in Table 4.11, but a much larger number should exist, which are mostly unpublished.

The second class includes the semi-empirical methods, which normally make use of some more or less simple theoretical framework to represent the phenomenon. This enables them to take into account some more fundamental variables, but yet, to a large degree, they rely on empirically developed procedures.

This group can be divided into two subclasses depending on whether the assumed type of representation for the ground medium is continuum or particulate. Some methods, in fact, combine theoretical elements derived from these two types of media to reach their goals (e.g., Limanov, 1957 or Schmidt, 1969).

The continuum theories model the ground as an ideally elastic, plastic or elasto-plastic medium. Examples of these are the methods by Limanov (1957), which calculates the maximum elastic surface settlement, by Murayama and Matsuoka (1969), which estimates settlements in granular soils represented by a plastic continuum, and by Lo et.al. (1984) which calculate settlements assuming the ground to be a linear elastic perfectly plastic material. Though these methods address some of the fundamental mechanisms involved in the process of settlement generation, they are formally approximate as they neglect some other aspects or variables of the problem, as well as including factors which were empirically derived. The degree of generality of these approximate solutions are clearly larger than that of a fully empirical method, but they still can be applied only to certain particular conditions.

The second subclass of the semi-empirical group includes those methods based on theories that recognize the discrete nature of the ground. These methods have in common the treatment of the subsidence as a stochastic problem, where the convergent downward particle flow towards an open

orifice is viewed as equivalent to a counterflow of voids entering the orifice and migrating upwards (Mullins, 1977:37). The number or volume of particles at a certain point in the ground passing through the orifice (a void space behind the liner, for instance) is a measure of the subsidence at this point. This volume, in turn is related to the probability of a particle located at that point to move down, as a result of the creation of an orifice (Schmidt, 1969;32). It follows that the ground surface subsidence can be approximated by a normal or Gaussian probability function.

The use of this theoretical framework was criticized by de Mello (1981) and de Mello and Sozio (1983). The criticism derived from the fact that under good ground control conditions, the basic nature of the physical phenomenon involved in the settlement generation is not addressed by the Stochastic Theory. The response of the ground mass upon the stress release induced by the construction of the tunnel is closely approximated by a continuum mechanics approach, and the fundamental soil behaviour involved is not probabilistic, unless localized collapses of the unsupported ground are the issues under investigation (de Mello and Sozio, 1983:18).

For good construction conditions, the normal probability function could be understood as being a simple curve-fitting tool to adjust measured settlement profiles. According to this view, this class of calculation methods

would be better defined as fully empirical, since they do not address any fundamental aspect of the ground behaviour. It is not debatable, however, that the normal probability curve does fit the observed settlement troughs well, unless the displacements are very large and the resulting trough is narrower than that predicted by Peck's boundaries (Cording and Hansmire, 1975:607). It is with interest that one notes, as indicated by Attewell (1977:935), that for these conditions, high shear strain concentration tends to develop and the settlement profile ceases to follow a normal probability curve. In other words, for poor ground control conditions, this approach would also not be suitable.

In all methods within this category (8 to 12 in Table 4.11), an independent estimate of the total volume of settlement is required. In this regard, an important contribution was made by Cording and Hansmire (1975). The settlement volume was defined by the sum of the volume of the soil lost into the tunnel plus the overall volume changes in the ground. The authors extended Schmidt's (1969:55) qualitative assessment of the sources of lost ground, and proposed a quantitative criterion, that allowed the identification of individual sources. For this, they assumed a two-dimensional approximation and neglected possible interactions between the different types of losses. This criterion, further extended by Attewell (1977), facilitates the estimate of the total volume of ground lost, but the volume of settlements remains undefined, as the

overall ground volume change is not readily determined.

A simpler alternative for settlement volume estimates was suggested by Negro (1979, 1983), who recognized that both the loss of ground and the volume changes are directly related to the quality of construction. By extending suggestions made by Peck et.al. (1972), Negro (Op.cit.) proposed four levels of construction quality, to which total volumes of surface settlements, $V_{\rm s}$, are directly associated. These are defined as a percentage of the tunnel volume, $V_{\rm t}$:

- a. High construction quality: $V_s = 0.5\% \ V_t$
- b. Normal construction quality: $V_s = 1.0\% V_t$
- c. Poor construction quality: $V_s=3.0\%\ V_t$
- d. Failure condition: V_s=40% V_t

Though entirely empirical and involving rather subjective qualifications of the contruction operation, this criterion was able to explain improved ground responses noted in tunnels built in Sao Paulo and in Frankfurt over an extended period of time (see Heinz, 1984:32). The experience gained in applying particular construction methods to specific ground conditions, led to increasingly smaller ground settlement volumes reflecting a better quality of construction.

Interesting contributions were made by Yoshikoshi et.al. (1978) and Attewell and co-workers (Table 4.11, item 12). These authors extended the assumption of normal probability for the transverse settlement to the distribution in the longitudinal direction, which should

result in a cumulative probability curve. This is because it reflects the summation of the subsidence surface generated by a 'point' source of loss, caused by the tunnel face advance. With this assumption, Attewell and co-workers were able to derive a curve fitting technique that seemed to adjust the complete displacement field above a tunnel. To achieve that, some additional simplifying assumptions had to be introduced, one of them being that the soil does not undergo volume changes. Applications of this technique to granular soils would, therefore, be less appropriate, though the probability approach was originally developed for this class of materials. This fact enhances the empirical nature of the method. The method requires an independent estimate of the loss of ground (equal to the volume of settlements), which is done empirically. Moreover, it assumes that the settlement of a point, when the tunnel face passes under it, is equal to 50% of the final settlement of this point.

The last group of methods to be discussed are those derived numerically. As explained in Section 4.3.2.6, these methods result from parametric numerical analyses, whose results are generalized through a normalized form using non-dimensional variables for certain ranges of conditions. Unlike other types of approach reviewed in the present section, these methods were developed from theoretical frameworks that take into account the fundamental aspects of the phenomenon. Their generality is controlled by the validity of their built-in assumptions, and by the range of

conditions covered in their development. As they were derived from basic mechanism representations, they tend to present broader ranges of application which allows an extrapolation of results which is not always possible by empirical methods. Some examples of those methods are given in Table 4.11.

The method by Sagaseta and co-workers was one of the first developed along these lines, using the finite element method as a modelling tool. The linear elastic behaviour it assumes for the soil is a fairly restrictive hypothesis, also shared by others (methods 15 and 16, Table 4.11). In their analyses, Sagaseta and co-workers overemphasized the role of Poisson's ratio on the ground response. In fact, the noted influence of Poisson's ratio, reflects more the effect of the in situ stress ratio, defined as a function of the former. In the development, they assumed a full stress release at the opening. To adjust this assumption to actual conditions, where a partial stress release occurs, the authors introduced an empirical multiplication factor smaller than unity, to be applied to the calculated settlements.

Resendiz and Romo (1981) went further and considered the non-linear, yet elastic, behaviour of the ground. They assumed a hyperbolic stress-strain relation for the soil, treated as a non-frictional material, and followed a development similar to one of those presented in Chapter 6. Thus, the application of the method is restricted to

saturated clay soils in undrained conditions. Further details of their method is given in Table 4.11. The account of the ground settlements induced by the stress release at the face, was approximated by a two-dimensional representation of the shallow tunnel in the longitudinal direction, in which the finite element nodes at the tunnel crown and floor were fixed (rigid lining). The resulting settlements caused by the stress release at the face tend to be excessive as a result of this assumption. Moreover, for certain conditions, the method tends to furnish final settlements at the tunnel crown which are smaller than those at the surface, a result which seems inconsistent with the expected ground response, under the assumptions made. It appears that this result again, is a reflection of the representation adopted for the evaluation of the settlements induced by the stress release at the face. The method requires an independent estimate of a uniform tunnel closure, to represent the loss of ground through the opening contour, which is an additional limitation of the method. These problems and limitations are solved however, if the tunnel closure solution derived in Section 5.3 of this thesis is used to evaluate, not only the losses through the tunnel contour, but also those occurring ahead of the tunnel face. The combination of these two procedures seems to yield more sensible results.

The last two methods included in Table 4.11 present some of the limitations of the method by Sagaseta and

co-workers. However, they take into account the three-dimensional nature of the problem. While the method by Pierau (1981, 1982) used a finite element formulation in its development and considered the tunnel to be lined, the one by Ito and Hisatake (1982), was based on a 3D boundary element analysis of unlined tunnels. As noted in Table 4.11, despite the account of 3D effects, both methods included other assumptions and features that largely restrict their practical application.

With the exception of the method by Pierau (Op.cit.), the other methods were developed in such a way that the prediction of ground settlements is dissociated from the prediction of lining loads. This is one of the most critical limitations of the methods reviewed in the present section.

4.3.4 Ground Stability Verification

The basic aspects of the ground stability problems involved in soil tunnelling were presented in other parts of this thesis, particularly in Section 3.2. It was shown there that tunnel stability is mainly governed by geometric conditions, defined by the cover to diameter ratio, H/D, and by the unsupported heading length to diameter, L/D.

On the other hand, the basic requirements for excavation stability assessment were presented in Section 4.2.3. It was discussed then, that conventional limit equilibrium calculations may not be recommended for stability assessment in practice, as they can provide unsafe



